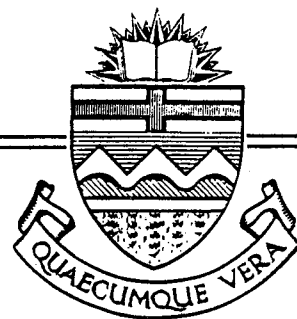


Structural Engineering Report No. 83



INELASTIC BEHAVIOR OF MULTISTORY STEEL FRAMES

by
MOHAMED H. EL-ZANATY
DAVID W. MURRAY
REIDAR BJORHOVDE

April 1980

RECENT STRUCTURAL ENGINEERING REPORTS

Department of Civil Engineering

University of Alberta

53. *Web Slenderness Limits for Non-Compact Beam-Columns* by D.S. Nash and G.L. Kulak, March 1976.
54. *A Monte Carlo Study of the Strength Variability of Rectangular Tied Reinforced Concrete Columns* by L.H. Grant and J.G. MacGregor, March 1976.
55. *An Elastic Stress Analysis of a Gentilly Type Containment Structure - Volume 1* by D.W. Murray and M. Epstein, April 1976.
56. *An Elastic Stress Analysis of a Gentilly Type Containment Structure - Volume 2 - (Appendices B to F)* by D.W. Murray and M. Epstein, April 1976.
57. *A System of Computer Programs for the Large Deformation In-Plane Analysis of Beams* by M. Epstein and D.W. Murray, May 1976.
58. *A Statistical Study of Variables Affecting the Strength of Reinforced Normal Weight Concrete Members* by S.A. Mirza and J.G. MacGregor, December 1976.
59. *The Destabilizing Forces Caused by Gravity Loads Acting on Initially Out-Of-Plumb Members in Structures* by D. Beaulieu and P.F. Adams, February 1977.
60. *The Second-Order Analysis and Design of Reinforced Concrete Frames* by G.S. Mathews and J.G. MacGregor, January 1977.
61. *The Effects of Joint Eccentricity in Open Web Steel Joists* by R.A. Matiisen, S.H. Simmonds and D.W. Murray, June 1977.
62. *Behaviour of Open Web Steel Joists* by R.A. Kaliandasani, S.H. Simmonds and D.W. Murray, July 1977.
63. *A Classical Flexibility Analysis for Gentilly Type Containment Structures* by D.W. Murray, A.M. Rohardt, and S.H. Simmonds, June 1977.
64. *Substructure Analysis of Plane Frames* by A.A. Elwi and D.W. Murray, June 1977.
65. *Strength and Behavior of Cold-Formed HSS Columns* by Reidar Bjorhovde, December 1977.
66. *Some Elementary Mechanics of Explosive and Brittle Failure Modes in Prestressed Containments* by D.W. Murray, June 1978.

67. *Inelastic Analysis of Prestressed Concrete Secondary Containments* by D.W. Murray, L. Chitnuyanondh, C. Wong and K.Y. Rijub-Agha, July 1978.
68. *Strength of Variability of Bonded Prestressed Concrete Beams* by D.K. Kikuchi, S.A. Mirza and J.G. MacGregor, August 1978.
69. *Numerical Analysis of General Shells of Revolution Subjected to Arbitrary Loading* by A.M. Shazly, S.H. Simmonds and D.W. Murray, September 1978.
70. *Concrete Masonry Walls* by M. Hatzinikolas, J. Longworth and J. Warwaruk, September 1978.
71. *Experimental Data for Concrete Masonry Walls* by M. Hatzinikolas, J. Longworth and J. Warwaruk, September 1978.
72. *Fatigue Behaviour of Steel Beams with Welded Details* by G.R. Bardell and G.L. Kulak, September 1978.
73. *Double Angle Beam-Column Connections* by R.M. Lasby and Reidar Bjorhovde, April 1979.
74. *An Effective Uniaxial Tensile Stress-Strain Relationship for Prestressed Concrete* by L. Chitnuyanondh, S. Rizkalla, D.W. Murray and J.G. MacGregor, February 1979.
75. *Interaction Diagrams for Reinforced Masonry* by C. Feeg and J. Warwaruk, April 1979.
76. *Effects of Reinforcement Detailing for Concrete Masonry Columns* by C. Feeg, J. Longworth, and J. Warwaruk, May 1979.
77. *Interaction of Concrete Masonry Bearing Walls and Concrete Floor Slabs* by N. Ferguson, J. Longworth and J. Warwaruk, May 1979.
78. *Analysis of Prestressed Concrete Wall Segments* by B.D.P. Koziak and D.W. Murray, June 1979.
79. *Fatigue Strength of Welded Steel Elements* by M.P. Comeau and G.L. Kulak, October 1979.
80. *Leakage Tests of Wall Segments of Reactor Containments* by S.K. Rizkalla, S.H. Simmonds and J.G. MacGregor, October 1979.
81. *Tests of Wall Segments from Reactor Containments* by S.H. Simmonds, S.H. Rizkalla and J.G. MacGregor, October 1979.
82. *Cracking of Reinforced and Prestressed Concrete Wall Segments* by J.G. MacGregor, S.H. Rizkalla and S.H. Simmonds, October 1979.
83. *Inelastic Behavior of Multistorey Steel Frames* by M. EL Zanaty, D.W. Murray and R. Bjorhovde, April 1980.

THE UNIVERSITY OF ALBERTA

INELASTIC BEHAVIOR OF MULTISTORY STEEL FRAMES

BY

MOHAMED H. EL-ZANATY

DAVID W. MURRAY

and

REIDAR BJORHOVDE

Department of Civil Engineering

University of Alberta

April, 1980

ABSTRACT

The research work in this report deals with the inelastic behavior of multistory, planar steel frames. The study includes a review of different types of formulation for stability and strength analyses. A method to compute elastic buckling loads for multistory frames is discussed.

A general approach to the elastic and inelastic nonlinear analyses of multistory frames is presented and a finite element formulation is developed. A technique to determine the load-deformation characteristics of frames, using the finite element equations is discussed. The inelastic analysis includes the effect of axial loads on the stiffness of the frame, gradual penetration of yielding in the cross section, and the spread of inelastic zones along the member length. The effects of residual stresses and strain hardening have been taken into account in the analysis.

The features of the elastic-plastic response of frames for first and second order analyses are presented. Throughout the study numerical examples are given and compared with available results.

In the final section the behavior of a number of frames is examined through inelastic and elastic-plastic analyses. Comparisons are made between the two approaches and the effects of residual stresses and strain hardening on the behavior of frames are studied.

ACKNOWLEDGEMENTS

This study was performed in the Department of Civil Engineering at the University of Alberta. Financial support provided by the Civil Engineering Department and the National Research Council is acknowledged with thanks.

TABLE OF CONTENTS

| | Page |
|--|-------|
| Title | i |
| Abstract | v |
| Acknowledgements | vi |
| Table of Contents | vii |
| List of Tables | xiii |
| List of Figures | xiv |
| List of Symbols | xviii |
| CHAPTER I INTRODUCTION | 1 |
| 1.1 Types of Frame Analysis | 1 |
| 1.2 Inelastic Frame Analysis | 4 |
| 1.3 Objective | 7 |
| 1.4 Outline of Contents | 7 |
| CHAPTER II REVIEW OF STABILITY THEORY | 9 |
| 2.1 Introduction | 9 |
| 2.2 Introduction to Linearly Elastic Formulation | 9 |
| 2.2.1 Bifurcation and Buckling | 9 |
| 2.2.2 Linearly Elastic Formulation for Frames | 18 |
| 2.2.2a Flexibility Approach | 23 |
| 2.2.2b Stiffness Approach | 27 |

| | Page |
|---|--------|
| 2.3 Elastic Nonlinear Formulation | 32 |
| 2.3.1 Large Deformation Formulation for Columns (The Elastica) | 33 |
| 2.3.2 Elastic Nonlinear Analysis of Frames | 38 |
| 2.4 Inelastic First Order Stability Theory | 41 |
| 2.4.1 Tangent Modulus Theory | 41 |
| 2.4.2 Reduced Modulus Theory | 43 |
| 2.4.3 Shanley's Contribution | 44 |
| 2.4.4 Inelastic Behavior of Beam-Columns | 44 |
| 2.4.5 Simple Plastic Analysis | 47 |
| 2.5 Inelastic Nonlinear Analysis | 49 |
| 2.5.1 The Step-by-Step Method of Analysis | 51 |
| 2.5.2 Development of Second Order Plastic Analysis. . | 51 |
| CHAPTER III ELASTIC FORMULATIONS AND SOLUTIONS | 54 |
| 3.1 Review of the Finite Element Method | 55 |
| 3.2 Basic Equations and Assumptions | 57 |
| 3.3 Formulation of Linear Stability Equations | 60 |
| 3.3.1 Secant Stiffness for Elastic Element | 60 |
| 3.3.2 Structure Secant Stiffness Matrix | 62 |
| 3.3.3 Frame Critical Load | 65 |
| 3.3.4 Inverse Power Iteration Method | 67 |
| 3.3.5 Computer Program | 69 |
| 3.4 Numerical Results of Elastic Buckling Problems | 70 |
| 3.4.1 Sample Solutions | 70 |
| 3.4.2 Comments on Results | 79 |

| | Page |
|--|---------|
| 3.5 Formulation of Nonlinear Equations | 79 |
| 3.5.1 Description of Basic Formulation | 79 |
| 3.5.2 Finite Element Model | 84 |
| 3.5.3 Assembly of Finite Element Equations | 85 |
| 3.5.4 Newton-Raphson Solution Procedure | 92 |
| 3.5.5 Summary | 94 |
| 3.5.6 Computer Program | 94 |
| 3.6 Nonlinear Elastic Solutions | 95 |
| 3.6.1 Examples of Beam-Columns | 95 |
| 3.6.2 Examples of Frames | 98 |
| 3.6.3 Comments on Results | 103 |
| CHAPTER IV BEHAVIOR OF ELASTIC-PLASTIC FRAMES | 106 |
| 4.1 Basic Assumptions and Limitations | 106 |
| 4.2 The Incremental Method of Analysis | 108 |
| 4.2.1 Incremental First Order Analysis | 108 |
| 4.2.2 Incremental Second Order Analysis | 111 |
| 4.3 The Iterative Method of Analysis | 112 |
| 4.3.1 First Order Analysis | 112 |
| 4.3.2 Iterative Second Order Analysis | 115 |
| 4.4 Comparison Between Incremental and Iterative Approaches | 115 |
| 4.5 Computer Programs | 116 |
| 4.6 Elastic-Plastic Solutions | 117 |
| 4.6.1 Sample Solutions | 117 |
| 4.6.2 Comments on Results | 125 |

| | Page |
|---|------|
| CHAPTER V NONLINEAR INELASTIC FORMULATION AND SOLUTIONS . . . | 126 |
| 5.1 Basic Formulation For Inelastic Behavior | 127 |
| 5.1.1 Main Assumptions | 127 |
| 5.1.2 Evaluation of Incremental Forces | 128 |
| 5.1.3 Evaluation of Element Tangent Stiffness Matrix | 128 |
| 5.2 Transformation and Assembly | 129 |
| 5.3 Newton-Raphson With Gradient Test | 130 |
| 5.4 Residual Stresses and Strain Hardening of the Material | 130 |
| 5.5 Plastification of the End Zones | 131 |
| 5.6 Computer Program | 132 |
| 5.7 Inelastic Solutions | 132 |
| 5.7.1 Sample Examples | 132 |
| 5.7.2 Comments on Results | 138 |
| CHAPTER VI BEHAVIORAL STUDIES | 140 |
| 6.1 Behavioral Study of a Beam-Column | 141 |
| 6.1.1 Inelastic Analysis Vs. Rajasekaran Method . . . | 141 |
| 6.1.2 Inelastic Vs. Elastic-Plastic Analysis | 141 |
| 6.1.3 Effects of Residual Stresses and Strain Hardening | 144 |
| 6.2 Behavioral Study of Single Story Frames | 151 |
| 6.2.1 Inelastic Vs. Elastic-Plastic Analysis | 151 |
| 6.2.2 Effects of Residual Stresses and Strain Hardening | 154 |

| | Page |
|--|------|
| 6.3 Behavioral Study of Multistory Frames | 161 |
| 6.3.1 Frames and Loading | 161 |
| 6.3.2 Presentation of Results | 165 |
| CHAPTER VII SUMMARY AND CONCLUSIONS | 173 |
| 7.1 Nonlinear Strain-Displacement Relationship | 174 |
| 7.2 Inelastic Vs. Elastic-Plastic Analysis | 174 |
| 7.3 Gradual Penetration of Yielding | 175 |
| 7.4 Effects of Residual Stresses and Strain Hardening . . | 176 |
| 7.5 Incremental Vs. Iterative Method in the Elastic- Plastic Analysis | 177 |
| LIST OF REFERENCES | 178 |
| APPENDIX A ELEMENT STIFFNESS MATRIX FOR BEAM-COLUMNS | 189 |
| A.1 Virtual Work Equations for Linear Stability Problems | 190 |
| A.2 The Finite Element Model | 192 |
| APPENDIX B DETAILS OF NONLINEAR ELASTIC FORMULATION | 198 |
| B.1 Basic Equations | 199 |
| B.2 Nonlinear Elastic Response | 201 |
| B.3 Evaluation of Unbalanced Forces Vector for Finite Element Model | 205 |
| B.3.1 Vector of Incremental Forces of Flexural Element | 206 |
| B.3.2 Vector of Incremental Forces of Truss Element | 208 |
| B.3.3 Assembly of Unbalanced Forces | 210 |
| B.4 Evaluation of Stiffness Matrix $[K_T]$ | 210 |
| B.4.1 Element Stiffness Matrix For a Flexural Element | 210 |

| | Page |
|--|------|
| B.4.2 Element Stiffness Matrix For a Truss Element | 217 |
| B.4.3 Assembly of Structural Stiffness $[K_T]$ | 221 |
| APPENDIX C LARGE DISPLACEMENT TRANSFORMATION | 222 |
| APPENDIX D CALCULATIONS OF SECTION PROPERTIES AND STRESS RESULTANTS FOR I-SECTION | 227 |
| D.1 Determination of Transformed Section | 228 |
| D.2 Evaluation of Cross-Section Properties | 234 |
| D.3 Evaluation of the Stress Resultants | 237 |
| APPENDIX E INCREMENTAL STRESS RESULTANT VECTORS FOR INELASTIC ELEMENT | 239 |
| E.1 Incremental Stress Resultant Vectors | 240 |
| | |

LIST OF TABLES

| TABLE | | PAGE |
|-------|--|------|
| 3-1 | Transformation Matrix | 63 |
| 3-2 | Critical Buckling Load of Columns | 72 |
| 3-3 | Numerical Results of Frame (a) | 75 |
| 3-4 | Numerical Results of Frame (b) | 76 |
| 3-5 | Transformation Matrix For a Flexural Element | 90 |
| 3-6 | Transformation Matrix For a Truss Element | 91 |
| 3-7 | Comparison Between Incremental Solutions For Cantilever Beam NL-4 | 101 |
| 5-1 | Mechanical Properties | 136 |
| 5-2 | Member Properties | 136 |
| 6-1 | Loading; Frame 24-3 | 166 |
| 6-2 | Beam Sections; Frame 24-3 | 167 |
| 6-3 | Column Sections; Frame 24-3 | 168 |
| B-1 | Incremental Stress Resultant Vectors For Flexural Element (Elastic) | 215 |
| B-2 | Incremental Stress Resultant Vectors For Truss Element (Elastic) | 220 |
| E-1 | Incremental Stress Resultant Vectors For Flexural Element (Inelastic) | 245 |
| E-2 | Incremental Stress Resultant Vectors For Truss Element (Inelastic) | 248 |

LIST OF FIGURES

| FIGURE | | PAGE |
|--------|---|------|
| 1-1 | Types of Analysis | 2 |
| 1-2 | Idealized Moment-Curvature Relationship | 6 |
| 2-1 | Load-Displacement Relation for Beam Clamped at Both Ends | 11 |
| 2-2 | Equilibrium Paths for Initially Straight Column . . . | 12 |
| 2-3 | Load-Deflection Relation for Imperfect Column | 16 |
| 2-4 | Fixed End Column | 19 |
| 2-5 | Behavior of Frames | 22 |
| 2-6 | Column Behavior for Large Deflections | 34 |
| 2-7 | Sway Forces Due to Vertical Loads | 40 |
| 2-8 | General Stress Strain Relationship | 42 |
| 2-9 | Load-Deflection Curve of Shanley's Model | 42 |
| 2-10 | Maximum Carrying Capacity Interaction Curves | 46 |
| 2-11 | Idealized Moment-Curvature Relationship | 50 |
| 3-1 | Element Deformation | 59 |
| 3-2 | Nodal Displacements and Forces | 61 |
| 3-3 | Types of Columns | 71 |
| 3-4 | One Story-One Bay Frame | 73 |
| 3-5 | Two Story-Two Bay Frame | 77 |
| 3-6 | Multistory-Multibay Frame | 78 |
| 3-7 | Local Nodal Displacements For Flexural Element | 86 |
| 3-8 | Local Nodal Displacements For Truss Element | 87 |
| 3-9 | Global Nodal Displacements | 89 |
| 3-10 | Newton-Raphson Procedure | 93 |
| 3-11 | Solution for The 'Elastica' | 96 |

| FIGURE | | PAGE |
|--------|---|------|
| 3-12 | Solution for Cantilever Under Pure Moment | 97 |
| 3-13 | Load-Deflection Curves for Cantilever Beam | 99 |
| 3-14 | Cantilever Beam With Two Lateral Loads | 100 |
| 3-15 | Load-Deflection Curves for One Story Bent | 102 |
| 3-16 | Load-Deformation Curves for Two Story--Two Bay Frame | 104 |
| 3-17 | Load-Deformation Curve for Multistory Multibay Frame | 105 |
| 4-1 | Interaction Curve | 107 |
| 4-2 | Load-Deformation Response | 114 |
| 4-3 | Frame EP-1 | 118 |
| 4-4 | Load-Deformation Relationship for Frame EP-1 | 119 |
| 4-5 | Frame EP-2 | 121 |
| 4-6 | Load-Deflection Curve for Frame EP-2 | 122 |
| 4-7 | Frame EP-3 | 123 |
| 4-8 | Load-Deformation Characteristics For Frame EP-3 | 124 |
| 5-1 | Results of Example IN-1 | 133 |
| 5-2 | Example Frame IN-2 | 135 |
| 5-3 | Example Frame IN-3 | 135 |
| 5-4 | Load-Deformation Curves of Frame IN-2 | 137 |
| 5-5 | Load-Deformation Curves of Frame IN-3 | 139 |
| 6-1 | Cantilever Beam-Column | 142 |
| 6-2 | Inelastic Vs. Rajasekaran (1971) | 143 |
| 6-3 | Inelastic Vs. Elastic-Plastic (Cantilever) | 145 |
| 6-3a | Column Interaction Curves | 146 |
| 6-4 | Load-Deformation Characteristics; Cantilever ($L/r = 14.4$; $P/P_y = 0.15$) | 147 |
| 6-5 | Load-Deformation Characteristics; Cantilever ($L/r = 14.4$; $P/P_y = 0.91$) | 148 |

| FIGURE | | PAGE |
|--------|---|------|
| 6-6 | Load-Deformation Characteristics; Cantilever ($L/r = 80$; $P/P_y = 0.15$) | 149 |
| 6-7 | Load-Deformation Characteristics; Cantilever ($L/r = 80$; $P/P_y = 0.3$) | 150 |
| 6-8 | Single Story Frame | 152 |
| 6-9 | Inelastic Vs. Elastic-Plastic (Single Story-Hinged Bases) | 153 |
| 6-10 | Maximum Strength of Beam-Columns in Portal Frames ($L/r = 40$) | 155 |
| 6-11 | Maximum Strength of Beam-Columns in Portal Frames ($L/r = 60$) | 156 |
| 6-12 | Load-Deformation Characteristics; Single Story Frame ($L/r = 40$; $P/P_y = 0.15$) | 157 |
| 6-13 | Load-Deformation Characteristics; Single Story Frame ($L/r = 40$; $P/P_y = 0.6$) | 158 |
| 6-14 | Load-Deformation Characteristics; Single Story Frame ($L/r = 60$; $P/P_y = 0.15$) | 159 |
| 6-15 | Load-Deformation Characteristics; Single Story Frame ($L/r = 60$; $P/P_y = 0.4$) | 160 |
| 6-16 | Configuration and Working Loads; Frame 8-1 | 162 |
| 6-17 | Configuration and Working Loads; Frame 6-2 | 163 |
| 6-18 | Geometry; Frame 24-3 | 164 |
| 6-19 | Load-Deformation Characteristics; Frame 8-1 | 169 |
| 6-20 | Load-Deformation Characteristics; Frame 6-2 | 170 |
| 6-21 | Load-Deformation Characteristics; Frame 24-3 | 171 |
| A-1 | Basic Functions for Linear Displacements | 194 |
| A-2 | Basic Functions for Cubic Polynomial | 195 |
| C-1 | Element Transformation | 224 |
| D-1 | Residual Strain Distribution | 230 |

| FIGURE | | PAGE |
|--------|--|------|
| D-2 | Trilinear Stress-Strain Diagram | 231 |
| D-3 | Transformed Section of a Plate Segment | 233 |
| D-4 | Cross Section | 235 |
| D-5 | Stresses in a Typical Plate Segment | 235 |

LIST OF SYMBOLS

In this dissertation, the notation generally corresponds with the notation commonly encountered in textbooks. All symbols are defined where they first appear in the text. However, in certain cases it has not been possible to maintain uniform symbology throughout the thesis.

Special Symbols

| | |
|-------------------|---|
| $\{ \}$ | denotes a column vector |
| $\langle \rangle$ | denotes a row vector |
| $[]$ | denotes a matrix |
| $[]^T$ | denotes a matrix transpose |
| $[]^{-1}$ | denotes a matrix inverse |
| $ $ | denotes a determinant |
| \sum | denotes a summation |
| Δ | prefixed to other term denotes an increment |
| δ | prefixed to other term denotes a virtual variation |
| ∂ | denotes partial differentiation |
| d | denotes ordinary differentiation |
| c, s | denote $\cos\alpha$ and $\sin\alpha$, respectively |
| $'$ | denotes differentiation with respect to the single argument |

Roman Symbols

| | |
|---------------------------------|--|
| A | area of the cross section; arbitrary point in Fig. 3-1 |
| A, A_n | arbitrary constants in Sect. 2.2.1 |
| A_k | transformed area of the k^{th} segment |
| A^t | transformed area of the cross section |
| a | initial midspan deflection (Fig. 2-3a) |
| a_1, a_2, a_3 | quantities defined by Eqs. 3.5.10 |
| $[A]$ | compatibility matrix in Eq. 2.2.36 |
| $[\bar{A}]$ | equilibrium matrix in Eq. 2.2.48 |
| B | arbitrary constant |
| b_r, b_r^t | original and transformed thickness, respectively, of a particular region |
| b_{1j}, b_{2j}, b_{3j} | quantities defined by Eqs. E.1.5 |
| C | constant of integration; stability function in Eq. 2.2.59 |
| C_1, C_2, C_3, C_4 | integration constants |
| C_m | equivalent moment factor |
| $\{C\}$ | vector of integration constants C_1, C_2, C_3 , and C_4 |
| $[D]$ | diagonal matrix obtained during decomposition of the stiffness matrix |
| E, E_p, E_{st} | Young's modulus, plastic modulus, and strain hardening modulus, respectively |
| E_r, E_t | reduced modulus and tangent modulus, respectively |
| e_{1j}, e_{2j}, e_{3j} | quantities defined by Eqs. B.1.3 |
| $\{F(r)\}$ | a function to be integrated |
| $\{F(r_1)\}, \dots, \{F(r_n)\}$ | vector $\{F(r)\}$ evaluated at points r_1, r_2, \dots, r_n |
| $[F]$ | structure flexibility matrix |
| $[\bar{F}]$ | element flexibility matrix |

| | |
|------------------------------|---|
| $[F]$ | matrix contains the element flexibility matrices on the principal diagonal |
| G | ratio of column stiffness to beam stiffness (see Eq. 3.3.1) |
| $[G]$ | matrix defined by Eq. 3.3.26b |
| $[G_1], [G_2]$ | the matrices of Eqs. 2.2.27b and 2.2.29b, respectively |
| H'_i | fictitious sway force at level i |
| h | story height |
| I, I_x | moment of inertia |
| I_c, I_g | column and girder moment of inertia, respectively |
| $I_1^t, I_2^t, I_3^t, I_4^t$ | transformed section properties defined by Eqs. D.2.2 |
| $(I_{xx})_k$ | moment of inertia of segment k about centroidal axis $x-x$ |
| $I_4, (I_{4xx})_k$ | quantities defined by Eq. B.2.2e |
| K | complete elliptic integral of the first kind; effective length factor in Chapter 6 |
| k | plate segment index; quantity defined by Eq. 2.2.2 |
| $\langle k \rangle_i$ | the i^{th} row of matrix $[k]$ |
| $[k], [k_s], [k_T], [k_g]$ | element flexural, secant, tangent, and geometric stiffness matrices, respectively |
| $[k_T^I]$ | inelastic element tangent stiffness matrix |
| $[k_1], [k_2], [k_3]$ | submatrices defined in Eqs. B.4.5 |
| $[K]$ | matrix contains element stiffness matrices on its principal diagonal |
| $[K], [K_s], [K_T], [K_G]$ | flexural, secant, tangent, and geometric stiffness matrices, respectively, assembled for the entire structure |
| $[K_T^I]$ | inelastic tangent stiffness matrix for the entire structure |
| $[\bar{K}_G]$ | geometric stiffness matrix corresponding to some reference value of the applied loading |

| | |
|---|--|
| L | member length |
| L_c, L_g | column length and girder length, respectively |
| ℓ, ℓ_r | element length and plate region length, respectively |
| $[L]$ | lower triangular matrix obtained during decomposition process |
| $M, M(z)$ | moment and moment at distance z , respectively |
| M_c, M_v | moments due to constant and variable sets of applied loads, respectively |
| M_o | applied moment |
| M_p | plastic moment |
| M_{pc} | reduced plastic moment due to presence of axial load |
| M_u | ultimate moment capacity in the absence of axial load |
| $\{M\}$ | vector of member end forces |
| $\{M^F\}$ | vector of fixed end forces |
| $\{M_p\}$ | vector of member end forces from a particular solution |
| n, m, m^* | stress resultants defined by Eqs. 3.5.9 |
| n | arbitrary number in Sect. 2.2.1 |
| $\{\frac{\partial n}{\partial q}\}, \{\frac{\partial m}{\partial q}\}, \{\frac{\partial m^*}{\partial q}\}$ | incremental stress resultant vectors |
| O | arbitrary point on the centroidal axis in Fig. 3-1 |
| P | axial load |
| P_{cr}, P_e | critical and Euler buckling loads, respectively |
| P_p | rigid plastic collapse load |
| P_r, P_t | reduced and tangent modulus loads, respectively |
| P_y | yield load |
| P_u | ultimate load |
| p | percentage ratio of $(Q_u)_{in}$ to $(Q_u)_{el-pl}$ |

| | |
|--------------------------------|--|
| Q | an applied lateral load |
| Q_1 | a force coordinate |
| $(Q_u)_{in}, (Q_u)_{el-pl}$ | ultimate values of the lateral load Q obtained from inelastic and elastic-plastic analysis, respectively |
| $q(z)$ | intensity of distributed load |
| q_1 | a displacement coordinate |
| $\{Q\}$ | the local vector of nodal forces; unbalanced forces in Sect. 2.2.2 |
| $\{Q_c\}, \{Q_v\}$ | vectors of member end forces due to constant and variable sets of applied loads, respectively |
| $\{Q^*\}$ | a set of generalized forces in Eq. 2.2.39 |
| $\{Q_p\}$ | vector of unbalanced forces in Sect. 2.2.2 |
| $\{Q^R\}$ | vector of resisting forces |
| $\{\Delta Q^I\}$ | vector of incremental forces evaluated for an inelastic element |
| $\{q\}$ | local vector of nodal displacements |
| $\{q^*\}$ | vector of generalized relative displacements |
| $\{q_p\}$ | vector of incompatible displacements |
| r | radius of gyration |
| $\{R\}, \{R^*\}$ | vectors of nodal forces |
| $\{R_c\}, \{R_v\}$ | constant set of global nodal forces and variable set of global nodal forces, respectively |
| $\{\bar{R}\}$ | reference load vector |
| $\{R_E\}$ | element forces |
| $\{R_g\}$ | vector defined in Eq. 3.3.24b |
| $\{R_p\}$ | vector of particular solution nodal forces |
| $\{\Delta R\}, \{\Delta R^I\}$ | unbalanced load vectors for elastic and inelastic analysis, respectively |
| $\{r\}$ | global vector of nodal displacements |

| | |
|------------------------|---|
| $\{r^*\}$ | vector of generalized displacements |
| $\{\bar{r}\}$ | vector defined in Eq. 3.3.27b |
| $\{r_c\}, \{r_v\}$ | global vectors of nodal displacements due to constant and variable set of applied loads, respectively |
| $\{r_E\}_G$ | element displacements |
| $\{r_p\}$ | vector of particular solution displacements |
| S | stability function |
| s | distance along a curve |
| t_k | plate segment thickness |
| $[T], [\bar{T}]$ | transformation matrix for a flexural element and a truss element, respectively |
| U^I, u^I | global and local displacements, respectively, at joint I in the x-direction |
| \tilde{U}, \tilde{u} | global and local displacements in Appendix C |
| u, u_o | horizontal displacements of points A and o, respectively (Fig. 3-1) |
| $\{\bar{U}\}$ | generalized displacements defined in Figs. 3-7 and 3-8 for a flexural element and truss element, respectively |
| V | shear force; volume |
| V^I, v^I | global and local displacements, at joint I in the y-direction, respectively |
| \tilde{V}, \tilde{v} | global and local displacements in Appendix C |
| V'_i, v'_{i-1} | fictitious shear forces at story i and (i-1), respectively |
| v | displacement; vertical displacement of point A in Fig. 3-1 |
| v_o | initial imperfection; vertical displacement of point O in Fig. 3-1 |
| $v_p(z)$ | particular solution displacement at distance z |
| $\{\bar{V}\}$ | generalized displacements defined in Figs. 3-7 and 3-8 for a flexural element and truss element, respectively |

| | |
|------------------|--|
| W | work of external forces |
| X, Y, Z | reference axes in global coordinate system |
| x, y, z | reference axes in local coordinate system |
| y, z | distance in the y and z -direction, respectively |
| Y_k | vertical distance between the centroid of the cross section and the transformed centroid of the k th plate segment |
| y_{ir}, y_{jr} | the distances of the i th and j th nodal points of the r th region with respect to the centroid of the cross section |

Greek Symbols

| | |
|---------------------------------------|---|
| α | slope of end of member; angle of inclination of local axes to global axes |
| $\alpha_1, \alpha_2, \dots, \alpha_n$ | arbitrary constants |
| β | ratio between axial to critical load |
| γ | shear strain |
| Δ, Δ_1 | sway deflection |
| δ | midspan deflection |
| $\{\Delta\}$ | vector of member end displacements |
| $\{\Delta_p\}$ | vector of particular solution member end displacements |
| ϵ, ϵ_z | strain; strain in z -direction |
| ϵ_A, ϵ_B | strain at points A and B, respectively |
| ϵ_R | residual strain |
| $\epsilon_y, \epsilon_{st}$ | yield and strain hardening strain, respectively |
| ϵ_{zt} | total strain in z -direction |
| θ | slope or rotation |
| θ^I | rotation at joint I |

| | |
|----------------------------|--|
| λ | load factor; instability factor in Sect. 3.3 |
| λ_{cr} | critical value of λ |
| ζ | dimensionless parameter |
| σ, σ_z | stress and stress in z-direction, respectively |
| σ_{cr} | critical stress |
| σ_{ir}, σ_{jr} | the stresses at the i^{th} and j^{th} nodal points of the region r |
| σ_R | residual stress |
| σ_{ult} | ultimate stress |
| σ_y | yield stress |
| ϕ | angle change per unit length |
| $\{\phi\}, \{\bar{\phi}\}$ | shape functions for a flexural element and truss element, respectively |
| $\{\phi(z)\}$ | shape function defined in Eq. 2.2.26b |
| ψ_1 | the unbalanced forces of Eq. 3.5.12 |

CHAPTER I

INTRODUCTION

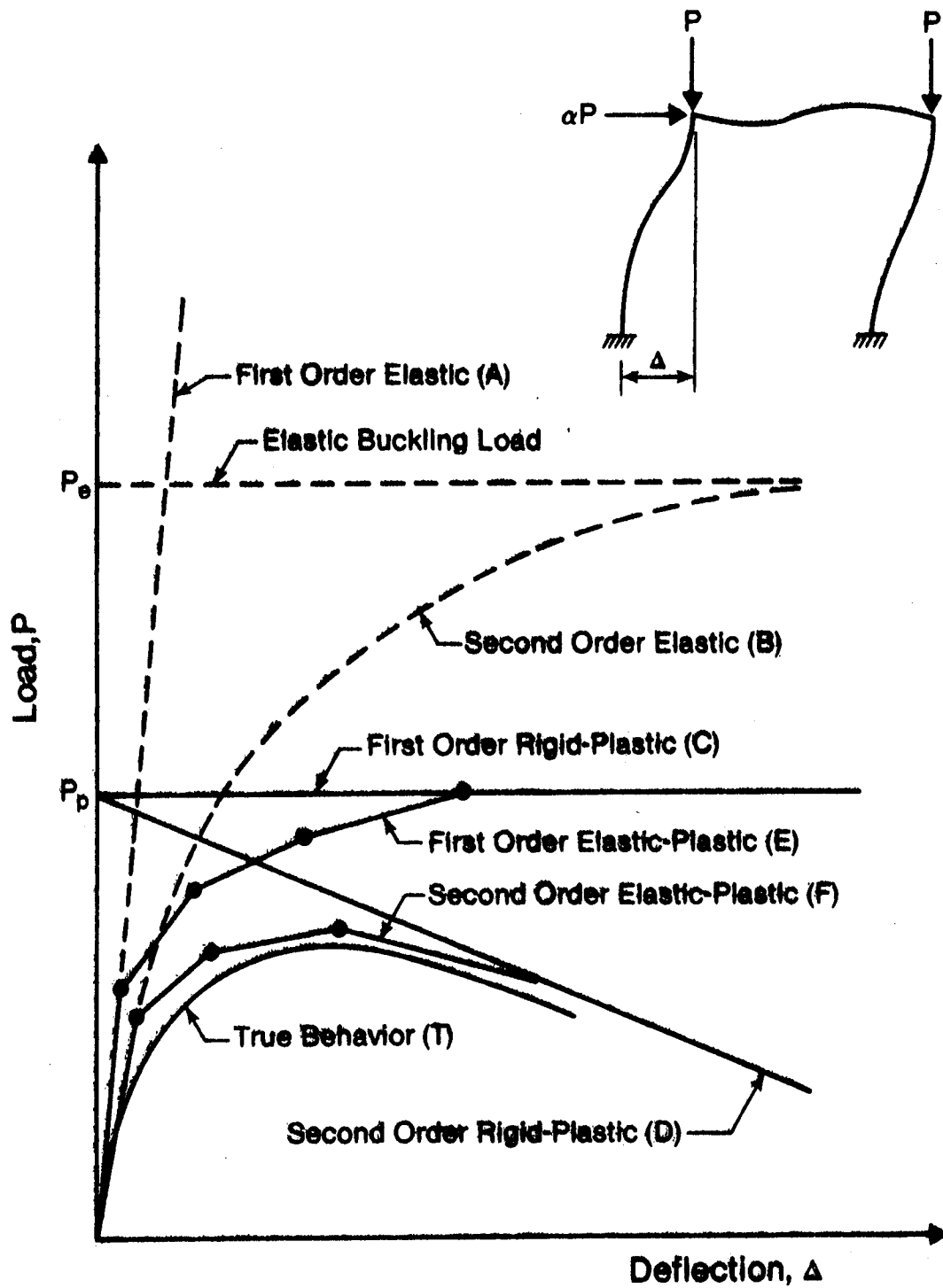
Almost all analysis carried out in engineering practice is based on linear theory. Linear analysis, rather than nonlinear, is performed because of its relative simplicity.

In recent years, there has been a considerable amount of theoretical work carried out on the effects of geometric and material nonlinearities on the behavior of structures. Nonlinear analyses by the finite element method were first introduced for geometric nonlinearity by Turner *et al.* (1960), and for elastic-plastic analysis by Gallagher *et al.* (1962). More recent work has dealt with large strains (Hofmeister *et al.* 1971), creep strains (Greenbaum and Rubinstein 1968), dynamic forces (Stricklin *et al.* 1971), and variation of material properties with temperature (Marcal 1972).

1.1 Types of Frame Analysis

Several types of frame analysis may be illustrated with reference to Fig. 1-1. This figure shows the relationship between the gravity load, P , and the lateral deflection at the top, Δ , for a simple portal frame, as predicted by various approaches.

The simplest form of frame analysis is one which predicts the elastic critical load of the frame, P_e . In this method the material is assumed to be elastic, the horizontal loads applied to the frame are zero, and all prebuckling deformations (e.g. initial out-of-



Load-Deformation Relationships

FIGURE 1-1 Types of Analysis

straightness) are ignored. When the deformations due to lateral loads are included, a linear load-deflection curve, A, is produced. This solution is usually referred to as a 'first order elastic analysis'. When nonlinear effects, such as nonlinear strain-displacement relationship and the effect of deformations on the equilibrium equations, are considered, the formulation results in a nonlinear load-deflection response, curve B. This method is usually called a 'second order elastic analysis'. The elastic analyses give no indication of the ultimate capacity of the frame or the true behavior in the region of ultimate load.

If the material response of the frame is no longer perfectly elastic, another critical load may be reached before the elastic buckling load. This critical load, P_p , results from the formation of a plastic mechanism, ignoring all prebuckling deformations. This method is referred to as a first order rigid-plastic analysis, and is illustrated by curve C of Fig. 1-1. A second order rigid-plastic approach considers the effect of the mechanism deflections on the equilibrium equations, and the loads therefore must decrease to maintain equilibrium, as shown by curve D.

In first order elastic-plastic analysis the material is assumed elastic-perfectly plastic, and prebuckling deformations are considered. The load-deformation response for such a solution is shown as curve E. The upper limit of the first order elastic-plastic analysis is the first order rigid-plastic limit, P_p . When the effects of sway deformations on the equilibrium equations are considered, the formulation results in a second order elastic-plastic analysis, shown as curve F, in Fig. 1-1.

The 'true' behavior of the frame is shown as curve T. The difference between the results of a second order elastic-plastic analysis and the 'true' behavior is due to gradual penetration of the yielded zones, residual stresses, initial imperfection, and strain hardening. The magnitude of the difference depends on the geometry and stiffness of the frame, material properties, and loading conditions.

1.2 Inelastic Frame Analysis

Extensive research has been conducted in recent years to investigate the behavior of multistory frames and their components. Much of this work has been aimed at the development of practical design procedures which could account for material nonlinearity (Majumdar and Adams 1971; Davison and Adams 1974).

Several authors (Hodge 1959; McNamee and Lu 1972) have assumed that yielding takes place only at generalized plastic hinges of zero length (the concept of concentrated plasticity). The researchers have considered multidimensional yield surfaces, with proposed procedures for modifying the elastic stiffness of a frame member to account for yielding. General computational procedures have not been developed and only simple cases have been considered. A few researchers (Moses 1964; Kitipornchai and Trahair 1975) considered extended regions of plastic deformations rather than discrete hinges, but no conclusions were reached regarding their effect on the behavior of frames.

Although steel exhibits some strain hardening, most investigators have assumed that the material is ideally elastic-plastic. The influence of strain hardening on the ultimate load was studied by

Hrennikoff (1965), Sawko (1965), and Horne and Medland (1966). In most cases an idealized moment-curvature relationship, as shown in Fig. 1-2, was assumed. However, a rigorous solution that takes strain hardening into account is at best a cumbersome and impractical approach.

A few authors (Alvarez and Birnstiel 1969) considered the effect of axial load on the stiffness of columns and girders. Others (Korn and Galambos 1968) developed stability functions for columns on the assumption that the axial forces in the girders were small enough to neglect their effect on girder stiffness. Parikh (1966) modified the column moment-curvature relationship to compensate for the decrease in bending stiffness due to the yielded condition of the cross section, for axial loads greater than $0.7 P_y$, where P_y represents the yield load of the column.

The influence of residual stresses was considered by Parikh (1966) and Alvarez and Birnstiel (1969). The latter formulated the member stiffness matrix so as to account for the gradual penetration of yielding, the presence of residual stresses, the spread of inelastic zones along the member length, and strain reversal in previously yielded fibers. However, their method was applicable only to relatively small structures.

Extensive experimental work has been performed to investigate the 'true' behavior of frames. Results of combined gravity and lateral loading tests on large scale multistory frames have been reported by Yura (1965), Yarimci (1966), and Majumdar *et al.* (1970). Schilling *et al.* (1956), and Arnold *et al.* (1968) performed some tests on single story steel frames.

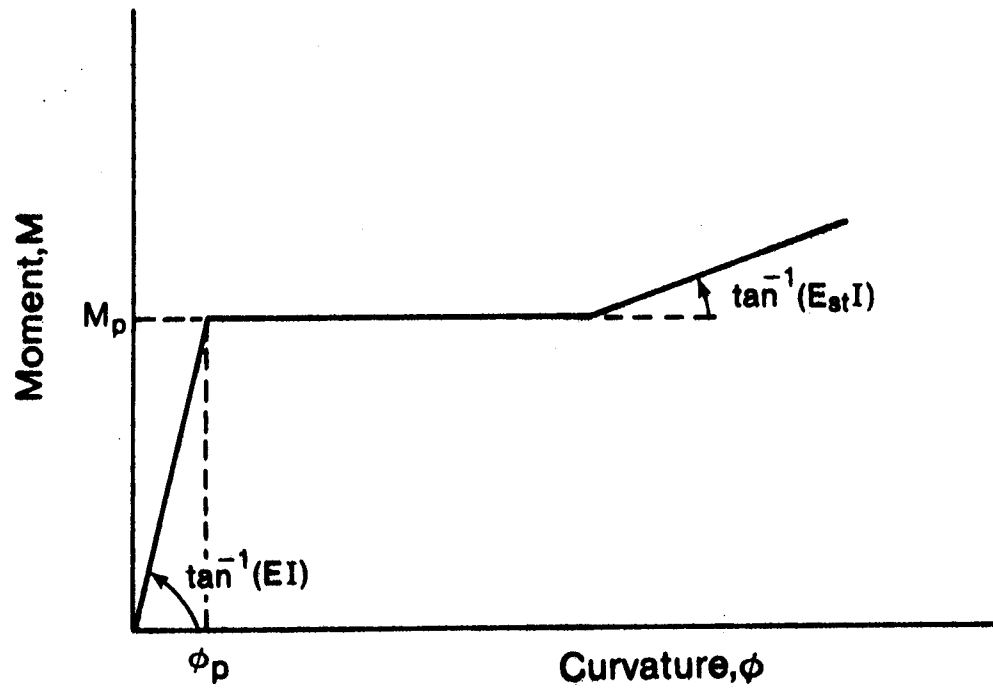


FIGURE 1-2 Idealized Moment-Curvature Relationship

1.3 Objective

The purpose of this investigation is to develop a nonlinear method of frame analysis, based on large deformation theory, that is applicable to both elastic and inelastic solutions of plane frame problems under any conditions of loading and geometry.

In the inelastic formulation the effect of axial loads on the stiffness of the structure is considered. Gradual penetration of yielding, the spread of inelastic zones along the member length, the presence of residual stresses, and strain hardening of the material are also accounted for.

Numerical solutions are obtained by developing a set of finite element equations applicable to stability problems. However, general purpose computer programs have been developed to solve a variety of problems. The most advanced of these can handle very complex nonlinear analyses, but does not require an excessive amount of computer time.

1.4 Outline of Contents

Chapter 2 reviews stability theory and discusses different types of formulation for stability and strength analyses.

Chapter 3 is divided into two parts. An elastic buckling formulation is presented in the first part, with a solution technique to determine the elastic critical load of frames. Numerical results for a variety of problems are compared with those obtained through classical techniques. The detailed derivation of the equations for this approach is carried out in Appendix A.

The second part of Chapter 3 presents the nonlinear formulation, based on large deformation theory. The equations are then specialized to elastic response, and a finite element model is developed for this case. A solution method to solve for the response of the frame using the finite element equations is discussed and a variety of problems are solved to determine the accuracy and efficiency of the proposed technique. The detailed derivation of the equations for this method is presented in Appendix B, with a large displacement transformation matrix derived in Appendix C.

Features of the elastic-plastic response of frames for first and second order analyses are presented in Chapter 4. Two techniques are discussed, namely, the incremental method and the iterative technique. The two methods and their results are compared with some published data.

The extension of the approach presented in part 2 of Chapter 3, to the case of inelastic response, is presented in Chapter 5. The finite element equations are formulated with respect to local reference axes through the original centroid. Some experimental results are compared with those obtained using the inelastic formulation. The detailed derivation of the section properties and stress resultants for an inelastic element is given in Appendix D, and details of the inelastic formulation are shown in Appendix E.

Chapter 6 illustrates a behavioral study for a number of frames subjected to combined vertical and lateral loads. Comparison is made between the inelastic and the elastic-plastic methods of analysis. The effects of residual stresses and strain hardening on the behavior of frames are also studied.

A summary of the investigation and the conclusions reached are presented in Chapter 7.

CHAPTER II

REVIEW OF STABILITY THEORY

2.1 Introduction

Knowledge of structural stability theory is of paramount importance to the practicing structural engineer. In many instances, buckling is a primary consideration in the design of various structural configurations. Because of this, and because the formulation for stability problems is more complex than for strength problems, few other fields within structural engineering have such a varied history as the theory of stability of metal structures (Bleich 1952).

This chapter presents a review of the basic concepts of stability. The various methods of analysis used in solving stability problems are discussed.

2.2 Introduction to Linearly Elastic Formulation

In elastic first order strength analysis two main assumptions are considered. The material of the structure is assumed to be linearly elastic, and the equilibrium equations are formulated on the undeformed shape of the structure. In elastic first order stability analysis the material is assumed to behave linearly elastic, but the formulation of the equilibrium equations must include the effect of displacements.

2.2.1 Bifurcation and Buckling

A structure is considered to be in a state of stable equilibrium when slight changes in loading do not produce disproportionate

distortions of the system. A load-displacement history such as the one shown in Fig. 2-1 is called an equilibrium path. Each point on the path represents an equilibrium configuration of the structure. In linear elastic analysis all equilibrium paths are straight lines that pass through the origin (Brush and Almroth 1975).

Consider a straight, simply supported column of length L , subject to a concentric applied compressive load, P , as illustrated in Fig. 2-2a. Under the assumptions of "small" deflections, v , and constant moment of inertia, I_x , the equilibrium equation of the elastic curve is given by Timoshenko and Gere (1961) as

$$EI_x \frac{d^2 v}{dz^2} + P v = 0 \quad (2.2.1)$$

Introducing the notation

$$k^2 = \frac{P}{EI_x} \quad (2.2.2)$$

Equation 2.2.1 can be written in the form

$$v'' + k^2 v = 0 \quad (2.2.3)$$

For constant k , this equation is a linear homogeneous differential equation the general solution of which is the homogeneous solution and can be written as

$$v = A \sin kz + B \cos kz \quad (2.2.4)$$

For simply supported ends the boundary condition equations are

$$v = 0 \quad \text{at} \quad z = 0 \quad (2.2.5a)$$

$$v = 0 \quad \text{at} \quad z = L \quad (2.2.5b)$$

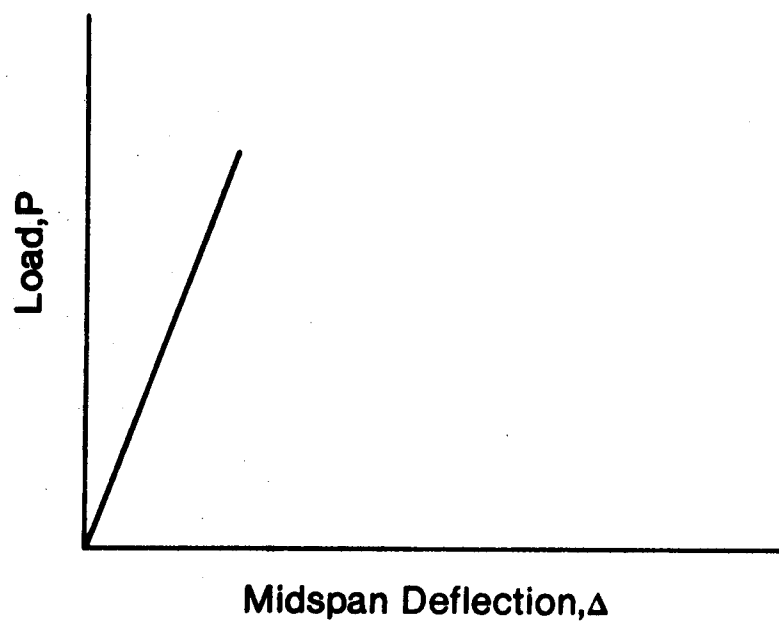
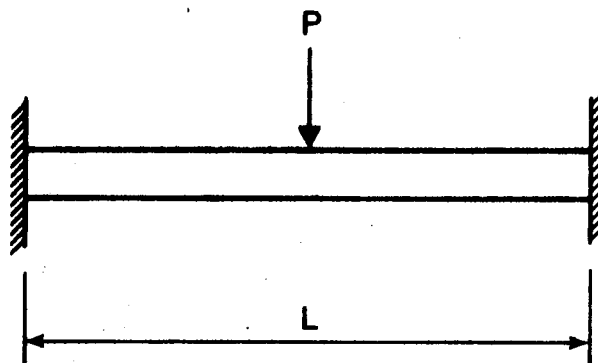
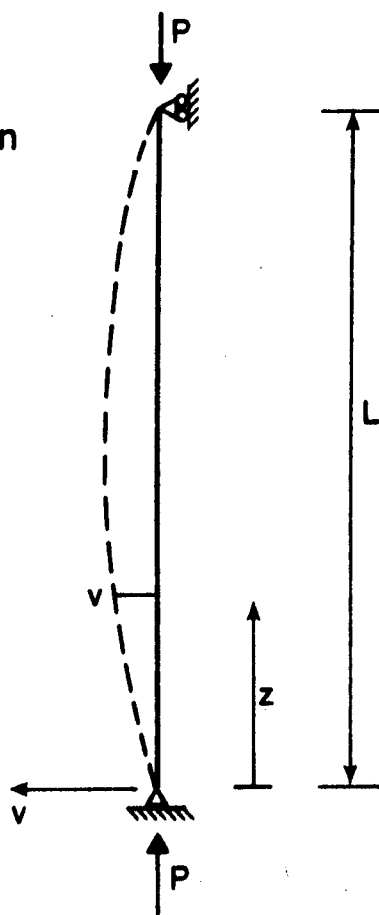


FIGURE 2-1 Load-Displacement Relation for Beam Clamped at Both Ends

(a) Euler Column



(b) Load-Deflection Relationship

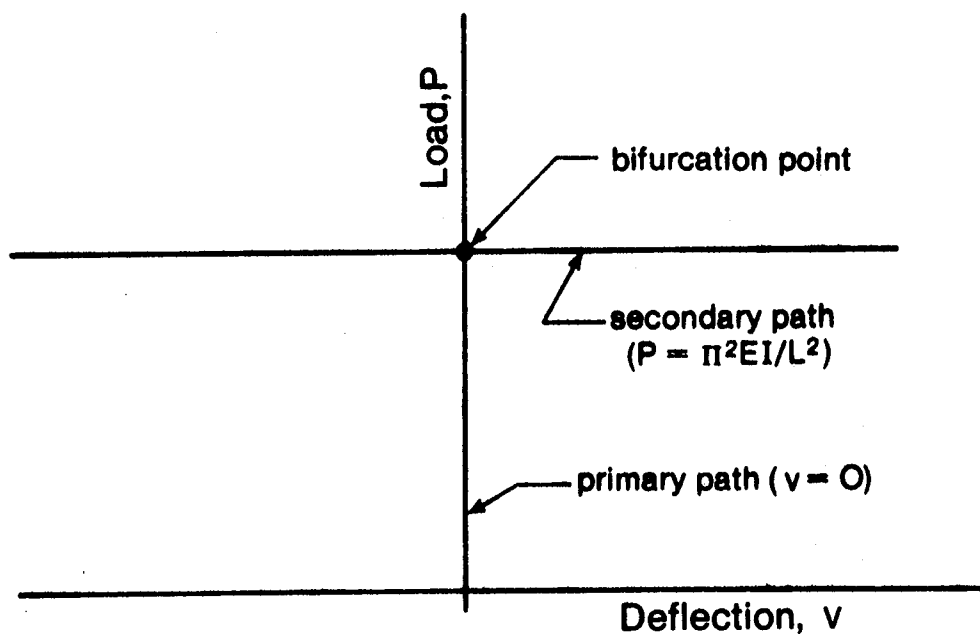


FIGURE 2-2 Equilibrium Paths for Initially Straight Column

Substituting condition 2.2.5a into Eq. 2.2.4 leads to $B = 0$.

Consequently

$$v = A \sin kz \quad (2.2.6)$$

From condition 2.2.5b one obtains

$$A \sin kL = 0 \quad (2.2.7)$$

Equation 2.2.7 can be satisfied in one of two ways, either

$$A = 0 \quad (2.2.8a)$$

or

$$\sin kL = 0 \quad (2.2.8b)$$

If $A = 0$, k and consequently P can have any value. But if $A \neq 0$, the displacement, v , of Eq. 2.2.6 is identically zero. This result is known as the trivial solution, in which a column is in equilibrium under any value of axial load, P , as long as the member remains perfectly straight.

There are an infinite number of values of k for which $\sin kL = 0$. These are

$$k_n L = n \pi \quad (2.2.9)$$

Substituting this expression into Eq. 2.2.2 gives the loads for which nontrivial solutions of Eq. 2.2.1 can be obtained as

$$P_n = \frac{n^2 \pi^2 EI_x}{L^2} \quad (2.2.10)$$

Problems of this type are called eigenvalue problems (Ziegler 1968). The values k_n or the corresponding loads P_n are called eigenvalues of the problem, and the corresponding displacements

$$v_n = A_n \sin \frac{n \pi z}{L} \quad (2.2.11)$$

are called eigenfunctions.

The only significant value of P arises from the lowest eigenvalue obtained by setting n equal to 1 and is known as the "Euler buckling load":

$$P_e = \frac{\pi^2 EI}{L^2} \quad (2.2.12)$$

Equilibrium paths for this column may be obtained by plotting P versus midspan deflection (v at $z = \frac{L}{2}$). Such a plot for $n = 1$ is shown in Fig. 2-2b. In this figure the primary equilibrium path (i.e. the trivial solution) is intersected by a secondary equilibrium path. The point at which equilibrium paths intersect is called a bifurcation point. At such a point the equilibrium equations have multiple solutions, one corresponding to each branch. This leads to the classical concept of bifurcation as a condition in which two (or more) adjacent equilibrium configurations exist at the same load.

In theory, the change in deformation that takes place when the structure passes from a point on the primary equilibrium path to a point on a secondary equilibrium path is generally known as buckling. For a linearly elastic stability formulation, buckling occurs at the bifurcation point. In general the load at which this happens is known as the critical load.

Bifurcation of rectilinear framed structures occurs only if the members remain straight during loading. Thus, if a column with an initial imperfection $v_0(z)$ is considered, as illustrated in Fig. 2-3a, the moment at any section along the column is

$$M = P (v + v_0) \quad (2.2.13)$$

and hence the differential equation of equilibrium takes the form

$$EI_x \frac{d^2v}{dz^2} + P (v + v_0) = 0 \quad (2.2.14)$$

Dividing by EI_x and using the notation of Eq. 2.2.2 leads to

$$v'' + k^2v = -k^2v_0 \quad (2.2.15)$$

For constant k , this equation is a linear inhomogeneous differential equation, and the solution consists of two parts. The first is the homogeneous solution, identical to Eq. 2.2.4, which can be obtained by setting the right hand side in Eq. 2.2.15 equal to zero. The second term is any particular solution which satisfies Eq. 2.2.15.

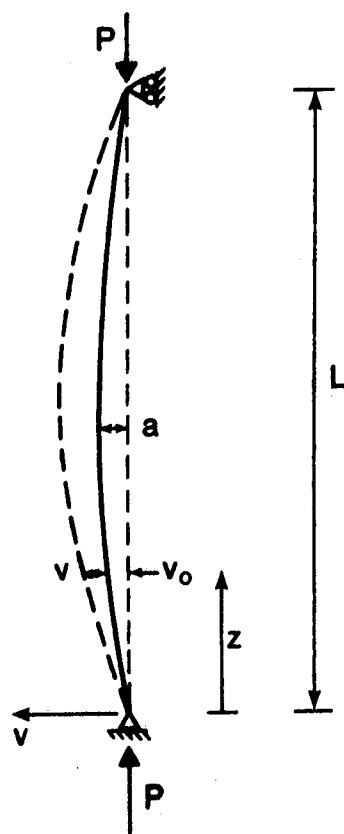
If the initial shape of the axis of the bar is assumed to be

$$v_0(z) = a \sin \frac{\pi z}{L} \quad (2.2.16)$$

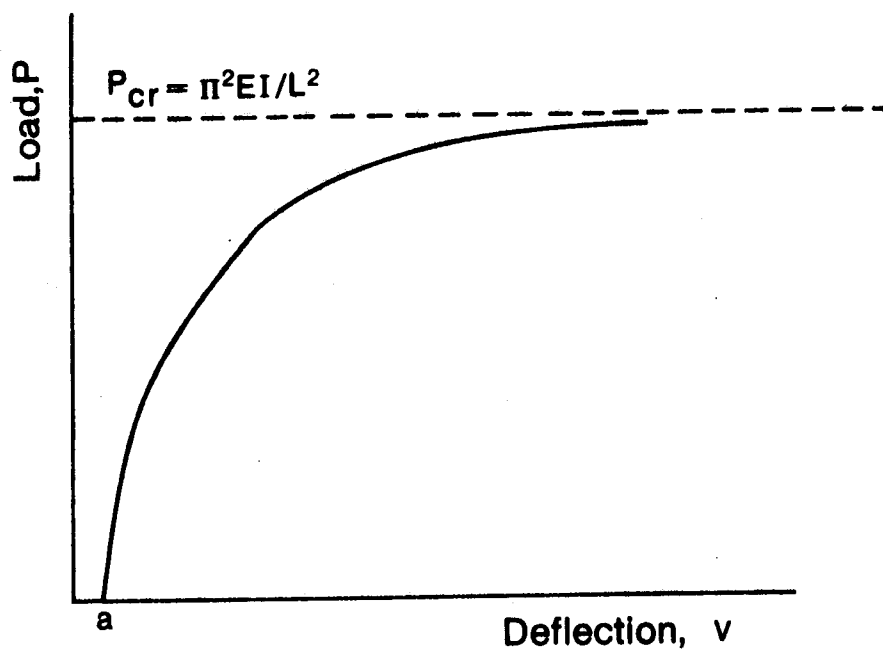
in which a is the initial midspan deflection, then Eq. 2.2.15 becomes

$$v'' + k^2v = -k^2 a \sin \frac{\pi z}{L} \quad (2.2.17)$$

and the general solution of this equation is (Timoshenko and Gere 1961)



(a) Imperfect Column



(b) Load-Deflection Curve

FIGURE 2-3 Load-Deflection Relation for Imperfect Column

$$v = A \sin kz + B \cos kz + \frac{1}{(\pi^2/k^2 L^2) - 1} a \sin \frac{\pi z}{L} \quad (2.2.18)$$

To satisfy the boundary conditions ($v = 0$ at $z = 0$ and $z = L$) for any value of k , A and B both must be equal to zero. If the ratio between the applied load and the critical load is defined as

$$\beta = \frac{P}{P_{cr}} = \frac{P}{\pi^2 EI/L^2} = \frac{k^2 L^2}{\pi^2} \quad (2.2.19)$$

then Eq. 2.2.18 becomes

$$v = \frac{\beta}{1 - \beta} a \sin \frac{\pi z}{L} \quad (2.2.20)$$

and the final ordinates of the deflected curve can be obtained by adding Eq. 2.2.16 to Eq. 2.2.20, which yields

$$v = \frac{a}{1 - \beta} \sin \frac{\pi z}{L} \quad (2.2.21)$$

The load-deflection curve for this imperfect column, as P varies, is nonlinear as shown in Fig. 2-3b. The deflection increases without limit as P approaches P_{cr} .

The solution to the homogeneous equation (Eq. 2.2.1) is unique and identically zero until the load reaches the critical load which corresponds to the lowest eigenvalue of the differential equation. At this point the magnitude of the deflection is undefined, because Eq. 2.2.7 is satisfied for arbitrary values of A . The solution to the inhomogeneous equation (Eq. 2.2.15) is unique and nontrivial, until the load reaches the critical load of the homogeneous problem, at which point it increases without limit. Therefore, for this type of problem,

the critical load of the homogeneous solution is adequate to determine the stability limit of the structure.

It should be noted that the above conclusion is valid for any arbitrary initial imperfection, since it can always be expanded in a Fourier series (Timoshenko and Gere 1961). The conclusion also remains valid for a column with transverse loads, since these simply lead to a different form of the inhomogeneous term in Eq. 2.2.15.

2.2.2 Linearly Elastic Formulation for Frames

The study of frame stability is associated with the determination of the buckling condition of a system of interconnected members as well as with the determination of the maximum capacity of such a system. Frame critical loads have been the subject of numerous investigations (Lu 1962), and many classical techniques are available for evaluating such critical loads (Bleich 1952). The following discussion attempts to place these methods in a general context.

The most fundamental method of determining critical loads for frames is a direct analytical solution. It is analogous to the solution of the buckling problem for a pin-ended column (see Sect. 2.2.1).

Equation 2.2.1 is valid only for pin-ended columns. If a column is fixed at both ends and loaded as shown in Fig. 2-4, the differential equation can be expressed as

$$EI \frac{d^2 v}{dz^2} = -M(z) \quad (2.2.22)$$

in which $M(z)$ is the moment at any point on the column, due to the end effects and the transverse loads. The boundary conditions influence $M(z)$ in an indeterminate manner. However, as shown by Timoshenko and

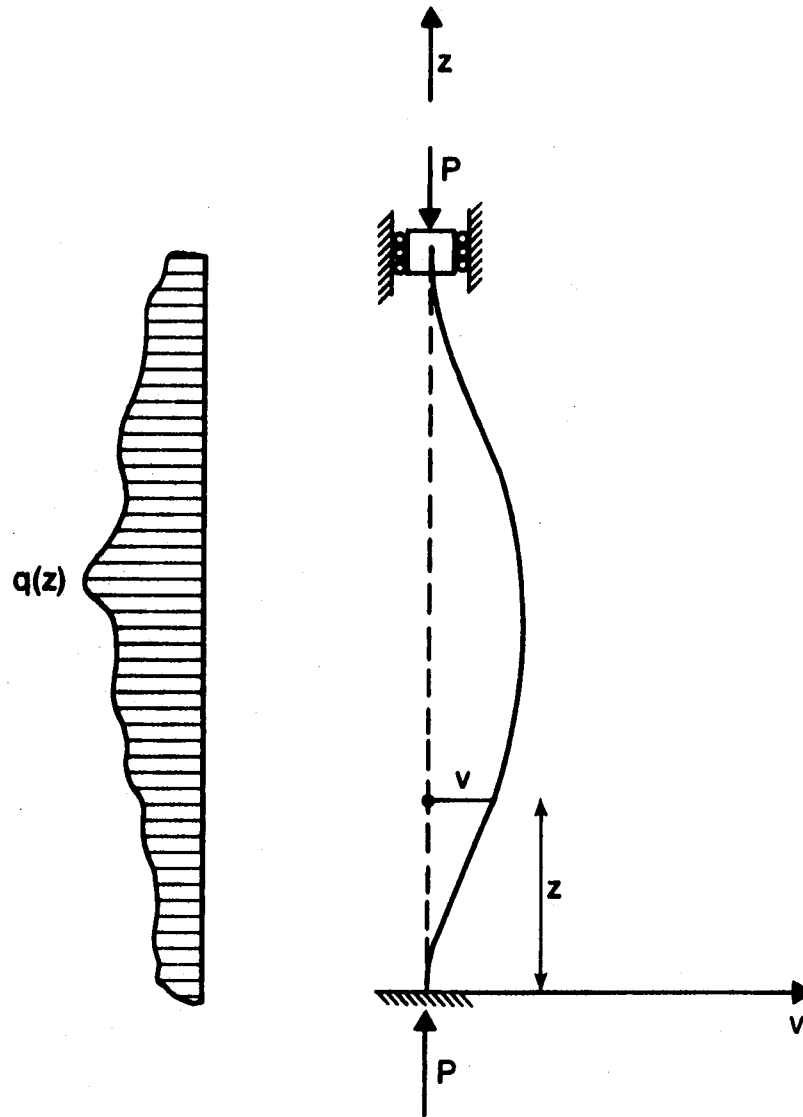


FIGURE 2-4 Fixed End Column

Gere (1961), a single fourth order equation, applicable to any prismatic column regardless of the boundary conditions, can be employed.

Differentiating Eq. 2.2.22 twice with respect to z yields

$$EI \frac{d^4 v}{dz^4} + P \frac{d^2 v}{dz^2} = q(z) \quad (2.2.23)$$

Dividing by EI , and using Eq. 2.2.2, leads to

$$\frac{d^4 v}{dz^4} + k^2 \frac{d^2 v}{dz^2} = \frac{1}{EI} q(z) \quad (2.2.24)$$

The general solution of Eq. 2.2.24 is

$$v = C_1 + C_2 z + C_3 \sin kz + C_4 \cos kz + v_p(z) \quad (2.2.25)$$

in which the integration constants C_1 , C_2 , C_3 , and C_4 are determined from the boundary conditions of the case under investigation.

In most structures the ends of the columns are neither hinged nor fixed. In frames the columns may be rigidly connected to the other members, which permits a limited amount of rotation to occur at the ends of the columns. Supports of this type are referred to as elastic restraints (Chajes 1974).

Both flexibility solutions and stiffness solutions of frame buckling problems can be obtained directly from the solution of the differential equation expressed by Eq. 2.2.25. All the classical elastic approaches which use stability functions, become special cases of this method. A general treatment of the problem may be carried out as follows.

Equation 2.2.25 may be written in matrix form as

$$v(z) = \langle \phi(z) \rangle \{C\} + v_p(z) \quad (2.2.26a)$$

in which

$$\langle \phi \rangle = \langle 1, z, \sin kz, \cos kz \rangle \quad (2.2.26b)$$

and

$$\{C\} = \langle C_1, C_2, C_3, C_4 \rangle^T \quad (2.2.26c)$$

Using Eqs. 2.2.26 to evaluate the transverse displacements and rotations at the ends of the member, and adopting the notation of Fig. 2-5a, yields

$$\begin{Bmatrix} \delta(0) \\ \theta(0) \\ \delta(L) \\ \theta(L) \end{Bmatrix} = \begin{Bmatrix} \langle \phi(0) \rangle \\ \langle \phi'(0) \rangle \\ \langle \phi(L) \rangle \\ \langle \phi'(L) \rangle \end{Bmatrix} \{C\} + \begin{Bmatrix} v_p(0) \\ v_p'(0) \\ v_p(L) \\ v_p'(L) \end{Bmatrix} \quad (2.2.27a)$$

which may be written, symbolically, as

$$\{\Delta\} = [G_1] \{C\} + \{\Delta_p\} \quad (2.2.27b)$$

Similarly, the end forces may be evaluated from Eqs. 2.2.26. Using the fundamental relations for moment and shear (Timoshenko and Gere 1961), the following expressions can be written

$$M = -EI v'' \quad (2.2.28a)$$

and

$$V = -EI v''' - P v' \quad (2.2.28b)$$

Adopting the notation of Fig. 2-5a, Eqs. 2.2.28 yield

$$\begin{Bmatrix} V(0) \\ M(0) \\ V(L) \\ M(L) \end{Bmatrix} = \begin{Bmatrix} EI \langle \phi'''(0) \rangle - P \langle \phi'(0) \rangle \\ -EI \langle \phi''(0) \rangle \\ -EI \langle \phi'''(L) \rangle - P \langle \phi'(L) \rangle \\ EI \langle \phi''(L) \rangle \end{Bmatrix} \{C\} + \begin{Bmatrix} EI v_p'''(0) - P v_p'(0) \\ -EI v_p''(0) \\ -EI v_p'''(L) - P v_p'(L) \\ EI v_p''(L) \end{Bmatrix} \quad (2.2.29a)$$

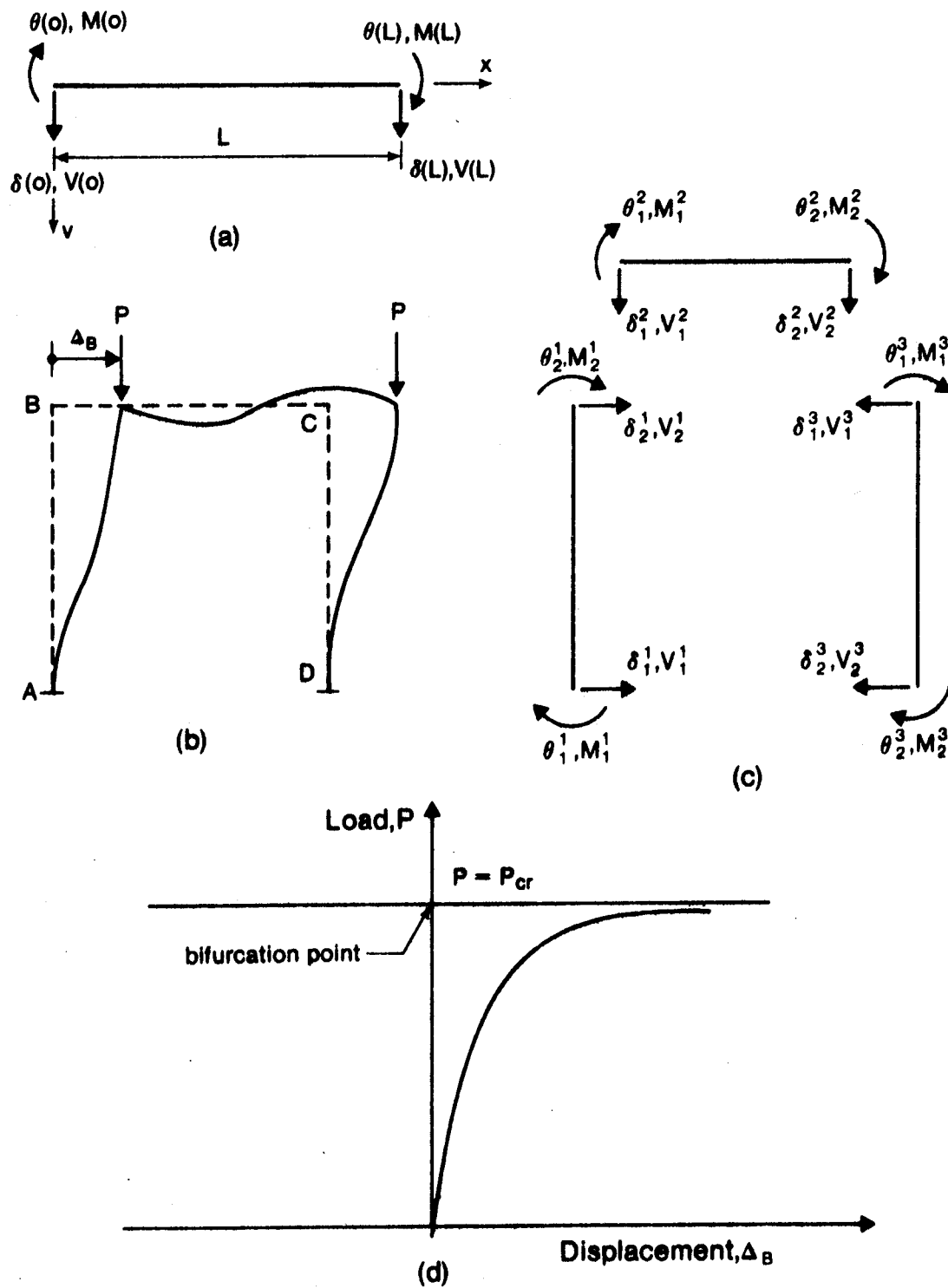


FIGURE 2-5 Behavior of Frames

Using the notation of Eq. 2.2.2 leads to

$$\begin{Bmatrix} V(0) \\ M(0) \\ V(L) \\ M(L) \end{Bmatrix} = EI \begin{bmatrix} \langle \phi'''(0) \rangle - k^2 \langle \phi'(0) \rangle \\ - \langle \phi''(0) \rangle \\ - \langle \phi'''(L) \rangle - k^2 \langle \phi'(L) \rangle \\ + \langle \phi''(L) \rangle \end{bmatrix} \{C\} + EI \begin{Bmatrix} v_p'''(0) - k^2 v_p'(0) \\ - v_p''(0) \\ - v_p'''(L) - k^2 v_p'(L) \\ v_p''(L) \end{Bmatrix} \quad (2.2.29b)$$

which may be written, symbolically, as

$$\{M\} = [G_2] \{C\} + \{M_p\} \quad (2.2.29c)$$

Equations 2.2.27 and 2.2.29 become the basis for the following developments.

2.2.2a Flexibility Approach

Solving Eq. 2.2.29c, for $\{C\}$, yields

$$\{C\} = [G_2]^{-1} \{M - M_p\} \quad (2.2.30)$$

Substituting this result into Eq. 2.2.27b yields

$$\{\Delta\} = [G_1][G_2]^{-1}\{M - M_p\} + \{\Delta_p\} \quad (2.2.31a)$$

or

$$\{\Delta\} = [\bar{F}] \{M - M_p\} + \{\Delta_p\} \quad (2.2.31b)$$

The matrix $[\bar{F}]$ in Eq. 2.2.31b is the (4x4) member flexibility matrix for the displacement coordinates and their associated forces (Murray *et al.* 1977), as indicated in Fig. 2-5a.

A classical flexibility analysis can now be carried out by arranging all the element vectors appearing in Eq. 2.2.31b sequentially into global vectors, and writing the result as

$$\{r\} = [F] \{R^*\} + \{r_p\} \quad (2.2.32)$$

For the frame illustrated in Fig. 2-5b and 2-5c the vector $\{r\}$ would appear as

$$\langle r \rangle = \langle \delta_1^1, \theta_1^1, \delta_2^1, \theta_2^1, \delta_1^2, \theta_1^2, \delta_2^2, \theta_2^2, \delta_1^3, \theta_1^3, \delta_2^3, \theta_2^3 \rangle \quad (2.2.33)$$

The vector $\{r_p\}$ is a similar array of particular solution displacements, whereas the vector $\{R^*\}$ is the associated array of end forces and moments, in which each component represents the difference between the total value and that associated with the particular solution. The matrix $[F]$ contains the element flexibility matrices of Eq. 2.2.31b on its principal diagonal.

Compatibility equations for the frame illustrated in Fig. 2-5b, are

$$\delta_1^1 - \theta_1^1 - \delta_1^2 = \delta_2^2 - \delta_2^3 - \theta_2^3 = 0 \quad (2.2.34)$$

$$\delta_2^1 + \delta_1^3 = 0 \quad (2.2.35a)$$

$$\theta_2^1 - \theta_1^2 = 0 \quad (2.2.35b)$$

$$\theta_2^2 - \theta_1^3 = 0 \quad (2.2.35c)$$

Equations 2.2.34 and 2.2.35 may be written as

$$[A] \{r\} = \{0\} \quad (2.2.36)$$

in which all elements of the compatibility matrix $[A]$ are either 0, 1 or -1. Substituting Eq. 2.2.32 into Eq. 2.2.36 yields

$$[A] \{F\} \{R^*\} = - [A] \{r_p\} \quad (2.2.37)$$

This compatibility equation cannot yet be solved for the indeterminate forces $\{R^*\}$, since there are only 9 equations but there are 12 unknowns.

To complete the solution, the left-hand side of Eq. 2.2.36 may be considered to define a set of relative displacements $\{q\}$, such that

$$\{q\} = [A] \{r\} \quad (2.2.38)$$

A set of generalized forces $\{Q^*\}$ may be associated with these relative displacements and, for work equivalence; it is necessary that (Przemieniecki 1968)

$$\{R^*\} = [A]^T \{Q^*\} \quad (2.2.39)$$

Substituting Eq. 2.2.39 into Eq. 2.2.37 yields

$$[A] \{F\} [A]^T \{Q^*\} = - [A] \{r_p\} \quad (2.2.40a)$$

which may be written symbolically as

$$[F] \{Q^*\} = - \{q_p\} \quad (2.2.40b)$$

Equation 2.2.40b is a set of compatibility equations which permit the solution for the generalized redundant forces $\{Q^*\}$, which restore continuity to the frame by counteracting the incompatibility

displacements $\{q_p\}$. The matrix $[F]$ is the flexibility matrix associated with these relative displacements.

For the condition where distributed loads are applied to the frame, the particular solution $v_p(z)$ of Eq. 2.2.25 is non-zero. Hence, $\{q_p\}$ of Eq. 2.2.40b is non-zero. For any value of distributed load and axial forces, Eq. 2.2.40b can be solved for $\{Q^*\}$; $\{R^*\}$ can be determined from Eq. 2.2.39; $\{c\}$ from Eq. 2.2.30, and hence the solution of Eq. 2.2.26a is known for each member. However, as

$$|| F || \rightarrow 0 \quad (2.2.41)$$

in which $|| F ||$ indicates the determinant of $[F]$, the redundants $\{Q^*\}$, and hence all displacements, increase without limit. Similarly, if all $v_p(z)$ are identically equal to zero, only the trivial solution is possible until

$$|| F || = 0 \quad (2.2.42)$$

at which time the eigenvectors of the homogeneous form of Eq. 2.2.40b can be determined, and forces and the associated displacements of arbitrary magnitude may exist. Thus, a bifurcation solution of the homogeneous problem and unbounded solutions of the inhomogeneous problem arise in the same manner as for a simple column, and permit the same interpretation, as illustrated in Fig. 2-5d.

The above technique is a general approach and has been used for simple structures. Normally an analyst imposes the boundary conditions of Eq. 2.2.34 on the differential equations prior to writing the intermember compatibility conditions of Eq. 2.2.35

(Timoshenko and Gere 1961). This reduces the size of the flexibility matrix in the illustrative problem from 9×9 to 3×3 . In non-computerized analysis this could reduce the problem from an intractable solution to a tractable one. However, determining critical loads by the flexibility method is still formidable. It is necessary to assume or calculate the value of the axial force in each member, in order to determine the values of k in the general solution, Eq. 2.2.25. It may then be assumed that these axial forces, and hence the k -values of the members, are proportional to the applied loads. If the load factor from the reference load is denoted by λ , the stability condition (Eq. 2.2.42) becomes a transcendental function of λ . It is necessary to find the smallest root, λ_{cr} , of this 'characteristic' equation.

The most practical method of doing this is by trial and error, and this is called the 'determinant search' technique. Values of λ are assumed, and $\|F\|$ is evaluated for each assumed value. By plotting, or interpolating between pairs of values, the value of λ_{cr} can be determined (Bleich 1952).

2.2.2b Stiffness Approach

A classical stiffness formulation, exactly parallel to the flexibility formulation, may be derived as follows. For a stiffness formulation Eq. 2.2.27b, instead of Eq. 2.2.29c, is solved for $\{C\}$, to yield

$$\{C\} = [G_1]^{-1} \{\Delta - \Delta_p\} \quad (2.2.43)$$

Substitution into Eq. 2.2.29c, yields

$$\{M\} = [G_2] [G_1]^{-1} \{\Delta - \Delta_p\} + \{M_p\} \quad (2.2.44a)$$

which may be written symbolically as

$$\{M\} = [k] \{\Delta - \Delta_p\} + \{M_p\} \quad (2.2.44b)$$

in which the matrix $[k]$ is the (4×4) member stiffness matrix, expressing the member end forces of Fig. 2-5a in terms of the corresponding displacements.

Arranging the element vectors appearing in Eq. 2.2.44b sequentially into global vectors, Eq. 2.2.44b for all members may be combined into the single matrix equation

$$\{R\} = [K] \{r^*\} + \{R_p\} \quad (2.2.45)$$

For the frame illustrated in Figs. 2-5b and 2-5c the vector $\{R\}$ would be

$$\langle R \rangle = \langle V_1^1, M_1^1, V_2^1, M_2^1, V_1^2, M_1^2, V_2^2, M_2^2, V_1^3, M_1^3, V_2^3, M_2^3 \rangle \quad (2.2.46)$$

The vector $\{R_p\}$ is a similar array of particular solution end forces, and the vector $\{r^*\}$ is the corresponding array of end displacements, where each term represents the difference between the total value and the particular solution value of the variable. The matrix $[k]$ contains the element stiffness matrices of Eq. 2.2.44b on its principal diagonal.

Equilibrium equations may now be written which, for the frame of Fig. 2-5b, are

$$M_1^1 + M_2^1 + v_2^1 \cdot L_1 = 0 \quad (2.2.47a)$$

$$M_1^2 + M_2^2 + v_2^2 \cdot L_2 = 0 \quad (2.2.47b)$$

$$M_1^3 + M_2^3 + v_2^3 \cdot L_1 = 0 \quad (2.2.47c)$$

$$v_2^1 + v_1^1 = 0, \quad v_1^2 + v_2^2 = 0, \quad v_1^3 + v_2^3 = 0 \quad (2.2.47d)$$

$$M_2^1 + M_1^2 = 0, \quad M_2^2 + M_1^3 = 0, \quad v_1^1 - v_2^3 = 0 \quad (2.2.47e)$$

Equations 2.2.47 may be expressed symbolically as

$$[\bar{A}] \{R\} = \{0\} \quad (2.2.48)$$

in which the elements of the equilibrium matrix $[\bar{A}]$ are either 0, 1, or -1.

Substituting Eq. 2.2.45 into Eq. 2.2.48 yields

$$[\bar{A}] [K] \{r^*\} = -[\bar{A}] \{R_p\} \quad (2.2.49)$$

Since Eq. 2.2.49 contains only 9 equations, and there are 12 unknowns in $\{r^*\}$, it cannot be solved directly. However, Eq. 2.2.48 can be considered to define a set of unbalanced forces $\{Q\}$, such that

$$\{Q\} = [\bar{A}] \{R\} \quad (2.2.50)$$

for which the associated work equivalent set of generalized relative displacements $\{q^*\}$ are related to the displacements $\{r^*\}$ by the equation

$$\{r^*\} = [\bar{A}]^T \{q^*\} \quad (2.2.51)$$

Substituting Eq. 2.2.51 into Eq. 2.2.49 yields

$$[\bar{A}] [K] [\bar{A}]^T \{q^*\} = -[\bar{A}] \{R_p\} \quad (2.2.52a)$$

which may be written symbolically as

$$[K] \{q^*\} = - \{Q_p\} \quad (2.2.52b)$$

Equations 2.2.52 are a set of equilibrium equations that permit the evaluation of the generalized displacements $\{q^*\}$ which establish equilibrium between members of the frame. The matrix $[K]$ is the stiffness matrix associated with the generalized displacements. For any distributed loading and axial forces, the particular solution forces and the vector $\{Q_p\}$ may be formed. Similarly, the matrix $[K]$ may be constructed. Once $\{q^*\}$ has been determined from Eq. 2.2.52b, $\{r^*\}$ may be determined from Eq. 2.2.51 and all member end forces from Eq. 2.2.45.

The stability condition is determined in the same manner as was done for the flexibility formulation of Sect. 2.2.2a. A unique set of finite displacements arises from the solution of the equilibrium equations (Eq. 2.2.52b). However, as axial forces increase and

$$\| K \| \rightarrow 0 \quad (2.2.53)$$

displacements increase without limit. For the homogeneous case, the solution to Eq. 2.2.52b is the trivial solution unless

$$\| K \| = 0 \quad (2.2.54)$$

in which case nontrivial eigenvectors of arbitrary magnitude exist as solutions. The interpretation of these solutions is, again, as illustrated in Fig. 2-5d. The determination of the critical load can be accomplished by a determinant search technique as discussed in Sect. 2.2.2a.

The above stiffness technique represents a general approach. It has been widely used in the more conventional form of the slope-deflection technique or the moment distribution procedure. The element slope-deflection matrix arises directly from Eq. 2.2.44b, as shown in the following:

Equation 2.2.44b can be written as

$$\{M\} = [k] \{\Delta\} + \{M_p\} - [k] \{\Delta_p\} \quad (2.2.55)$$

For zero member displacements the total forces, called the fixed end forces and denoted by $\{M^F\}$, are obtained from Eq. 2.2.55 as

$$\{M^F\} = \{M_p\} - [k] \{\Delta_p\} \quad (2.2.56)$$

Consequently Eq. 2.2.55 may be written as

$$\{M\} = [k] \{\Delta\} + \{M^F\} \quad (2.2.57)$$

In the slope-deflection method, only the end moments are selected from the vector $\{M\}$, to yield

$$\begin{Bmatrix} M_1 \\ M_2 \end{Bmatrix} = \begin{bmatrix} < k >_1 \\ < k >_2 \end{bmatrix} \{\Delta\} + \begin{Bmatrix} M_1^F \\ M_2^F \end{Bmatrix} \quad (2.2.58)$$

in which $<k>_i$ is the i th row of the matrix $[k]$. Recognizing that the coefficients of δ_1 and δ_2 in these rows are numerically the same but opposite in sign permits Eq. 2.2.58 to be written as

$$\begin{Bmatrix} M_1 \\ M_2 \end{Bmatrix} = \begin{bmatrix} S & C & -(C + S) \\ C & S & -(C + S) \end{bmatrix} \begin{Bmatrix} \theta_1 \\ \theta_2 \\ \frac{\delta_2 - \delta_1}{L} \end{Bmatrix} + \begin{Bmatrix} M_1^F \\ M_2^F \end{Bmatrix} \quad (2.2.59)$$

in which C and S are the standard stability functions (Galambos 1968).

Assembly of Eq. 2.2.59 into the equilibrium equations Eq. 2.2.47 by a standard slope deflection technique gives Eq. 2.2.52b, and the solution procedure then follows as described above. Thus, the magnitude of the axial forces which satisfy Eq. 2.2.54 are sought by a determinant search technique.

Equation 2.2.59 is also the starting point for a moment distribution search for critical loads (Hoff 1941). In this technique the magnitudes of the axial forces are assumed and the stiffnesses, S , and carry-over factors, C , are evaluated. Distribution factors are computed with these. At the critical load the moment distribution process diverges, leading to end forces and displacements which become arbitrarily large (Winter *et al.* 1948). This is, in effect, a test that Eq. 2.2.54 has been satisfied.

2.3 Elastic Nonlinear Formulation

An elastic nonlinear formulation may be carried out to determine the behavior of the structure after the deflections are large enough to cause significant changes in the geometry. This phenomenon is referred to as geometric nonlinearity. To account for the effects of changes in the geometry as the applied loading is increased, an exact expression for the curvature must be used.

In Sect. 2.2.1 the deflection of a column was found to be indeterminate at the critical load. This is strictly correct only as long as the deflection remains "small" and may be better understood by recognizing that the governing equation, Eq. 2.2.1, is based on the approximate expression for the curvature of the buckled column $\frac{d^2v}{dz^2}$. If the exact expression is used, the solution will not exhibit indefiniteness in the value of the deflection. The shape of the elastic curve of a simple column, when developed on the basis of the "exact" differential equation, is called the 'elastica'.

2.3.1 Large-Deformation Formulation For Columns (The Elastica)

To obtain a solution for the 'elastica', consider the simply supported column shown in Fig. 2-6a. Except for the now invalid assumption of "small" deflections, all idealizations are the same as those of the Euler column. If the y-z coordinate system is taken as shown in Fig. 2-6a, and the column is in equilibrium in a bent configuration, then the moment (Pv) at any section is equal to the resisting moment ($-EI\phi$). Thus,

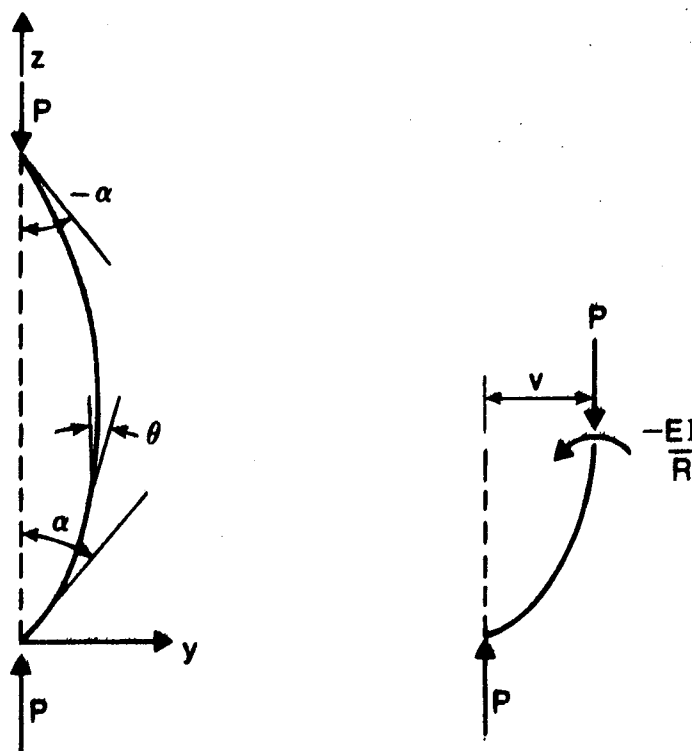
$$-EI\phi = Pv \quad (2.3.1)$$

in which ϕ is the angle change per unit length. If the slope is given by θ , and the distance along the curve from the origin to the point is s , then

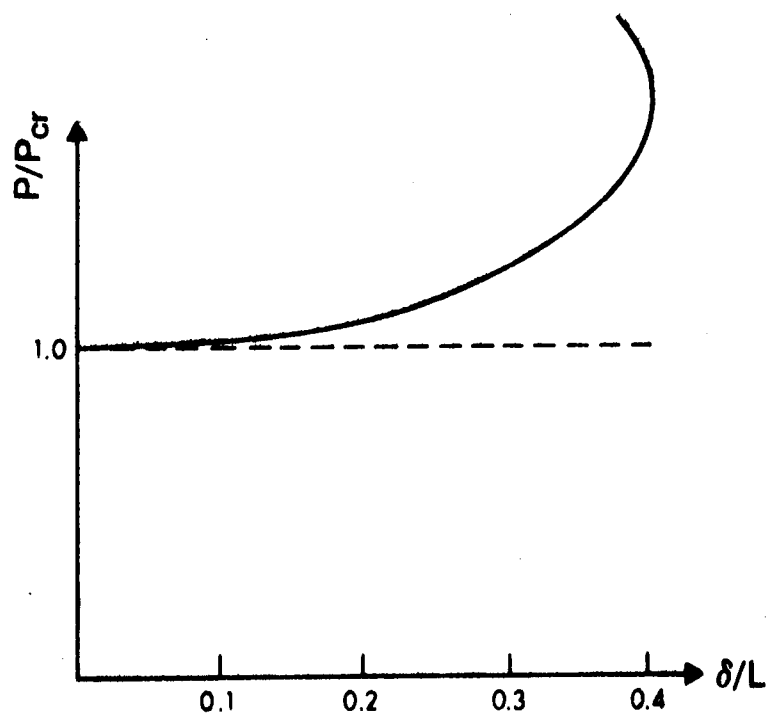
$$\phi = \frac{d\theta}{ds} \quad (2.3.2)$$

Substituting this expression into Eq. 2.3.1 leads to

$$EI \frac{d\theta}{ds} + Pv = 0 \quad (2.3.3a)$$



(a) Large Deflections of a Column



(b) Load-Deformation Curve

FIGURE 2-6 Column Behavior for Large Deflections

or

$$\frac{d\theta}{ds} + k^2 v = 0 \quad (2.3.3b)$$

Differentiating Eq. 2.2.3b with respect to s and replacing $\frac{dv}{ds}$ by $\sin\theta$, yields

$$\frac{d^2\theta}{ds^2} + k^2 \sin\theta = 0 \quad (2.3.4)$$

which is a nonlinear differential equation in θ .

Multiplying Eq. 2.3.4 by $(2 d\theta)$ and integrating gives

$$\left(\frac{d\theta}{ds}\right)^2 - 2 k^2 \cos\theta = C \quad (2.3.5)$$

The integration constant, C , is evaluated from the boundary conditions of Fig. 2-6a, namely,

$$\theta = \alpha \text{ and } \frac{d\theta}{ds} = 0 \text{ at } z = 0 \quad (2.3.6)$$

Hence

$$C = -2 k^2 \cos\alpha \quad (2.3.7)$$

and Eq. 2.3.5 becomes

$$\left(\frac{d\theta}{ds}\right)^2 = 2 k^2 (\cos\theta - \cos\alpha) \quad (2.3.8)$$

or

$$\frac{d\theta}{ds} = \pm k \sqrt{2} \sqrt{\cos\theta - \cos\alpha} \quad (2.3.9)$$

Solving for ds gives

$$ds = - \frac{d\theta}{k \sqrt{2} \sqrt{\cos\theta - \cos\alpha}} \quad (2.3.10)$$

in which the positive sign has been dropped because θ always decreases as s increases.

The total length of the column is obtained from

$$L = \int_0^L ds = - \int_{+\alpha}^{-\alpha} \frac{d\theta}{k \sqrt{2} \sqrt{\cos\theta - \cos\alpha}} \quad (2.3.11)$$

Equation 2.3.11 may be written as (Timoshenko and Gere 1961)

$$L = \frac{2K}{\sqrt{P/EI}} \quad (2.3.12)$$

in which

$$K = \int_{-\alpha}^{+\alpha} \frac{d\theta}{4 \sqrt{\sin^2 \frac{\alpha}{2} - \sin^2 \frac{\theta}{2}}} \quad (2.3.13)$$

is a complete elliptic integral of the first kind, which is tabulated in mathematical handbooks (Jahnke and Emde 1945).

Solving Eq. 2.3.12 for P yields

$$\frac{P}{P_{cr}} = \frac{4K^2}{\pi^2} \quad (2.3.14)$$

in which $P_{cr} = \pi^2 EI / L^2$

If the deflection of the member is very small the value of K approaches $\frac{\pi}{2}$. Equation 2.3.14 then becomes

$$P = P_{cr} = \frac{\pi^2 EI}{L^2} \quad (2.3.15)$$

The nonlinear theory thus leads to the same critical load as the linear theory.

The load-deformation characteristic of the column can be obtained as follows.

Noting that $dv = \sin\theta \, ds$, and making use of Eq. 2.3.10, gives

$$dv = - \frac{\sin\theta \, d\theta}{k \sqrt{2} \sqrt{\cos\theta - \cos\alpha}} \quad (2.3.16)$$

The midheight deflection, δ , is obtained as

$$\delta = - \int_{\delta}^0 dv = \int_0^{\alpha} \frac{\sin\theta \, d\theta}{k \sqrt{2} \sqrt{\cos\theta - \cos\alpha}} \quad (2.3.17)$$

from which it can be shown that (Timoshenko and Gere 1961)

$$\frac{\delta}{L} = \frac{2 \sin \alpha/2}{\pi \sqrt{P/P_{cr}}} \quad (2.3.18)$$

Using Eqs. 2.3.14 and 2.3.18 it is possible to compute for various values of α the corresponding values of P/P_{cr} and δ/L . The load-deformation characteristic is shown in Fig. 2-6b. Comparison

between this figure and Fig. 2-2b shows that large deformation theory leads to the same critical load as linear theory, but predicts a very slight increase in load with increasing deflection above the critical load. The increase in load becomes pronounced only after considerable deformation has taken place. This indicates that the prediction of bending at constant load, as implied by the linear theory, is a good approximation for a considerable range of deformations.

2.3.2 Elastic Nonlinear Analysis of Frames

In a structural framework made from a linearly elastic material, nonlinearity arises when the effect of the deformations on the equilibrium equations is considered.

In Sect. 2.2.2 an approximate expression for the curvature was used, and the axial force in each column was assumed to remain constant during buckling. These assumptions result in a linear formulation of the problem. The classical solutions, as presented in Sect. 2.2.2, may be modified to account for geometric nonlinearity. In this case an exact expression for the curvature is used, resulting in an 'exact' differential equation (See Sect. 2.3.1). The axial force also may be assumed to be changing in each column during buckling. A modified classical formulation, however, would not be easy to solve. A few authors have considered the nonlinear strain-displacement relationship (Turner *et al.* 1960; Martin 1965), and many others have incorporated the effect of joint displacement on the overall behavior of the structure (Nair 1975).

An approximate method of analysis for elastic nonlinear problems has been described by Adams (1972). The effect of joint

displacements on the overall behavior of a multistory frame is accounted for by modifying the results of a standard (linear formulation) analysis. The method is usually referred to as the P- Δ method, and the secondary effects as the P- Δ effects.

The mechanics of the P- Δ method can be described as follows, using Fig. 2-7 (Johnston 1976).

- 1 - The loads are applied to the frame, and the lateral displacements Δ_i due to primary moments are computed.
- 2 - The additional story shears that are caused by the displaced vertical loads are calculated as

$$V'_i = \frac{\Sigma P_i}{h_i} (\Delta_{i+1} - \Delta_i) \quad (2.3.19)$$

in which V'_i is the additional shear in story i due to the sway forces, ΣP_i is the sum of the column axial loads in story i , h_i is the height of story i , and Δ_{i+1} and Δ_i are the lateral displacements of the frame at levels $i+1$ and i , respectively.

- 3 - The fictitious sway forces, H'_i , are computed at each floor level as

$$H'_i = V'_{i-1} - V'_i \quad (2.3.20)$$

- 4 - The sway forces, H'_i , are added to the applied loads and a new linear analysis is performed.
- 5 - When the deflected shape remains unchanged from one iteration cycle to the next, the solution has converged, and the resulting forces now include the secondary moments.

In practical applications the convergence is fast, and the first iteration produces acceptable results (Springfield and Adams

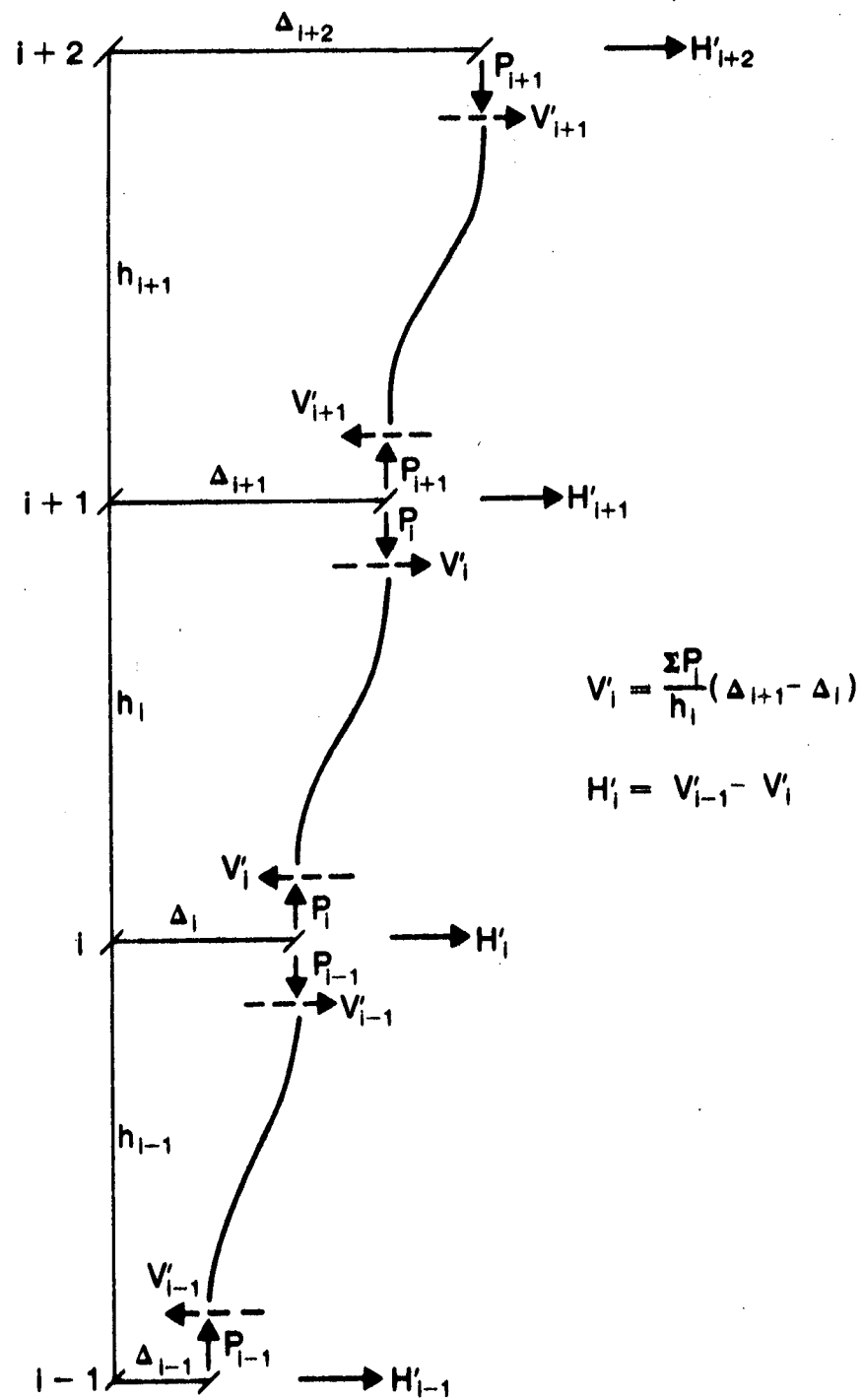


FIGURE 2-7 Sway Forces Due to Vertical Loads

1972). Slow convergence is a sign that the structure is excessively flexible, and lack of convergence indicates that the structure is unstable (Wood *et al.* 1976).

2.4 Inelastic First Order Stability Theory

Early tests of steel columns of practical proportions showed that failure occurred at loads less than the Euler load. The difference can be attributed to the assumptions made in deriving the Euler load. In each of the preceding sections it has been assumed that the material behaves linearly elastic, but in order for this to be valid, the total stresses in the member must remain below the proportional limit of the material. However, in most columns the elastic limit is exceeded before the load reaches the Euler load. The results of the elastic analysis therefore are not valid and the buckling load must be determined by taking inelastic behavior into account.

2.4.1 Tangent Modulus Theory

Engesser (1889) suggested that if column failure occurred at a stress above the proportional limit of the material, the column strength could be obtained by simply replacing E by E_t , the tangent modulus, in the Euler formula (Eq. 2.2.12). The slope of the tangent to the stress-strain curve of the material at any point A is E_t , as shown in Fig. 2-8. That is

$$E_t = \frac{d\sigma}{d\epsilon} \quad (2.4.1)$$

To justify the substitution of E_t instead of E , it is assumed that the column remains straight and that the stress-strain

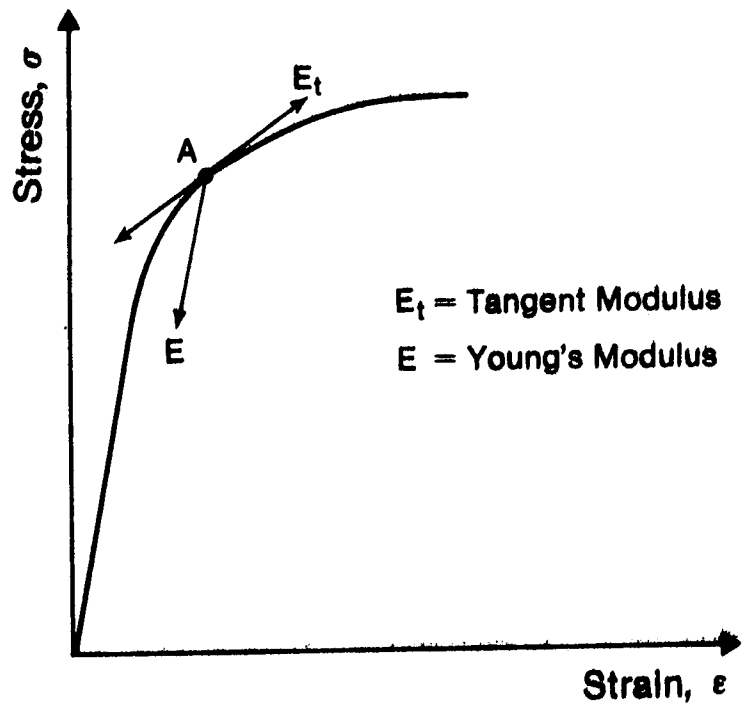


FIGURE 2-8 General Stress Strain Relationship

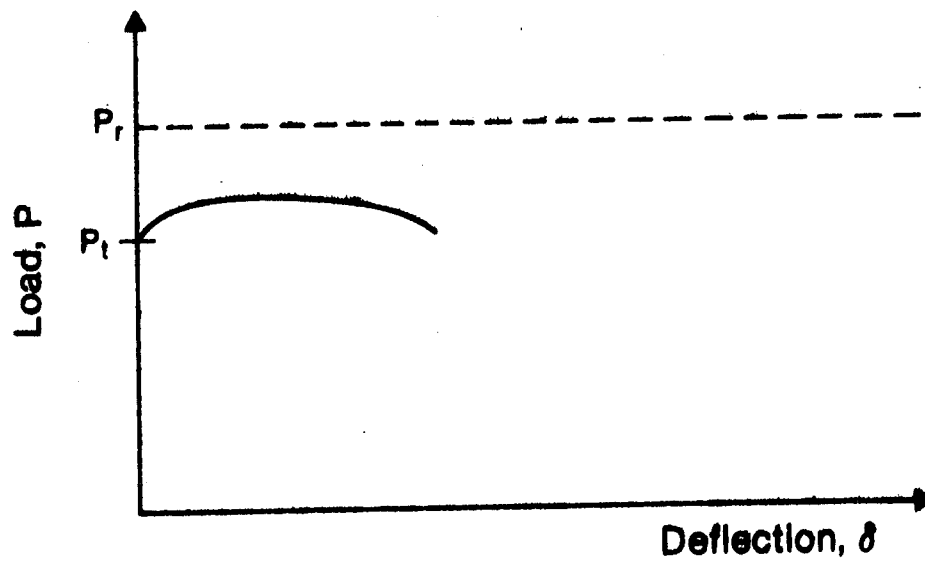


FIGURE 2-9 Load-Deflection Curve of Shanley's Model

characteristics are the same throughout the length of the member. Thus, the average stress at the tangent modulus load for a short column, such as the one shown in Fig. 2-2a, is

$$\sigma_{cr} = \frac{\pi^2 E_t}{(L/r)^2} \quad (2.4.2)$$

2.4.2 Reduced Modulus Theory

When a column begins to bend at the critical load, there is a possibility that stresses on the convex side decrease. Referring to Fig. 2-8, any incremental decrease in the compressive strain from point A involves a decrease in stress equal to $(\Delta\epsilon)E$, whereas an incremental increase in the strain involves an increase in stress equal to $(\Delta\epsilon)E_t$. This line of reasoning is the basis for the reduced modulus theory, or as it is sometimes called, the double modulus theory.

Based on the above reasoning, Engesser (1895) realized the theoretical contradictions inherent in the tangent modulus theory, and suggested the use of a reduced modulus, E_r , for E in the Euler formula. The magnitude of E_r lies between those of E and E_t . The expression for E_r and the position of the axis of bending at critical load are determined so as to satisfy the traditional buckling concept that the load remains constant during buckling.

Von Karman (1910) revised the theory, and determined the expressions for the reduced modulus for a rectangular cross section and for the idealized I-section. His subsequent experimental work showed that the actual buckling loads were closer to the tangent modulus values than to the reduced modulus values. In contradiction

to the understanding of column behavior at that time, this problem was not resolved for another 35 years.

2.4.3 Shanley's Contribution

Shanley (1947) resolved the apparent contradiction between theory and tests through a revised tangent modulus model. He demonstrated that upon reaching the tangent modulus load, P_t , there is nothing to prevent the column from bending and at the same time support an increasing axial load.

Figure 2-9 illustrates the load-deflection curve according to Shanley's model. He concluded that the column load may exceed the tangent modulus load, but cannot be greater than the reduced modulus load, P_r . Shanley also noted that the tangent modulus theory predicts more accurately the maximum load that an inelastic column may support.

2.4.4 Inelastic Behavior of Beam-Columns

Inelastic action must be considered in the determination of the ultimate strength of a beam-column. The behavior of beam-columns is different from the behavior of either columns or beams. The term defines a member subjected to axial load as well as bending moment. A set of tests was performed by Ketter *et al.* (1955) on W8 x 31 beam-columns loaded up to failure. The results showed that the fully plastic moment capacity of a beam-column cannot be reached. The study concluded that the maximum moment capacity of members is a function of the axial force as well as the moment applied to the member.

Galambos and Ketter (1961) presented theoretical ultimate strength interaction curves for beam-columns with various end

conditions, correlating the analysis with earlier tests by Mason *et al.* (1958). One set of such curves is shown in Fig. 2-10, representing strong axis bending of a W8 x 31, subjected to equal end moments. The curves are a reasonable approximation for most typical wide-flange sections. The validity of such interaction curves has been verified by extensive experiments (Van Kuren and Galambos 1964), and the correlation between tests and theory is good.

The strength of members subjected to bending moments and axial loads can be approximated by interaction formulas in terms of the ratios P/P_u and M_o/M_u as

$$\frac{P}{P_u} + \frac{C_m M_o}{M_u (1 - P/P_e)} \leq 1.0 \quad (2.4.3)$$

in which P is the axial load at failure, P_u is the ultimate load for a concentrically loaded pin-ended column, M_o is the maximum applied moment (not including second order effects), and M_u is the ultimate moment capacity in the absence of axial load. The coefficient C_m is the equivalent moment factor that accounts for unequal end moments, and P_e is the elastic critical load for buckling in the plane of the applied moments. The term $1/(1 - P/P_e)$ in Eq. 2.4.3 is the amplification factor, covering the effect of the axial load acting on the deflected column.

Equation 2.4.3 is based on failure of the beam-column due to instability. It approximates the experimental interaction curves, and is the basis for the Canadian Standards Association Specification (CSA 1974).

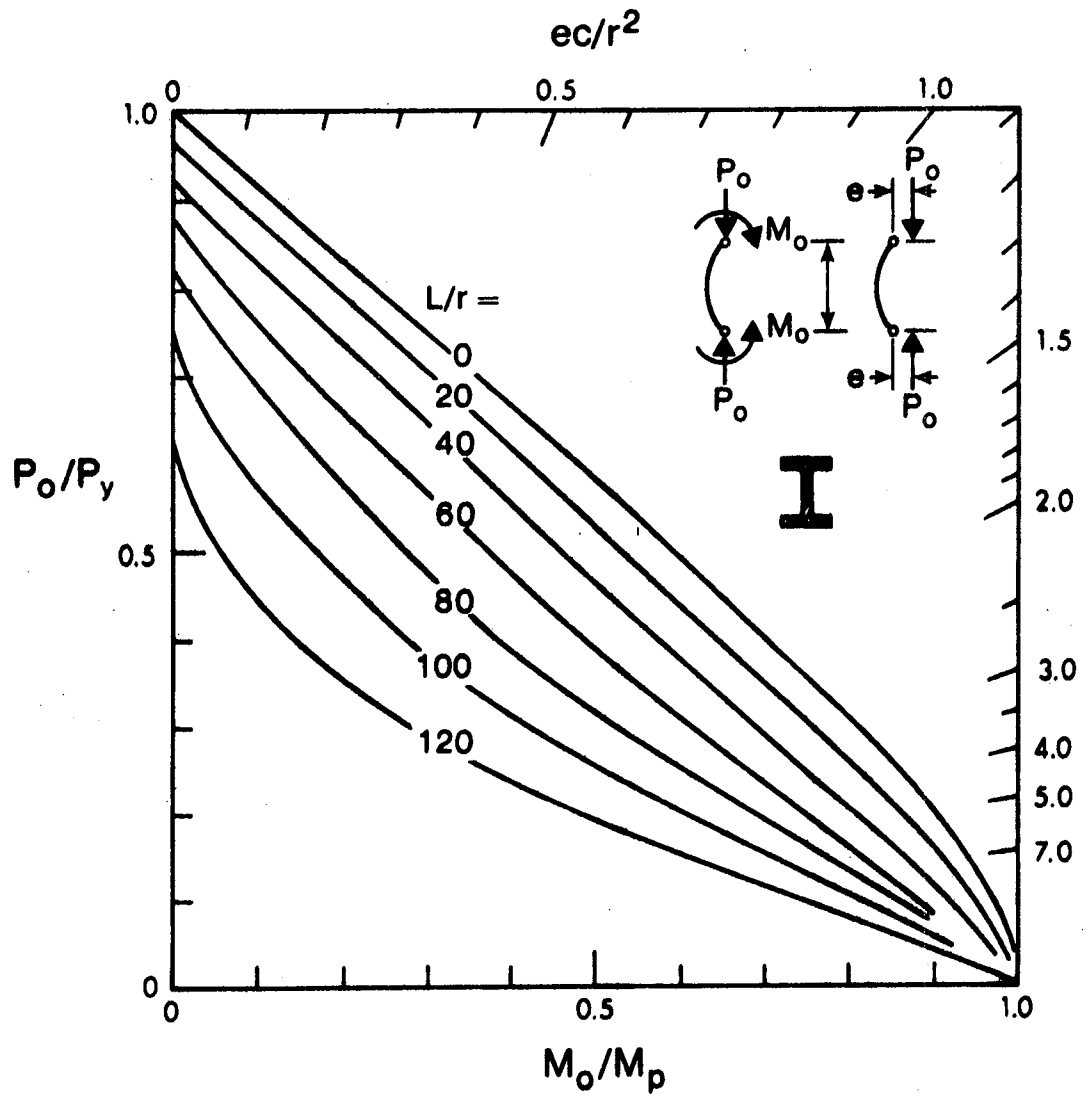


FIGURE 2-10 Maximum Carrying Capacity Interaction Curves

2.4.5 Simple Plastic Analysis

The objective of the plastic methods of analysis is to predict the loads at which a structure may fail by the development of excessive deflections. It is assumed that whenever the moment at any section reaches the plastic moment capacity, M_p , a plastic hinge forms, which can undergo extensive rotation while the moment remains constant. The arrangement of plastic hinges together with real hinges which are functioning at collapse is known as the collapse mechanism or, simply, mechanism (Neal 1977). The plastic limit load for a frame is the maximum load it can carry, assuming that no increases will take place after a mechanism has formed.

Two approaches were commonly used in plastic analysis in early studies (Pippard and Baker 1968) namely, the equilibrium method and the mechanism method.

The equilibrium method of analysis consists of constructing a moment diagram for the structure after it has been rendered statically determinate by replacing a sufficient number of the redundant moments with the fully plastic moment M_p (Phillips 1956). Since it is not always possible to choose the correct locations of the plastic hinges, the method essentially is based on trial and error. If M_p is not exceeded at any point in the moment diagram, but is attained at a sufficient number of points to form a mechanism, the proper plastic moment diagram has been found. If a moment greater than M_p appears at any point, it becomes necessary to assume another moment distribution. When the correct moment diagram has been found, the plastic limit load may be evaluated by statics.

The mechanism method is often less cumbersome than the equilibrium method. It consists of equating the external work done by the loads acting on the deflected structure to the internal work performed by plastic hinge rotations during a virtual displacement of an assumed mechanism. As in the case of the equilibrium method, a trial and error procedure is needed where there are two or more possible mechanisms. The mechanism which yields the smallest collapse load governs the solution of the problem.

The above methods predict the failure load, but give no indication of the load-deformation characteristics of the structure. The methods also are difficult to use for large frames, since the number of possible mechanisms may be very large.

The complete load-deformation response of complex frames can be determined by a computerized step-by-step analysis (Wang 1963). In this approach the difficulty of locating and verifying plastic mechanisms for large structures is avoided. During the first step a linear elastic computation is performed, based on the original geometry and stiffness of the structure. The search for the location of the first plastic hinge is conducted, and the loads on the structure are increased until the section with the highest moment has reached the plastic moment of the member at that point. The first plastic hinge now has formed, and the stiffness of the structure must be modified by changing the particular member stiffness. The search for the next hinge to be formed is then conducted by the same procedure, which is continued until a plastic mechanism has been formed.

Two different step-by-step approaches can be utilized. One is an elastic-plastic analysis, where elastic behavior is assumed

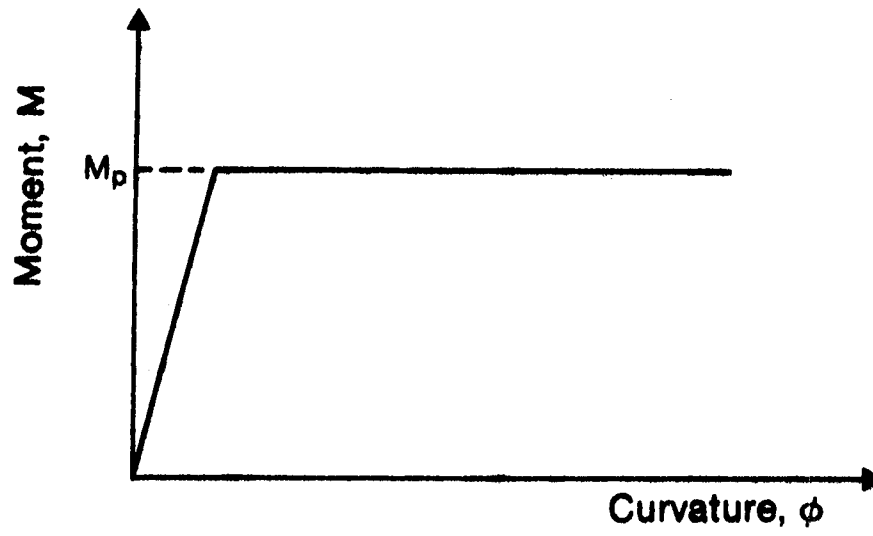
until the hinge has formed, and the moment-curvature relationship shown in Fig. 2-11a is used. According to this assumption, the segments of the frame between the hinges will remain elastic. The resulting load-deformation characteristic is termed the first order elastic-plastic curve, and is illustrated by curve E in Fig. 1-1.

The second approach based on the step-by-step method is a rigid-plastic analysis, which gives a first estimate of the ultimate load of the frame (Beedle 1958). According to this theory the frame remains undeformed until a mechanism has formed. This is consistent with the moment-curvature relationship assumed in Fig. 2-11b. The behavior is termed first order rigid-plastic and is illustrated by curve C in Fig. 1-1.

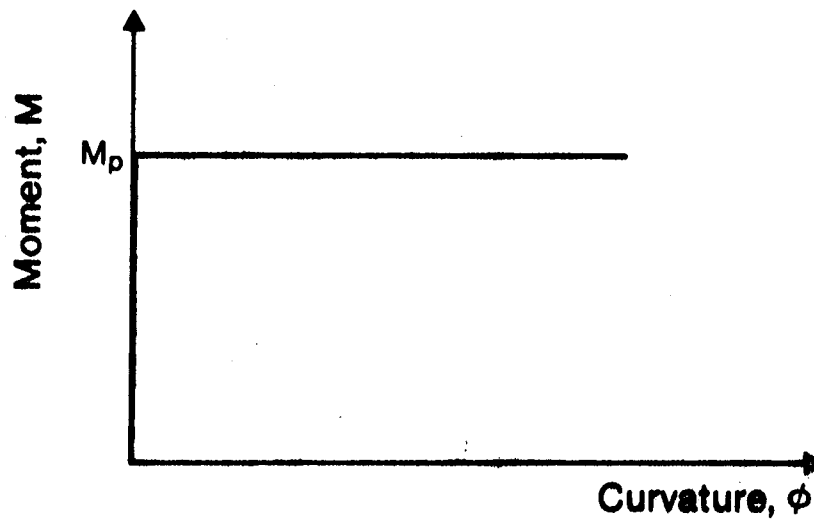
2.5 Inelastic Nonlinear Analysis

The determination of the ultimate strength of a frame is a nonlinear bending problem (Alvarez and Birnstiel 1969). The nonlinearity results from changes in stiffnesses of the members due to axial force and plastification, and from changes in the geometry of the structure due to displacements. The true ultimate strength has been reached when the combination of yielding, axial force, and joint displacements reduce the stiffness of the structure to such an extent that the frame cannot carry any more load.

Experiments have shown that the ultimate strength is less than that predicted by simple plastic theory based on the plastic hinge concept. The actual and the predicted values differ because nonlinear effects are neglected in the simple plastic theory.



(a) Elastic-Plastic Material



(b) Rigid-Plastic Material

FIGURE 2-11 Idealized Moment-Curvature Relationship

2.5.1 The Step-by-Step Method of Analysis

The step-by-step method described by Korn and Galambos (1968), and outlined in Sect. 2.4.5, can be modified to account for nonlinear effects. In this case the analysis is formulated on the deformed structure thus incorporating both strength and stability effects into the analysis. This can be done by performing a $P-\Delta$ analysis, discussed in Sect. 2.3.2, on a frame with plastic hinges.

If the moment-curvature relationship is of the type shown in Fig. 2-11a, indicating an elastic-plastic material, a second order elastic-plastic analysis can be performed. Such a model can adequately represent complex inelastic behavior within the limitations imposed by confining inelastic effects to individual cross sections. The results of the analysis is the complete load-deformation response of a frame, and is shown as curve F in Fig. 1-1. A second order rigid-plastic analysis can be performed on the frame for which the moment-curvature relationship for the material is as illustrated in Fig. 2-11b. In this approach the frame remains undeformed until a mechanism is developed, at which point the frame exhibits lateral deformation with a decrease in load. This behavior is shown in Fig. 1-1 as curve D. The plastic collapse load obtained from the rigid-plastic analysis will always give an upper bound value for the true maximum load.

2.5.2 Development of Second Order Plastic Analysis

A technique for the inelastic stability analysis of portal frames with hinged bases, neglecting the effect of axial forces, has been presented by Ang (1960). Ojalvo and Lu (1961) developed a

procedure for the analysis of portal frames, symmetrically loaded into the inelastic region. Moses (1964) showed a procedure for the inelastic analysis of portal frames with hinged bases, considering the spread of the inelastic zones and the effects of axial forces. In this procedure the frame is given a lateral displacement and the compatible forces and moments are determined by iterations. Adams (1964) presented a similar method, but neglected the axial force in the beam, as did Chu and Pabarcus (1964). The latter also assumed elastic behavior of the beam.

The effect of lateral joint displacements on the inelastic behavior of a hinged base portal frame was included in a paper by Yura and Galambos (1965). The influence of beam axial force was neglected. This is the method called the P- Δ approach, as discussed in Sect. 2.3.2.

Horne and Majid (1966) incorporated both design and analysis features into a second order program capable of considering reductions in plastic moment capacity due to axial forces, but restrictions are placed on the column plastic hinges. The program is limited to considering only bending deformations.

Davison and Adams (1971) considered the effect of a finite column width on the lateral stiffness of the structure. Considering the width of vertical members reduces the clear span of girders, thus increasing the bending stiffness and decreasing the fixed end moments.

McNamee and Lu (1972) examined the frame buckling problem, and presented an engineering solution for inelastic buckling loads of multistory frames. In this approach only flexural deformations are considered, and small deformation theory is used. The plastic hinges

are assumed to take place at discrete points, and an idealized elastic-plastic behavior is implied.

Davison and Adams (1974) developed a method to analyze the stability of braced and unbraced frames. The formulation is based on the slope-deflection equations, modified to incorporate the effect of plastic hinging and finite column widths. The material is assumed elastic-perfectly plastic, and $P-\Delta$ effects are covered. The plastic moment capacity of the column is reduced for axial force, and the effect of axial force on the stiffness and carry-over factors for a column is considered by using elastic stability functions.

Frame collapse analysis has been presented by Tranberg *et al.* (1976). The concepts of geometric and tangent stiffness are used, together with an initial strain procedure. An attempt was made to incorporate most of the factors that influence frame collapse into a single analysis. Extended plastic zones, axial deformations, and strain hardening are considered, but residual stresses are ignored.

Cohn and Rafay (1977) investigated second order analysis using the $P-\Delta$ method. The analysis made use of the plastic hinge concept, as well as considering the axial forces in the members. Residual stresses and strain hardening were neglected, and only stress distribution at collapse is obtained, with no information about the complete load-deformation characteristics.

CHAPTER III

ELASTIC FORMULATIONS AND SOLUTIONS

In Chapter 2 a number of different kinds of classical formulations were reviewed for the solution of member and frame stability problems. Relatively recently, the finite element method has proven itself as one of the most versatile techniques available for the numerical solution of complex structural problems (Gallagher and Padlog 1963). In this chapter the elastic solutions of frame stability problems, using the finite element method, are compared with those obtained by the classical solutions, reviewed in Chapter 2.

The finite element method as a solution technique is reviewed in Sect. 3.1. Section 3.2 is devoted to the basic equations and assumptions. The formulation of stability equations of equilibrium is derived in Sect. 3.3 together with a solution technique to solve for the elastic critical load of frames. Numerical results for a variety of problems are presented in Sect. 3.4. Formulation of nonlinear equilibrium equations as well as finite element models are developed in Sect. 3.5, which also contains a solution technique to solve for the load-deformation response of a framed structure using the finite element equations. A variety of nonlinear problems are checked, for accuracy and efficiency of the solution technique, in Sect. 3.6.

3.1 Review of the Finite Element Method

The development of the finite element method as an analysis tool was initiated with the advent of the electronic digital computer. In the solution of a continuum problem it is necessary to establish and solve a system of governing differential equations. Using the finite element method and a digital computer it is possible to discretize and solve the governing equations for complex system in a very effective way (Zienkiewicz 1971).

In the finite element method structures can be visualized as an assemblage of structural elements interconnected at a discrete number of nodal points. In an elastic continuum the true number of interconnection points is infinite and therein lies the difficulty of its numerical solution. The concept of finite element as originally introduced by Turner *et al.* (1956) attempts to overcome this difficulty by assuming the real continuum to be divided into elements interconnected only at a finite number of nodal points at which work equivalent fictitious forces are introduced. If such an idealization is possible the problem reduces to that of a conventional structural type well suited to numerical treatment.

Although finite element formulations can be based on either stress fields or displacement fields, most often a displacement based finite element formulation is applied in practice since it can easily be programmed for digital computers. The procedure of the finite element method as applied to a frame can be described by the following steps (Chen and Atsuta 1977).

- (a) Each member is separated by imaginary lines into a number of finite elements.

- (b) The elements are assumed to be interconnected at a discrete number of nodal points. The displacements of these nodal points become the unknown parameters of the problem, as in simple structural analysis.
- (c) A set of functions is chosen to uniquely define the state of displacement within each finite element in terms of its nodal displacements. These functions are so chosen that they ensure continuity throughout the member.
- (d) The displacement functions uniquely define the state of strain within an element in terms of nodal displacements. These strains together with any initial strain define the state of stress throughout the element and also at its boundaries.
- (e) A system of forces concentrated at the nodes of the element, equilibrating the boundary stresses and any distributed loads, is determined. This results in a stiffness relationship of the form

$$[k] \{q\} = \{Q\} \quad (3.1.1)$$

in which $\{q\}$ is the vector of nodal displacements, $\{Q\}$ is the vector of nodal forces, and $[k]$ is the element stiffness matrix whose typical influence coefficient k_{ij} is the force Q_i due to a unit displacement q_j when all other displacements (q 's) are zero.

- (f) Once this stage has been reached the solution procedure can follow the standard direct stiffness structural analysis.

Variational principles may be regarded as one of the most important bases for the finite element method (Washizu 1969). They have contributed to the development of structural analysis by leading

to rigorous finite element formulations. Numerous types of finite element models may be derived based on variational principles. Since continuum problems cannot usually be solved 'exactly', the variational method provides an approximate formulation of the problem which yields a solution compatible with the assumed degree of approximation. The variational technique used herein, for the formulation of equations such as Eq. 3.1.1, is the principle of virtual work (Fung 1965).

3.2 Basic Equations and Assumptions

The following assumptions are used to formulate the basic equations of beams and beam-columns throughout this work, unless otherwise stated.

- 1 - The member is straight, prismatic and symmetric about the plane of the frame (the y-z plane). The member z axis (the reference axis) coincides with the centroidal axis of the cross-section.
- 2 - Loads are applied in the plane of the frame only at the ends of an element.
- 3 - Only in-plane deformations occur and sections that were originally normal to the z axis will remain undistorted and normal to the beam axis after deformation.
- 4 - The slope at any point along the reference axis is given by

$$v'_0 = \frac{\Delta v_0}{\Delta z} = \sin\theta \quad (3.2.1)$$

Assumption 4 is basic to the nonlinear formulation developed herein. Since a Lagrangian coordinate system is used, this expression is 'exact' when the elemental length of beam (Δz) does not change in

length. Since the axis of a member may be expected to undergo only very small deformations up to the point of collapse (of the order of 1 or 2 percent), Eq. 3.2.1 permits accurate solutions for large displacement problems of frames, as will subsequently be demonstrated.

The above assumptions permit the displacements u and v of an arbitrary point A on a beam cross section to be expressed in terms of the displacements of the reference axis of the beam. Thus, referring to Fig. 3-1, the displacements can be written as

$$u = u_0 - y \sin\theta \quad (3.2.2a)$$

and

$$v = v_0 - y (1 - \cos\theta) \quad (3.2.2b)$$

Assumption 4 permits Eqs. 3.2.2 to be written as

$$u = u_0 - y v'_0 \quad (3.2.3a)$$

and

$$v = v_0 - y (1 - \cos\theta) \quad (3.2.3b)$$

The axial strain at the arbitrary point A may now be obtained from the large displacement strain-displacement equations (Saada 1974) as

$$\epsilon_z = u' + \frac{1}{2} [(u')^2 + (v')^2] \quad (3.2.4)$$

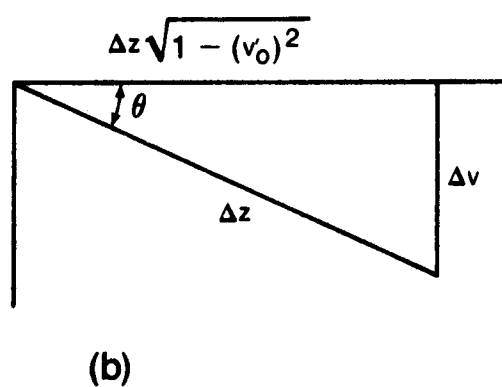
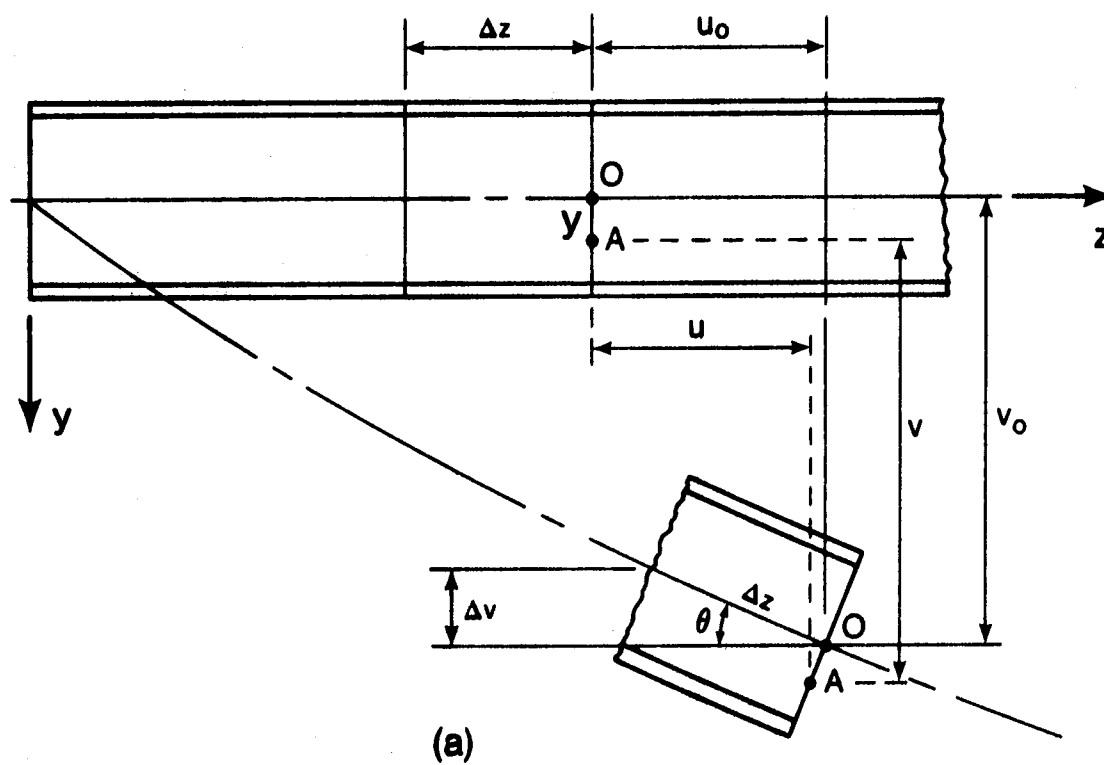


FIGURE 3-1 Element Deformation

Substitution of Eqs. 3.2.3 into Eq. 3.2.4 permits the strain to be determined throughout the beam in terms of displacements of the reference axes.

A variety of beam formulations are now available depending on the degree to which Eqs. 3.2.3 and 3.2.4 are approximated during the formulation. The assumptions that yield the classical linear stability equations are followed in Sect. 3.3. However, a large displacement formulation, which retains all terms implied by Eqs. 3.2.1, 3.2.3 and 3.2.4, is developed in Sect. 3.5.

3.3 Formulation of Linear Stability Equations

In this section a linear stability formulation is derived and a solution technique to solve for the elastic critical load of plane frame is described.

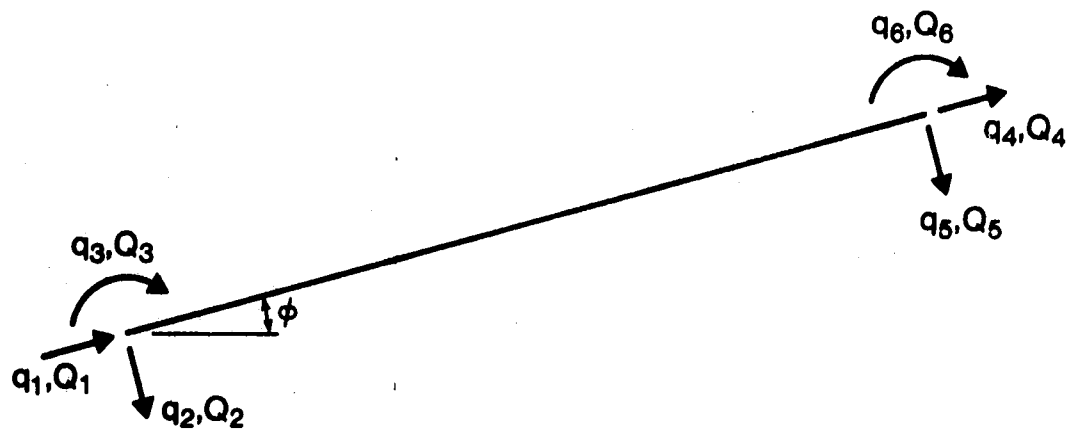
Detailed derivation of the equations of this section is carried out in Appendix A.

3.3.1 Secant Stiffness for Elastic Element

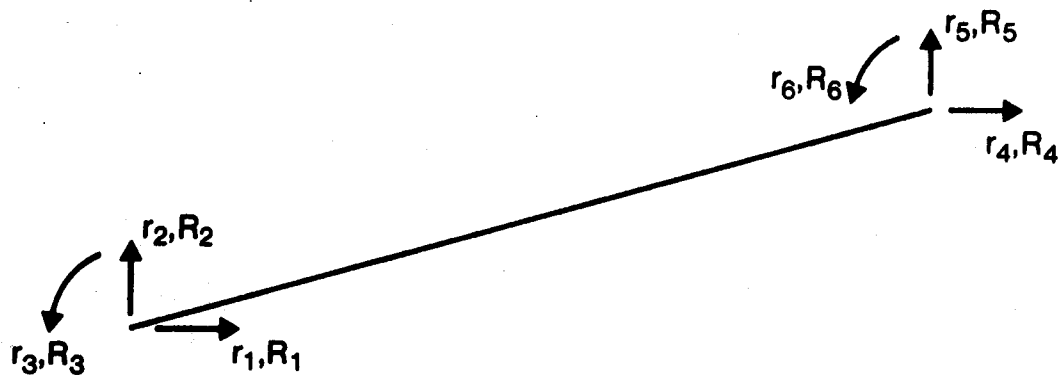
Within the limitation of "small" displacements and elastic stresses the equilibrium equation for an element, as shown in Fig. 3-2a, can be written as (Ghali and Neville 1972)

$$[k] \{q\} = \{Q\} \quad (3.3.1)$$

in which $\{q\}$ is the vector of nodal displacements, $\{Q\}$ is the vector of nodal forces, and $[k]$ is the element stiffness matrix given by Eq. A.2.6c.



(a) Local Nodal Displacements and Forces



(b) Global Nodal Displacements and Forces

FIGURE 3-2 Nodal Displacements and Forces

When the element is subjected to both axial force and bending the stiffness of the element, which in this case may be called the secant stiffness matrix, becomes a function of the axial load. The equation of equilibrium, Eq. 3.3.1, in this case becomes (Chajes 1974)

$$[k_s] \{q\} = \{Q\} \quad (3.3.2)$$

in which

$$[k_s] = [k] + [k_g] \quad (3.3.3)$$

The elastic stiffness $[k]$ is that commonly used for frame analysis (Eq. A.2.6c). For finite element analysis $[k]$ is usually based on a cubic displacement assumption with shear deformations ignored. The matrix $[k_g]$ is called the geometric stiffness matrix (Eq. A.2.6d) and is a function of the element axial force.

3.3.2 Structure Secant Stiffness Matrix

The vector of element local nodal displacements $\{q\}$ can be expressed in terms of the element global nodal displacements $\{r_E\}_G$, shown in Fig. 3-2b, as

$$\{q\} = [T] \{r_E\}_G \quad (3.3.4)$$

in which $[T]$ is a transformation matrix given in Table 3-1.

If $\{R_E\}_G$ is the vector of nodal forces associated with nodal displacements $\{r_E\}_G$ then, by the reasoning of Sect. 2.2

$$\langle q \rangle \{Q\} = \langle r_E \rangle_G \{R_E\}_G \quad (3.3.5)$$

$$[T] = \left[\begin{array}{ccc|ccc} c & s & 0 & & & \\ s & -c & 0 & & & \\ 0 & 0 & -1 & & & \\ \hline & & & c & s & 0 \\ & & & s & -c & 0 \\ & & & 0 & 0 & -1 \end{array} \right]$$

$$c = \cos \phi$$

$$s = \sin \phi$$

TABLE 3-1 Transformation Matrix

Substituting Eq. 3.3.4 into Eq. 3.3.5 yields

$$\langle r_E \rangle_G [T]^T \{Q\} = \langle r_E \rangle_G \{R_E\}_G \quad (3.3.6)$$

or

$$\langle r_E \rangle_G \left\{ [T]^T \{Q\} - \{R_E\}_G \right\} = 0 \quad (3.3.7)$$

Since this must be true for all $\langle r_E \rangle_G$, Eq. 3.3.7 implies that

$$\{R_E\}_G = [T]^T \{Q\} \quad (3.3.8)$$

Premultiplying Eq. 3.3.2 by $[T]^T$ yields

$$[T]^T [k_s] \{q\} = [T]^T \{Q\} \quad (3.3.9)$$

Substituting Eqs. 3.3.4 and 3.3.8 into Eq. 3.3.9 yields

$$[T]^T [k_s] [T] \{r_E\}_G = \{R_E\}_G \quad (3.3.10a)$$

or

$$[k_s]_G \{r_E\}_G = \{R_E\}_G \quad (3.3.10b)$$

The formation of the complete stiffness matrix for the entire structure is obtained by direct addition for all the interface nodes. The equilibrium equations for the entire structure can then be written as

$$[K_s] \{r\} = \{R\} \quad (3.3.11)$$

in which $\{r\}$ is the assembled vector of global nodal displacements, $\{R\}$ is the assembled vector of global nodal forces, and $[K_s]$ is the structure secant stiffness matrix and is a function of the element axial forces. The matrix $[K_s]$ consists of two parts as

$$[K_s] = [K] + [K_G] \quad (3.3.12)$$

in which $[K]$ is the structure stiffness matrix, and $[K_G]$ is the geometric stiffness matrix assembled for the overall structure.

Equation 3.3.11 is an inhomogeneous equilibrium equation that can be used to obtain a unique solution for the frame behavior under a set of loads $\{R\}$. In addition, the equation can be used to obtain the frame critical load by the reasoning discussed in Sect. 2.2.2.

3.3.3 Frame Critical Load

Solving, symbolically, for the displacement vector $\{r\}$ in Eq. 3.3.11 yields

$$\{r\} = [K_s]^{-1} \{R\} \quad (3.3.13)$$

The displacement vector $\{r\}$ increases without limit, for finite values of $\{R\}$, only when the inverse of the secant stiffness matrix becomes infinitely large. Since the inverse of the matrix is obtained by dividing the adjoint matrix by the determinant, the elements of the inverse will become indefinitely large when the determinant is equal to zero. Thus

$$|| K_s || = 0 \quad (3.3.14)$$

gives the stability criterion as discussed in Sect. 2.2.2.

Equation 3.3.14 can be rewritten as

$$|| [K] + [K_G] || = 0 \quad (3.3.15)$$

In dealing with linear stability problems it is assumed that the buckling deformations are independent of all deformations prior to instability. This leads to the possibility of expressing the axial force for each element, at the buckling condition, as a multiple of the axial force occurring for some reference loading. Since the critical load is unknown a factor λ , an arbitrary multiple of the reference load vector $\{\bar{R}\}$, is introduced to represent the relative magnitude of the applied loads. Thus

$$\{R\} = \lambda \{\bar{R}\} \quad (3.3.16)$$

The factor λ is called the instability factor or eigenvalue. Since the geometric stiffness matrix, derived from Eq. A.2.6d, is proportional to the internal axial forces it follows that

$$[K_G] = \lambda [\bar{K}_G] \quad (3.3.17)$$

in which $[\bar{K}_G]$ is the geometric stiffness matrix for the reference value of the applied loading. Thus Eq. 3.3.15 can be written as

$$|| [K] + \lambda [\bar{K}_G] || = 0 \quad (3.3.18)$$

which is the requirement for nontrivial solution of the homogeneous form of Eq. 3.3.11 and gives the eigenvalue, λ_{cr} , that represents the critical load.

Equation 3.3.18 can be solved, using the determinant search technique discussed in Sect. 2.2.2, for the critical load, P_{cr} . However, since Eq. 3.3.18 is a classical eigenvalue problem an inverse power iteration method becomes more practical.

3.3.4 Inverse Power Iteration Method

The inverse power iteration method is described by Householder (1964) and Wilkinson (1965). It is one of the most efficient methods available for solving for the lowest eigenvalue in the case of large systems. It has the advantage of providing the buckling eigenvalue λ_{cr} and the associated buckling mode simultaneously. Stability eigen-systems of over 20,000 degrees of freedom have been handled efficiently with the use of this method (Skogh *et al.* 1972).

To solve for the critical load of a frame the homogeneous form of Eq. 3.3.11 is used. That is

$$[K_g] \{r\} = \{0\} \quad (3.3.19)$$

or

$$[[K] + [K_G]] \{r\} = \{0\} \quad (3.3.20)$$

Substituting Eq. 3.3.17 into Eq. 3.3.20 yields

$$[[K] + \lambda [\bar{K}_G]] \{r\} = \{0\} \quad (3.3.21)$$

which can be written in the form

$$[K] \{r\} = -\lambda [\bar{K}_G] \{r\} \quad (3.3.22)$$

To solve for the lowest value of λ , Eq. 3.3.22 can be rearranged as

$$\frac{1}{\lambda} [K] \{r\} = - [\bar{K}_G] \{r\} \quad (3.2.23)$$

At this stage the inverse power iteration method is performed, using 'Cholesky Decomposition' (Elwi and Murray 1977), to solve for the eigenvalue λ_{cr} and the associated buckling mode $\{r\}$. The method

can be described by the following procedure.

- 1 - The structure elastic stiffness matrix $[K]$ is assembled.
- 2 - For a particular set of loads, a simple linear elastic analysis is performed and the axial force in each element is determined.
- 3 - Using the axial forces obtained in Step 2, the geometric stiffness matrix $[\bar{K}_G]$ can be assembled.
- 4 - An approximate normalized buckling mode $\{r\}$ is assumed.
- 5 - By substituting the vector $\{r\}$ into the right hand side of Eq.

3.3.23, the equation can be rewritten as

$$[K] \left\{ \frac{r}{\lambda} \right\} = \{R_g\} \quad (3.3.24a)$$

in which

$$\{R_g\} = - [\bar{K}_G] \{r\} \quad (3.3.24b)$$

- 6 - Equation 3.3.24a can be put in the form

$$[L] [D] [L]^T \left\{ \frac{r}{\lambda} \right\} = \{R_g\} \quad (3.3.25)$$

or

$$[L] [G] \left\{ \frac{r}{\lambda} \right\} = \{R_g\} \quad (3.3.26a)$$

in which

$$[G] = [D] [L]^T \quad (3.3.26b)$$

The solution is then obtained as

$$\left\{ \frac{r}{\lambda} \right\} = [G]^{-1} \{r\} \quad (3.3.27a)$$

in which

$$\{\bar{r}\} = [L]^{-1} \{R_g\} \quad (3.3.27b)$$

By forward substitution one can solve Eq. 3.3.27b, for the vector $\{\bar{r}\}$. Then substituting $\{\bar{r}\}$ into Eq. 3.3.27a and back substitution yields $\{\frac{r}{\lambda}\}$.

- 7 - The largest value in the new vector $\{\frac{r}{\lambda}\}$ is determined and the vector is divided by this value to obtain a new normalized buckling mode $\{r\}$.
- 8 - The new buckling mode $\{r\}$, obtained from Step 7, is compared with the previous one.
- 9 - Steps 5 to 8 are repeated using the new vector $\{r\}$, until the difference between the buckling modes from two successive iterates is arbitrarily small.
- 10 - The largest value in vector $\{r\}$, obtained in Step 7 after convergence, is equal to $\frac{1}{\lambda}$ and the critical load on the frame is obtained by multiplying the particular set of loads assumed in Step 2 by the inverse of this value.

3.3.5 Computer Program

A computer program, called Eigenvalue Stability Analysis of Frames (ESTANF), has been developed to perform an eigenvalue analysis based on the formulation presented in this section. The results for some example applications are presented in the next section.

3.4 Numerical Results of Elastic Buckling Problems

The formulation given in Sect. 3.3 enables the solution of a wide variety of problems. At this stage it is appropriate to examine the numerical accuracy that may be attained in the solution and also to check the efficiency of the computer program. In general the adequacy and validity of numerical formulation may be measured by comparing its performance on problems for which accurate solutions have been derived by classical methods.

3.4.1. Sample Solutions

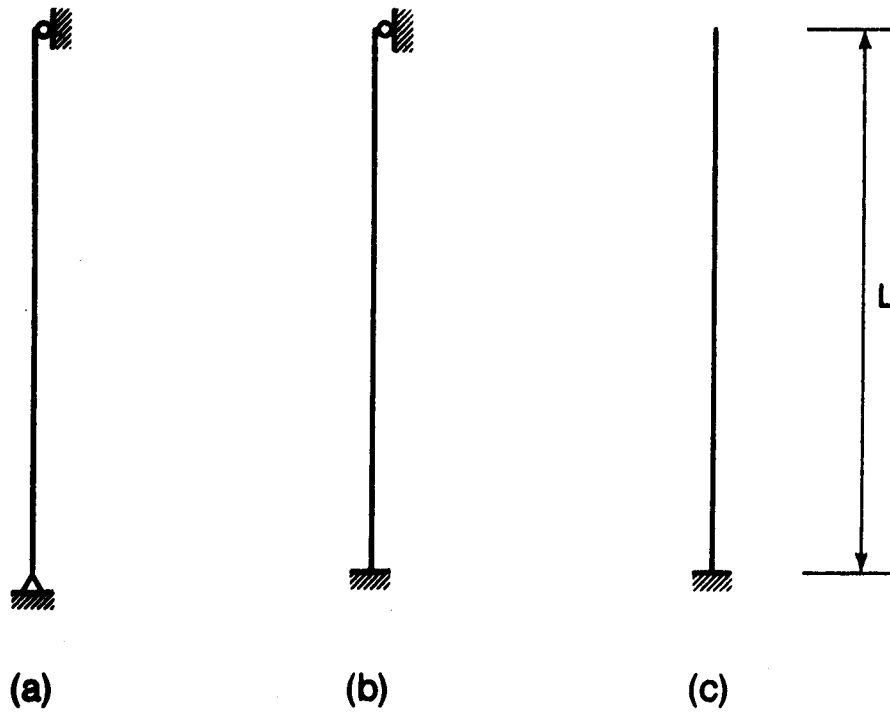
In order to demonstrate the efficiency of the finite element method in the solution of linear stability problems several examples are solved in this section and compared with classical solutions. For each problem the cpu computer time is given as a measure of the cost of running the program.

E-1 Critical Buckling Load of Columns

Three column types, shown in Fig. 3-3, are analyzed. Each type is solved twice, by dividing the member into two elements and then four elements. As can be observed from the results, in Table 3-2, the difference between the classical solutions given by Timoshenko and Gere (1961) and the present analysis is less than 1.0%. For all types of columns analyzed the cpu time ranges between .15 and 0.2 seconds.

E-2 One Story - One Bay Example Frame

Each of the frames shown in Fig. 3-4 is solved using different values of G where G is given by

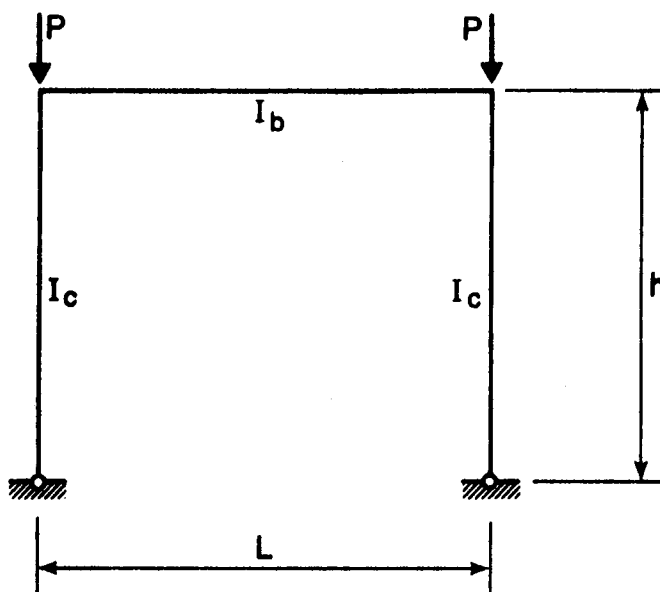


$$\begin{aligned}L &= 120 \text{ in} \\I &= 100 \text{ in}^4 \\E &= 30,000 \text{ ksi}\end{aligned}$$

FIGURE 3-3 Types of Columns

| Type of Column | Classical Solution P_{cr} | Present Analysis | | | | | |
|----------------|--------------------------------|---------------------|--------------|---------------------|--------------|----------|--------------|
| | | No. of Elements = 2 | | No. of Elements = 4 | | | |
| | | P_{cr} | % Difference | P_{cr} | % Difference | P_{cr} | % Difference |
| (a) | 2056.2 | 2073.5 | 0.85 | 2058.5 | 0.1 | | |
| (b) | 4239.5 | 4279.6 | 0.95 | 4250.4 | 0.25 | | |
| (c) | 514.0 | 515.7 | 0.33 | 514.1 | 0.02 | | |

TABLE 3-2 Critical Buckling Load of Columns



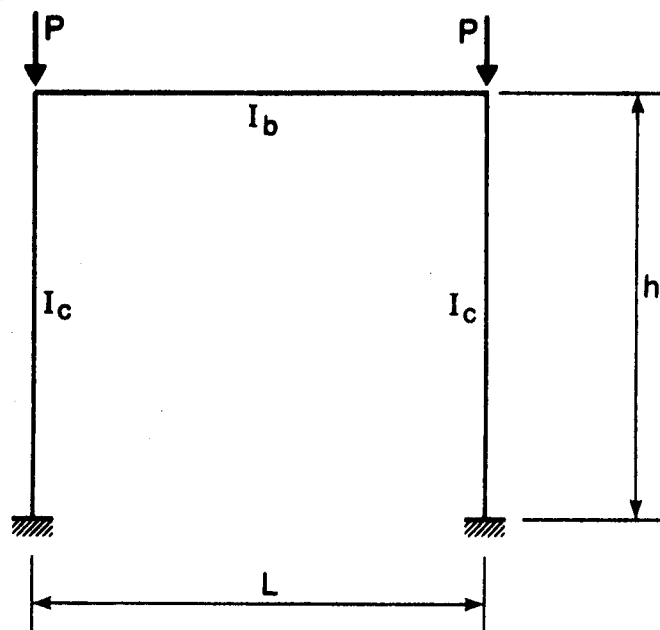
Frame (a)

$$E = 30,000 \text{ ksi}$$

$$L = h = 120 \text{ in}$$

$$I_c = 100 \text{ in}^4$$

$$I_b = 50, 100 \text{ or } 200 \text{ in}^4$$



Frame (b)

FIGURE 3-4 One Storey - One Bay Frame

$$G = \frac{I_c/L_c}{I_g/L_g} \quad (3.3.1)$$

in which I_c and I_g are the moment of inertia of the column and beam, and L_c and L_g are the length of column and beam respectively. For each value of G the frame is solved twice, first assuming the member as one element and second by dividing each member into three elements with the central element being 80% of the length of the member. The reason for the unusual subdivision with three elements will be given later in the thesis, when inelastic behavior is considered.

The results for frame (a), with hinged bases, is given in Table 3-3 while the numerical results for frame (b), with fixed bases, is shown in Table 3-4. The differences in critical loads between the present analysis and the classical solutions tabulated by Lu (1962) are less than 1% even when treating each member as one element. It is noted that the present analysis gives an upper bound to the classical solution. The cpu time ranges between 0.25 to 0.35 seconds.

E-3 Two Story - Two Bay Example Frame

The frame shown in Fig. 3-5 is solved treating each member as one element. An energy formulation derived by Johnson (1960) gives a critical load of 780.2 kips while the present formulation provides a critical load of 778.4 kips with a difference of 0.23%. Unfortunately there was not an exact solution available for this problem. The computer cpu time is about 0.5 sec.

E-4 Multistory Multibay Example Frame

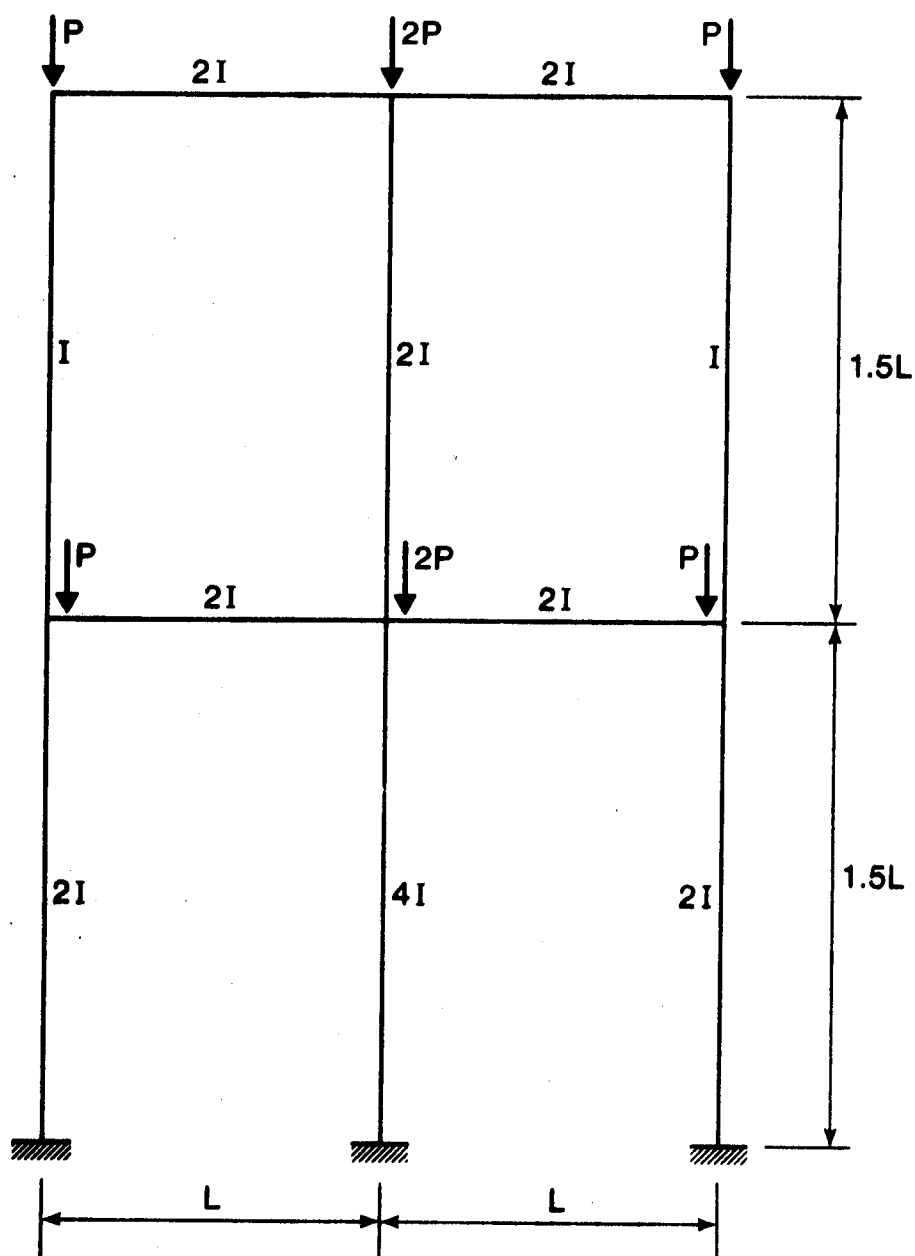
A classical method of analysis based on the energy formulation, for the large frame shown in Fig. 3-6, is presented by Johnson (1960).

| G | Classical Solution P _{cr} | Present Analysis | | | |
|-----|--|---------------------|--------------|---------------------|--------------|
| | | No. of Elements = 1 | | No. of Elements = 3 | |
| | | P _{cr} | % Difference | P _{cr} | % Difference |
| 0.5 | 438.3 | 440.3 | 0.45 | 439.5 | 0.27 |
| 1.0 | 379.4 | 380.5 | 0.3 | 380.1 | 0.18 |
| 2.0 | 296.1 | 296.6 | 0.17 | 296.5 | 0.13 |

TABLE 3-3 Numerical Results of Frame (a)

| G | Classical Solution | Present Analysis | | | |
|-----|-----------------------|---------------------|--------------|---------------------|--------------|
| | | No. of Elements = 1 | | No. of Elements = 3 | |
| | | P _{cr} | % Difference | P _{cr} | % Difference |
| 0.5 | 1756.3 | 1773.1 | 0.95 | 1765.4 | 0.52 |
| 1.0 | 1536.0 | 1549.9 | 0.90 | 1544.7 | 0.57 |
| 2.0 | 1255.0 | 1267.4 | 0.99 | 1263.7 | 0.70 |

TABLE 3-4 Numerical Results of Frame (b)



$$I = 75 \text{ in}^4$$

$$L = 96 \text{ in}$$

$$E = 30,000 \text{ ksi}$$

FIGURE 3-5 Two Storey - Two Bay Frame

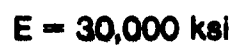


FIGURE 3-6 Multistory - Multibay Frame

It gives a critical load of 1189.6 kips compared to 1187.4 kips obtained from the present analysis furnishing a difference of 0.2%. No exact solution was available. The cpu computer time is, approximately, 1 second.

3.4.2 Comments on Results

The examples presented in this section have been selected to test the ability of the computer program to analyze a variety of rectilinear framed structures. The analysis, as it can be seen from the previous examples, exhibits good results.

3.5 Formulation of Nonlinear Equations

In this section a technique for nonlinear stability formulation of elastic multistory frames is presented. The formulation of nonlinear equilibrium equations is derived, based on the principle of virtual work. Nonlinearities enter the formulation as a result of nonlinear strain-displacement relationships, which contain strain products of the same order of magnitude as the engineering strains.

The Newton-Raphson method is used to solve for the overall load-displacement characteristics of multistory building frames.

3.5.1 Description of Basic Formulation

The basic equations from which a nonlinear formulation may be derived have been given in Sect. 3.2. In Appendix A approximations were made which produced a linear stability formulation. An effort is made in this section to retain all nonlinear terms. Retaining the $(1 - \cos\theta)$ term in Eq. 3.2.2b, the expression for v' required in Eq. 3.2.4 is obtained by differentiating Eq. 3.2.2b. This yields

$$v' = v'_0 - y \sin \theta \frac{d\theta}{dz} \quad (3.5.1)$$

To evaluate the term $d\theta/dz$, differentiate the expression for v'_0 appearing in Eq. 3.2.1 to obtain

$$v''_0 = \cos \theta \frac{d\theta}{dz} \quad (3.5.2)$$

from which

$$\frac{d\theta}{dz} = \frac{v''_0}{\cos \theta} \quad (3.5.3a)$$

The physical interpretation of v'_0 contained in Fig. 3-1b allows $\cos \theta$ to be approximated as

$$\cos \theta = \sqrt{1 - (v'_0)^2} \quad (3.5.3b)$$

Substituting Eqs. 3.5.3 into Eq. 3.5.1, and using Eq. 3.2.1 yields

$$v' = v'_0 - \frac{y v'_0 v''_0}{\sqrt{1 - (v'_0)^2}} \quad (3.5.4)$$

In contrast to the linear formulation (Sect. A.1), both nonlinear terms in Eq. 3.2.4 are now retained. Substituting Eqs. 3.5.4 and 3.2.3a into Eq. 3.2.4 yields the strain-displacement equation for the nonlinear formulation as

$$\begin{aligned} \epsilon_z = & u'_0 + \frac{1}{2} \left[(u'_0)^2 + (v'_0)^2 \right] - y v'_0 \left[1 + u'_0 + \frac{(v'_0)^2}{\sqrt{1 - (v'_0)^2}} \right] \\ & + \frac{1}{2} y^2 (v''_0)^2 \left[1 + \frac{(v'_0)^2}{1 - (v'_0)^2} \right] \end{aligned} \quad (3.5.5)$$

The variation in strain $\delta\epsilon_z$ can be obtained from Eq. 3.5.5, noting that u'_0 , v'_0 , and v''_0 may vary independently. The result is

$$\begin{aligned} \delta\epsilon_z = & [1 + u'_0 - y v''_0] \delta u'_0 + \left[v'_0 - \frac{2y v'_0 v''_0}{\sqrt{1 - (v'_0)^2}} \right. \\ & \left. - \frac{y (v'_0)^3 v''_0}{[1 - (v'_0)^2]^{3/2}} + \frac{y^2 v'_0 (v''_0)^2}{1 - (v'_0)^2} + \frac{y^2 (v'_0)^3 (v''_0)^2}{[1 - (v'_0)^2]^2} \right] \delta v'_0 \\ & + \left[-y (1 + u'_0) + y^2 v''_0 - \frac{y (v'_0)^2}{\sqrt{1 - (v'_0)^2}} + \frac{y^2 (v'_0)^2 v''_0}{1 - (v'_0)^2} \right] \delta v''_0 \end{aligned} \quad (3.5.6)$$

As in Appendix A, the principle of virtual work may be written as

$$\delta W = \int_V \sigma_z \delta\epsilon_z dV - \langle Q \rangle \{ \delta q \} = 0 \quad (3.5.7)$$

Substituting Eq. 3.5.6 into Eq. 3.5.7 results in the equilibrium equation.

$$\begin{aligned} & \left(\int \int \int \sigma_z \left\{ [1 + u'_0 - y v''_0] \delta u'_0 + \left[v'_0 - \frac{2y v'_0 v''_0}{\sqrt{1 - (v'_0)^2}} - \frac{y (v'_0)^3 v''_0}{(1 - (v'_0)^2)^{3/2}} \right. \right. \right. \\ & \quad \left. \left. + \frac{y^2 v'_0 (v''_0)^2}{1 - (v'_0)^2} + \frac{y^2 (v'_0)^3 (v''_0)^2}{(1 - (v'_0)^2)^2} \right] \delta v'_0 + \left[-y (1 + u'_0) + y^2 v''_0 \right. \right. \\ & \quad \left. \left. - \frac{y (v'_0)^2}{\sqrt{1 - (v'_0)^2}} + \frac{y^2 (v'_0)^2 v''_0}{1 - (v'_0)^2} \right] \delta v''_0 \right\} \cdot dA \cdot dz \Bigg) \\ & - \langle Q \rangle \{ \delta q \} = 0 \end{aligned} \quad (3.5.8)$$

Let stress resultants be defined as

$$n = \int_A \sigma_z \cdot dA \quad (3.5.9a)$$

$$m = \int_A \sigma_z \cdot y \cdot dA \quad (3.5.9b)$$

$$m^* = \int_A \sigma_z \cdot y^2 \cdot dA \quad (3.5.9c)$$

then Eq. 3.5.8 can be rewritten, using the definitions in Eqs. 3.5.9, as

$$\left(\int_{\ell} (a_1 \delta u'_0 + a_2 \delta v'_0 + a_3 \delta v''_0) dz \right) - \langle Q \rangle \{ \delta q \} = 0 \quad (3.5.10a)$$

in which

$$a_1 = n (1 + u'_0) - m v''_0 \quad (3.5.10b)$$

$$\begin{aligned} a_2 = n v'_0 - m \frac{v'_0 v''_0}{\sqrt{1 - (v'_0)^2}} \left(2 + \frac{(v'_0)^2}{1 - (v'_0)^2} \right) \\ + m^* \frac{v'_0 (v''_0)^2}{1 - (v'_0)^2} \left(1 + \frac{(v'_0)^2}{1 - (v'_0)^2} \right) \end{aligned} \quad (3.5.10c)$$

and

$$a_3 = -m \left(1 + u'_0 + \frac{(v'_0)^2}{\sqrt{1 - (v'_0)^2}} \right) + m^* v''_0 \left(1 + \frac{(v'_0)^2}{1 - (v'_0)^2} \right) \quad (3.5.10d)$$

Equations 3.5.10 are approximate only to the extent introduced by assumption 4 of Sect. 3.2.

If the displacements, u_o and v_o , are functions of a discrete set of N displacement coordinates, q_i , Eq. 3.5.10a may be written as

$$\psi_1 = 0 \quad (3.5.11)$$

in which

$$\psi_1 = \int_{\ell} \left(a_1 \frac{\partial u'_o}{\partial q_1} + a_2 \frac{\partial v'_o}{\partial q_1} + a_3 \frac{\partial v''_o}{\partial q_1} \right) dz - Q_1 \quad (3.5.12)$$

and for which i has a range of N . (In this and the following equations $N = 4$). Equations 3.5.11 are nonlinear. If Eqs. 3.5.11 are not satisfied, corrections to the q_i may be obtained by Newton-Raphson iteration according to (Murray *et al.* 1979)

$$\Delta\psi_1 = \frac{\partial\psi_1}{\partial q_j} \Delta q_j = -\psi_1 \quad (3.5.13)$$

in which the summation convention is used for repeated indices and j also has a range of N .

Substituting Eq. 3.5.12 into Eq. 3.5.13 results in

$$\begin{aligned} & \left(\int_{\ell} \left(\frac{\partial a_1}{\partial q_j} \frac{\partial u'_o}{\partial q_1} + \frac{\partial a_2}{\partial q_j} \frac{\partial v'_o}{\partial q_1} + \frac{\partial a_3}{\partial q_j} \frac{\partial v''_o}{\partial q_1} \right) \cdot dz \right) \Delta q_j \\ & = Q_1 - \int_{\ell} \left(a_1 \frac{\partial u'_o}{\partial q_1} + a_2 \frac{\partial v'_o}{\partial q_1} + a_3 \frac{\partial v''_o}{\partial q_1} \right) dz \end{aligned} \quad (3.5.14)$$

Equation 3.5.14 is the basic Newton-Raphson equation and may be adapted to geometric and material nonlinearity.

Once the expressions for u_0 and v_0 are defined in terms of the q 's, all terms in Eq. 3.5.14 may be evaluated and numerical integration with respect to z may be carried out to form an incremental tangent stiffness matrix $[k_T]$ and unbalanced load vector $\{\Delta Q\}$. Equation 3.5.14 may then be written symbolically as

$$[k_T] \{\Delta q\} = \{\Delta Q\} \quad (3.5.15)$$

in which the influence coefficient $(k_T)_{ij}$ is evaluated as

$$(k_T)_{ij} = \int_L \left(\frac{\partial a_1}{\partial q_j} \frac{\partial u'_0}{\partial q_1} + \frac{\partial a_2}{\partial q_j} \frac{\partial v'_0}{\partial q_1} + \frac{\partial a_3}{\partial q_j} \frac{\partial v''_0}{\partial q_1} \right) \cdot dz \quad (3.5.16)$$

; and the unbalanced load ΔQ_1 , is evaluated as

$$\Delta Q_1 = Q_1 - \int_L \left(a_1 \frac{\partial u'_0}{\partial q_1} + a_2 \frac{\partial v'_0}{\partial q_1} + a_3 \frac{\partial v''_0}{\partial q_1} \right) dz \quad (3.5.17)$$

All equations derived above are applicable to inelastic as well as elastic behavior. The equations are specialized for elastic response in Appendix B resulting in a tangent stiffness matrix $[k_T]$, given by Eq. B.4.4 for a flexural element, or Eq. B.4.11 for a truss element. The unbalanced load vector $\{\Delta Q\}$ is given by Eqs. B.3.4 and B.3.11 for flexural and truss elements, respectively.

3.5.2 Finite Element Model

For computational purposes a finite element model is developed to obtain a set of algebraic equations using a beam element function. In the finite element approach the displacements at any point are

represented by interpolating functions denoted as $\{\phi\}$, and the generalized displacements $\{\bar{U}\}$ and $\{\bar{V}\}$ at the nodes. Thus

$$u_o = \langle \phi \rangle \{\bar{U}\} \quad (3.5.18a)$$

and

$$v_o = \langle \phi \rangle \{\bar{V}\} \quad (3.5.18b)$$

in which $\{\bar{U}\}$ and $\{\bar{V}\}$ are defined in Fig. 3-7 for a flexural element and, in Fig. 3-8 for a truss element.

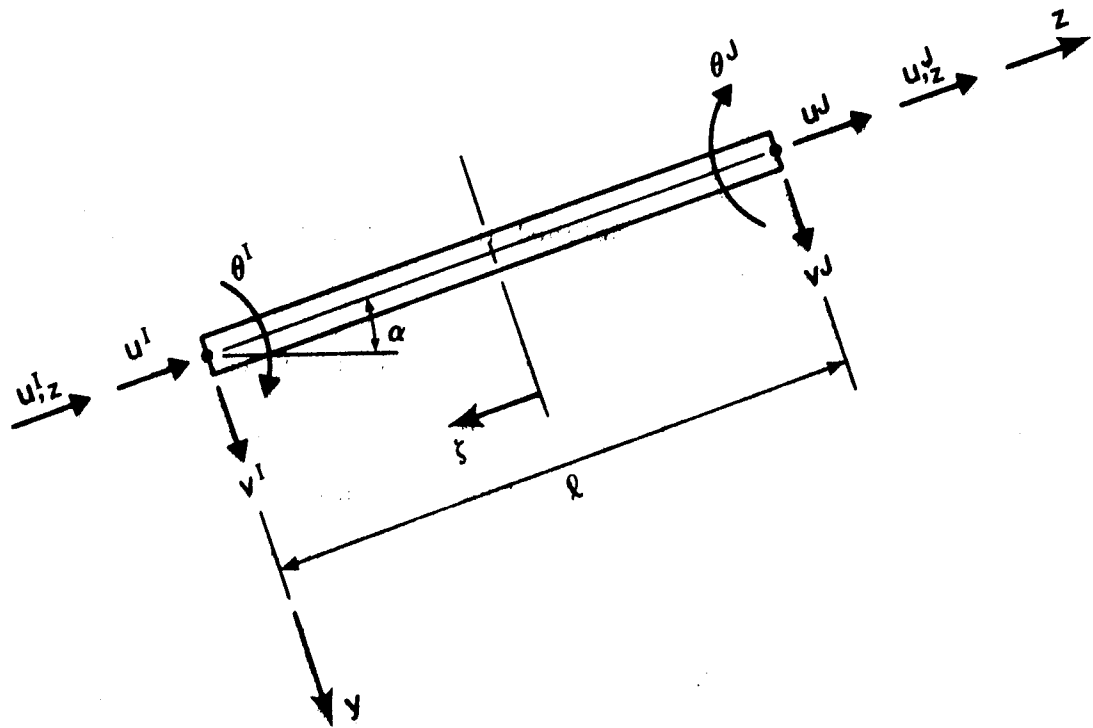
The formulation developed in this study uses two types of interpolating functions for two types of element, namely a flexural element and a truss element. The functions selected for the flexural element are cubic polynomials that can be expressed as linear combination of the four base functions illustrated in Fig. A-2 and given by Eq. A.2.3b.

For a truss element, linear functions are used that may be expressed as combination of the two base functions illustrated in Fig. A-1 and given in Eq. A.2.3a.

Equations 3.5.18 are used in Appendix B to evaluate the finite element equations, Eq. 3.5.15.

3.5.3 Assembly of Finite Element Equations

Equation 3.5.15 is the incremental equilibrium equation, for an element. In this equation the element stiffness matrix has been evaluated with respect to nodal displacements $\{q\}$, referenced to a local coordinate system shown in Fig. 3-7 for a flexural element and Fig. 3-8 for a truss element. The local nodal displacements can be written as

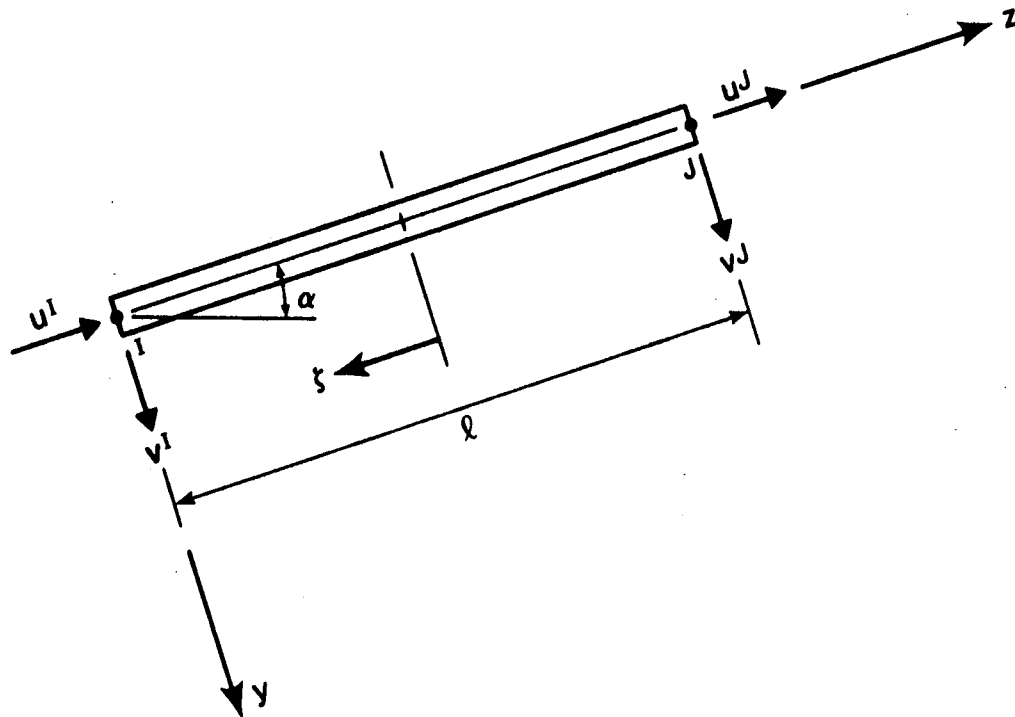


$$\{\bar{U}\}^T = \langle u^I, (u_z^I), u^J, (u_z^J) \rangle$$

$$\{\bar{V}\}^T = \langle v^I, \theta^I, v^J, \theta^J \rangle$$

$$\{q^I\}^T = \langle u^I, (u_z^I), v^I, \theta^I \rangle$$

FIGURE 3-7 Local Nodal Displacements for Flexural Element



$$\{\bar{U}\}^T = \langle u^I, u^J \rangle$$

$$\{\bar{V}\}^T = \langle v^I, v^J \rangle$$

$$\{q^I\}^T = \langle u^I, v^I \rangle$$

FIGURE 3-8 Local Nodal Displacements for Truss Element

$$\langle q \rangle = \langle \langle \bar{U} \rangle, \langle \bar{V} \rangle \rangle \quad (3.5.19a)$$

or

$$\langle q \rangle = \langle u^I, \left(\frac{\partial u}{\partial z}\right)^I, u^J, \left(\frac{\partial u}{\partial z}\right)^J, v^I, \theta^I, v^J, \theta^J \rangle \quad (3.5.19b)$$

for a flexural element; and

$$\langle q \rangle = \langle u^I, u^J, v^I, v^J \rangle \quad (3.5.19c)$$

for a truss element; and I and J are nodal numbers.

In frame analysis it is convenient to select a different set of reference axis for the global system of nodal displacements $\{r_E\}_G$ as shown in Fig. 3-9. The global nodal displacements can be written as

$$\langle r_E \rangle_G = \langle r_E^I, r_E^J \rangle_G \quad (3.5.20a)$$

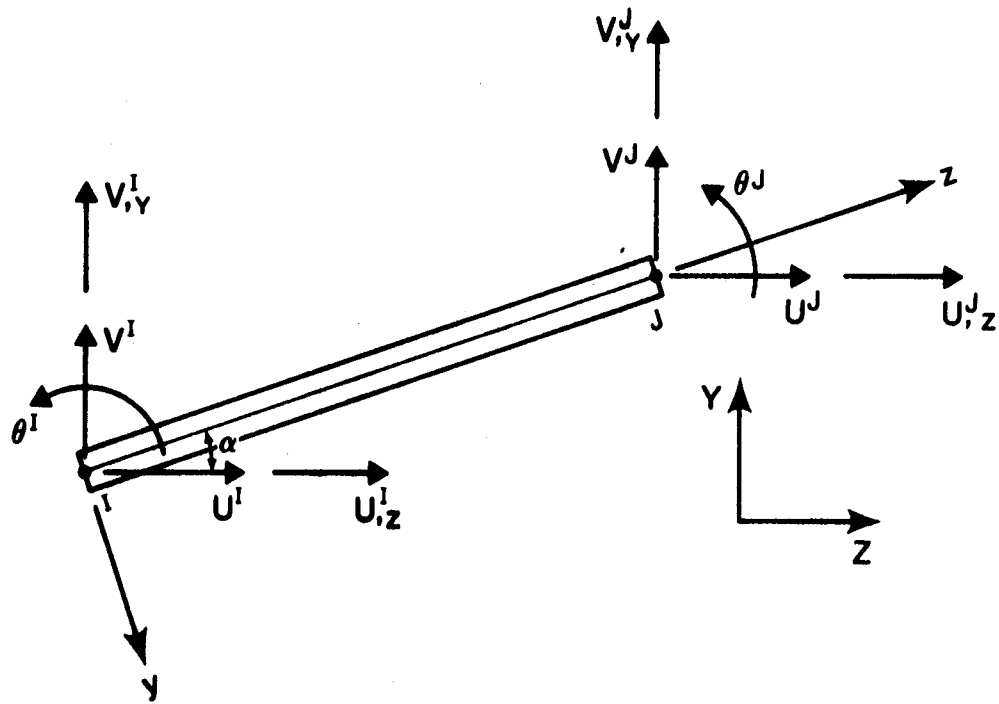
in which

$$\langle r_E^I \rangle_G = \langle U^I, V^I, \theta^I, \left(\frac{\partial U}{\partial Z}\right)^I, \left(\frac{\partial V}{\partial Y}\right)^I \rangle \quad (3.5.20b)$$

The element displacements with respect to the local coordinate system can be related to those in the global coordinate system by the transformation

$$\{q\} = [T] \{r_E\}_G \quad (3.5.21)$$

in which the transformation matrix $[T]$ for a flexural element is derived in Appendix C and given in Table 3-5. Also, the transformation matrix $[\bar{T}]$ for a truss element is given in Table 3-6.



$$\{r^I\}_G^T = \langle U^I, V^I, \theta^I, (U_{,z})^I, (V_{,y})^I \rangle_G$$

FIGURE 3-9 Global Nodal Displacements

$$[\bar{T}] = \begin{bmatrix} \cos \alpha & \sin \alpha & 0 & 0 & 0 & 0 & 0 & 0 & 0 \\ 0 & 0 & 0 & 0 & 0 & 0 & 0 & 0 & 0 \\ 0 & 0 & 0 & 0 & 0 & 0 & 0 & 0 & 0 \\ 0 & 0 & 0 & \cos \alpha & \sin \alpha & 0 & 0 & 0 & 0 \\ 0 & 0 & 0 & -\sin \alpha & \cos \alpha & 0 & 0 & 0 & 0 \\ 0 & 0 & 0 & 0 & 0 & 0 & 0 & 0 & 0 \\ 0 & 0 & 0 & 0 & 0 & 0 & 0 & 0 & 0 \\ 0 & 0 & 0 & 0 & 0 & 0 & 0 & 0 & 0 \\ 0 & 0 & 0 & 0 & 0 & 0 & 0 & 0 & 0 \end{bmatrix}$$

TABLE 3-6 Transformation Matrix For a Truss Element

Using the transformation procedure described in Sect. 3.3.2 results in

$$[k_T]_G \{\Delta r_E\}_G = \{\Delta R_E\}_G \quad (3.5.22)$$

The element stiffness matrices can now be assembled to form

$$[K_T] \{\Delta r\} = \{\Delta R\} \quad (3.5.23)$$

in which $[K_T]$ is the structural tangent stiffness matrix assembled for the entire structure, $\{\Delta r\}$ is the assembled vector of incremental nodal displacements, and $\{\Delta R\}$ is the assembled vector of incremental nodal forces, called the unbalanced forces.

Once Eq. 3.5.23 is assembled the Newton-Raphson method can be used to solve for the load-deformation characteristics of the structure.

3.5.4 Newton-Raphson Solution Procedure

The Newton-Raphson method has proven to be one of the most useful solution techniques available for nonlinear analysis (Rajasekaran and Murray 1973). Many investigators have adapted the method quite successfully. Walker and Hall (1968) used it to study large deflections of beams while Brebbia and Connor (1969) used it to study the geometrically nonlinear behavior of arbitrary shells.

The Newton-Raphson solution technique can be best described with reference to Fig. 3-10 and the following algorithm.

- 1 - For any approximate $\{r\}_n$, the stiffness matrix $[K_T]$ and the vector of unbalanced forces $\{\Delta R\}_n$ are evaluated.

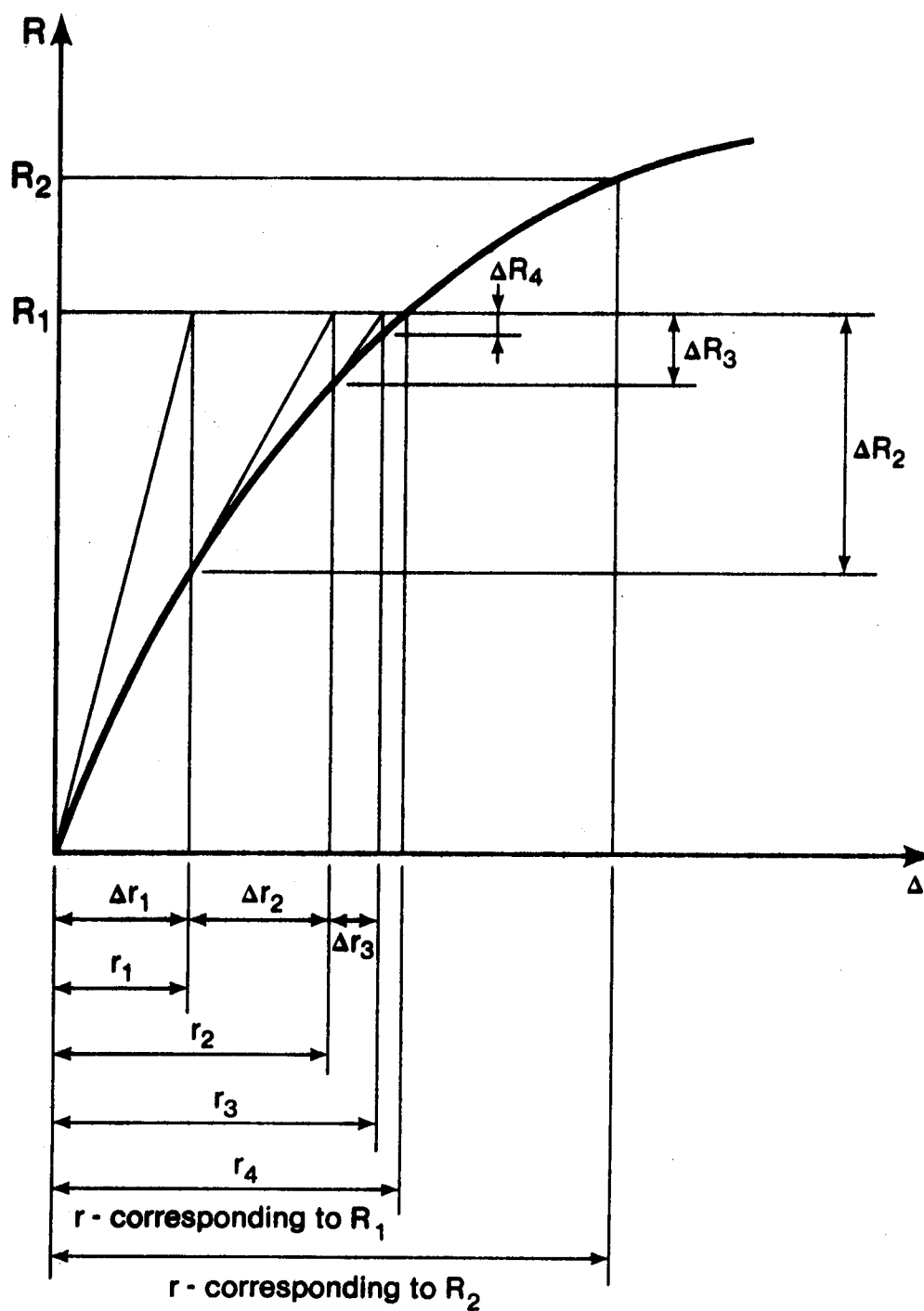


FIGURE 3-10 Newton - Raphson Procedure

- 2 - The increment in displacements $\{\Delta r\}$ necessary to equilibrate the unbalanced forces, evaluated in step 1, are evaluated using Eq. 3.5.23 as

$$\{\Delta r\}_n = [K_T]_n^{-1} \{\Delta R\}_n \quad (3.5.24)$$

- 3 - The displacements are updated. That is

$$\{r\}_{n+1} = \{r\}_n + \{\Delta r\}_n \quad (3.5.25)$$

- 4 - Steps 1 to 3 are repeated until the vector of unbalanced forces $\{\Delta R\}$ is arbitrarily small. At this stage a point on the load-displacement diagram is obtained.
- 5 - A new load level is applied and steps 1 to 4 are repeated to obtain the load-deformation characteristics of the structure.

3.5.5 Summary

A large deformation theory for plane frame problems has been formulated in this section. A finite element method has been developed and a Newton-Raphson solution procedure, to solve for the complete load-deformation curve, is explained.

3.5.6 Computer Program

To show the capability of the theory, formulated above, a computer program, called Nonlinear Elastic Analysis (NONELA), is developed to solve the set of equations presented in this section for the case of linearly elastic material. The method of Newton-Raphson is used; the stiffness matrix $[K_T]$ being evaluated at each step of the procedure. Some applications are presented in the next section to demonstrate the capability of the theory and the efficiency of the computer program.

3.6 Nonlinear Elastic Solutions

The examples presented in Sect. 3.4 have dealt with elastic buckling or bifurcation problems. When large deformation theory, presented in Sect. 3.5, is considered the problem becomes nonlinear. For this type of problem the load-deformation response is obtained by applying the load incrementally and iterating to find the equilibrium configuration for each loading condition as described in Sect. 3.5.4.

3.6.1 Examples of Beam-Columns

NL-1 'The Elastica' Problem

This example considers the elastic post-buckling behavior of a simply supported beam-column. A small transverse load was applied to act as an initial imperfection. Results are shown in Fig. 3-11. Agreement with the 'Elastica' solution, discussed in Sect. 2.3.1, (Timoshenko and Gere 1961) is very good. The number of elements used was 4 elements. The average number of iterations to get from one load level to the next with a relative error of 1×10^{-4} was 4, with an average cpu time per iteration of 0.1 sec.

NL-2 Cantilever Under Pure Moment

In this example a cantilever beam acted upon by a moment at its free end is analyzed. A very good agreement with the solution of Epstein and Murray (1976), was obtained with four elements for deformations up to the semicircumference. Then the number of elements was increased to six and deformations pursued up to the complete circumference. Fig. 3-12 shows some of the exact deformed configuration with the corresponding positions of the nodes as obtained from the

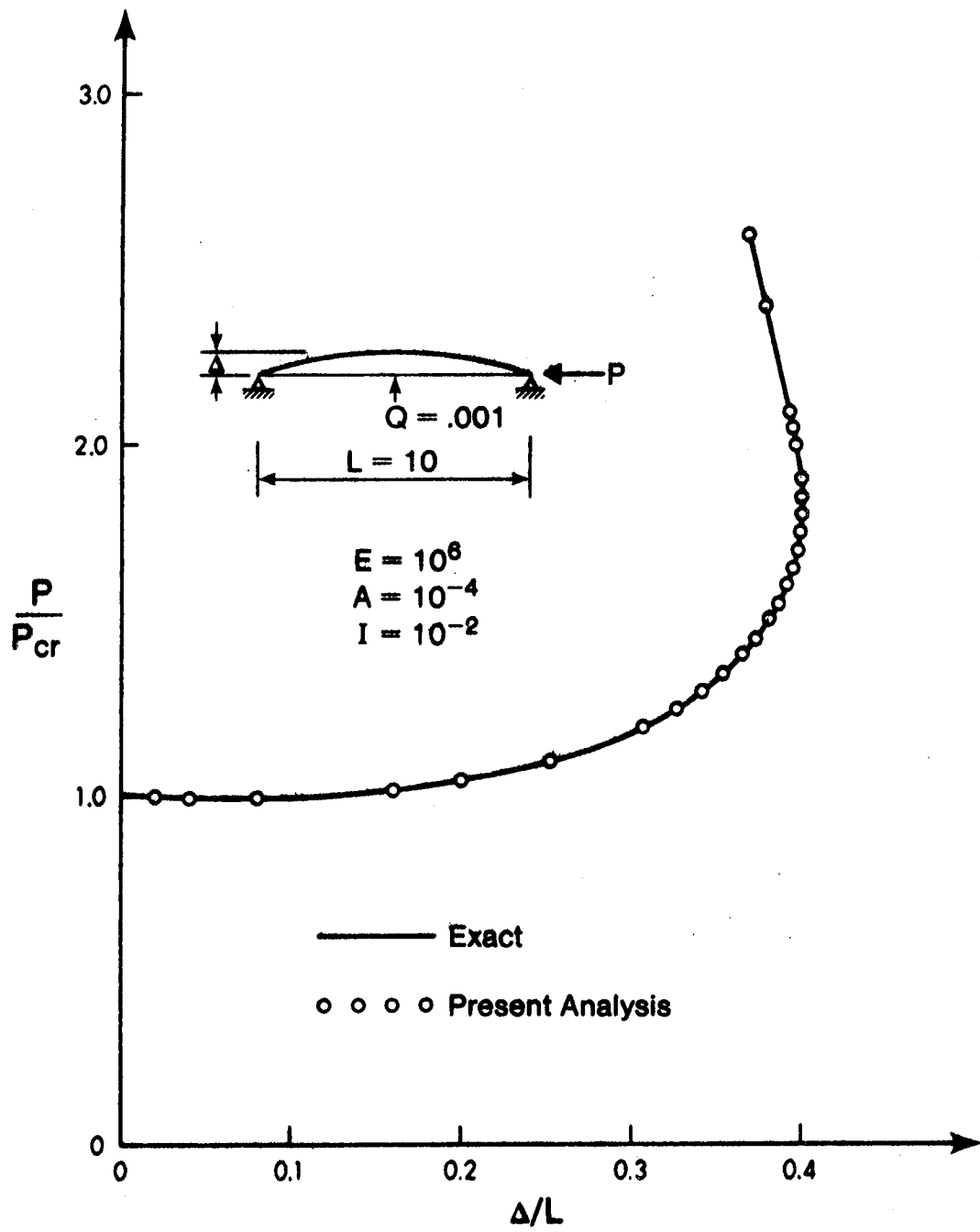


FIGURE 3-11 Solution for the 'Elastica'

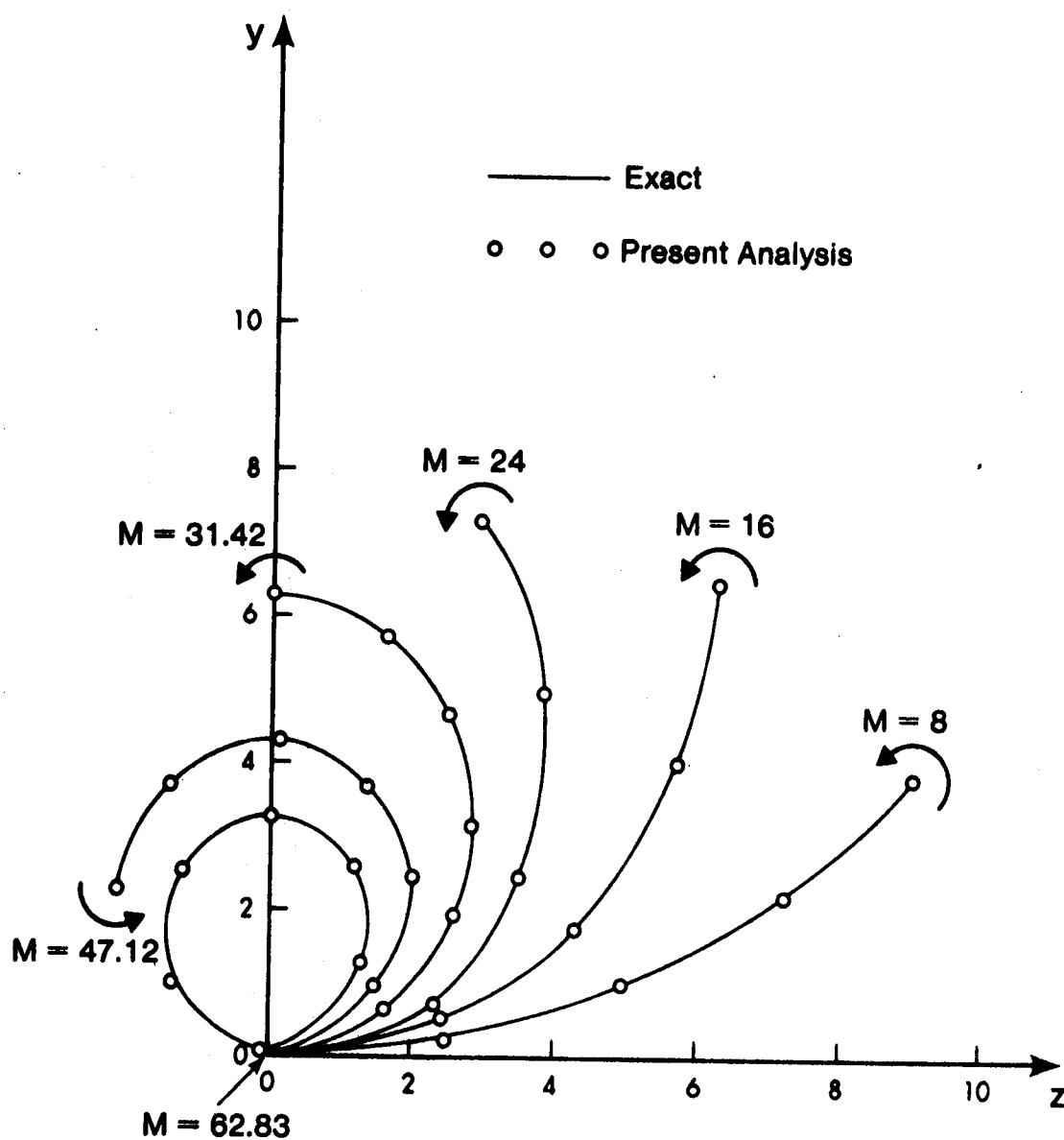


FIGURE 3-12 Solution for Cantilever Under Pure Moment

computer program. The number of iterations averaged 4 iterations per each load increment with an average cpu time of 0.1 sec./iteration.

NL-3 Cantilever Beam With One Concentrated Load

The results summarized in Fig. 3-13 are for a cantilever beam loaded, with a concentrated load, at its tip. The solid line represents the exact solution, given by Bisshop and Drucker (1945). Two solutions for the present formulation are introduced. One using 2 elements and the other using 4 elements. It is seen that the solution obtained using 4 elements is in excellent agreement with the exact solution.

NL-4 Cantilever Beam With Two Concentrated Loads

A comparative study by Ebner and Ucciferro (1972) gives numerical results obtained by several different finite element techniques for the cantilever beam shown in Fig. 3-14. The results reported are reproduced in Table 3-7 along with results obtained by the present formulation. It is seen that the present solution with two elements is as accurate as the solution by various other versions of the finite element approach.

3.6.2 Examples of Frames

NL-5 One Story Frame

The results obtained for a simple one story bent are shown in Fig. 3-15. The results are compared with an approximate solution presented by Oran and Kassimali (1976). It is important to note that the formulation developed as part of the present investigation did function properly, with no significant convergence difficulties, up to even beyond the critical load of the limiting case of the perfect bent. It

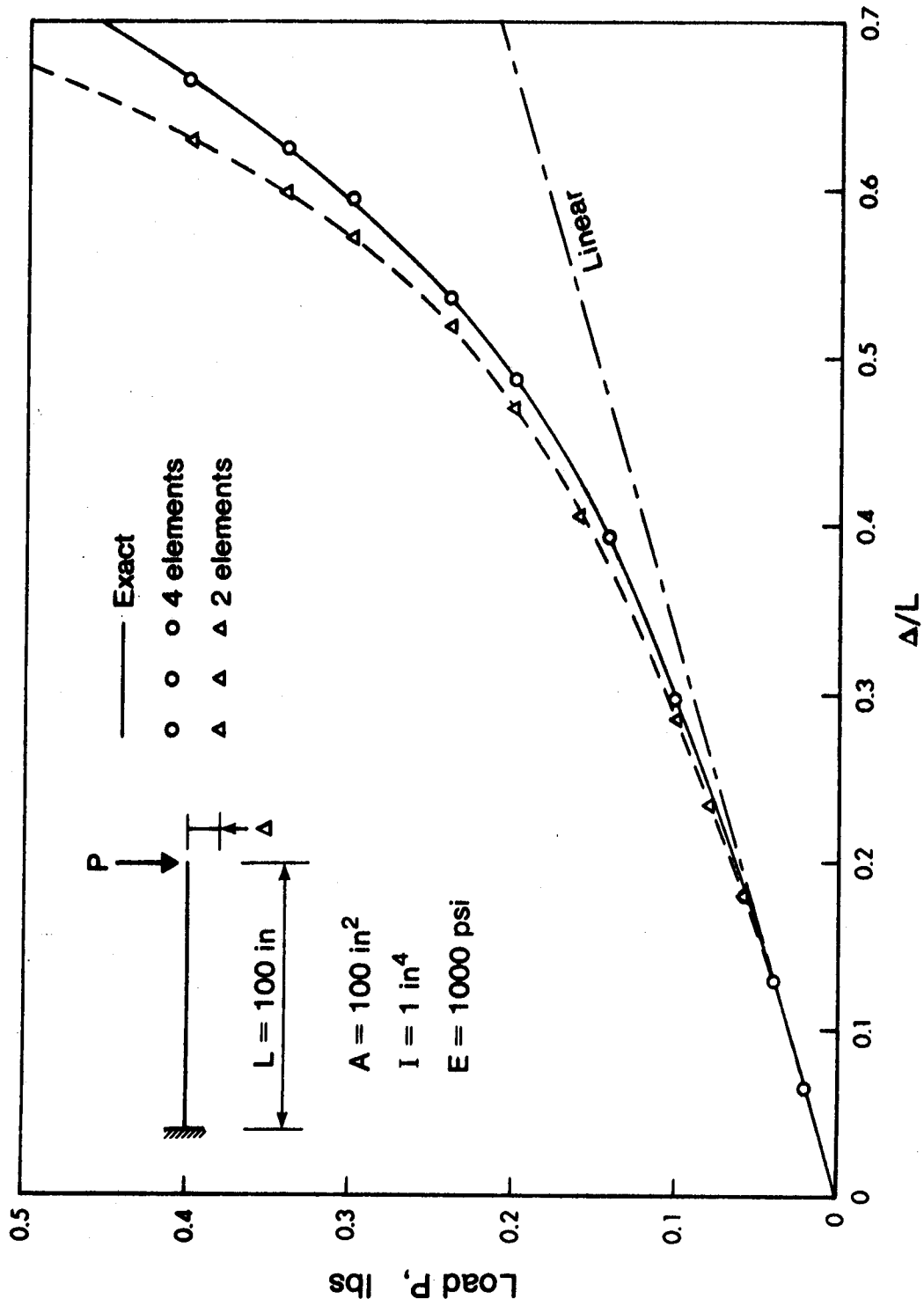
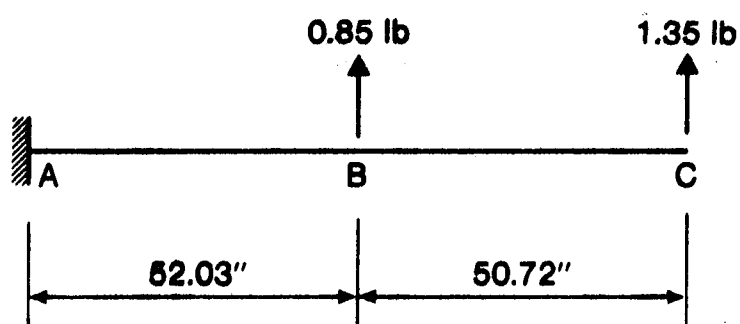


FIGURE 3-13 Load Deflection Curves for Cantilever Beam



$$E = 30 \times 10^6 \text{ lb/in}^2$$

$$A = 1/5 \text{ in}^2$$

$$I = 1/6000 \text{ in}^4$$

FIGURE 3-14 Cantilever Beam with Two Lateral Loads

| Formulation | Number of Elements | Number of Increments | Horizontal Deflection pt. B(in.) | Vertical Deflection pt. B(in.) | Horizontal Deflection pt. C(in.) | Vertical Deflection pt. C(in.) |
|----------------------------|--------------------|----------------------|----------------------------------|--------------------------------|----------------------------------|--------------------------------|
| Martin (1965) | 2 | 20 | -8.97 | 27.49 | -36.02 | 74.20 |
| | 20 | 100 | -9.11 | 26.29 | -34.37 | 70.60 |
| Argyris (1964) | 2 | 20 | -9.06 | 29.04 | -36.20 | 75.20 |
| | 20 | 100 | -9.12 | 26.30 | -35.00 | 70.75 |
| Jennings (1968) | 2 | 20 | - .01 | 2.20 | - .03 | 6.40 |
| | 20 | 100 | -4.94 | 20.60 | -15.01 | 51.15 |
| Present | 2 | 4 | -7.8 | 24.25 | -30.45 | 66.40 |
| Exact by Frisch-Fay (1961) | - | - | -8.3 | 25.10 | -31.01 | 67.30 |

TABLE 3-7 Comparison Between Incremental Solutions
for Cantilever Beam NL-4

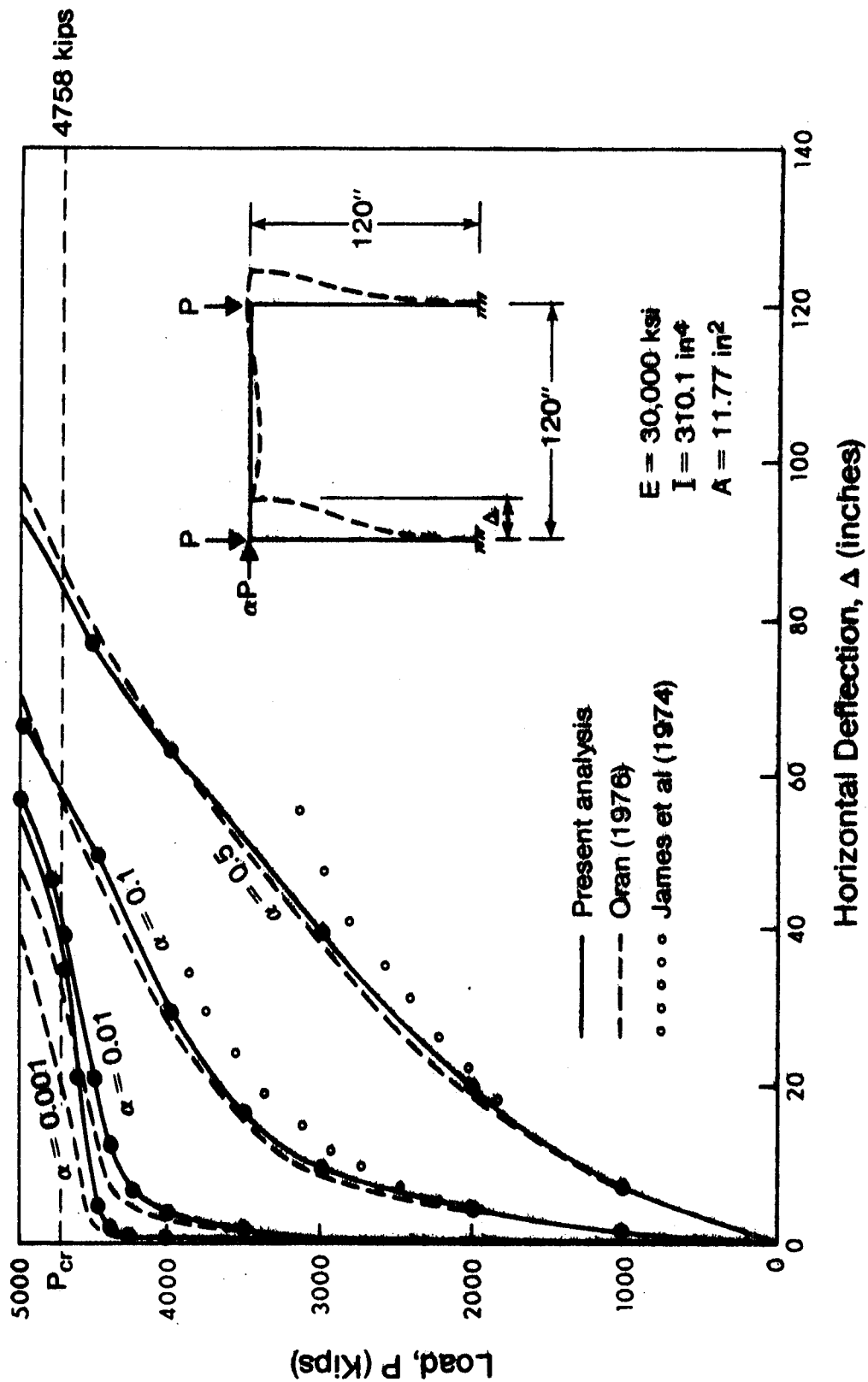


FIGURE 3-15 Load Deflection Curves for One Story Bent

may be of interest to note, in this connection, that an alternate iterative technique, suggested by James *et al.* (1974), failed to converge at substantially lower load levels. A lack of convergence in the iterative process was viewed by those authors as an indication of instability. In the light of data presented herein, such a conclusion would not necessarily be justified.

The solution obtained averaged about 4 iterations per each load increment with average cpu time per iteration of 0.1 sec.

NL-6 Multistory Frames

The two frames shown in Fig. 3-5 and Fig. 3-6 are analyzed here. The results for the two story-two bay frame are shown in Fig. 3-16. In this example the average number of iterations to get from one load level to the next was 5 with an average cpu time per iteration of 0.2 second. The results obtained for the multistory multibay frame are illustrated in Fig. 3-17. In this case the number of iterations averaged 6 iterations per load increment with an average cpu time of 1.2 seconds per iteration.

Unfortunately there is no exact, or approximate, solution available for these frames to compare with. However, according to the results obtained from the previous examples, the author strongly feels that the present formulation provides good results for these frames.

3.6.3 Comments on Results

Results obtained in this section compared favorably to the exact and approximate solutions available. The examples demonstrate that the computer program developed is capable of analyzing a wide variety of nonlinear frame problems with very good results.

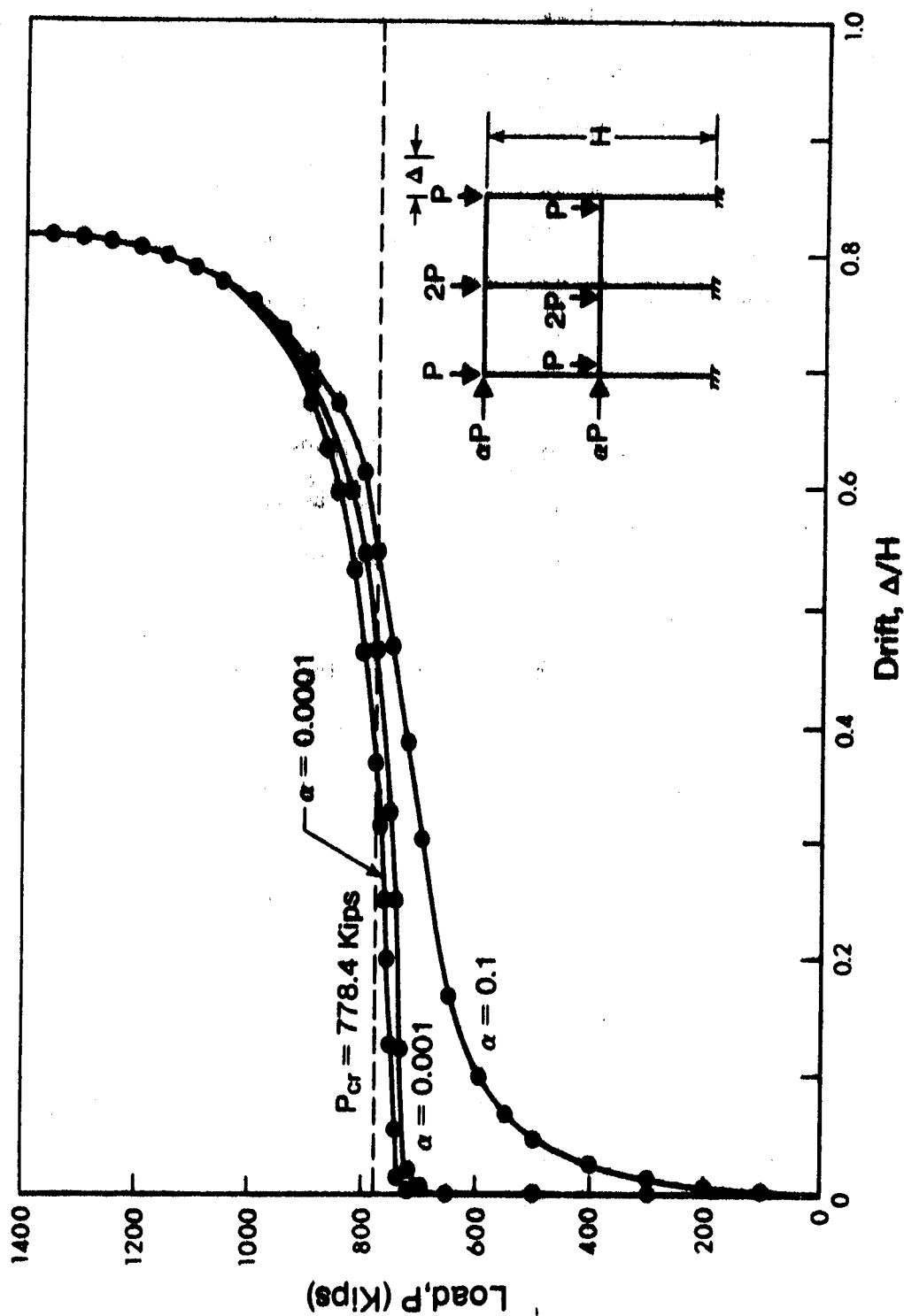


FIGURE 3-16 Load Deformation Curves for Two Story-Two Bay Frame.

CHAPTER IV

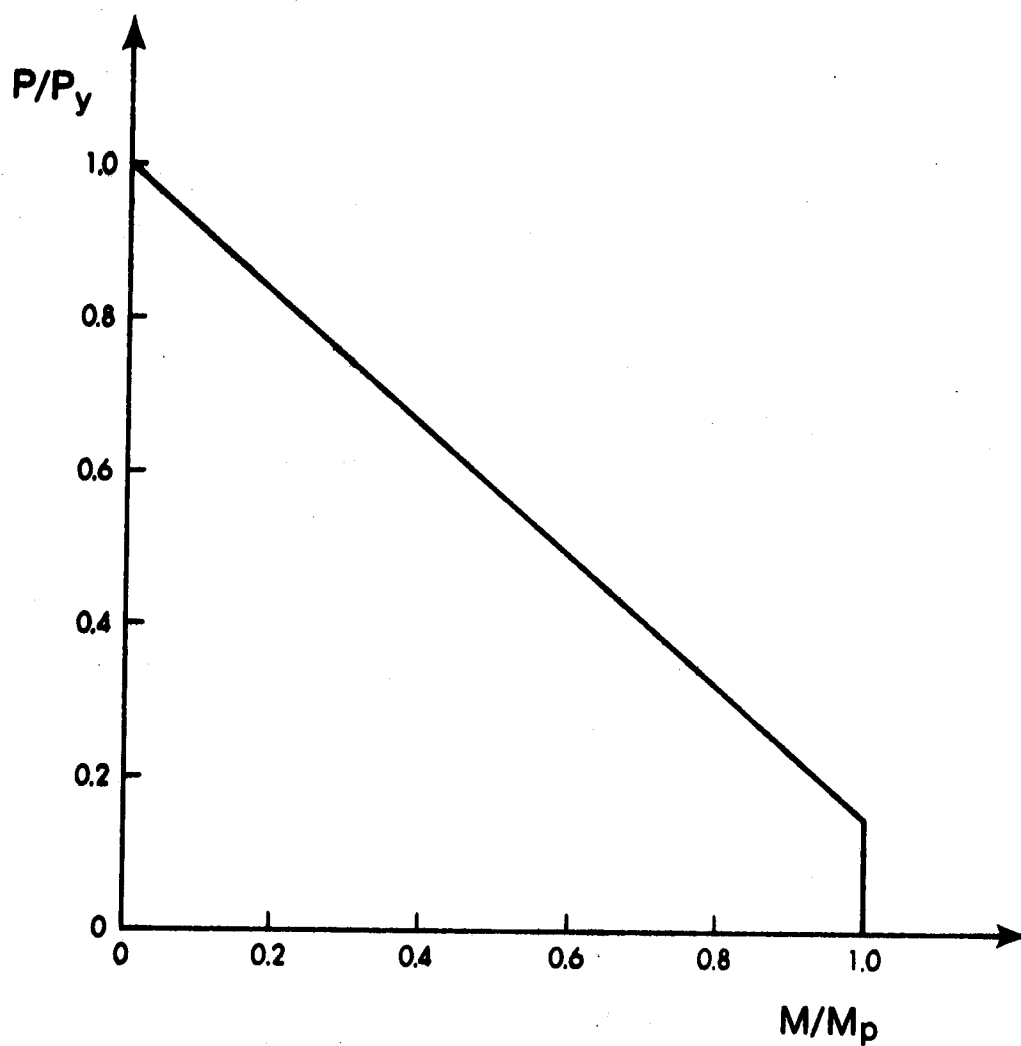
BEHAVIOR OF ELASTIC - PLASTIC FRAMES

The determination of the complete load-deformation response for plane frames, loaded to the inelastic range, is possible by a computerized step-by-step elastic-plastic analysis, described in Sect. 2.4.5. In this chapter, features of elastic-plastic analysis of frames are presented. Two methods have been adapted, one is an incremental solution while the other is an iterative technique. For each technique first and second order analyses are presented. A comparison between the methods is furnished and results are compared to published reports.

4.1 Basic Assumptions and Limitations

In addition to the first three assumptions presented in Sect. 3.2, the following assumptions are also considered.

- 1 - The material is assumed to be linearly elastic-perfectly plastic (i.e. strain hardening is not considered).
- 2 - Residual stresses are ignored.
- 3 - Plastic deformations are concentrated in generalized hinges.
- 4 - Plastic moment capacity, M_{pc} , in the presence of axial load, P , at a particular section is reduced in accordance with the interaction yield curve shown in Fig. 4-1.



$$\begin{array}{ll}
 M = M_p & \text{For } 0 \leq P/P_y \leq .15 \\
 M = 1.18 (1 - P/P_y) M_p & \text{For } .15 \leq P/P_y \leq 1.0
 \end{array}$$

FIGURE 4-1 Interaction Curve

4.2 The Incremental Method of Analysis

Equation 3.3.11 is the equilibrium equation, for a structure, assembled in a global coordinate system. In that equation the geometric stiffness matrix $[K_G]$ depends on the axial forces in the individual members which in turn depend on the level of loading.

Since the geometric stiffness matrix $[K_G]$ varies between two levels of loading, Eq. 3.3.11 can be put in an incremental form as

$$[K] \{\Delta r\} + [K_G] \{\Delta r\} + [\Delta K_G] \{r\} = \{\Delta R\} \quad (4.2.1)$$

Equation 4.2.1 can be written, symbolically, as

$$[K_T] \{\Delta r\} = \{\Delta R\} - [\Delta K_G] \{r\} \quad (4.2.2)$$

which is an incremental equilibrium equation that can be used in the step-by-step elastic-plastic analysis to obtain the complete load-deformation characteristics of a frame.

4.2.1 Incremental First Order Analysis

Consider a frame subjected to two sets of loads, one of which is constant, $\{R_c\}$, while the other, $\{\Delta R_v\}$, varies proportionately. In conducting a first order analysis the geometric stiffness is not considered and Eq. 4.2.2 becomes

$$[K_T] \{\Delta r\} = \{\Delta R\} \quad (4.2.3)$$

in which $[K_T]$ is the tangent stiffness matrix not including the geometric nonlinearity.

The step-by-step, elastic-plastic first order analysis, to obtain the load-deformation response of a frame, can be best described using the following procedure.

- 1 - An elastic analysis is performed based on the original elastic stiffness matrix of the structure. The vectors of nodal displacements $\{r_c\}$ and $\{\Delta r_v\}$ as well as the vectors of member forces $\{Q_c\}$ and $\{\Delta Q_v\}$, due to the two sets of loads considered above, are obtained.
- 2 - The moment capacity of each critical section is calculated as

$$(M_{pv})_i = (M_{pc})_i - (M_c)_i \quad (4.2.4)$$

in which $(M_{pv})_i$ is the moment capacity that would resist the moment at the i th section due to the variable set of loads $\{\Delta R_v\}$, $(M_{pc})_i$ is the plastic moment capacity of the i th section and, $(M_c)_i$ is the moment at the i th section due to the constant set of loads $\{R_c\}$.

- 3 - The load factors λ_i are calculated, for each section, as

$$\lambda_i = \frac{(M_{pv})_i}{(\Delta M_v)_i} \quad (4.2.5)$$

in which $(\Delta M_v)_i$ is the moment at the i th section, due to the variable set of loads, $\{\Delta R_v\}$. The section having the smallest load factor will be the first section to be plastified. This load factor then is called λ_1 which will cause the first hinge to be formed.

- 4 - The applied loads, nodal displacements, and member forces are updated, using the factor λ_1 , as

$$\{R_1\} = \{R_c\} + \lambda_1 \{\Delta R_v\} \quad (4.2.6a)$$

$$\{r_1\} = \{r_c\} + \lambda_1 \{\Delta r_v\} \quad (4.2.6b)$$

and

$$\{Q_1\} = \{Q_c\} + \lambda_1 \{\Delta Q_v\} \quad (4.2.6c)$$

in which $\{R_1\}$, $\{r_1\}$, and $\{Q_1\}$ are vectors of applied loads, nodal displacements, and member forces respectively at the formation of the first plastic hinge.

- 5 - Now the first plastic hinge has been formed. A real hinge is placed at this section and the incremental stiffness matrix of the structure is modified by changing the particular member stiffness matrix where the plastic hinge has appeared.
- 6 - An increment in the variable set of loads $\{\Delta R_v\}$ is applied to the structure and a new elastic analysis is performed on the basis of the modified stiffness matrix. The member forces, nodal displacements and plastic deformations due to the load increment can then be evaluated.
- 7 - The moment capacity remaining in each section may then be calculated as

$$(M_{pv})_i = (M_{pc})_i - (M_1)_i \quad (4.2.7)$$

in which $(M_1)_i$ is the moment at the i th section developed at the formation of the first plastic hinge and can be obtained from the updated vector of member forces $\{Q_1\}$, given in step 4.

- 8 - The search for the next section to be plastified is conducted, as described in step 3, and the applied loads, nodal displacements and member forces are updated accordingly as

$$\{R_2\} = \{R_1\} + \lambda_2 \{\Delta R_v\} \quad (4.2.8a)$$

$$\{r_2\} = \{r_1\} + \lambda_2 \{\Delta r_v\} \quad (4.2.8b)$$

and

$$\{Q_2\} = \{Q_1\} + \lambda_2 \{\Delta Q_v\} \quad (4.2.8c)$$

in which λ_2 is the smallest load factor obtained.

The above procedure is continued until a failure mechanism is formed. The failure criterion, as far as the incremental analysis is concerned, is the singularity of the global tangent stiffness matrix of the structure. When a mechanism forms, a zero element appears on the main diagonal of the triangularized structure stiffness matrix and the solution is completed.

4.2.2 Incremental Second Order Analysis

In the case of a second order analysis, geometric nonlinearity is considered and Eq. 4.2.2 is used. The same procedure for first order analysis, described in Sect. 4.2.1, is used for second order analysis with few changes.

First, a new geometric stiffness matrix $[K_G]$ has to be assembled at the beginning of each load increment. This matrix is a function of the axial forces in the members up to this stage of loading.

The second change, that has to be introduced, is to modify the vector of incremental loads $\{\Delta R_v\}$ to account for the quantity $[\Delta K_G]\{r\}$ in Eq. 4.2.2. The incremental geometric stiffness matrix $[\Delta K_G]$ is a function of the incremental axial forces in the members due to $\{\Delta R_v\}$ while $\{r\}$ is the vector of total nodal displacements obtained from a previous step.

To account for the reduction in plastic moment capacity due to the presence of axial forces in the members, the interaction curve shown in Fig. 4-1 is used. Two alternative methods are suggested. The first method is to estimate, approximately, the final axial force in each member and reduce the moment capacity according to this estimate. The other alternative is to calculate the moment capacity based on the axial force developed at the beginning of the load increment, neglecting any change in this value due to any change in axial force once a hinge has formed at this particular location. Both alternatives suggested above are approximate solutions and result in some error. The second suggestion is adapted in the analysis presented in this section. A more precise method is presented in the following section.

Once the above modifications are introduced, the procedure described in Sect. 4.2.1 is followed until a mechanism is formed. When a mechanism forms the determinant of the decomposed structure stiffness matrix will have a negative sign. At this stage a negative increment in load is applied to the structure to obtain the descending line of load-deformation characteristic, shown in Fig. 1-1 (Curve F).

4.3 The Iterative Method of Analysis

In this section the equilibrium equation, Eq. 3.3.11, is satisfied at each equilibrium position, (i.e. at the formation of each hinge).

4.3.1 First Order Analysis

For first order analysis, the geometric nonlinearity that appears in Eq. 3.3.12 is not considered. In such a case, Eq. 3.3.11 can be written as

$$[K] \{r\} = \{R\} \quad (4.3.1)$$

in which $[K]$ is the elastic stiffness matrix assembled for the entire structure.

The procedure presented in Sect. 4.2.1 can be used here, with Eq. 4.3.1, up to and including step 5. However, the new stiffness matrix in this case, obtained from step 5, is a tangent stiffness matrix.

The loads that produced the first plastic hinge are then applied to the modified structure together with an applied moment equal to the plastic moment capacity, M_{pc} , at the location of the hinge. The first set of loads $\{R_v\}$ increases until the formation of the second hinge while the applied moment which can be assembled into the load vector $\{R_c\}$ is kept constant. It is important to note that because the stiffness matrix is a tangent stiffness, the set of displacements $\{r_v\}$ and $\{r_c\}$ are fictitious displacements. However, the difference is the real displacement vector $\{r\}$ defined in Fig. 4-2.

The maximum moment capacity left in any section after the first hinge was formed can be obtained from Eq. 4.2.4 and the search for the second section to be plastified is based on the smallest factor λ defined by Eq. 4.2.5.

Once λ is determined, the applied loads, nodal displacements and member forces are updated. Also, the constant set of forces $\{R_c\}$ is modified to include the plastic moment capacity as an applied moment at the second hinge preparing for the next equilibrium position.

The above procedure is continued until a mechanism forms.

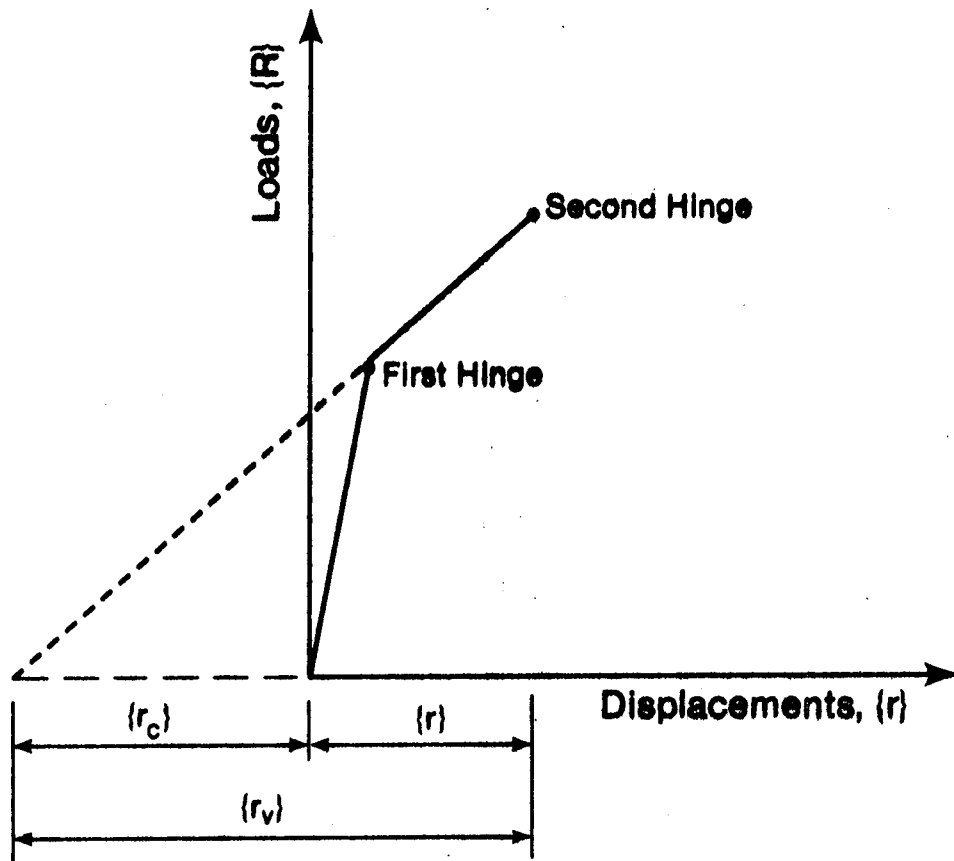


FIGURE 4-2 Load-Deformation Response

4.3.2 Iterative Second Order Analysis

The first order analysis as described in Sect. 4.3.1 neglects the effects of axial forces in the members as they influence the geometric nonlinearity of the structure.

To account for the geometric nonlinearity, the geometric stiffness matrix is included in the analysis (Eq. 3.3.12). In this case, a new geometric stiffness matrix is formed at each load level based on the previous load level. This geometric stiffness matrix is to be corrected through an iterative process up to the new level of loading to be consistent with the updated applied loads $\{R_v\}$.

The reduction in moment capacity M_p due to the presence of axial force P at any section is considered based on the interaction curve shown in Fig. 4-1. The ratio P/P_y at any section is checked to ensure that the moment capacity of the section does not exceed the plastic moment capacity, M_{pc} .

A new moment capacity M_{pc} should be calculated at each iteration to account for the change in the axial forces. Consequently, the constant set of forces $\{R_c\}$, described in Sect. 4.3.1, must be modified in accordance with the new moment capacity, M_{pc} , at each iteration.

The same procedure, described in Sect. 4.3.1, is then used for an iterative second order analysis.

4.4 Comparison Between Incremental and Iterative Approaches

In the incremental method the geometric stiffness matrix is evaluated at the beginning of the load increment as a function of the total axial forces in the members up to this step. In the iterative

approach, however, the geometric stiffness matrix is re-evaluated with each iteration as a function of the total member axial forces. This results in a more accurate geometric stiffness matrix and, consequently, a more accurate solution.

As discussed in Sect. 4.2.2, the incremental procedure does not allow any change in the plastic moment capacity, M_{pc} , of a section due to any change in the axial force, once a hinge has formed at this particular section. Two alternative solutions were suggested in Sect. 4.2.2 to overcome this problem. However, both alternatives are approximate and result in some error when evaluating the load-deformation response of the structure. In the iterative procedure, the plastic moment capacity of each section is re-evaluated with each iteration to account for any change in the axial forces. This results in a more accurate analysis.

The effect of the approximations made in the incremental method will be demonstrated by some example applications in Sect. 4.6.

4.5 Computer Programs

Two computer programs have been developed to solve for the load-deformation characteristics of frames by plastic analysis. The first program performs an incremental plastic analysis of frames, based on the procedure described in Sect. 4.2, and is called INPLAF. The second program performs plastic analysis of frames using the iterative technique, described in Sect. 4.3, and is called PLAFIT. Each program has the option to perform first or second order analysis.

4.6 Elastic-Plastic Solutions

Three example frames are checked in this section using the incremental and iterative procedures presented in Sects. 4.2 and 4.3, respectively. The load-deformation characteristics for each frame are obtained using the different analyses and the results are compared with published results. For each analysis the cpu computer time is given as a measure of the cost of running the program.

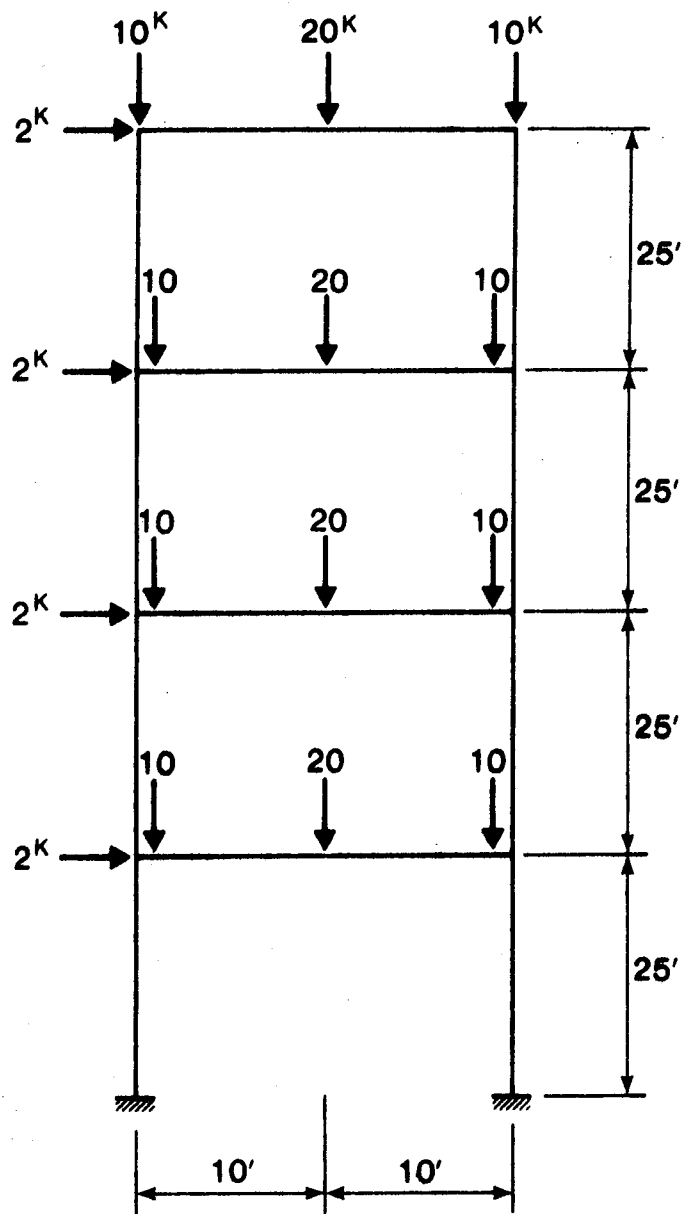
4.6.1 Sample Solutions

EP-1 Four Story Frame

The frame shown in Fig. 4-3 was analyzed by Korn and Galambos (1968). In the analysis the loads were increased proportionately. Figure 4-4 illustrates the load-deformation curves obtained by the different analyses. Curves (1), (2), (3), and (4) represent iterative first order, iterative second order, incremental first order, and incremental second order analysis, respectively. The results obtained by Korn and Galambos (1968) are identical to curves (1) and (2).

The cpu computer time for first order analysis is about 1.7 seconds using the incremental approach and 5 seconds for the iterative approach. For second order analysis the incremental technique used about 1.3 sec. compared to 20 sec. for the iterative technique.

As can be observed from Fig. 4-4 the incremental second order analysis (curve 4) is considerably different from the iterative second order analysis (curve 2). This difference basically occurs during the formation of the first hinge as the geometric stiffness matrix in the incremental analysis is formulated at the beginning of the load increment which in this case results in a null geometric stiffness matrix.



All Members are Fictitious

$$A = 11.75 \text{ in}^2$$

$$I = 144 \text{ in}^4$$

$$M_p = 160 \text{ ft} \cdot \text{K}$$

$$E = 30,000 \text{ Ksi}$$

$$\sigma_y = 36 \text{ Ksi}$$

FIGURE 4-3 Frame EP-1

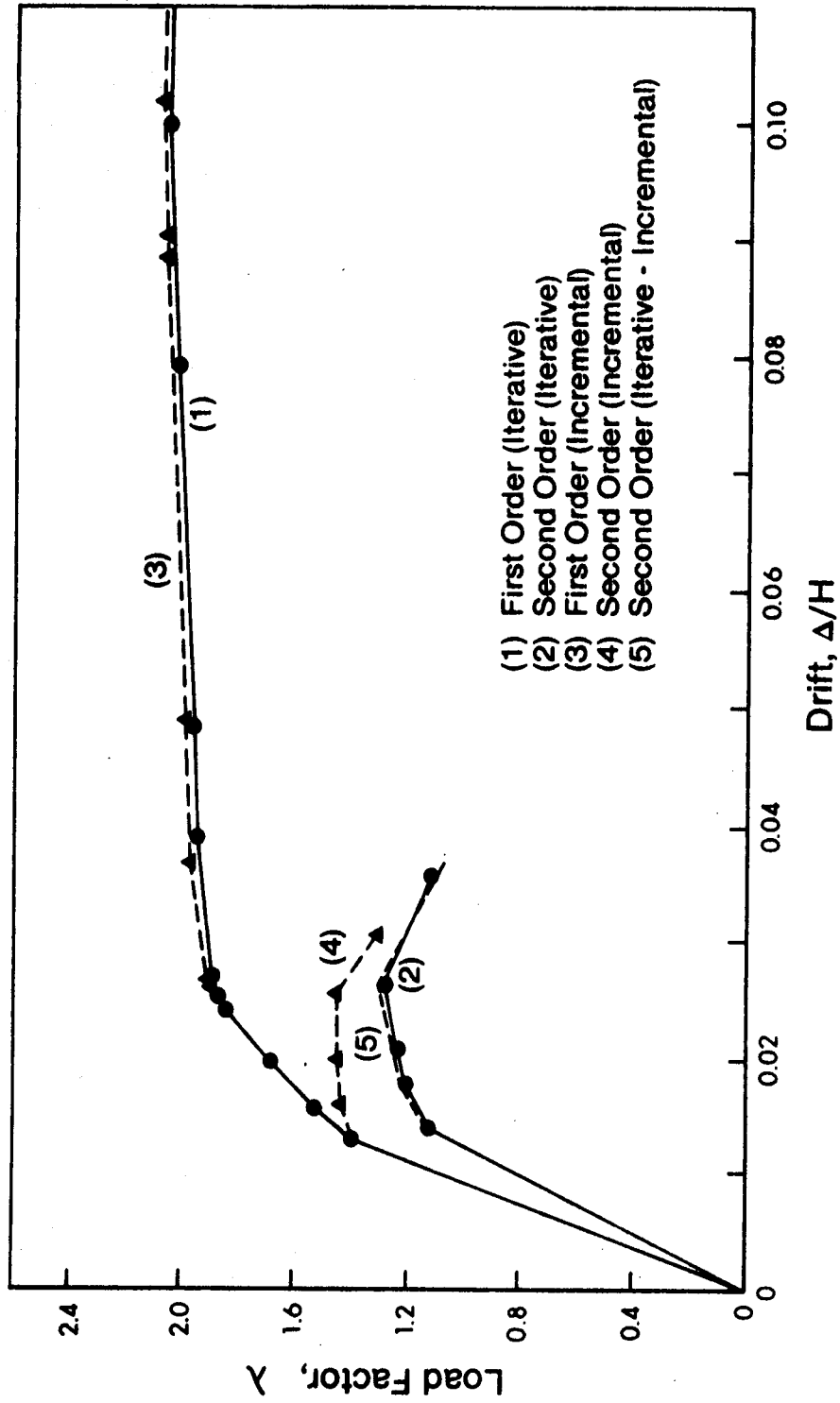


FIGURE 4-4 Load-Deformation Relationship for Frame EP-1

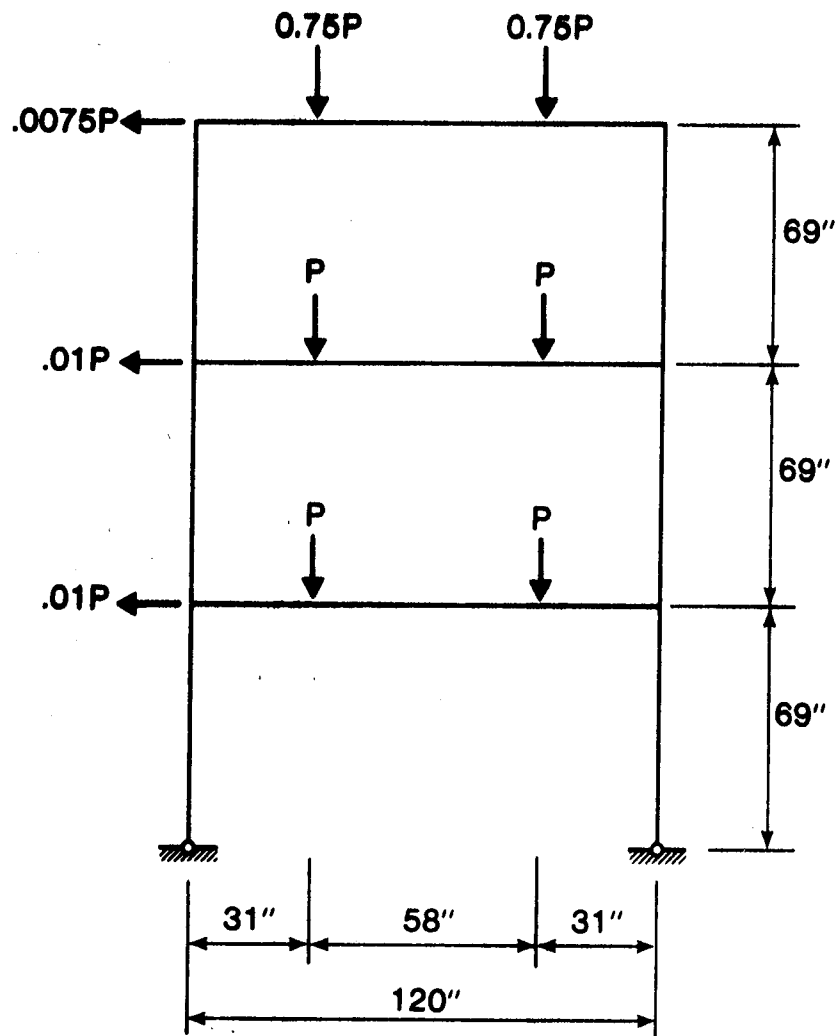
At this stage it was thought that better results could be obtained if an iterative procedure were applied only up to the development of the first hinge followed by an incremental procedure up to the collapse mechanism. This procedure, which may be called iterative-incremental second order analysis, results in a load-deformation relationship given by curve (5) in Fig. 4-4 and compares favorably to curve (2). The cpu computer time used to obtain curve (5) is about 5 sec. which is considerably less than that used to obtain curve (2).

EP-2 Three Story Frame

McNamee and Lu (1972) performed a second order analysis on the frame shown in Fig. 4-5 increasing the loads proportionally. The load-deflection curve they obtained is curve (2) in Fig. 4-6. Curves (1) and (3) represent the iterative and incremental second order analysis, respectively, presented in this chapter. While the cpu computer time for the iterative technique is about 4 seconds, it is 1.2 sec. for the incremental technique. It is important to note that an iterative-incremental analysis, suggested in the previous example, results in a load-deflection curve identical to curve (1) and uses only about 2 sec. cpu computer time.

EP-3 One Story Three Bay Frame

In the frame shown in Fig. 4-7 the vertical loads, P , are kept constant while increasing the horizontal force, H . The results of first and second order analyses presented by Galambos and Lay (1965) are given as curves (3) and (6), respectively, in Fig. 4-8. The present study gives an iterative first order analysis (curve 1) and an incremental first order analysis (curve 2) which are almost identical. The cpu time



Beams W6 x 16 (A36 steel)
Columns W4 x 13 (A441 steel)

FIGURE 4-5 Frame EP-2

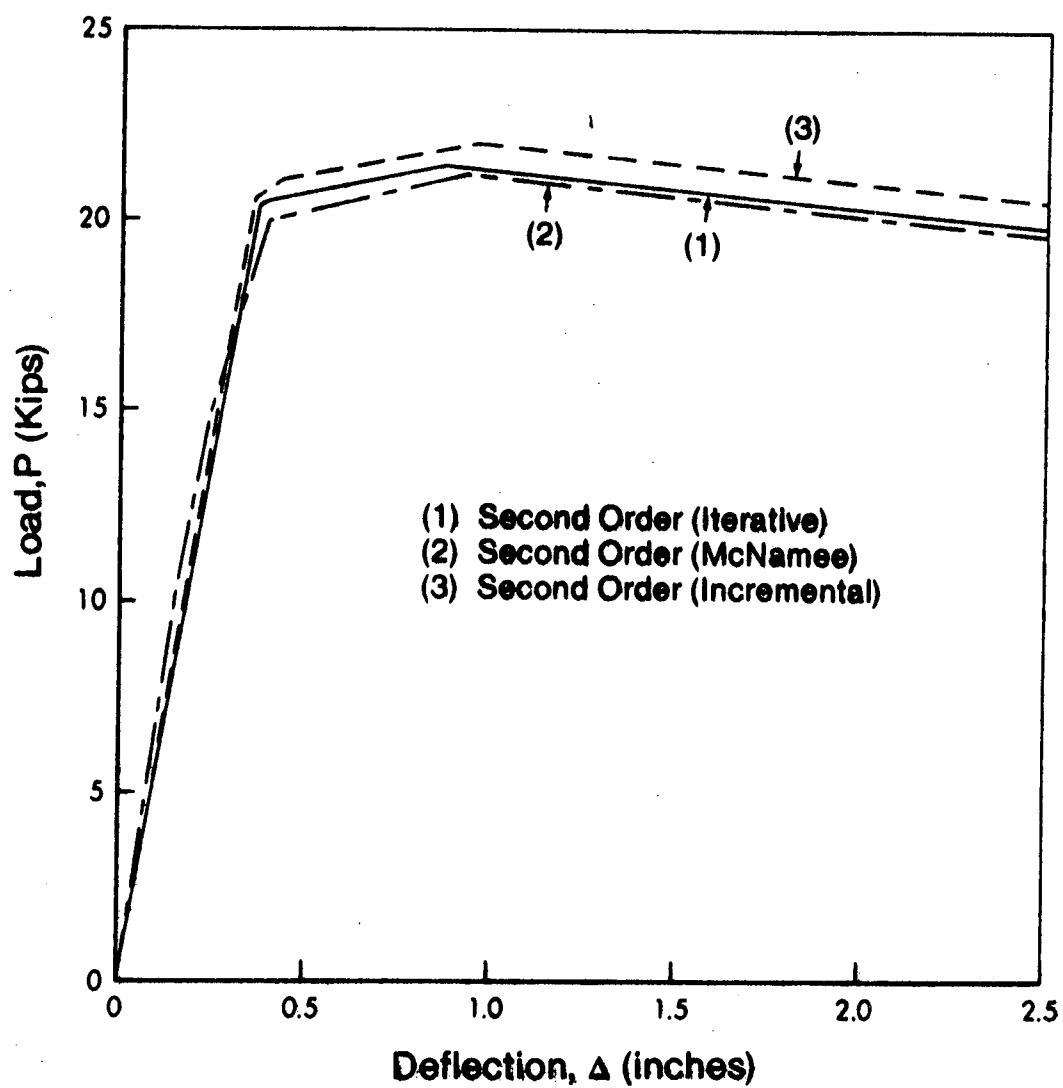
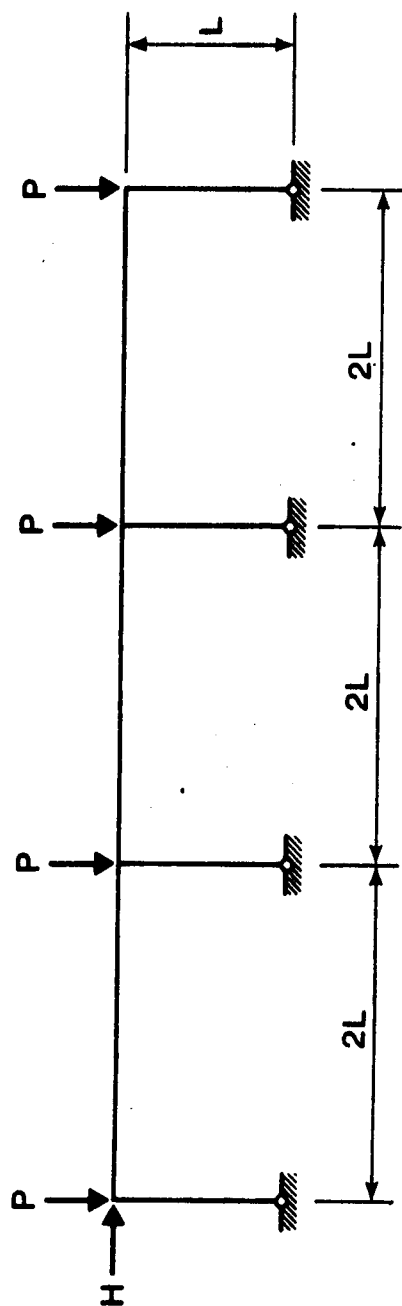


FIGURE 4-6 Load-Deflection Curve for Frame EP-2



All Members are W8 x 31

$$P = 0.3P_y$$

$$L = 104''$$

$$\sigma_y = 33 \text{ Ksi}$$

$$E = 30,000 \text{ Ksi}$$

FIGURE 4-7 Frame EP-3

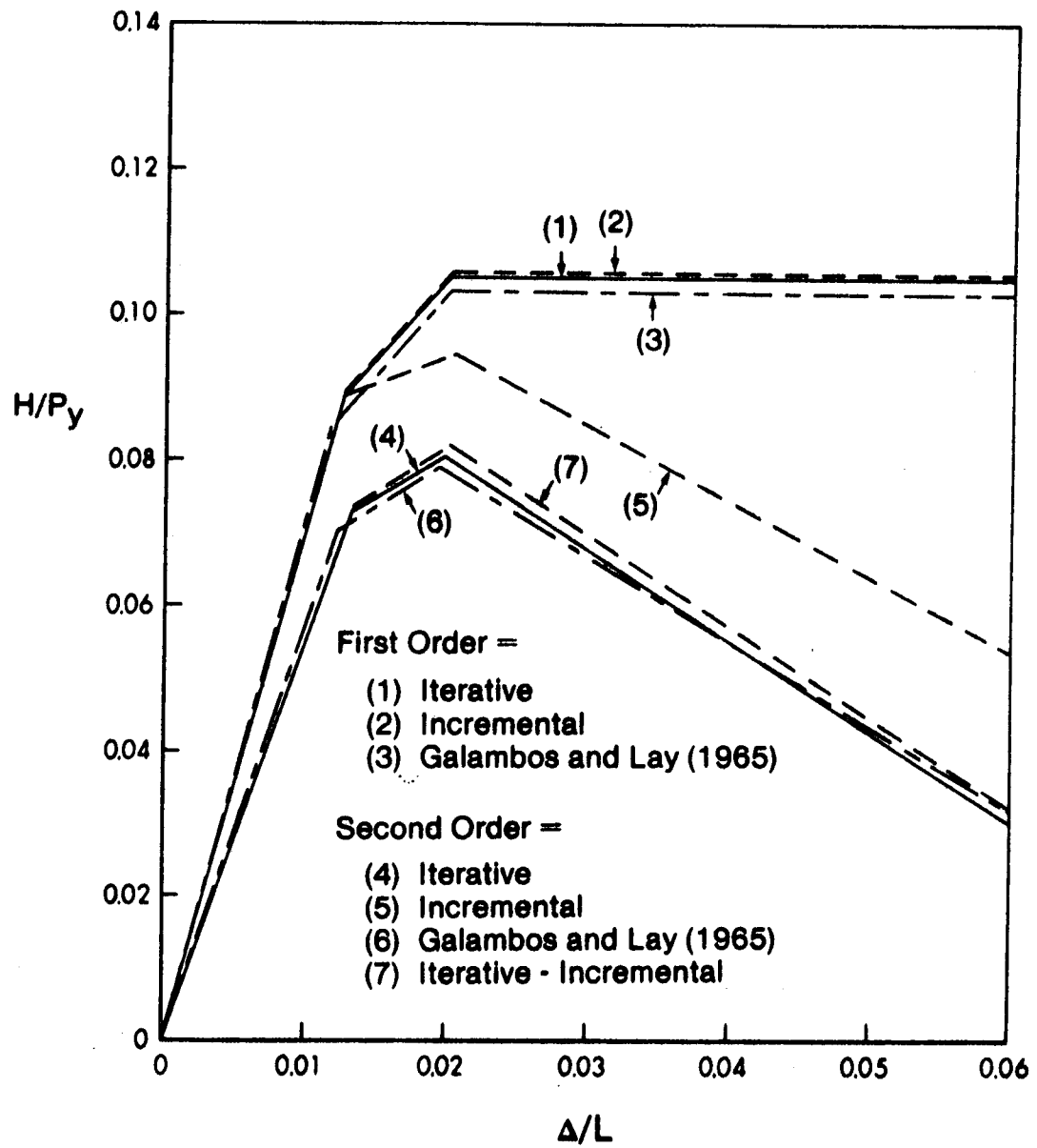


FIGURE 4-8 Load-Deformation Characteristics for Frame EP-3

is about 0.6 sec. for the iterative technique and 0.45 sec. for the incremental one.

The second order analyses result in curves (4) and (5) representing the iterative and incremental technique, respectively. The cpu computer time is about 2.4 sec. and .90 sec. for the iterative and incremental technique, respectively. When an iterative-incremental procedure is performed curve (7) is obtained with a cpu time of 1.4 sec.

4.6.2 Comments on Results

The examples presented above indicate that the iterative method of analysis, presented in Sect. 4.3, exhibits good results. However, an iterative method up to the development of the first hinge followed by an incremental procedure until collapse gives approximately the same results and does not cost as much as the iterative method.

CHAPTER V

NONLINEAR INELASTIC FORMULATION AND SOLUTIONS

Nonlinear formulations relating kinematic and mechanical variables may fall into one of the three categories: geometric nonlinearity, material nonlinearity, or combined geometric and material nonlinearities. The formulation presented in Chapter 3 falls into the first category while this chapter is devoted to problems falling into the third one.

In this chapter an inelastic stability analysis of multistory frames is presented based on a stiffness formulation which accounts for geometric as well as material nonlinearity. The formulation is an extension of that presented in Sect. 3.5 to include material nonlinearity. The formulation results in finite element equations and the Newton-Raphson method is then used to solve for the overall load-deformation characteristics of the structure.

In the analysis presented herein, the effect of axial load on the stiffness and strength of the individual members is considered. Partial plastification of sections is taken into account. The influence of residual stresses as well as strain hardening of the material is included in the analysis. The formulation also permits consideration of extended regions of plastic deformations rather than discrete hinges in beams and beam-columns.

Also in this chapter, the formulation is checked by comparing computed results with some of the available experimental test results.

5.1 Basic Formulation for Inelastic Behavior

Equation 3.5.14 is the basic incremental equilibrium equation, derived in Sect. 3.5.1, and is applicable to elastic and inelastic response. Equation 3.5.14 can be written in matrix form, for inelastic response, as

$$[k_T^I] \{\Delta q\} = \{\Delta Q^I\} \quad (5.1.1)$$

in which $[k_T^I]$ is the inelastic element tangent stiffness matrix and is a function of geometric and material nonlinearities and $\{\Delta Q^I\}$ is the vector of incremental forces, evaluated for an inelastic element.

The difference between the equilibrium equation for an elastic element, Eq. 3.5.15, and that for an inelastic element, Eq. 5.1.1, basically arises in the evaluation of the tangent stiffness matrix and the incremental load vector.

5.1.1 Main Assumptions

In deriving the tangent stiffness for a partially plastic section, it is assumed that no strain reversal occurs. If one considers a section which has already yielded and an infinitesimal increment in bending moment is applied, the resistance to this moment is a measure of incremental bending stiffness. The yielded zones increase somewhat, while some strain reversal may take place in the already yielded zones. These effects are neglected in this study and the additional moment is assumed to be resisted by all parts of the cross section with the stress increment determined from the tangent modulus of the material at the current value of strain. The section properties relating increments in stress resultants to increments in displacements may then be computed

by a transformed area concept as described in Sect. D.1. This concept is applicable to thin wall open beam sections since the stress is essentially uniaxial and the effect of shear stress on the principal stresses may be neglected.

5.1.2 Evaluation of Incremental Forces $\{\Delta Q^I\}$

To evaluate the vector of incremental forces $\{\Delta Q^I\}$, in Eq. 5.1.1, it is necessary to evaluate the stress resultants n , m , and m^* , defined by Eqs. 3.5.9, at any section prior to the load increment. Equations B.3.4 and B.3.11 give the vectors of incremental forces, for a flexural element and truss element, respectively, assuming an elastic response. The same equations are applicable to inelastic response provided that the stress resultants are evaluated by direct integration of stresses as detailed in Appendix D, Eqs. D.3.1 through D.3.3.

5.1.3 Evaluation of Element Tangent Stiffness Matrix

The element tangent stiffness matrix for an elastic element is given by Eq. B.4.4 for a flexural element, and by Eq. B.4.11 for a truss element. These equations are applied to inelastic response with two modifications.

First the stress resultants n , m and m^* are numerically evaluated by direct integration of stresses (Eqs. D.3.1b, D.3.2b, and D.3.3b).

The second modification that should be introduced for inelastic analysis is in the evaluation of the incremental stress resultants $\frac{\partial n}{\partial q_j}$, $\frac{\partial m}{\partial q_j}$, and $\frac{\partial m^*}{\partial q_j}$. These increments are evaluated in detail in Sect. B.2 for an elastic element. For an inelastic element detailed evaluation of the incremental stress resultants is given in Appendix E

and the incremental stress resultant vectors are given in Tables E-1 and E-2 for a flexural element and a truss element, respectively.

Once the stress resultants are evaluated and the incremental stress resultant vectors are formed the same formulation, presented in Sect. B.4 to derive the elastic tangent stiffness matrix can be used to derive the inelastic tangent stiffness matrix for an inelastic element. It should be noted that the finite element shape functions selected for an elastic analysis (Eqs. A.2.3) are also applicable to inelastic response evaluation.

5.2 Transformation and Assembly

The incremental equilibrium equation (Eq. 5.1.1) is formulated in the y-z coordinate directions which are the reference axes of the member. The local incremental displacements $\{\Delta q\}$ may be related to the incremental displacements in the global system $\{\Delta r\}$ for a typical element by the transformation matrices given in Tables 3-5 and 3-6 for a flexural element and a truss element, respectively. Assembly of the incremental equilibrium equation then proceeds by the direct stiffness method, presented in Sect. 3.3.2, to yield

$$[K_T^I] \{\Delta r\} = \{\Delta R^I\} \quad (5.2.1)$$

in which $[K_T^I]$ is the inelastic tangent stiffness matrix for the entire structure and is obtained by direct addition, $\{\Delta r\}$ is the assembled vector of incremental displacements, and $\{\Delta R^I\}$ is the assembled vector of incremental forces (called the unbalanced load vector).

Equation 5.2.1 is the equilibrium equation for the structure and becomes the basis for the Newton-Raphson solution.

5.3 Newton-Raphson With Gradient Test

The Newton-Raphson technique, described in Sect. 3.5.4, is used in this chapter to trace the behavior of inelastic structures. The procedure is identical to that of Sect. 3.5.4 except for the detailed evaluation of tangent stiffness matrix and the vector of unbalanced forces. The computational procedure and the associated incremental equilibrium equation (Eq. 5.2.1) are applicable up to the peak of the load-deflection curve.

To be able to trace the load-deflection characteristics beyond the peak of the curve, a special treatment must be adapted (Rajasekaran and Murray 1973). The descending branch of the load-deflection curve in the inelastic region is characterized by a negative definite stiffness matrix. This means that the structure can only withstand a decrease in the load.

To obtain the descending branch of the load-deflection curve, the determinant of the tangent stiffness matrix is checked for sign change to determine if the stiffness matrix is still positive definite. If this sign is negative the load is decremented. The test for sign is called a 'gradient test' and will determine exactly where to start decreasing the applied loads in order to maintain equilibrium.

5.4 Residual Stresses and Strain Hardening of the Material

Residual stresses are caused by a variety of factors and in some cases they may be as large as the yield stresses (Huber and Beedle 1954; Tall 1964). They are a result of thermal effects and plastic deformation during the manufacturing process. Tall (1964), Huber and

Beedle (1954), and Beedle and Tall (1960) provide a large number of illustrations showing the measured residual stresses caused by hot rolling, welding, or flange cutting for steel cross sections of various shapes and sizes.

In this investigation residual stresses are considered. These may have a considerable effect on the behavior of the structure, especially during the transition from the fully elastic to the partly yielded condition. Full treatment of residual stresses is discussed in Sect. D.1.

In most of the elastic-plastic formulations developed for frame analysis the material is assumed to be ideally elastic-plastic and the influence of strain hardening on the ultimate load is neglected. In the formulation presented in this chapter an attempt is made to include the strain hardening of the material in the analysis. In this case the idealized stress-strain relationship shown in Fig. D-2 is assumed. The treatment is detailed in Appendix D (Sect. D.1).

5.5 Plastification of the End Zones

Because of the distribution of the Gauss sampling points, discussed in Sect. B.3.1, plastification at the ends of members does not immediately show its effect on the element tangent stiffness matrix when treating each member as one element. For this reason better results may be obtained by subdividing the member into three elements with the central element being 80% of the length of the member. The result is that a number of Gauss points are located on each end within the outer 10% of member length. Therefore, the influence of inelastic strains is felt shortly after they are initiated at the member ends.

An element tangent stiffness matrix is formed for each element and a static condensation scheme, developed by Elwi and Murray (1977) is used to eliminate the internal degrees of freedom and to then assemble only the member end degrees of freedom into the structure stiffness matrix.

5.6 Computer Program

A computer program, called Inelastic Stability Analysis of Frames (INSTAF), has been developed to solve for the load-deformation characteristics of an inelastic structure. The program can analyze braced and unbraced frames and has the provision of including residual stresses and strain hardening of the material in the analysis.

5.7 Inelastic Solutions

To demonstrate the accuracy and to test the efficiency of the inelastic formulation presented in this chapter, some of the available experimental test results are checked using the computer program. The results are presented in this section.

5.7.1 Sample Examples

IN-1 Beam-Column Test

A W4 x 13 beam-column was tested by Van Kuren and Galambos (1964), in which the axial load, P , was kept constant while the applied moment, M_o , was increased until failure took place. Figure 5-1 shows the comparison between the test results (curve 1) and the theoretical moment-rotation curve obtained using the present formulation (curve 2). Residual stress data were not given by Van Kuren and Galambos and therefore

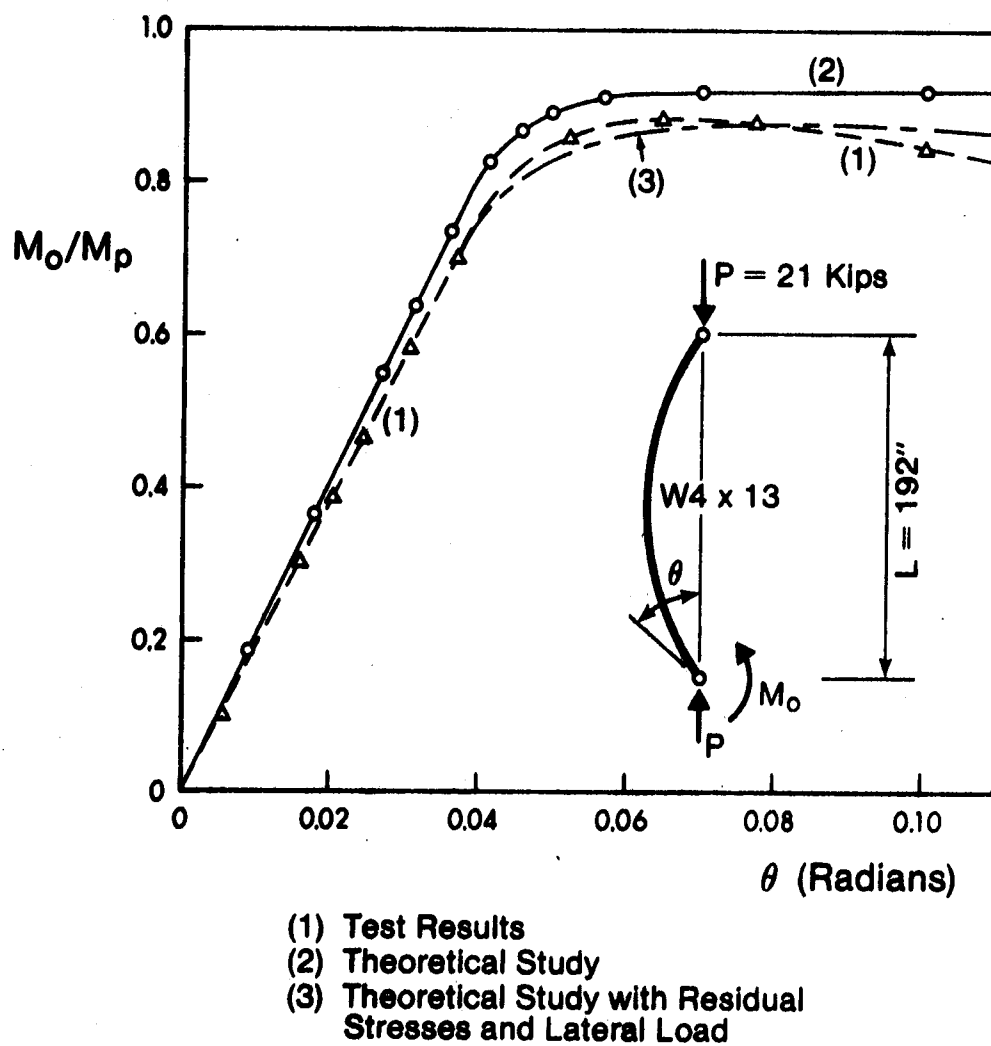


FIGURE 5-1 Results of Example IN-1

were not included in the theoretical study. This may explain the difference in ultimate capacities between the two curves. The fact that the slopes of the moment-rotation curves are different indicates that there was geometric imperfection in the member before testing. Using an analysis of the beam-column where a small lateral load (0.001 kips) was applied at midspan, the geometric imperfection was simulated. An assumed residual stress distribution was used, with a maximum compressive value of $0.3 \sigma_y$. The analysis gave curve 3, which compares favorably to the test results.

Twelve load increments were used to draw the complete moment-rotation curve, obtained in the present analysis, with an average of 5 iterations for each load increment and 0.15 second per iteration.

IN-2 One Story Frame with Fixed Base

The one story-one bay frame shown in Fig. 5-2 was tested by Arnold *et al.* (1968). The mechanical and member properties are given in Tables 5-1 and 5-2 respectively. Two sets of load were applied to the frame. The vertical set of load was kept constant while increasing the lateral load, H. Figure 5-4 illustrates the results obtained using different formulations. The load-deformation curves (1), (2), (3) and (4) represent the inelastic analysis presented in this chapter, the experimental test results, the second order elastic-plastic analysis and the first order elastic-plastic analysis, respectively. In the inelastic analysis the effects of residual stresses and strain hardening were considered. These effects are not included in the elastic-plastic analyses which were performed using the iterative method, described in Sect. 4.3. The results show good agreement between the behavior of the frame tested and the inelastic analysis.

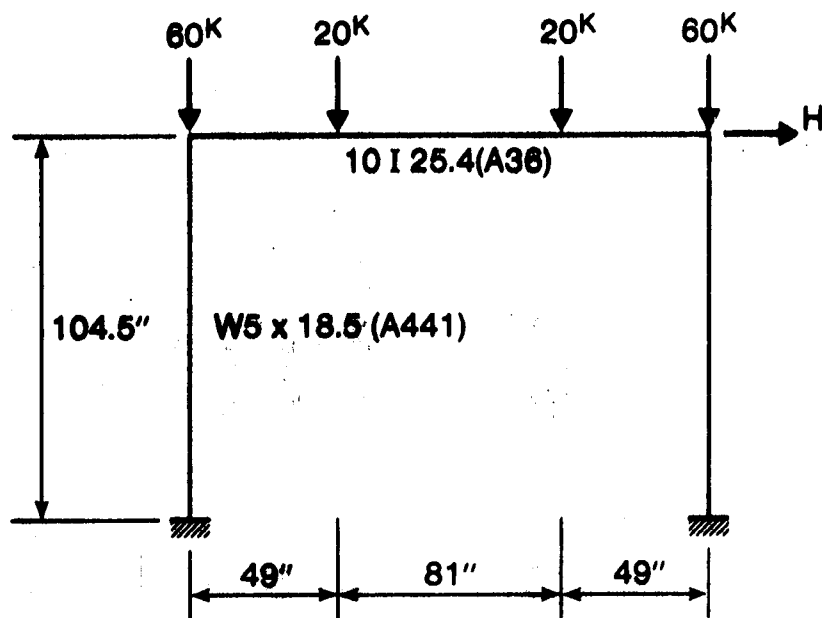


FIGURE 5-2 Example Frame IN-2

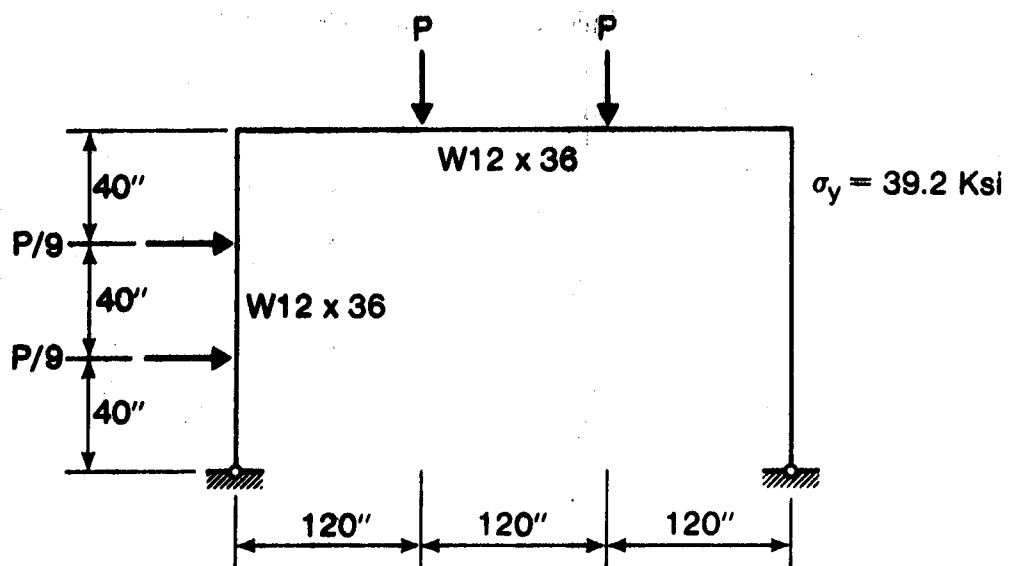


FIGURE 5-3 Example Frame IN-3

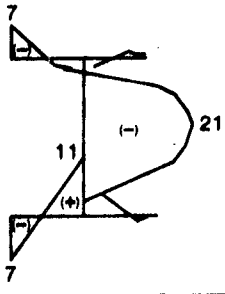
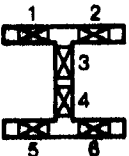
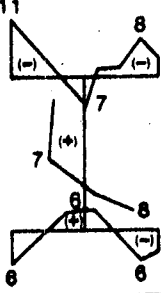
| Section | Specimen No. | σ_y ksi | ϵ_y | ϵ_{st} | Est ksi | σ_{ult} ksi | Elong % | Residual Stresses ksi (Tension +) |
|-----------|---|-------------------|--------------|-----------------|------------|-----------------------|------------|--|
| 10I25.4 | 1 | 37.5 | .00127 | .0182 | 732 | 64.7 | 28.8 |  |
| | 2 | 37.1 | .126 | .186 | 620 | 63.8 | 30.6 | |
| | 3 | 40.7 | .138 | .184 | 762 | 67.8 | 28.2 | |
| | 4 | 41.5 | .141 | .204 | 645 | 68.0 | 26.9 | |
| | 5 | 37.0 | .126 | .180 | 752 | 63.4 | 28.2 | |
| | 6 | 37.6 | .127 | .191 | 630 | 64.0 | 29.4 | |
| 5 WF 18.5 |  | | | | | | |  |
| | 1 | 56.3 | .00191 | — | — | 83.5 | 20.9 | |
| | 2 | 56.0 | .190 | .0184 | 677 | 81.2 | 19.4 | |
| | 3 | 56.0 | .140 | .172 | 594 | 83.0 | 20.0 | |
| | 4 | 56.6 | .192 | .177 | 896 | 82.4 | 20.0 | |
| | 5 | 56.8 | .189 | .176 | 648 | 81.2 | 21.0 | |
| | 6 | 56.3 | .191 | .195 | 718 | 81.4 | 21.2 | |

TABLE 5-1 Mechanical Properties

| Section | b, in inches | d, in inches | t, in inches | w, in inches | $\frac{b}{t}$ | $\frac{d}{w}$ | L or h, in inches | r_x , in inches | r_y , in inches | σ_y , in kips per square inch | M_p , in kip- inches | M_{pc} , in kip- inches | Z, in cubic inches |
|---------|--------------------|--------------------|--------------------|--------------------|---------------|---------------|-------------------------|-------------------------|-------------------------|--|---------------------------------|------------------------------------|-----------------------------|
| 10I25.4 | 4.660 | 10.00 | 0.491 | 0.310 | 9.49 | 32.3 | 179.0 | 4.07 | 0.97 | 38.57 | 1070.6 | — | 26.0 |
| 5WF18.5 | 5.025 | 5.12 | 0.420 | 0.265 | 11.96 | 19.3 | 104.5 | 2.16 | 1.28 | 56.17 | 640.34 | 558.4 | 11.4 |

TABLE 5-2 Member Properties

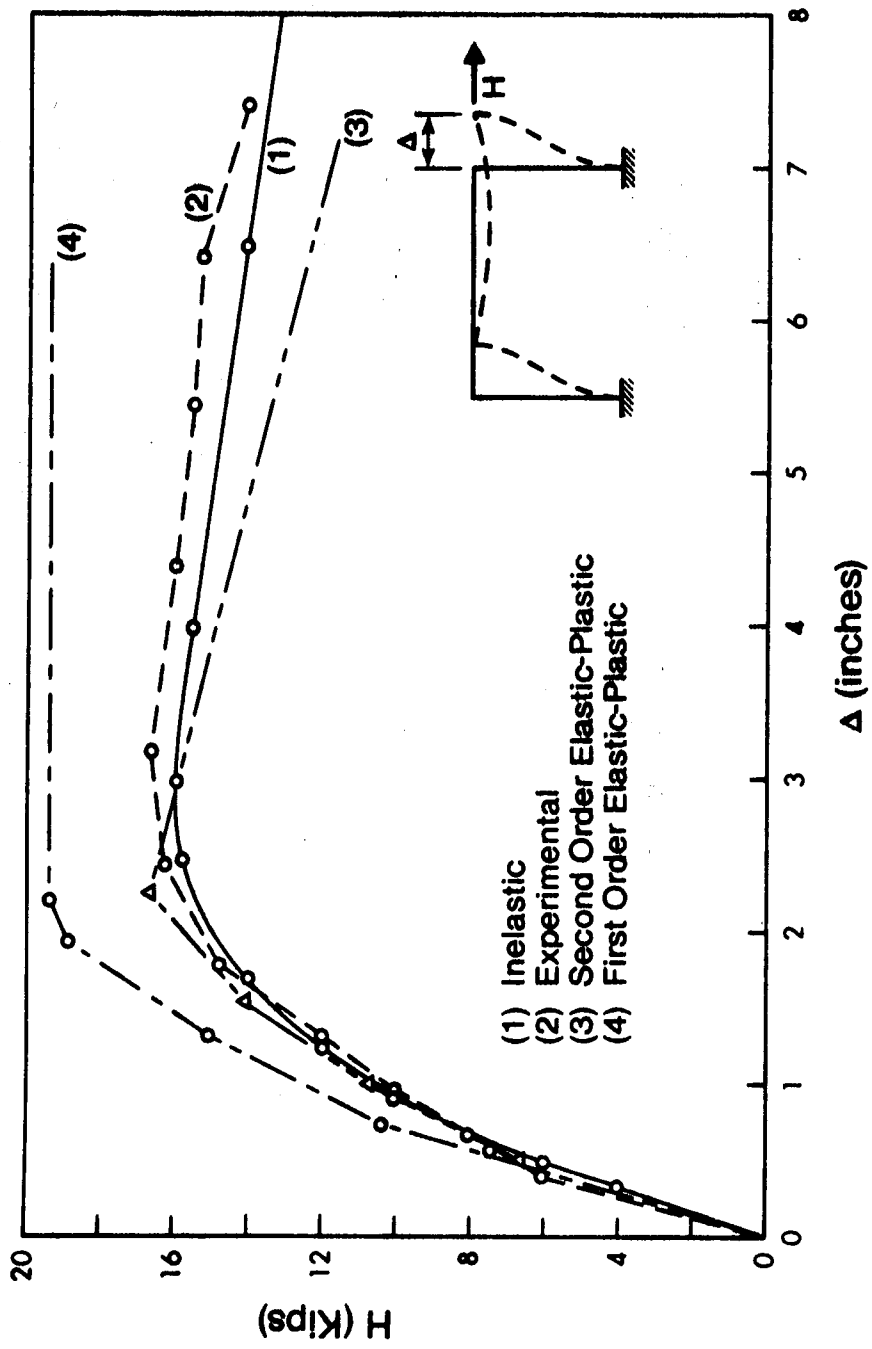


FIGURE 5-4 Load-Deformation Curves of Frame IN-2

IN-3 One Story Frame With Hinged Base

Schilling *et al.* (1956) tested the frame shown in Fig. 5-3. During the test the applied loads on the frame were increased proportionally. Good agreement between the test results (curve 2) and the inelastic analysis (curve 1) is observed from Fig. 5-5. The figure also shows the first order elastic-plastic analysis (curve 4) and the second order elastic-plastic analysis (curve 3), obtained using the iterative solution presented in Sect. 4.3.

In examples IN-2 and IN-3 about twelve load increments were needed in the inelastic analysis to obtain the load-deformation characteristics of the frames. The average number of iterations was 5 iterations for each load increment with an average of 0.25 second per iteration.

5.7.2 Comments on Results

Results obtained from the inelastic analysis compare favorably to the experimental test results available. The results show the capability of the computer program to analyze inelastic frame problems efficiently.

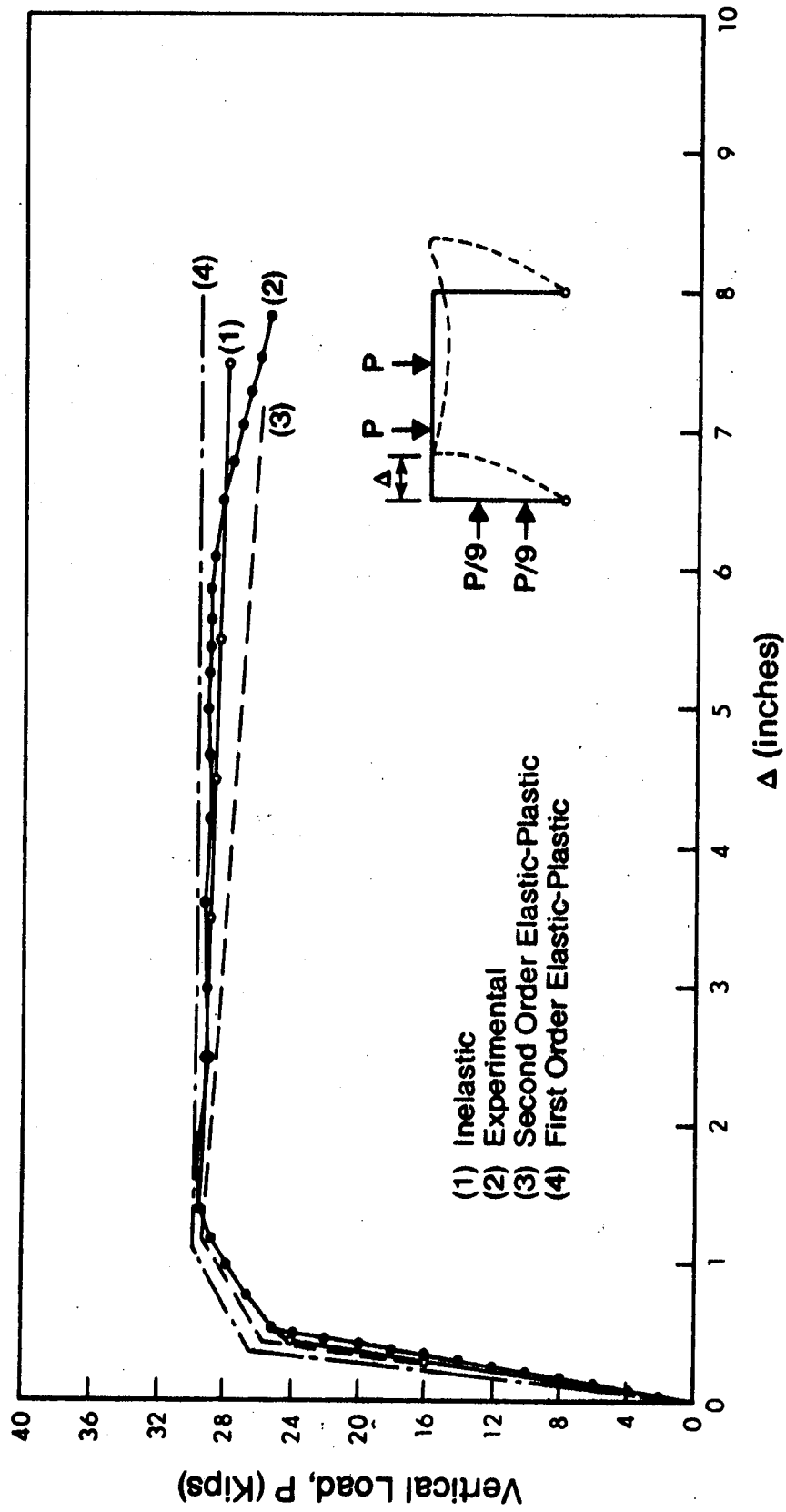


FIGURE 5-5 Load-Deformation Curve of Frame IN-3

CHAPTER VI

BEHAVIORAL STUDIES

In Chapter 5 an inelastic stability analysis based on a stiffness formulation was presented. The validity of the theory was then evaluated by comparing the results with some sample problems. The primary objective of this chapter is to compare the results obtained using the formulation given in Chapter 5 with those of the simple plastic theory given in Chapter 4 (i.e. elastic-plastic analysis). To this end, a cantilever beam-column and single story frames have been analyzed.

In addition to the basic study outlined above, the effects of residual stresses and strain hardening on the behavior of single story and multistory frames are examined. Although these effects have been investigated by many researchers, their influence on frame behavior and strength has not been considered in detail.

Mild steel with a yield stress of 36 ksi is used in the following analyses, unless otherwise specified. A maximum compressive residual stress of $\sigma_R = 0.3 \sigma_y$ is considered, and the residual strain distribution shown in Fig. D-1b is assumed. A strain hardening modulus of 900 ksi is used, and the strain-hardening strain is assumed equal to twelve times the yield strain. Although the strain hardening modulus is rather high it is thought to represent commercially available structural steel grades.

6.1 Behavioral Study of a Beam-Column

The cantilever beam-column shown in Fig. 6-1 is used in this study. The axial force, P , is kept constant, while the lateral load, Q , is increased monotonically.

6.1.1 Inelastic Analysis Vs. Rajasekaran's Method

This example problem was previously analyzed by Rajasekaran (1971) for a slenderness ratio ($\frac{L}{r}$) equal to 14.4 and P/P_y of 0.6. Rajasekaran used an iterative incremental technique based on an equilibrium balance to solve for inelastic beam-column problems. Figure 6-2 shows the load-deformation curves that were obtained using different solution approaches. It should be noted that in the inelastic analysis, the residual stresses are not considered. The results obtained by Rajasekaran are identical to curves 3 and 4 which were obtained using the present analysis.

6.1.2 Inelastic Vs. Elastic-Plastic Analysis

To compare the inelastic method to the elastic-plastic solution, the cantilever shown in Fig. 6-1 was analyzed using each method. In each approach the axial force was kept constant and the corresponding ultimate value of Q is calculated using the inelastic as well as the elastic-plastic analysis. In the inelastic approach, however, residual stresses and strain hardening are not considered, as they are not accounted for in the elastic-plastic formulation. The ratio p between the ultimate values of Q obtained by the two methods has then been computed as

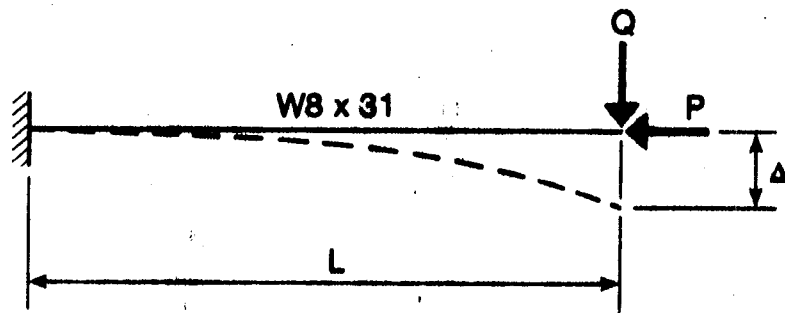


FIGURE 6-1 Cantilever Beam - Column

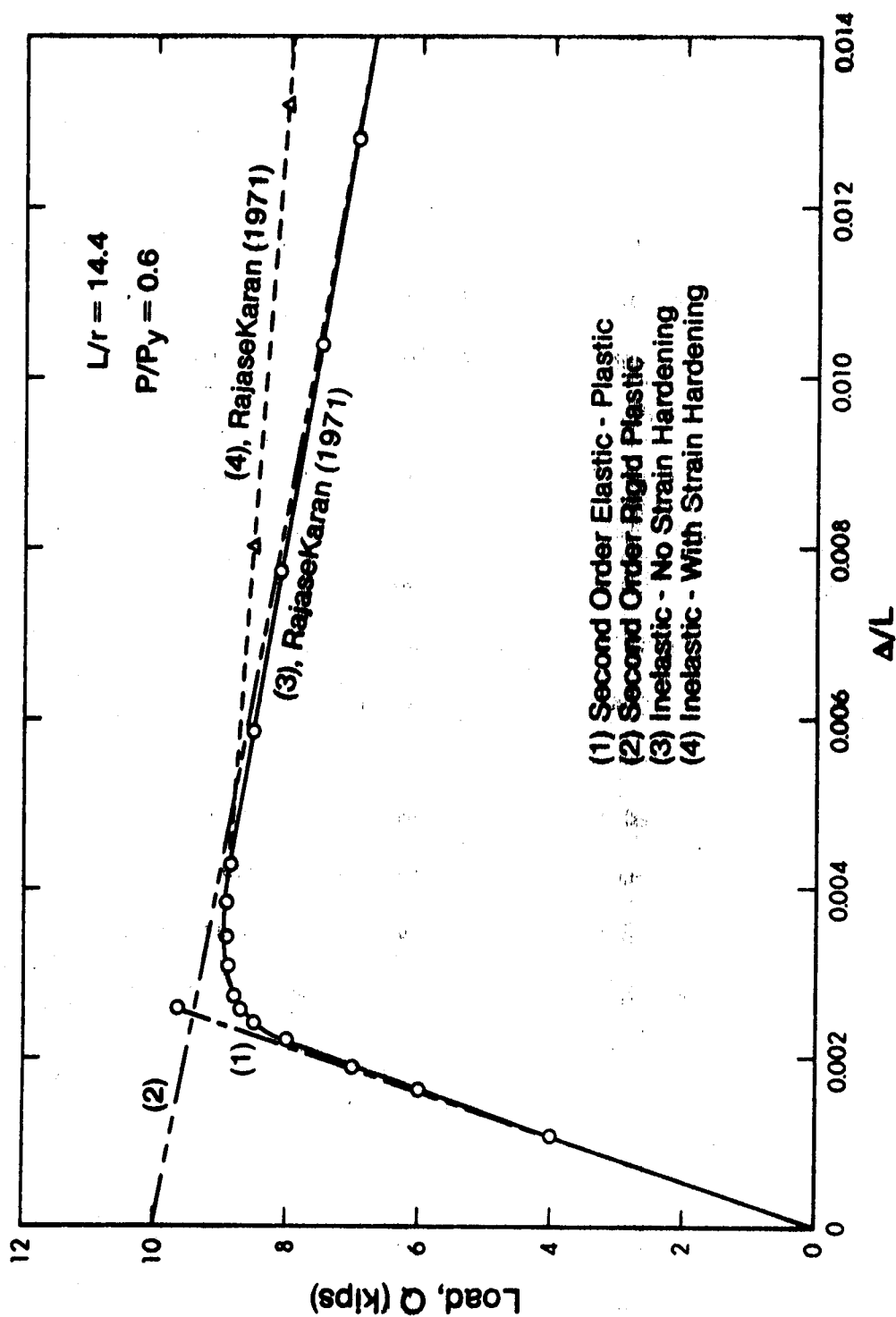


FIGURE 6-2 Inelastic Vs. Rajasekaran (1971)

$$p = \frac{(Q_u)_{in}}{(Q_u)_{el-pl}} \times 100 \text{ (in percent)} \quad (6.1.1)$$

in which $(Q_u)_{in}$ and $(Q_u)_{el-pl}$ are the ultimate values of Q obtained using the inelastic and the elastic-plastic analysis, respectively. Figure 6-3 shows the relationship between p and P/P_y for different values of L/r . The results show that the ultimate lateral load as predicted by the inelastic analysis is less than that obtained from the elastic-plastic approach. The plot also shows that p is a function of L/r and P/P_y .

The conclusions that can be drawn from Fig. 6-3 may be misleading. The figure actually compares the lateral strength of the cantilever, as predicted by the inelastic solution, to that obtained from the elastic-plastic approach. The overall strength of the cantilever as predicted by both methods is analyzed more appropriately through interaction curves as shown in Fig. 6-3a. In these curves the nondimensionalized first order moment, QL_c/M_p , at the maximum strength of the beam-column, is plotted against the nondimensionalized axial load, P/P_y . Figure 6-3a indicates that the difference between the overall strength given by the inelastic method and that obtained from the elastic-plastic analysis is very small. The reason for the difference in results between the two solutions will be examined in Chapter 7 (Sect. 7.2)

6.1.3 Effects of Residual Stresses and Strain Hardening

A cantilever beam-column with different L/r -values is used to study the effects of residual stresses and strain hardening. The data are illustrated in Figs. 6-4 through 6-7. These figures

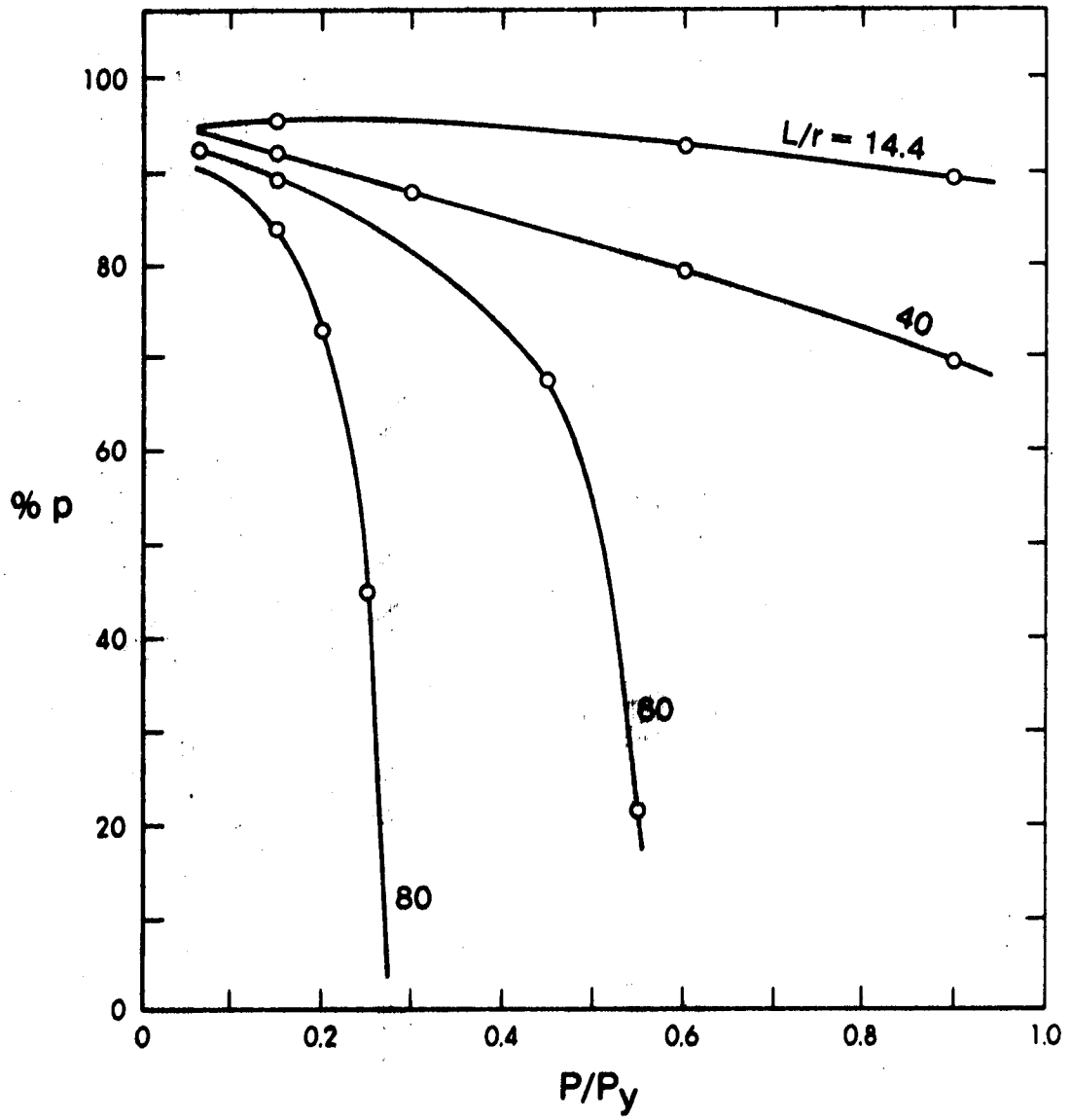


FIGURE 6-3 Inelastic Vs. Elastic-Plastic (Cantilever)

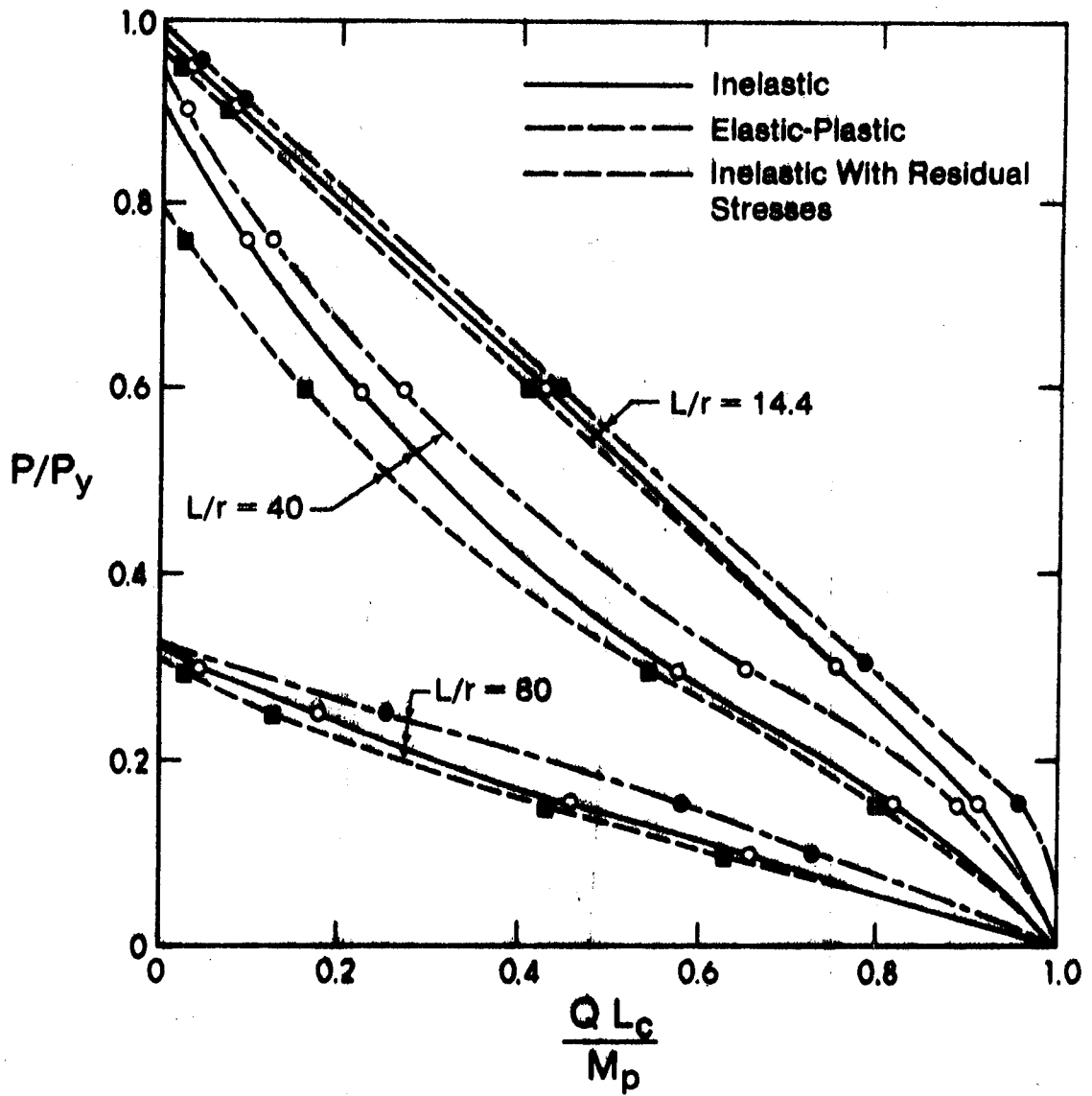


Figure 6-3a. Column Interaction Curves

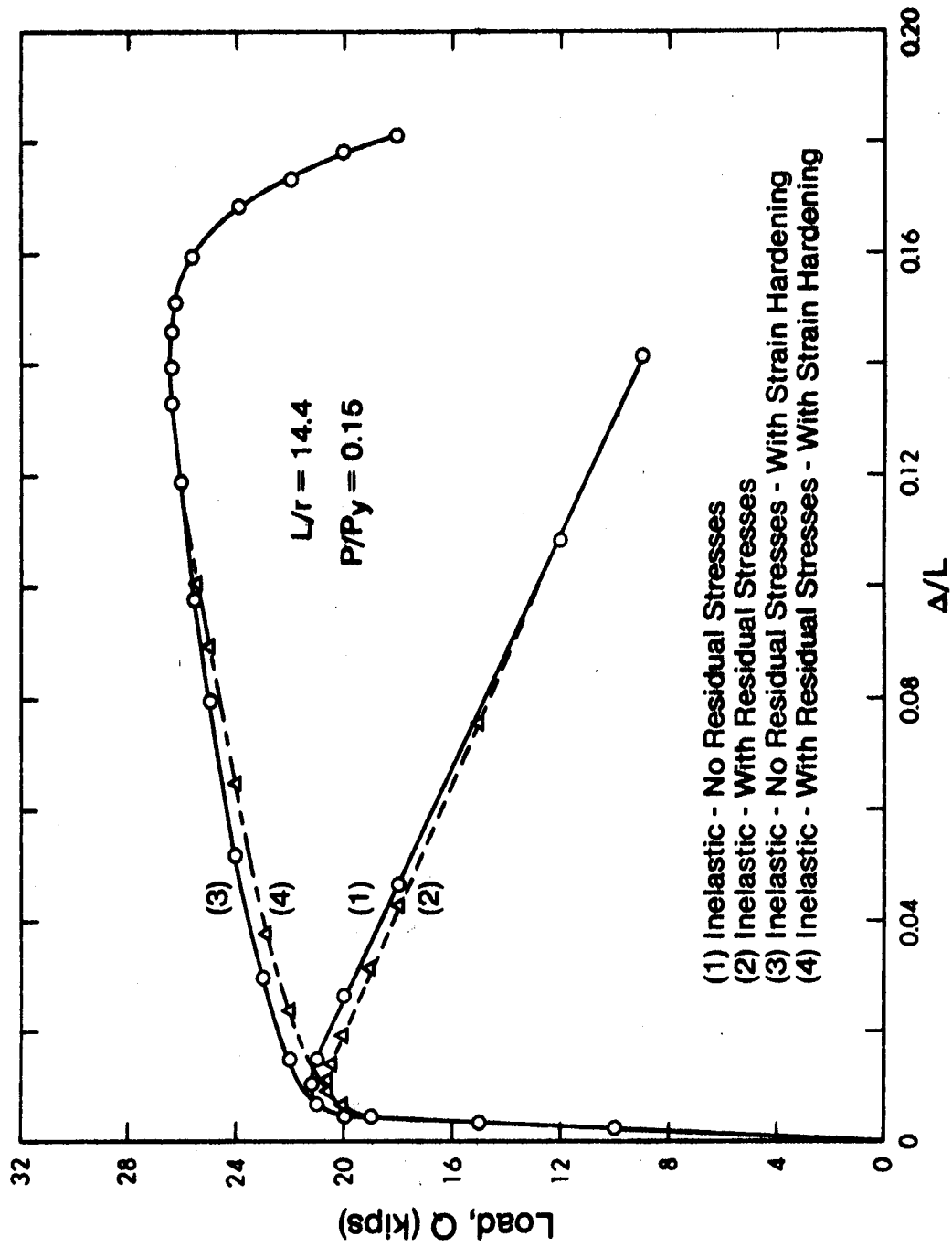


FIGURE 6-4 Load-Deformation Characteristics; Cantilever
($L/r = 14.4$; $P/P_y = 0.15$)

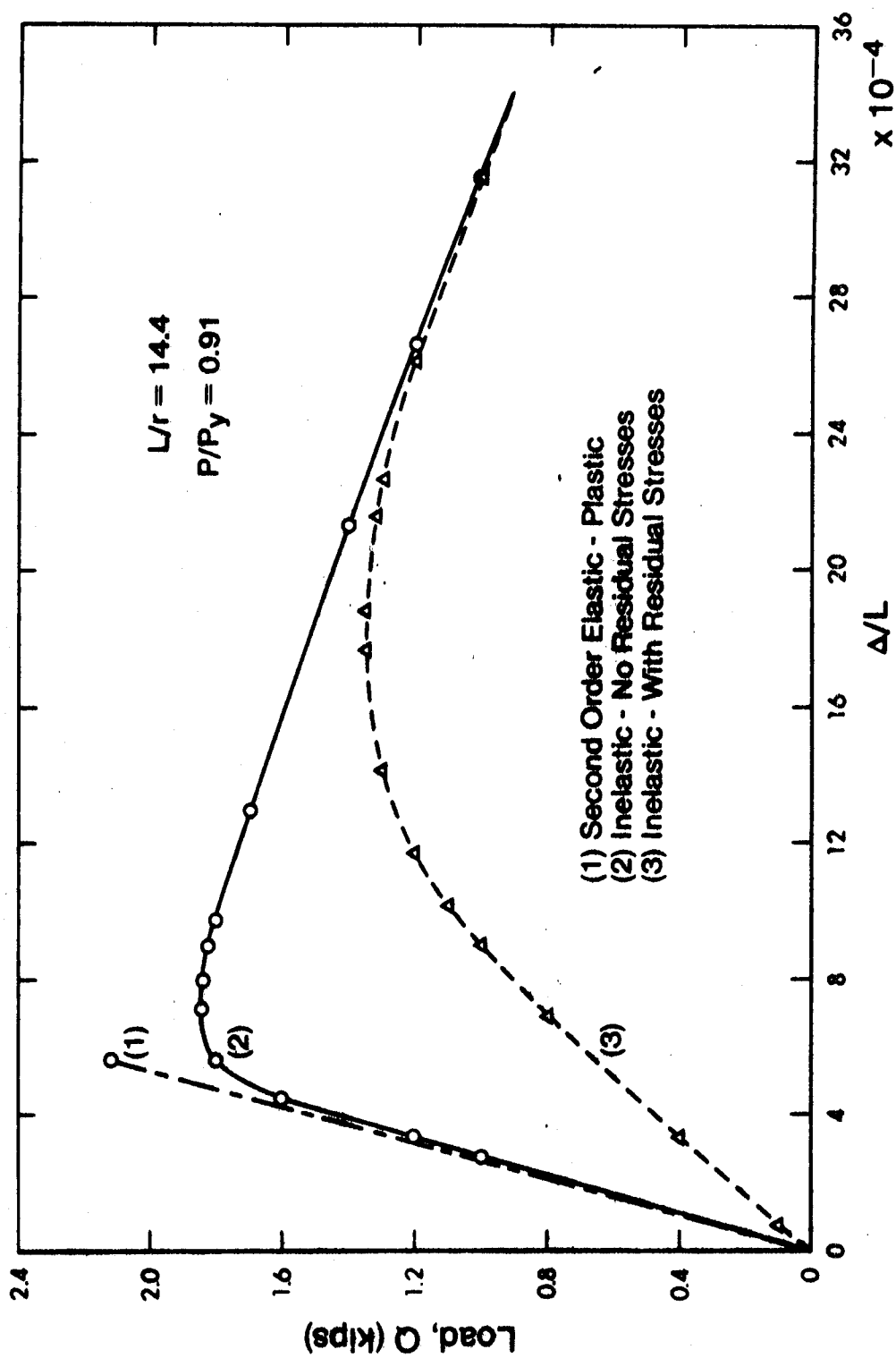


FIGURE 6-5 Load-Deformation Characteristics; Cantilever
 ($L/r = 14.4$; $P/P_y = 0.91$)

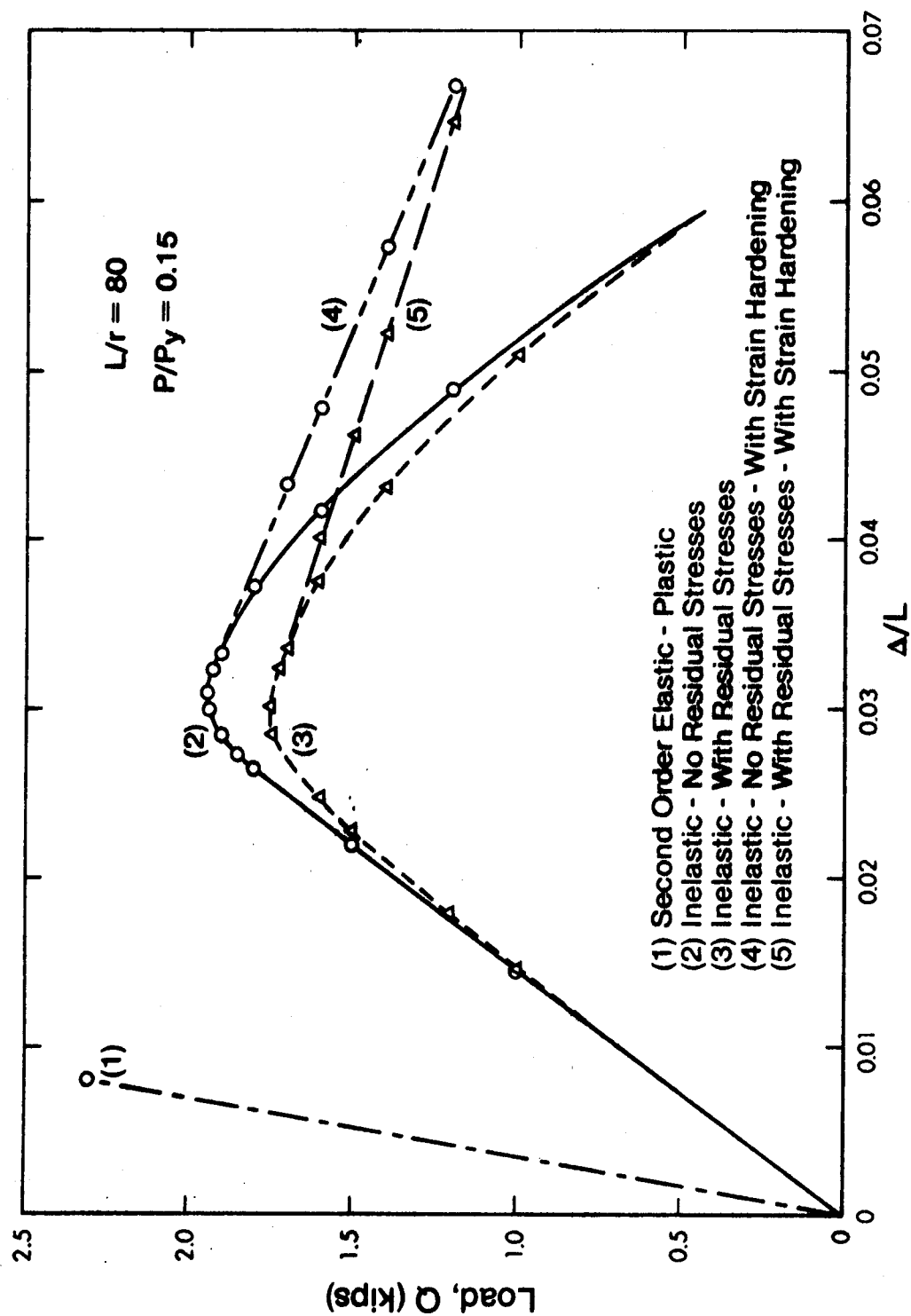


FIGURE 6-6 Load-Deformation Characteristics; Cantilever
($L/r = 80$; $P/P_y = 0.15$)

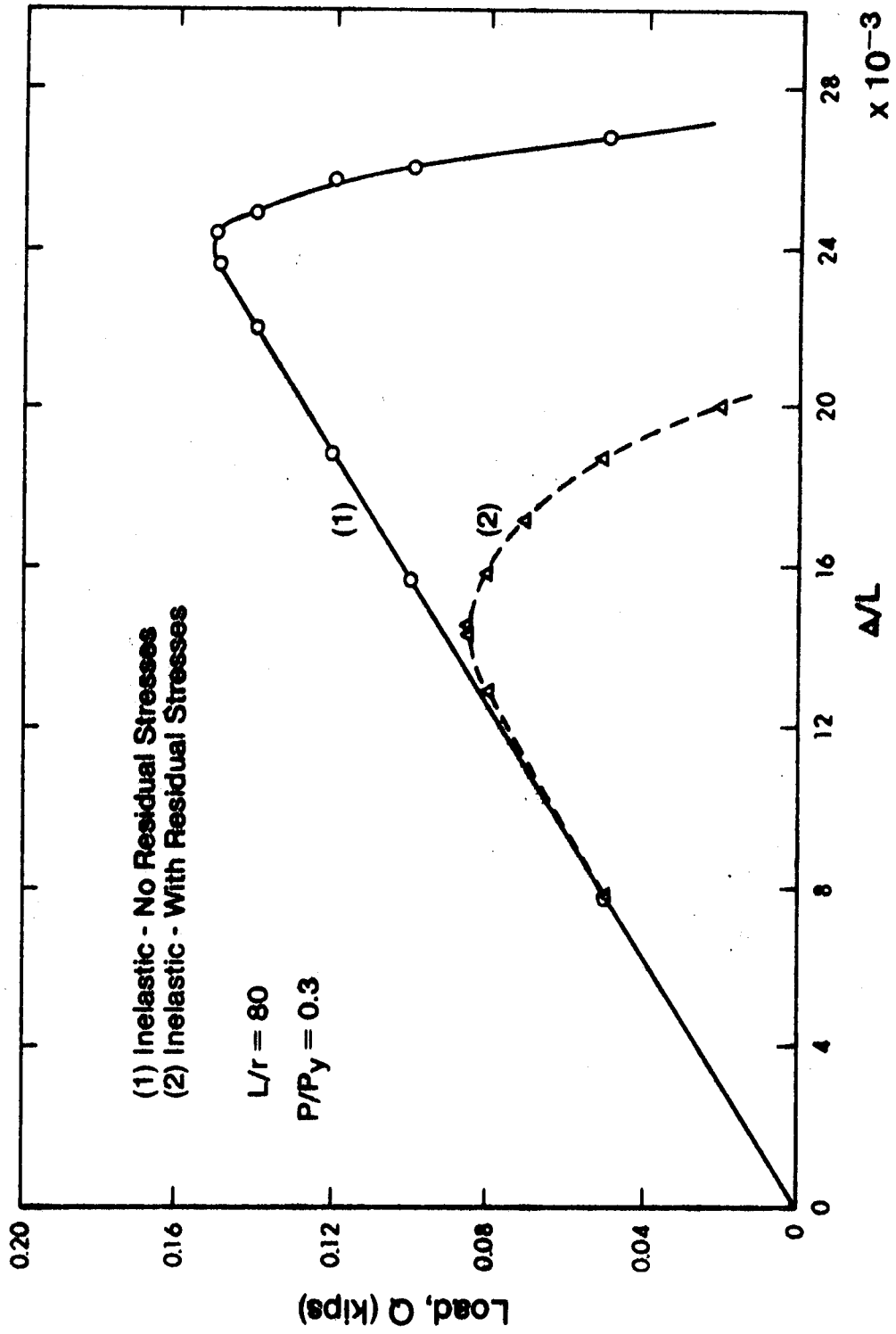


FIGURE 6-7 Load-Deformation Characteristics; Cantilever
 $(L/r = 80; P/P_y = 0.3)$

show that when only the lateral strength is considered, residual stresses will have significant effect on the maximum lateral capacity, especially for members with large axial loads. The results of the ultimate strength analysis, including the effect of residual stresses are plotted as dashed lines in Fig. 6-3a. The results show that when the overall strength is considered, the effect of residual stresses is relatively insignificant.

Except for the case of low values of L/r and P/P_y (Fig. 6-4), the data demonstrate that strain hardening of the material has no effect on the maximum value of Q . Actually, it was found that the strain hardening tends to affect only the slope of the descending line of the load-deformation characteristics. However, for the case of $L/r = 14.4$ and $P/P_y = 0.15$, the effect is pronounced. This can be attributed to the low slenderness ratio of the member.

6.2 Behavioral Study of Single Story Frames

6.2.1 Inelastic Vs. Elastic-Plastic Analysis

A study similar to that of Sect. 6.1.2 has been performed for the frame shown in Fig. 6-8, to compare the inelastic and the elastic-plastic analyses when applied to frames. The results are then illustrated on plots similar to Fig. 6-3.

As in the case of the cantilever, the elastic-plastic method tends to overestimate the lateral strength of the frame (Fig. 6-9). The results of the ultimate strength analysis are given in the form of interaction curves, where the nondimensionalized first order moment, $QL_c/2M_p$, at the maximum strength, is plotted again the nondimensionalized axial load, P/P_y . Three different values of G_T are

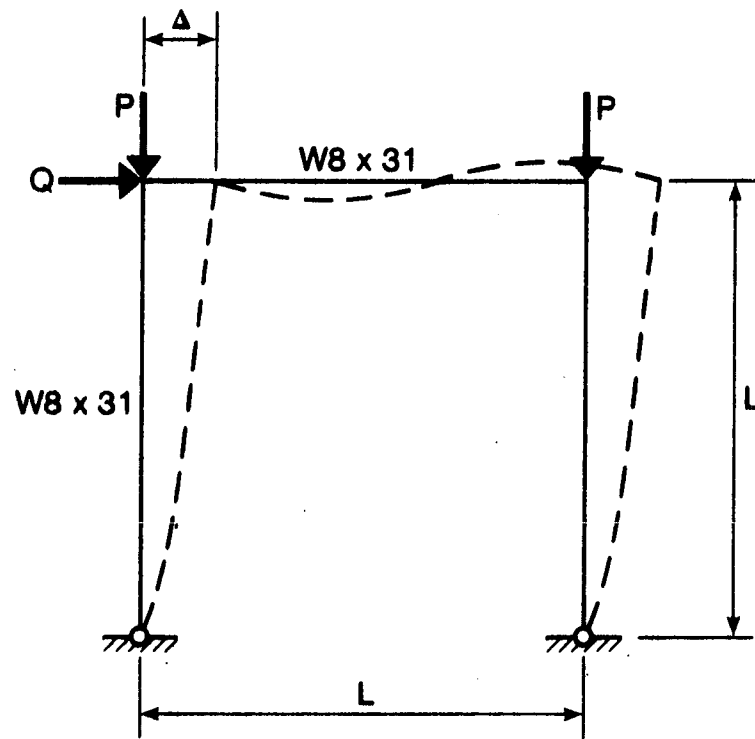


FIGURE 6-8 Single Story Frame

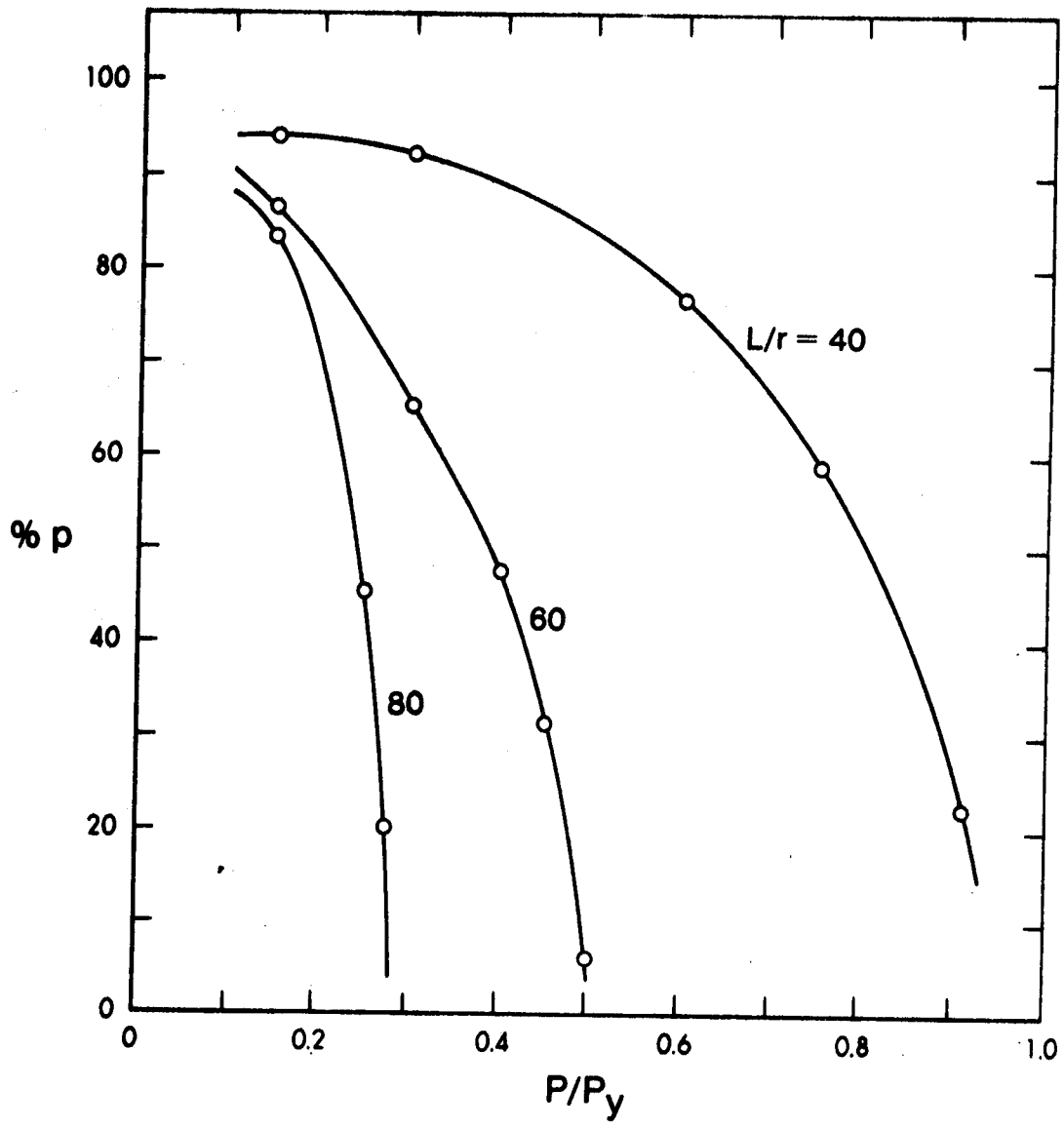


FIGURE 6-9 Inelastic Vs Elastic - Plastic
(Single Story - Hinged Bases)

considered (0, 1, and 3), where G_T is evaluated at the top joint from Eq. 3.3.1. The results are given in Fig. 6-10 ($L/r = 40$) and Fig. 6-11 ($L/r = 60$). The effective length factors corresponding to G_T values of 0, 1, and 3, with the bottom end of the column pinned ($G_B = \infty$), are 2.0, 2.3, and 2.92, respectively. This gives a range of effective slenderness ratios from $KL/r = 80$ ($K = 2.0$, $L/r = 40$) to $KL/r = 175.2$ ($K = 2.92$, $L/r = 60$).

Generally, the results show that the strength decreases as the slenderness ratio increases. Also, the results of Figs. 6-10 and 6-11 indicate that the difference in overall strength, as predicted by the two methods, is insignificant.

6.2.2 Effects of Residual Stresses and Strain Hardening

The effects of residual stresses and strain hardening are evaluated in a study of the frame shown in Fig. 6-8. The gravity loads are kept constant, and the relationship between Q and Δ/L is developed using different values of L/r and P/P_y . The results are given in Figs. 6-12 through 6-15.

It is clear that the residual stresses have a significant effect on the lateral strength of the frame, particularly for frames with high gravity loads (high P/P_y values). In Fig. 6-12, where $L/r = 40$ and $P/P_y = 0.15$, the reduction in ultimate lateral load due to residual stresses is about 2%. When the value of P/P_y is increased to 0.6 ($L/r = 40$) the ultimate lateral load of the frame (Q_u) is reduced by about 30% (Fig. 6-13). The reduction in ultimate lateral load is about 4% for the frame with $L/r = 60$ and $P/P_y = 0.15$ (Fig. 6-14). When P/P_y is increased to 0.4, for the same frame

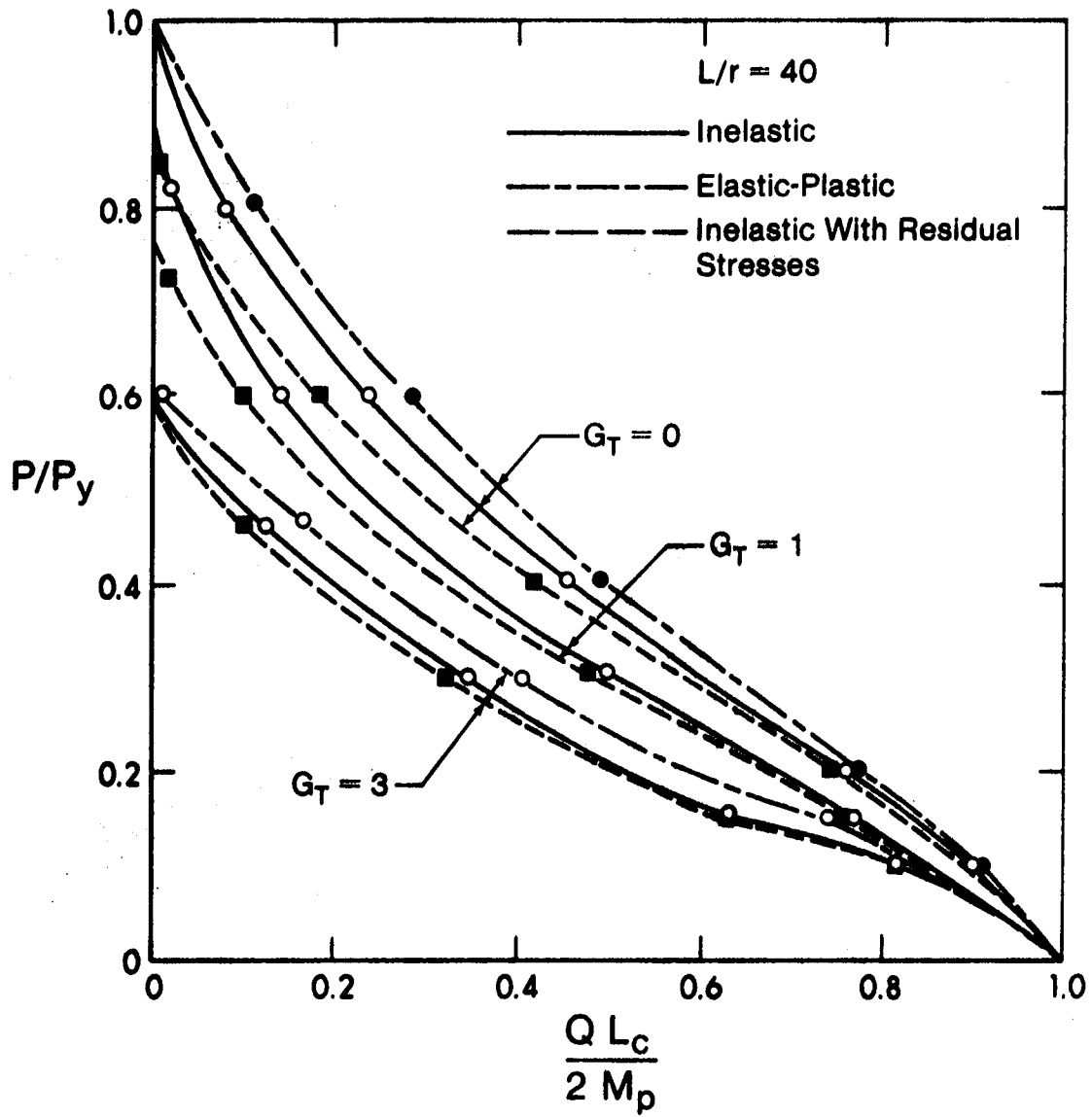


Figure 6-10. Maximum Strength of Beam-Columns in Portal Frames ($L/r = 40$)

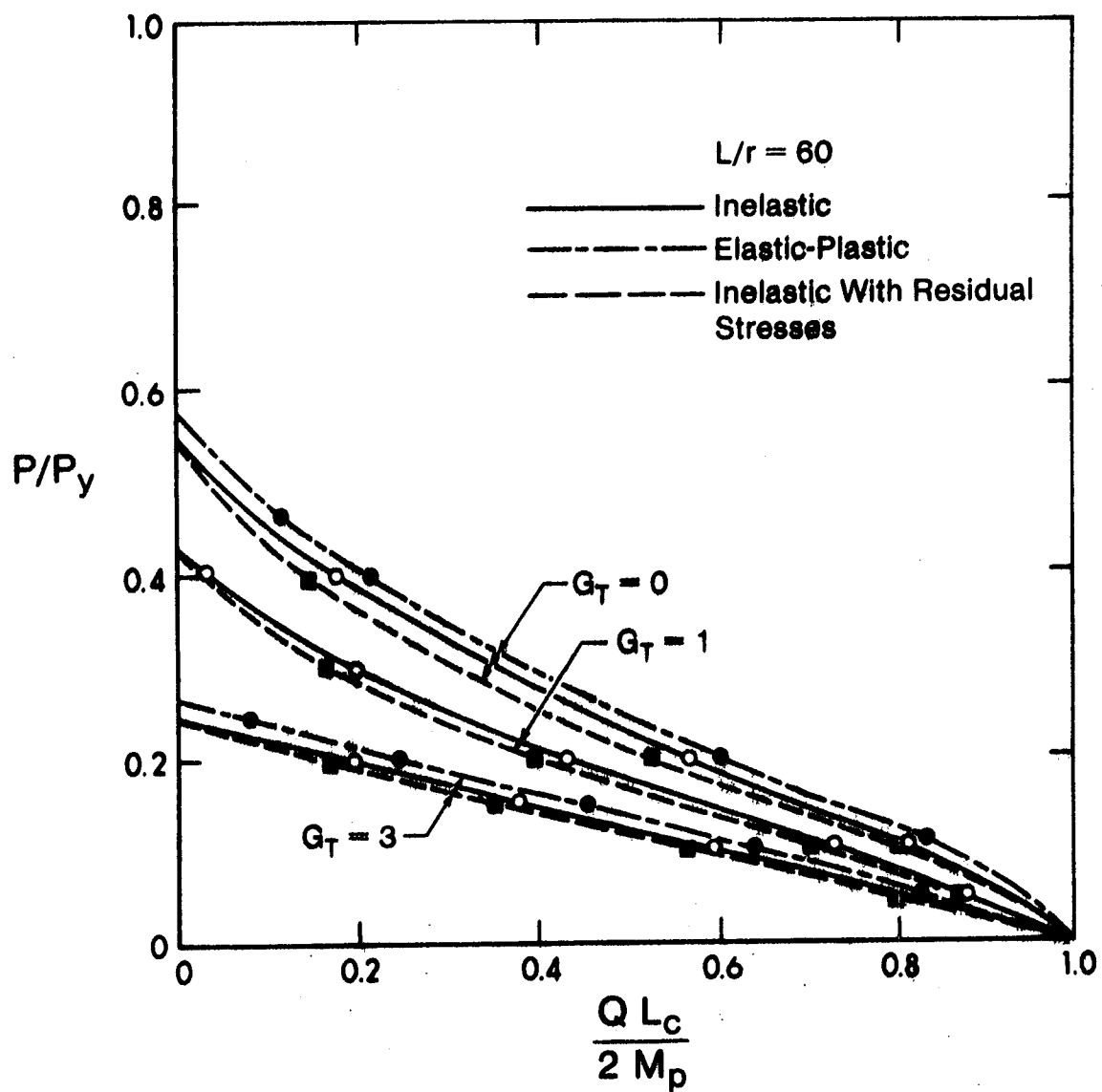


Figure 6-11. Maximum Strength of Beam-Columns in Portal Frames ($L/r = 60$)

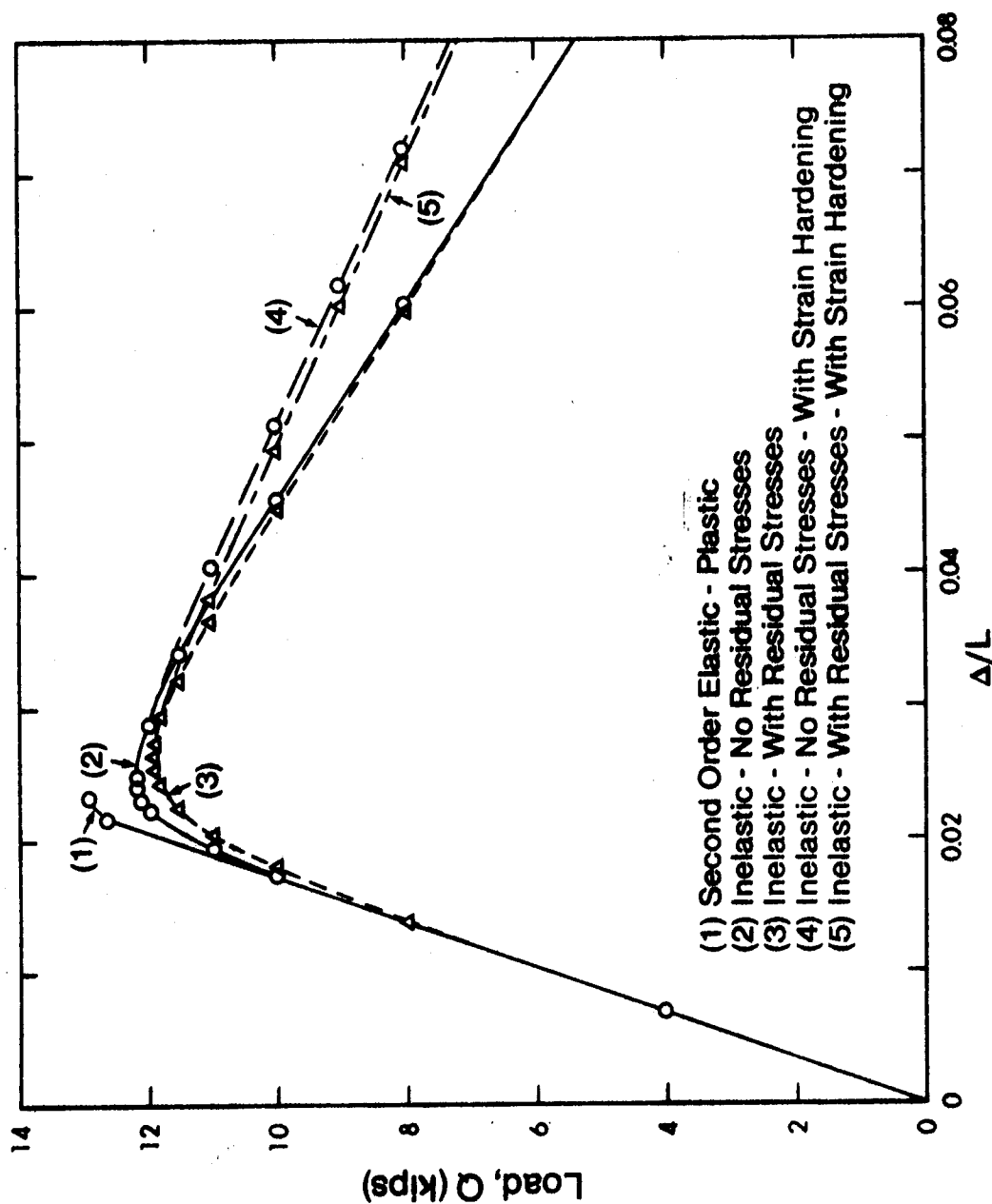


FIGURE 6-12 Load-Deformation Characteristics; Single Story Frame
 ($L/r = 40$; $P/P_y = .15$)

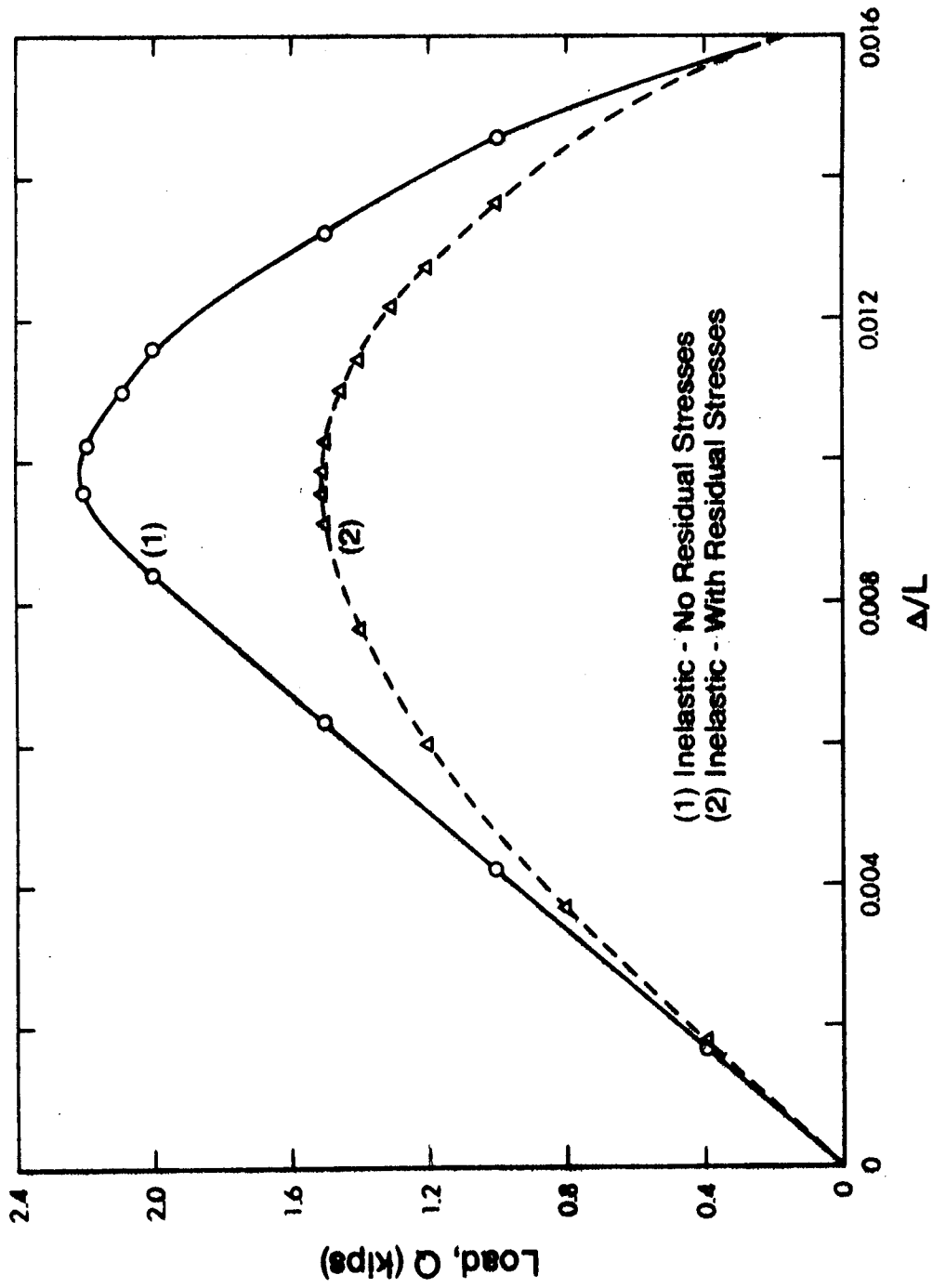


FIGURE 6-13 Load-Deformation Characteristics; Single Story Frame
($L/r = 40$; $P/P_y = 0.6$)

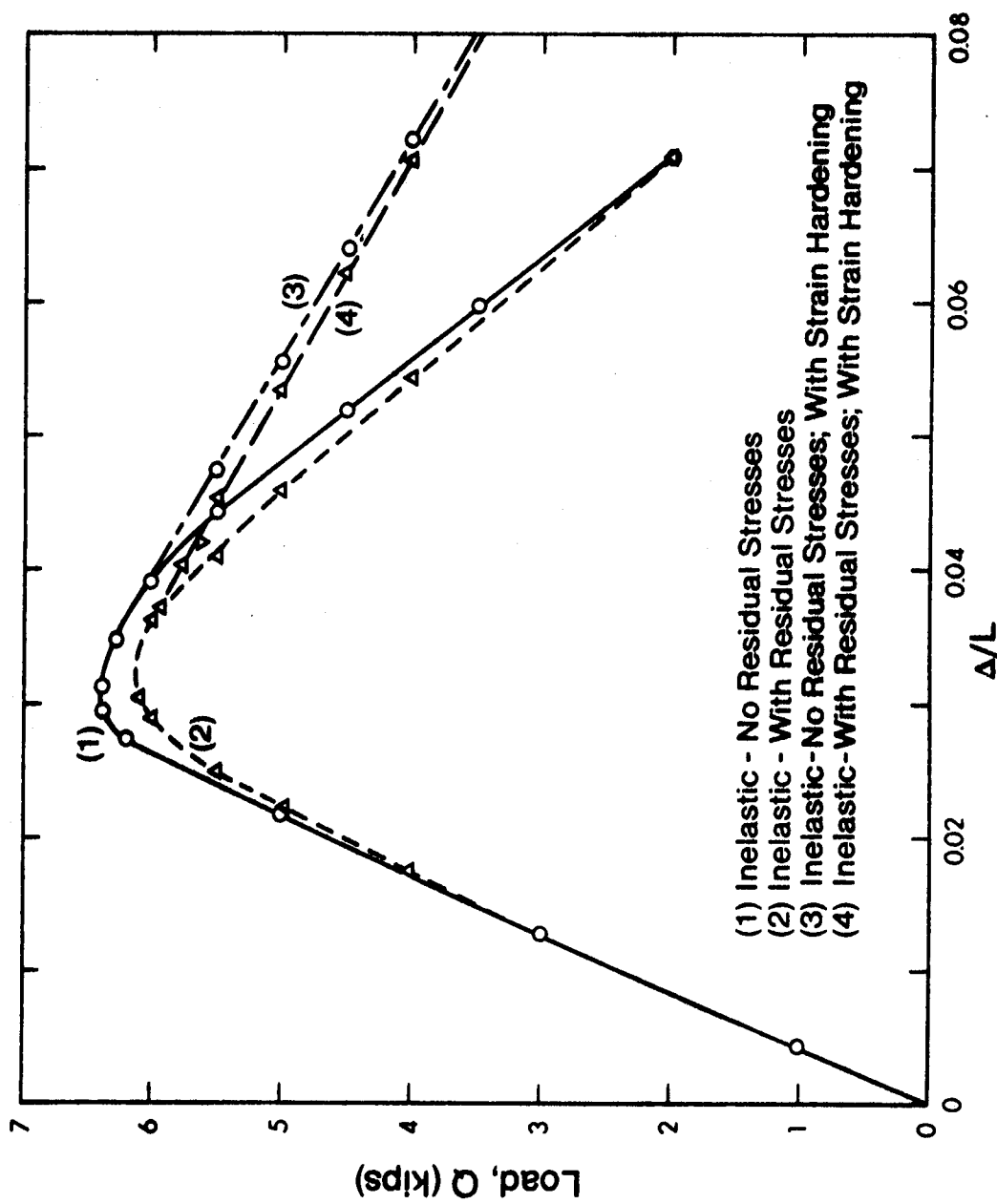


FIGURE 6-14 Load-Deformation Characteristics, Single Story Frame
 ($L/r = 60$; $P/P_y = 0.15$)

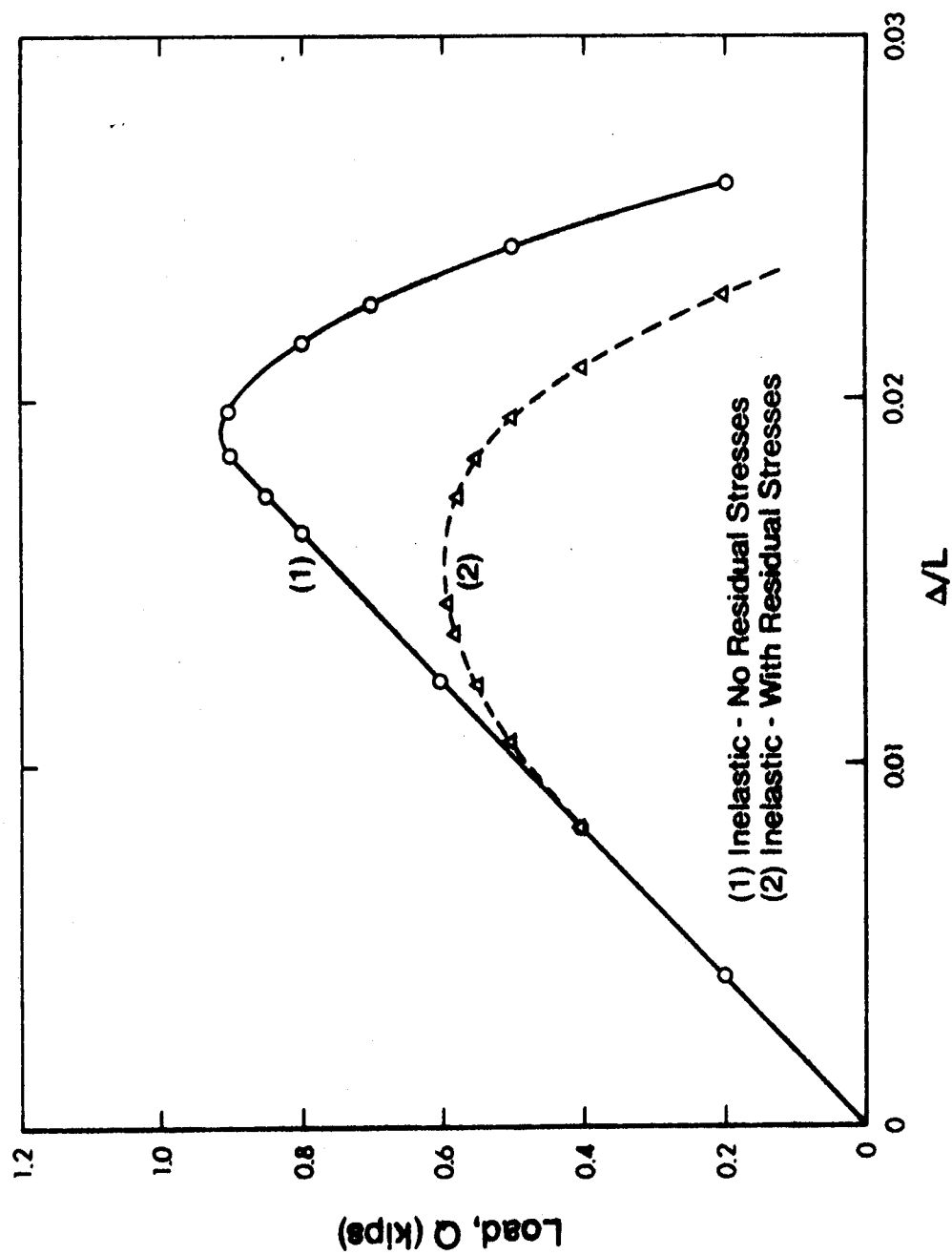


FIGURE 6-15 Load-Deformation Characteristics; Single Story Frame
($L/r = 60$; $P/P_y = 0.4$)

($L/r = 60$), the lateral load capacity is reduced by about 35% (Fig. 6-15).

The interpretation of the results shown in Figs. 6-12 through 6-15 may be misleading. In these figures only the lateral load capacity of the frame is considered. The results of the ultimate strength analysis, including the effect of residual stresses, are plotted as dashed lines in Figs. 6-10 and 6-11. The results show that the effect of residual stresses is actually small in comparison with the overall capacity. The figures also show that the residual stress effect decreases as the level of axial load decreases, and as the slenderness ratio increases.

Figures 6-12 through 6-15 show that strain hardening of the material have no effect on the ultimate lateral load of the frame. It may have an effect only on the slope of the descending portion of the load-deformation characteristic. The change in slope is particularly noticeable for frames with low values of P/P_y .

6.3 Behavioral Study of Multistory Frames

6.3.1 Frames and Loading

The formulation developed in Chapter 5 is intended primarily for the analysis of multistory frames. In the following, the three frames shown in Figs. 6-16 through 6-18 are used for this purpose. Material properties, column lengths, and girder lengths are shown for each frame. The frames are designated by a numeral indicating the number of stories, followed by a numeral indicating the number of bays. The loading on each frame is the service load, and it is

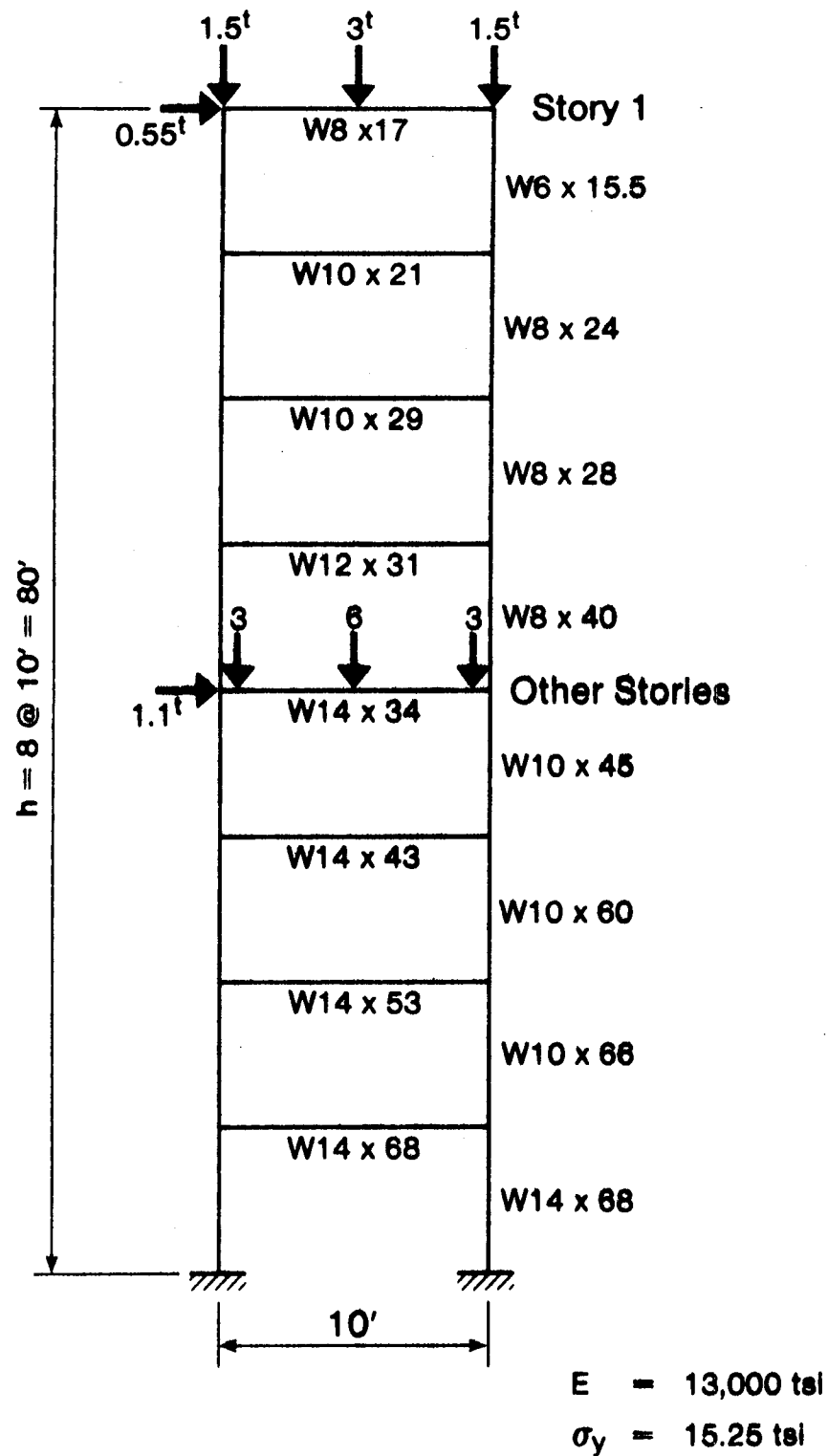


FIGURE 6-16 Configuration and Working Loads; Frame 8-1

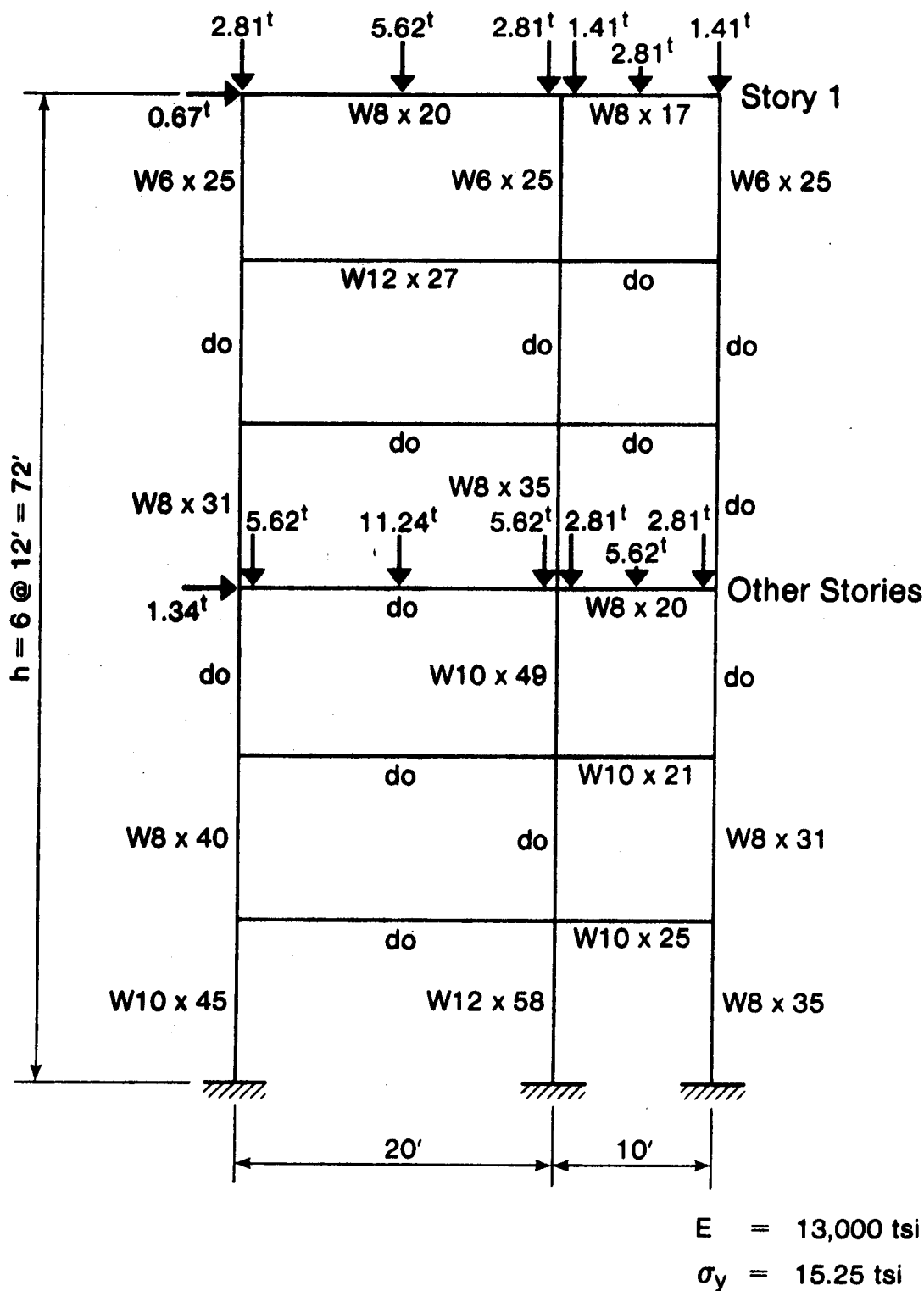
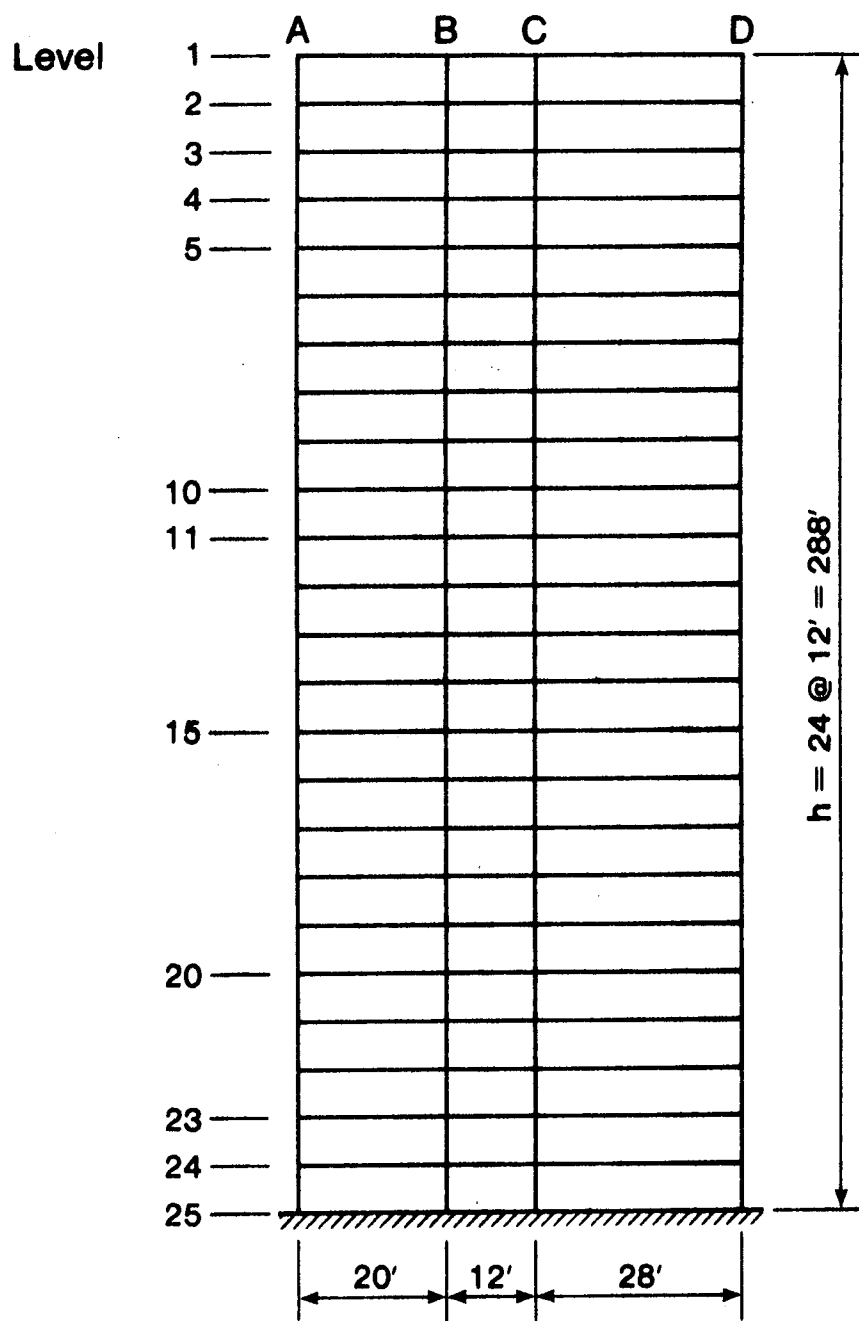


FIGURE 6-17 Configuration and Working Loads; Frame 6-2



Columns below Level 11 are A 441 Steel.
 Columns above Level 11 and all girders are A 36 Steel.
 $E = 30,000 \text{ ksi}$

FIGURE 6-18 Geometry; Frame 24-3.

assumed to be increased proportionally until collapse. Frames 8-1 and 6-2, analyzed by Korn and Galambos (1968), are subjected to concentrated loads, as shown in Figs. 6-16 and 6-17. The loading for both frames is given in ton units (1 ton = 2.24 kips). Frame 24-3, analyzed by Parikh (1966), is subjected to distributed loads given in Table 6-1. Beam and column sections for Frame 24-3 are given in Tables 6-2 and 6-3, respectively.

6.3.2 Presentation of Results

The load-deformation characteristics for the three frames are shown in Figs. 6-19, 6-20, and 6-21. Each frame was analyzed using different methods of analysis, as indicated on the figures. It can be observed that residual stresses have a limited effect on the ultimate capacity of frames. However, they have a slight effect on the load-deformation curve during the transition from the elastic into the fully plastic condition. It is believed that the effect of residual stresses for large frames will become more significant with increasing gravity loads.

The effect of strain hardening was found to be more significant for large frames than for single story frames. When considered, it caused an increase in the ultimate load ranging from 5 to 10%. This is due to the large number of sections that have to be plastified in order for the frame to reach its collapse load. When plasticity develops in the last few critical sections, the strain at a sufficient number of the sections that reached the full plastic moment earlier may have attained the strain hardening value. This does not occur

| | Unit | Working Load |
|----------|------|-----------------|
| Roof | k/ft | 3.00 |
| Floor AB | k/ft | 4.36 |
| Floor BC | k/ft | 4.73 |
| Floor CD | k/ft | 4.06 |
| Wind | K | 5.76 |
| Wall | K | 24.5 |
| Column | K | 7.5 |

TABLE 6-1 Loading; Frame 24-3

| Beams Floor | AB | BC | CD |
|----------------|-----------|-------------|-----------|
| 1 | W 14 x 26 | M 12 x 11.8 | W 16 x 45 |
| 2 | W 16 x 36 | W 12 x 16.5 | W 8 x 55 |
| 3 | do | do | do |
| 4 | do | do | do |
| 5 | do | W 16 x 31 | do |
| 6 | W 16 x 45 | W 16 x 40 | do |
| 7 | do | do | do |
| 8 | W 18 x 50 | W 18 x 50 | do |
| 9 | do | do | do |
| 10 | W 21 x 55 | W 21 x 55 | W 21 x 55 |
| 11 | do | do | do |
| 12 | W 21 x 62 | W 21 x 62 | W 21 x 62 |
| 13 | do | do | do |
| 14 | W 21 x 68 | W 21 x 68 | W 21 x 68 |
| 15 | do | do | do |
| 16 | W 24 x 68 | W 24 x 68 | W 24 x 68 |
| 17 | do | do | do |
| 18 | W 24 x 76 | W 24 x 76 | W 24 x 76 |
| 19 | do | do | do |
| 20 | do | do | do |
| 21 | W 24 x 84 | W 24 x 84 | W 24 x 84 |
| 22 | do | do | do |
| 23 | do | do | do |
| 24 | W 27 x 84 | W 27 x 84 | W 27 x 84 |

TABLE 6-2 Beam Sections; Frame 24-3

| Column Story | A | B | C | D |
|-----------------|------------|------------|------------|------------|
| 1 - 3 | W 12 x 40 | W 12 x 40 | W 12 x 58 | W 12 x 58 |
| 3 - 5 | W 12 x 58 | W 12 x 58 | W 12 x 79 | W 12 x 79 |
| 5 - 7 | W 14 x 78 | W 14 x 78 | W 14 x 111 | W 14 x 111 |
| 7 - 9 | W 14 x 111 | W 14 x 111 | W 14 x 136 | W 14 x 136 |
| 9 - 11 | W 14 x 127 | W 14 x 127 | W 14 x 158 | W 14 x 158 |
| 11 - 13 | W 14 x 136 | W 14 x 142 | W 14 x 193 | W 14 x 158 |
| 13 - 15 | W 14 x 142 | W 14 x 167 | W 14 x 211 | W 14 x 184 |
| 15 - 17 | W 14 x 167 | W 14 x 193 | W 14 x 246 | W 14 x 202 |
| 17 - 19 | W 14 x 211 | W 14 x 237 | W 14 x 314 | W 14 x 246 |
| 19 - 21 | W 14 x 246 | W 14 x 264 | W 14 x 342 | W 14 x 287 |
| 21 - 23 | W 14 x 287 | W 14 x 314 | W 14 x 370 | W 14 x 314 |
| 23 - 25 | W 14 x 314 | W 14 x 342 | W 14 x 398 | W 14 x 320 |

TABLE 6-3 Column Sections; Frame 24-3

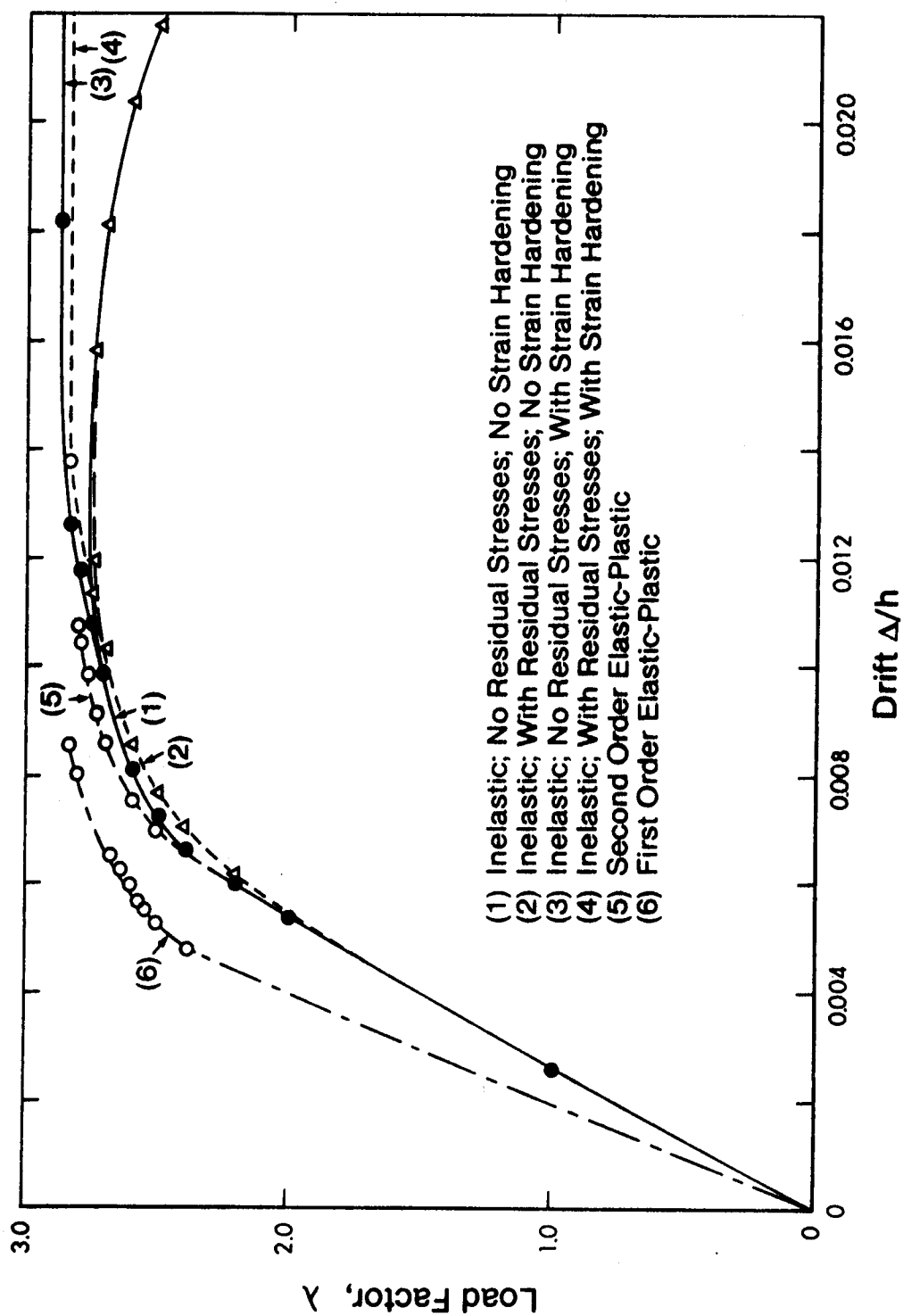


FIGURE 6-19 Load-Deformation Characteristics; Frame 8-1.

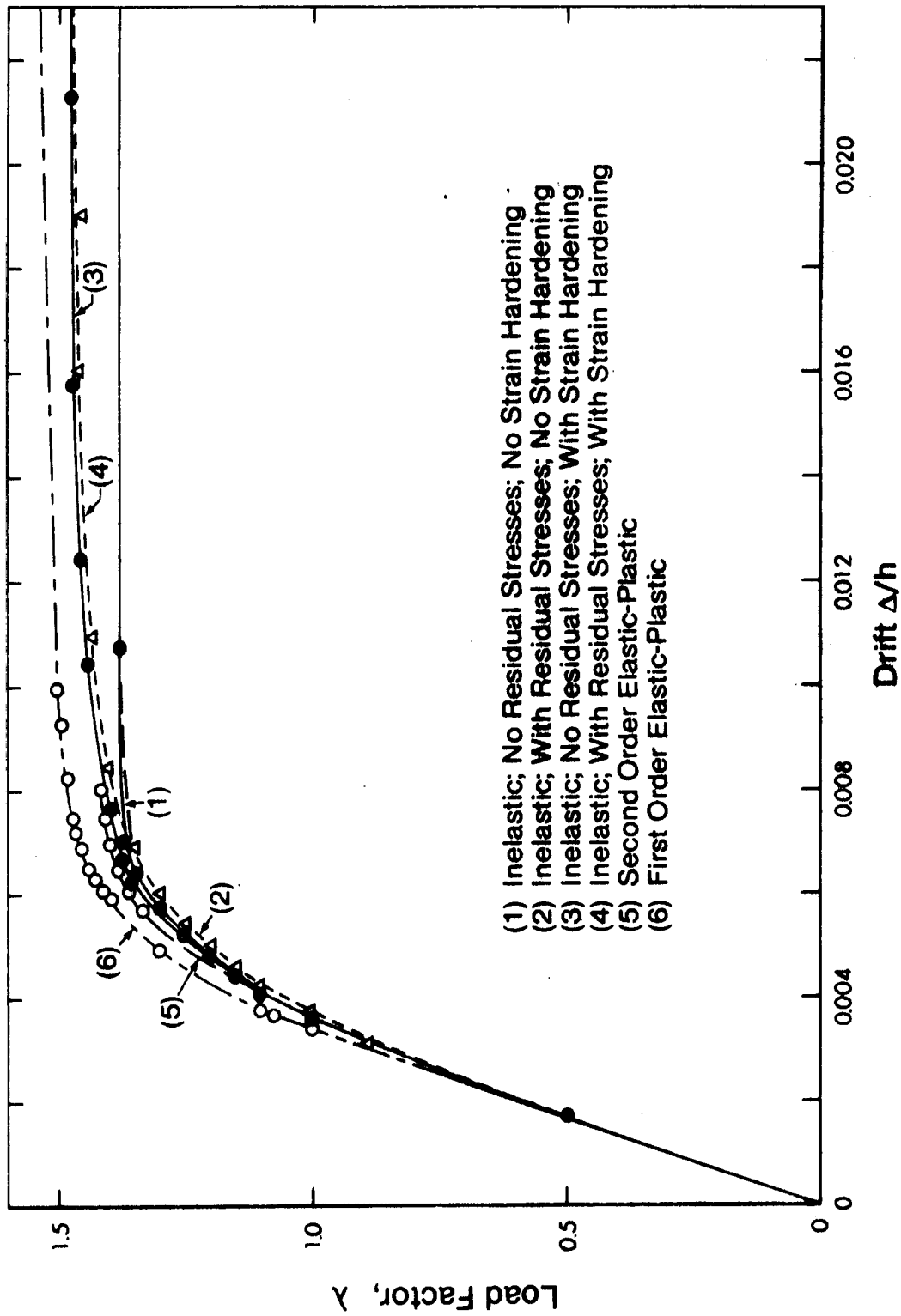


FIGURE 6-20 Load-Deformation Characteristics; Frame 6-2.

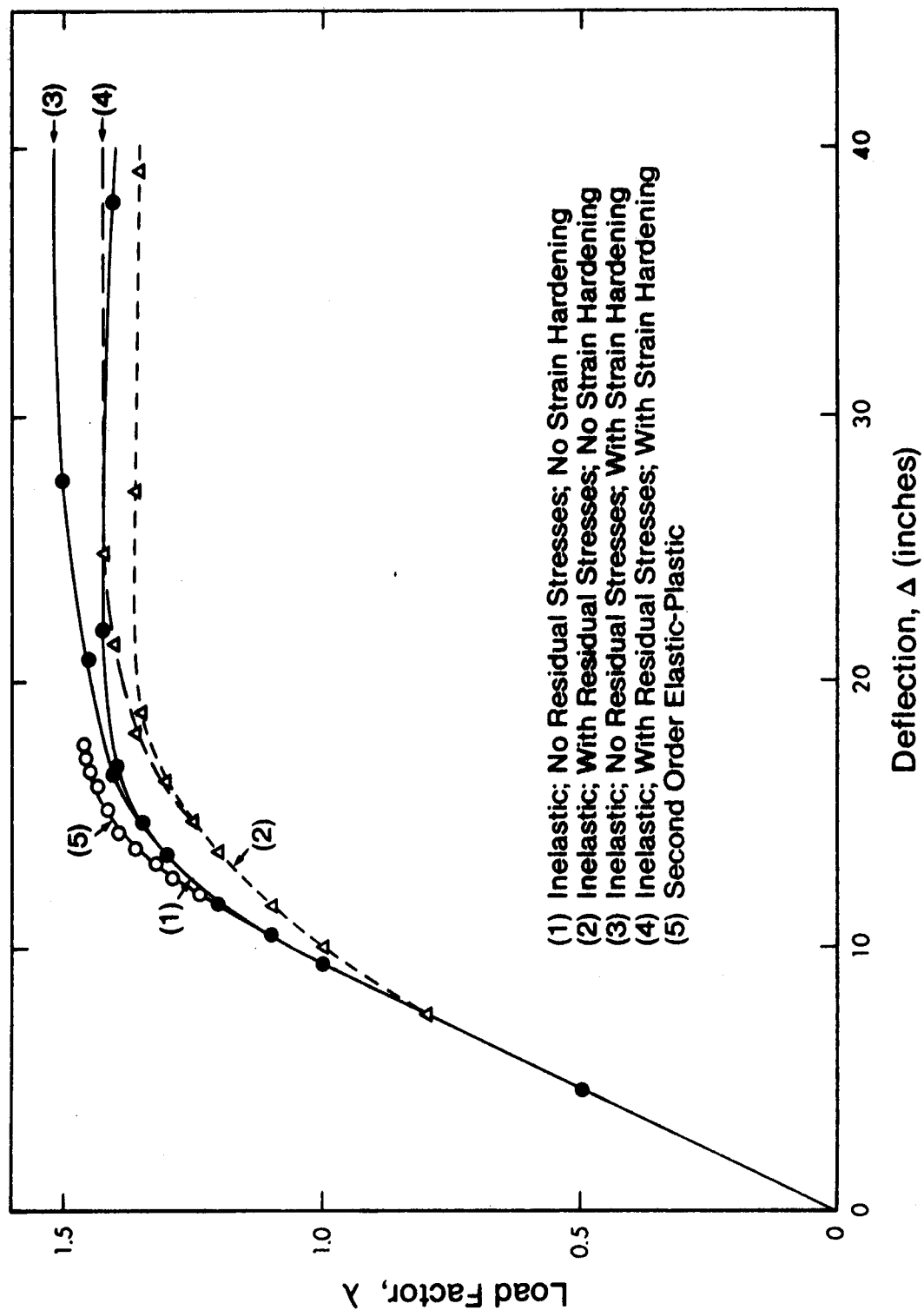


FIGURE 6-21 Load-Deformation Characteristics; Frame 24-3

in the single story--single bay frame, as the critical sections develop plasticity within a short time of one another.

It is important to note that the results of the first and second order elastic-plastic analyses for Frames 8-1 and 6-2, obtained using the iterative procedure described in Chapter 4, are identical to those obtained by Korn and Galambos (1968). The results obtained by Parikh (1966) for Frame 24-3 are very similar to curve (2) of Fig. 6-21 (up to the peak load). It is noted that Parikh took into consideration residual stresses in the columns.

In Figs. 6-19 through 6-21, a comparison between the inelastic response (curve 1) and the elastic-plastic response (curve 5) shows a slight difference only near the ultimate load. This difference, ranging between 2 to 4%, may be attributed to the gradual penetration of yielding. If the strain hardening effect is included in the inelastic analysis, there is no apparent difference between ultimate loads. Thus, when the overall behavior of the frame is considered, local losses in frame stiffness due to inelastic action are often compensated for by the behavior of other members and by the effects of strain hardening.

CHAPTER VII

SUMMARY AND CONCLUSIONS

An investigation of inelastic behavior of multistory steel frames has been presented. The investigation includes a review of stability theory, with a discussion of the different approaches to formulating stability and strength analyses. An elastic buckling formulation with a solution technique to determine the elastic critical load of frames is also given.

A nonlinear method of frame analysis, based on a simplified large deformation theory that is applicable to both inelastic and elastic responses has been developed. A finite element model has been used for this purpose, and a solution method to solve for the response of frames using the finite element equations is discussed. In the inelastic analysis the effect of axial loads on the stiffness of the structure is considered. Gradual penetration of yielding through the cross section, the spread of inelastic zones along the member length, the presence of residual stresses, and strain hardening of the material are also accounted for.

The investigation also includes the features of the elastic-plastic response of frames for first and second order analyses. The incremental and the iterative solution techniques are discussed in this context.

During the course of the investigation computer programs have been developed for all types of analyses. A variety of problems are solved to determine the accuracy and efficiency of the proposed

techniques and to demonstrate their performance in comparison with other methods.

The behavior of a number of frames under the action of combined vertical and lateral loads has been presented. Comparisons are made between the inelastic and the elastic-plastic methods of analysis. The effects of residual stresses and strain hardening are also studied.

The following sections outline the major conclusions.

7.1 Nonlinear Strain-Displacement Relationship

In an energy formulation, deformations affect the equilibrium equations through the nonlinear terms in the strain-displacement equations for virtual strains. Additional nonlinear terms must also be included in the formulation if the large geometric effects on stresses are to be considered. Thus, in the formulation presented in Sect. 3.5.1, the effect of the deformations on the equilibrium equations arises from the nonlinear terms of the expression for $\delta \epsilon_z$ in the virtual work equation (Eq. 3.5.7). The nonlinear terms as they affect stresses arise from the nonlinear strain-displacement equations. Thus, a stability formulation arises from the first effect, while the second effect simply gives a more accurate estimate of stresses in the deformed configuration of the structure.

7.2 Inelastic Vs. Elastic-Plastic Analysis

The elastic-plastic method of analysis is found to overestimate the ultimate capacity of frames under the action of lateral

loads, together with large axial loads and column slenderness ratios. When the overall capacity is considered, the difference between the inelastic method and the elastic-plastic solution is fairly small. This difference arises primarily because of two factors.

Firstly, the assumed interaction curve in the elastic-plastic analysis (Fig. 4-1) overestimates the capacity of the section. This curve is applicable only for strength analysis, since it applies to the case of $L/r = 0$. However, the actual ultimate strength interaction curves are functions of the slenderness ratio, L/r (Fig. 2-10). The true interaction curve values are the ones calculated as stress resultants in the inelastic method of analysis as presented in this investigation.

Secondly, the $P-\Delta$ moments which are included in the elastic-plastic analysis, through the geometric stiffness matrix, are underestimated. For a cantilever member with an axial compressive force, P , and a sway displacement at the top, Δ , the $P-\Delta$ method considers the maximum secondary moment at the bottom of the cantilever. This implies a triangular distribution of secondary moments along the member. The true distribution, however, is a parabola with zero moment at the top and $P\Delta$ at the bottom. This difference becomes more significant for members with large axial loads and slenderness ratios.

7.3 Gradual Penetration of Yielding

As the results of the examples presented in Chapter 5 show, the load-deformation curves obtained using the inelastic and the

elastic-plastic methods are almost identical for frames with low L/r values and P/P_y ratios. This indicates that gradual penetration of yielding has a negligible effect on the behavior of the frames. However, for the large frames presented in Sect. 6.3, there is a difference between the two analyses as the ultimate load is approached. This may be attributed to the gradual penetration of yield. The effect is apparent in large frames because of the large number of sections that develop fully plastic behavior before the ultimate frame load is reached. In single story frames, however, only a few sections had to be plastified for the frames to form mechanisms. Thus, partial plastification of sections does not show its effect immediately on the element tangent stiffness matrix.

7.4 Effects of Residual Stresses and Strain Hardening

The effect of residual stresses on the overall strength of a frame is found to be very small. It decreases as the axial load decreases, and as the slenderness ratio increases.

Strain hardening of the material is more significant for large frames than for single story frames. Although it only affects the slope of the descending portion of the load-deformation curve for a single story frame, it causes an increase in the ultimate strength of large frames by up to 10%.

7.5 Incremental Vs. Iterative Method in the Elastic-Plastic Analysis

Although more expensive, the iterative technique is found to give more accurate results than the incremental method. However, good results can be obtained if an iterative procedure is used until the first hinge is developed, followed by an incremental approach until the collapse mechanism has been reached. This procedure has been called the iterative-incremental technique, and it gives approximately the same results as the iterative method, but the cost of producing the solution is significantly less than that of the latter.

LIST OF REFERENCES

LIST OF REFERENCES

- 1 - Adams, P.F., (1964),
 "Load-Deformation Relationships for Simple Frames",
 Report 273.21, Fritz Engineering Laboratory, Lehigh
 University, Bethlehem, December.
- 2 - Adams, P.F., (1972),
 "Design of Steel Beam-Columns",
 Proceedings of the Canadian Structural Engineering Conference,
 Montreal.
- 3 - Alvarez, R.J., and Birnstiel, C., (1969),
 "Inelastic Analysis of Multistory Multibay Frames",
 Journal of the Structural Division, ASCE, Vol. 95, No. ST 11,
 November, pp. 2477-2503.
- 4 - Ang, A., (1960),
 "Analysis of Frames with Nonlinear Behavior",
 Journal of the Engineering Mechanics Division, ASCE, Vol. 86,
 No. EM3, June, pp. 1-23.
- 5 - Argyris, J.H., (1964),
 "Recent Advances in Matrix Methods of Structural Analysis",
 Progress In Aeronautical Sciences, Vol. 4, Pergamon Press
 Book, The MacMillan Comp., New York.
- 6 - Arnold, P., Adams, P.F., and Lu, W.L., (1968),
 "Strength and Behavior of an Inelastic Hybrid Frame",
 Journal of the Structural Division, ASCE, Vol. 94, No. ST1,
 January, pp. 243-266.
- 7 - Bathe, K.J., and Wilson, E.L., (1976),
 "Numerical Methods in Finite Element Analysis",
 Prentice-Hall, Inc., Englewood Cliffs, New Jersey.
- 8 - Beedle, L.S., (1958),
 "Plastic Design of Steel Frames",
 John Wiley and Sons, Inc., New York.
- 9 - Beedle, L.S., and Tall, L., (1960),
 "Basic Column Strength",
 Journal of the Structural Division, ASCE, Vol. 86, No. ST7,
 July, pp. 139-173.
- 10 - Bisshopp, K.E., and Drucker, D.C., (1945),
 "Large Deflection of Cantilever Beams",
 Quarterly Journal of Applied Mathematics, Vol. III (3),
 pp. 272-275.

- 11 - Bleich, F., (1952),
 "Buckling Strength of Metal Structures",
 McGraw-Hill Book Company, Inc., New York.
- 12 - Brebbia, C., and Connor, J., (1969),
 "Geometrically Nonlinear Finite Element Analysis",
 Journal of the Engineering Mechanics Division, ASCE,
 Vol. 95, No. EM2, April, pp. 463-483.
- 13 - Brush, D.O., and Almroth, B.O., (1975),
 "Buckling of Bars, Plates, and Shells",
 McGraw-Hill Book Comp., Inc., New York.
- 14 - Chajes, A., (1974),
 "Principles of Structural Stability Theory",
 Prentice-Hall, Inc., Englewood Cliffs, New Jersey.
- 15 - Chen, W.F., and Atsuta, T., (1977),
 "Theory of Beam-Columns; Vol. 2 - Space Behavior and Design",
 McGraw-Hill Book Comp., Inc., New York.
- 16 - Chu, K.H., and Pabarcus, A., (1964),
 "Elastic and Inelastic Buckling of Portal Frames",
 Journal of the Engineering Mechanics Division, ASCE,
 Vol. 90, No. EM5, October, pp. 221-249.
- 17 - Cohn, M.Z., and Rafay, T., (1977),
 "Deformations of Plastic Frames Considering Axial Forces",
 Journal of the Engineering Mechanics Division, ASCE, Vol. 103,
 No. EM4, August, pp. 725-745.
- 18 - CSA, (1974),
 "Steel Structures For Buildings - Limit States Design",
 CSA Standard S16.1 - 1974, Canadian Standards Association,
 Ottawa.
- 19 - Davison, J.H., and Adams, P.F., (1971),
 "Stability of Braced Frames",
 Structural Engineering Report, No. 37, Dept. of
 Civil Engineering, Univ. of Alberta, October.
- 20 - Davison, J.H., and Adams, P.F., (1974),
 "Stability of Braced and Unbraced Frames",
 Journal of the Structural Division, ASCE, Vol. 100, No. ST2,
 February, pp. 319-334.
- 21 - Ebner, A.M., and Ucciferro, J.J., (1972),
 *"A Theoretical and Numerical Comparison of Elastic Nonlinear
 Finite Element Methods"*,
 Computers and Structures, Vol. 2, pp. 1043-1061, Pergamon
 Press.

- 22 - Elwi, A.A., and Murray, D.W., (1977),
"Substructure Analysis of Plane Frames",
 Structural Engineering Report, No. 64, Dept. of Civil
 Engineering, Univ. of Alberta, June.
- 23 - Engesser, F., (1889),
"Ueber die Knickfestigkeit gerader Stäbe",
 Zeitschrift für Architekture and Ingenieurwesen, Vol. 35,
 pp. 455.
- 24 - Engesser, F., (1895),
"Knickfragen",
 Schweizerische Bauzeitung, Vol. 26, pp. 24.
- 25 - Epstein, M., and Murray, D.W., (1976),
"Large Deformation In-Plane Analysis of Elastic Beams",
 Computers and Structures, Vol. 6, pp. 1-9, Pergamon Press.
- 26 - Frisch-Fay, R., (1961),
*"A New Approach to the Analysis of Deflection of Thin
 Cantilevers"*,
 Journal of Applied Mechanics, Vol. 28, March, pp. 87-90.
- 27 - Fung, Y.C., (1965),
"Foundations of Solid Mechanics",
 Prentice-Hall, Inc., Englewood Cliffs, New Jersey.
- 28 - Galambos, T.V., and Ketter, R.L., (1961),
"Columns Under Combined Bending and Thrust",
 Transactions, ASCE, Vol. 126, Part I, pp. 1-24.
- 29 - Galambos, T.V., and Lay, M.G., (1965),
"Studies of the Ductility of Steel Structures",
 Journal of the Structural Division, ASCE, Vol. 91, No. ST4,
 August, pp. 125-151.
- 30 - Galambos, T.V., (1968),
"Structural Members and Frames",
 Prentice-Hall, Inc., Englewood Cliffs, New Jersey.
- 31 - Gallagher, R.H., Padlog, J., and Bijlaard, P.P., (1962),
"Stress Analysis of Heated Complex Shapes",
 American Rocket Society Journal, Vol. 32, May, pp. 700-707.
- 32 - Gallagher, R., and Padlog, J., (1963),
"Discrete Element Approach to Structural Instability Analysis",
 AIAA Journal, Vol. 1, No. 6, June, pp. 1437-1439.
- 33 - Ghali, A., and Neville, A.M., (1972),
"Structural Analysis",
 Intext Educational Publishers, Toronto.

- 34 - Greenbaum, G.A., and Rubinstein, M.F., (1968),
"Creep Analysis of Axisymmetric Bodies Using Finite Elements",
 Nuclear Engineering and Design, Vol. 7, pp. 379-397.
- 35 - Hodge, P.G., (1959),
"Plastic Analysis of Structures",
 McGraw-Hill Book Comp., Inc., New York.
- 36 - Hoff, N.J., (1941),
"Stable and Unstable Equilibrium of Plane Framework",
 Journal of the Aeronautical Sciences, Vol. 8, pp. 115-119.
- 37 - Hofmeister, L.D., Greenbaum, G.A., and Evenson, D.A., (1971),
"Large Strain, Elasto-Plastic Finite Element Analysis",
 AIAA Journal, Vol. 9, No. 7, July, pp. 1248-1254.
- 38 - Horne, M.R., and Majid, K.I., (1966),
"Elastic-Plastic Design of Rigid Jointed Sway Frames by Computer",
 First Report, Study of Analytical and Design Procedures for
 Elastic and Elastic-Plastic Structures, University of Manchester,
 England, March.
- 39 - Horne, M.R., and Medland, I.C., (1966),
*"Collapse Loads of Steel Frameworks Allowing for the Effect
 of Strain Hardening"*,
 Proceedings of the Institution of Civil Engineers, Vol. 33,
 March, pp. 381-402.
- 40 - Householder, A., (1964),
"The Theory of Matrices in Numerical Analysis",
 Blaisdell Publishing Company, Boston.
- 41 - Hrennikoff, A.P., (1965),
"Importance of Strain Hardening in Plastic Design",
 Journal of the Structural Division, ASCE, Vol. 91, No. ST4,
 August, pp. 23-34.
- 42 - Huber, A.W., and Beedle, L.S., (1954),
"Residual Stress and the Compressive Strength of Steel",
 Welding Journal, Vol. 33, December, pp. 589-s to 614-s.
- 43 - Jahnke, E., and Emde, F., (1945),
"Tables of Functions with Formulae and Curves",
 Fourth Edition, Dover Publications, New York.
- 44 - James, M.E., Kozik, T.J., and Martinez, J.E., (1974),
"Effect of Curvature on Nonlinear Frame Analysis",
 Journal of the Structural Division, ASCE, Vol. 100, No. ST7,
 July, pp. 1451-1457.

- 45 - Jennings, A., (1968),
 "Frame Analysis Including Change of Geometry",
 Journal of the Structural Division, ASCE, Vol. 94, No. ST3,
 March, pp. 627-644.
- 46 - Johnson, D.E., (1960),
 "Lateral Stability of Frames by Energy Method",
 Journal of the Engineering Mechanics Division, ASCE, Vol. 86,
 No. EM4, August, pp. 23-41.
- 47 - Johnston, B.G., (1976),
 "Guide to Stability Design Criteria for Metal Structures",
 Third Edition, John Wiley and Sons, Inc., New York.
- 48 - Ketter, R.L., Kaminsky, E.L., and Beedle, L.S., (1955),
 "Plastic Deformation of Wide-Flange Beam Columns",
 Transactions, ASCE, Vol. 120, pp. 1028-1061.
- 49 - Kitipornchai, S., and Trahair, N.S., (1975),
 "Buckling of Inelastic I-Beams Under Moment Gradient",
 Journal of the Structural Division, ASCE, Vol. 101, No. ST5,
 May, pp. 991-1004.
- 50 - Korn, A., and Galambos, T.V., (1968),
 "Behavior of Elastic-Plastic Frames",
 Journal of the Structural Division, ASCE, Vol. 94, No. ST5,
 May, pp. 1119-1142.
- 51 - Loxan, A.N., Davids, N., and Levenson, A., (1942),
 *"Tables of Zeros of the Legendre Polynomials of Order 1-16 and
 the Weight Coefficients of Gauss Mechanical Quadrature Formula"*,
 Bulletin of the American Mathematical Society, Vol. 48, pp.
 739-743.
- 52 - Lu, L.W., (1962),
 "A Survey of Literature on the Stability of Frames",
 Welding Research Council, Bulletin 81, September.
- 53 - Majumdar, S.N.G., MacGregor, J.G. and Adams, P.F., (1970),
 *"Experimental and Analytical Study of the Behavior of Steel
 Frame-Shear Wall Structures"*,
 Structural Engineering Report, No. 27, Dept. of Civil
 Engineering, Univ. of Alberta, August.
- 54 - Majumdar, S.N.G., and Adams, P.F., (1971),
 "Tests on Steel Frame, Shear-Wall Structures",
 Journal of the Structural Division, ASCE, Vol. 97, No. ST4,
 April, pp. 1097-1111.
- 55 - Marcal, P.V., (1972),
 "Thermal Mechanical Effects of Welding",
 Presented at National Symposium on Computerized Structural
 Analysis and Design, George Washington Univ., Washington, D.C.,
 March.

- 56 - Martin, H.C., (1965),
 "On the Derivation of Stiffness Matrices for the Analysis of Large Deflection and Stability Problems",
 Proceedings, Conference on Matrix Methods in Structural Mechanics, Wright Patterson Air Force Base, Ohio, October, pp. 697-716.
- 57 - Mason, R.E., Fisher, G.P., and Winter, G., (1958),
 "Eccentrically Loaded Hinged Steel Columns",
 Journal of the Engineering Mechanics Division, ASCE, Vol. 84, No. EM4, October, pp. 1792-1 to 1792-19.
- 58 - McNamee, B.M., and Lu, L.W., (1972),
 "Inelastic Multistory Frame Buckling",
 Journal of the Structural Division, ASCE, Vol. 98, No. ST7, July, pp. 1613-1631.
- 59 - Moses, F., (1964),
 "Inelastic Frame Buckling",
 Journal of the Structural Division, ASCE, Vol. 90, No. ST6, December, pp. 105-121.
- 60 - Murray, D.W., Rohardt, A.M., and Simmonds, S.H., (1977),
 "A Classical Flexibility Analysis for Gentilly Type Containment Structures",
 Structural Engineering Report, No. 63, Dept. of Civil Engineering, Univ. of Alberta, June.
- 61 - Murray, D.W., Chitnuyanondh, L., and Wong, C., (1979),
 "Implementation of an Elastic-Plastic Concrete Relationship",
 A Paper Accepted for Publication In Computer Methods in Applied Mechanics and Engineering.
- 62 - Nair, R.S., (1975),
 "Overall Elastic Stability of Multistory Buildings",
 Journal of the Structural Division, ASCE, Vol. 101, No. ST12, December, pp. 2487-2503.
- 63 - Neal, B.G., (1977),
 "The Plastic Methods of Structural Analysis",
 Third Edition, John Wiley and Sons, Inc., New York.
- 64 - Ojalvo, M., and Lu, L.W., (1961),
 "Analysis of Frames Loaded into the Plastic Range",
 Journal of the Engineering Mechanics Division, ASCE, Vol. 87, No. EM4, August, pp. 35-48.
- 65 - Oran, C., and Kassimali, A., (1976),
 "Large Deformations of Framed Structures Under Static and Dynamic Loads",
 Computer and Structures, Vol. 6, pp. 539-547, Pergamon Press.

- 66 - Parikh, B.P., (1966),
"Elastic-Plastic Analysis and Design of Unbraced Multistory Steel Frames",
Fritz Engineering Laboratory, Report No. 273.44, Lehigh University, Bethlehem, May.
- 67 - Phillips, A., (1956),
"Introduction to Plasticity",
The Ronald Press Company, New York.
- 68 - Pippard, A.J., and Baker, J., (1968),
"The Analysis of Engineering Structures",
Fourth Edition, Edward Arnold Publishers Ltd., London.
- 69 - Popov, E.P., (1976),
"Mechanics of Materials",
Second Edition, Prentice-Hall, Inc., Englewood Cliffs, New Jersey.
- 70 - Porter, F.L., and Powell, G.H., (1971),
"Static and Dynamic Analysis of Inelastic Frame Structures",
Univ. of California, Earthquake Engineering Research Centre, Report No. EERC 71-3, June.
- 71 - Przemieniecki, J.S., (1968),
"Theory of Matrix Structural Analysis",
McGraw-Hill Book Comp., Inc., New York.
- 72 - Rajasekaran, S., (1971),
"Finite Element Analysis of Thin-Walled Members of Open Sections",
Ph.D. Thesis, University of Alberta, Edmonton, September.
- 73 - Rajasekaran, S., and Murray, D.W., (1973),
"Solution Techniques for Geometrically Nonlinear Structures",
Structural Engineering Report, No. 42, Dept. of Civil Eng., Univ. of Alberta, March.
- 74 - Saada, A.S., (1974),
"Elasticity Theory and Applications",
Pergamon Press Inc., New York.
- 75 - Sawko, F., (1965),
"Collapse Load for Structures Allowing for Strain Hardening",
Proceedings of the Institution of Civil Engineering, Vol. 31, June, pp. 147-153.
- 76 - Schilling, C., Schutz, F., and Beedle, L.S., (1956),
"Behavior of Welded Single Span Frame Under Combined Loading",
Welding Journal, Vol. 35, May, pp. 234s-252s.

- 77 - Shanley, F.R., (1947),
 "Inelastic Column Theory",
 Journal of the Aeronautical Science, Vol. 14, No. 5, May,
 pp. 261-268.
- 78 - Skogh, J., Stern, P., and Brogan, F.A., (1972),
 "Instability Analysis of Skylab Structure",
 Presented at the National Symposium on Computerized Structural
 Analysis and Design, George Washington Univ., Washington, D.C.
- 79 - Springfield, J., and Adams, P.F. (1972),
 "Aspects of Column Design in Tall Steel Buildings",
 Journal of the Structural Division, ASCE, Vol. 98, No. ST5,
 May, pp. 1069-1083.
- 80 - Stricklin, J.A., Martinez, J.E., Tillerson, J.R., Hong, J.H.,
 and Haisler, W.E., (1971),
 *"Nonlinear Dynamic Analysis of Shells of Revolution by
 Matrix Displacement Method"*,
 AIAA Journal, Vol. 9, No. 4, April, pp. 629-636.
- 81 - Tall, L., (1964),
 "Compression Members in Structural Steel Design",
 The Ronald Press Company, New York.
- 82 - Timoshenko, S.P., and Gere, M.J., (1961),
 "Theory of Elastic Stability",
 Second Edition, McGraw-Hill Book Comp., Inc., New York.
- 83 - Tranberg, W., Swannell, P., and Meek, J.L., (1976),
 "Frame Collapse Using Tangent Stiffness",
 Journal of the Structural Division, ASCE, Vol. 102, No. ST3,
 March, pp. 659-675.
- 84 - Turner, M.J., Clough, R.W., Martin, H.C., and Topp, L.J., (1956),
 "Stiffness and Deflection Analysis of Complex Structures",
 Journal of the Aerospace Science, Vol. 23, No. 9, September,
 pp. 805-823.
- 85 - Turner, M.J., Dill, E.H., Martin, H.C., and Melosh, R.J., (1960),
 *"Large Deflections of Structures Subjected to Heating and
 External Loads"*,
 Journal of the Aerospace Science, Vol. 27, No. 2, February,
 pp. 97-106.
- 86 - Van Kuren, R.C., and Galambos, T.V., (1964),
 "Beam-Column Experiments",
 Journal of the Structural Division, ASCE, Vol. 90, No. ST2,
 April, pp. 223-255.

- 87 - Von Karman, T., (1910),
 "Untersuchungen über Knickfestigkeit",
 Mitteilungen über Forschungsarbeiten auf dem Gebiete des
 Ingenieurwesens, Berlin, No. 81.
- 88 - Walker, A.C., and Hall, D.G., (1968),
 *"Analysis of the Large Deflections of Beams Using Rayleigh-
 Ritz Finite element Method"*,
 Aeronautical Quarterly, Vol. 19, November, pp. 357-367.
- 89 - Wang, C.K., (1963),
 "General Computer Program for Limit Analysis",
 Journal of the Structural Division, ASCE, Vol. 89, No. ST6,
 December, pp. 101-117.
- 90 - Washizu, K., (1969),
 "Some Remarks on Basic Theory for Finite Element Method",
 Proc. Japan-U.S. Seminar on Matrix Methods in Structural
 Analysis and Design, Tokyo.
- 91 - Wilkinson, J.H., (1965),
 "The Algebraic Eigenvalue Problem",
 Oxford Univ. Press (Clarendon), London.
- 92 - Winter, G., Hsu, P.T., Koo, B., and Loh, M.H., (1948),
 "Buckling of Trusses and Rigid Frames",
 Cornell Univ. Eng. Exp. Station Bulletin No. 36, Ithaca,
 New York.
- 93 - Wood, B.R., Beaulieu, D., and Adams, P.F., (1976),
 "Column Design by P-Delta Method",
 Journal of the Structural Division, ASCE, Vol. 102, No. ST2,
 February, pp. 411-427.
- 94 - Yarimci, E., (1966),
 *"Incremental Inelastic Analysis of Framed Structures and Some
 Experimental Verifications"*,
 Fritz Engineering Laboratory, Report No. 273.45, Lehigh
 Univ., May.
- 95 - Yura, J.A., (1965),
 "The Strength of Braced Multistory Steel Frames",
 Fritz Engineering Laboratory, Report No. 273.28, Lehigh
 University, September.
- 96 - Yura, J.A., and Galambos, T.V., (1965),
 "Strength of Single Story Steel Frames",
 Journal of the Structural Division, ASCE, Vol. 91, No. ST5,
 October, pp. 81-101.

- 97 - Ziegler, H., (1968),
 "Principles of Structural Stability",
 Blaisdell Publishing Company, Toronto.
- 98 - Zienkiewicz, O.C., (1971),
 "The Finite Element Method in Engineering Science",
 McGraw-Hill Book Company, Inc., New York.

APPENDIX A

ELEMENT STIFFNESS MATRIX

FOR

BEAM-COLUMNS

APPENDIX A
ELEMENT STIFFNESS MATRIX FOR
BEAM-COLUMNS

In this Appendix the "small-displacement" element beam-column stiffness matrix is derived.

A.1 Virtual Work Equations for Linear Stability Problems

To formulate the virtual work equations for a linear stability formulation it is necessary to simplify the strain-displacement equations presented in Sect. 3.2. Assuming that θ , of Fig. 3-1, remains "small" such that

$$1 - \cos\theta \approx 0 \quad (A.1.1)$$

Eqs. 3.2.3 become

$$u = u_o - y v_o' \quad (A.1.2a)$$

$$v = v_o \quad (A.1.2b)$$

In addition, the $(u')^2$ term in Eq. 3.2.4 is assumed "small" with respect to the other two terms so that Eq. 3.2.4 becomes

$$\epsilon_z = u' + \frac{1}{2} (v')^2 \quad (A.1.3)$$

Substituting Eqs. A.1.2 into Eq. A.1.3 yields

$$\epsilon_z = u_o' - y v_o'' + \frac{1}{2} (v_o')^2 \quad (A.1.4)$$

Equation A.1.4 is the strain-displacement equation from which classical linear stability formulations arise.

The principle of virtual work may be written for the length of beam illustrated in Fig. 3-1 as

$$\delta W = \int_V \sigma_z \delta \epsilon_z dV - \langle Q \rangle \{\delta q\} = 0 \quad (\text{A.1.5})$$

From Eq. A.1.4

$$\delta \epsilon_z = \delta u'_0 - y \delta v''_0 + v'_0 \delta v'_0 \quad (\text{A.1.6})$$

Substituting Eq. A.1.6 into Eq. A.1.5; integrating over the area of cross-section A, and defining the stress resultants n and m as

$$n = \int_A \sigma_z dA \quad (\text{A.1.7a})$$

and

$$m = \int_A \sigma_z y dA \quad (\text{A.1.7b})$$

yields

$$\delta W = \int_L (n \delta u'_0 - m \delta v''_0 + n v'_0 \delta v'_0) dz - \langle Q \rangle \{\delta q\} = 0 \quad (\text{A.1.8})$$

For linear elastic response it is assumed that

$$\sigma_z = E \epsilon_z \quad (\text{A.1.9})$$

Substituting Eq. A.1.4 into Eq. A.1.9, and the result into Eqs. A.1.7, the stress resultants may be expressed in terms of displacements as

$$n = EA u'_0 \quad (A.1.10a)$$

and

$$m = -EI v''_0 \quad (A.1.10b)$$

in which I is the moment of inertia of the cross-section, and the first moment of area vanishes because the axis is the centroidal axis. A term involving $(v'_0)^2$ has been discarded from Eq. A.1.10a for simplicity of calculation.

To form the classical equation of linear stability, Eqs. A.1.10 are substituted into the first two terms of Eq. A.1.8, resulting in the equilibrium requirement that

$$\begin{aligned} & \int_{\ell} (EA u'_0 \delta u'_0 + EI v''_0 \delta v''_0) dz \\ & + \int_{\ell} n v'_0 \delta v'_0 dz - \langle Q \rangle \{ \delta q \} = 0 \end{aligned} \quad (A.1.11)$$

Equation A.1.11 is now used to determine finite element matrices.

A.2 The Finite Element Model

The displacements u_0 and v_0 may be approximated in terms of the displacement coordinates $\langle q \rangle$, of Fig. 3-2a, as

$$u_0 = \langle \bar{\phi} \rangle \begin{Bmatrix} q_1 \\ q_4 \end{Bmatrix} \quad (A.2.1)$$

and

$$v_o = \langle \phi \rangle \begin{Bmatrix} q_2 \\ q_3 \\ q_5 \\ q_6 \end{Bmatrix} \quad (A.2.2)$$

Standard linear shape functions (Fig. A-1) are used for $\langle \bar{\phi} \rangle$, and standard cubic shape functions (Fig. A-2) are used for $\langle \phi \rangle$. In terms of the nondimensional coordinate ζ , shown in Figs. A-1 and A-2, the shape functions are

$$\langle \bar{\phi} \rangle = \left\langle -\frac{1}{2} (\zeta - 1), \frac{1}{2} (\zeta + 1) \right\rangle \quad (A.2.3a)$$

and

$$\begin{aligned} \langle \phi \rangle = \left\langle \frac{1}{4} (\zeta + 2) (\zeta - 1)^2, \frac{\ell}{8} (\zeta + 1) (\zeta - 1)^2, \right. \\ \left. \frac{1}{4} (2 - \zeta) (\zeta + 1)^2, \frac{\ell}{8} (\zeta - 1) (\zeta + 1)^2 \right\rangle \quad (A.2.3b) \end{aligned}$$

The derivatives required for Eq. A.1.11 are now evaluated by differentiation of Eqs. A.2.1 and A.2.2 to yield

$$u'_o = \langle (\bar{\phi})' \rangle \langle q_1, q_4 \rangle^T \quad (A.2.4a)$$

$$v'_o = \langle \phi' \rangle \langle q_2, q_3, q_5, q_6 \rangle^T \quad (A.2.4b)$$

$$v''_o = \langle \phi'' \rangle \langle q_2, q_3, q_5, q_6 \rangle^T \quad (A.2.4c)$$

in which

$$\langle (\bar{\phi})' \rangle = \frac{1}{\ell} \langle -1, 1 \rangle \quad (A.2.5a)$$

$$\begin{aligned} \langle \phi' \rangle = \frac{1}{\ell} \left\langle \frac{1}{2} (3\zeta^2 - 3), \frac{\ell}{4} (3\zeta^2 - 2\zeta - 1), \right. \\ \left. -\frac{1}{2} (3\zeta^2 - 3), \frac{\ell}{4} (3\zeta^2 + 2\zeta - 1) \right\rangle \quad (A.2.5b) \end{aligned}$$

$$\langle \phi'' \rangle = \frac{1}{\ell^2} \langle 6\zeta, \ell(3\zeta - 1), -6\zeta, \ell(3\zeta + 1) \rangle \quad (A.2.5c)$$

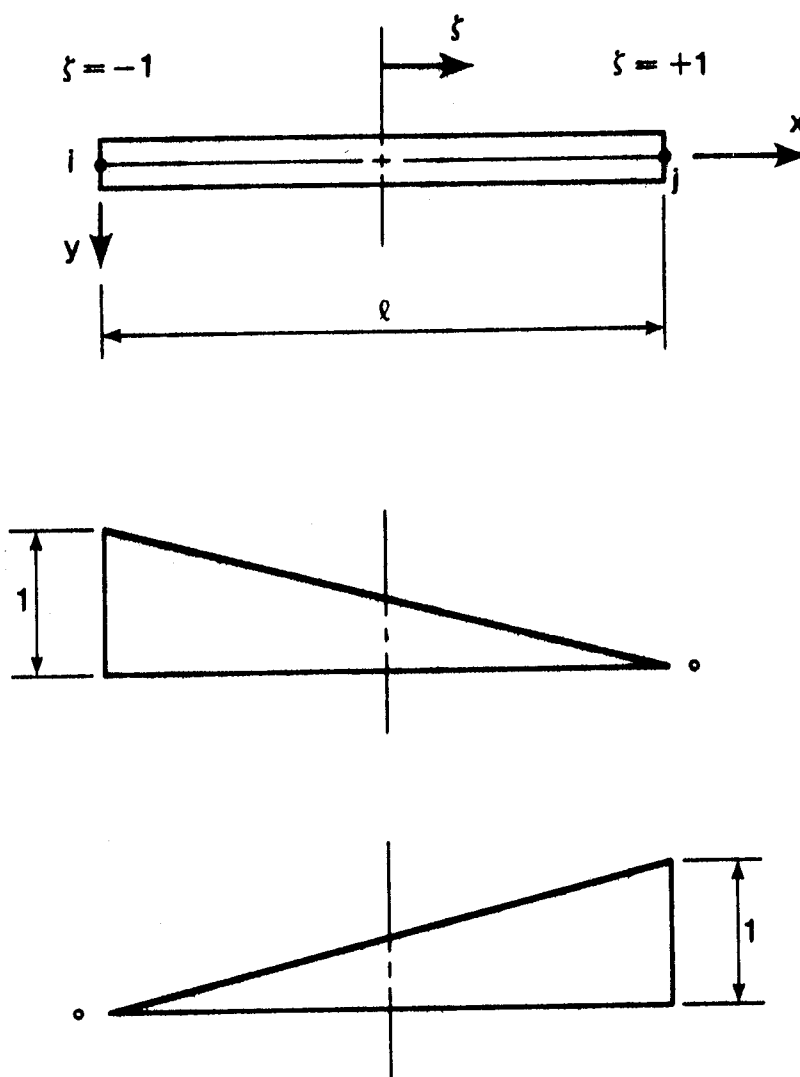


FIGURE A-1 Basic Functions for Linear Displacements

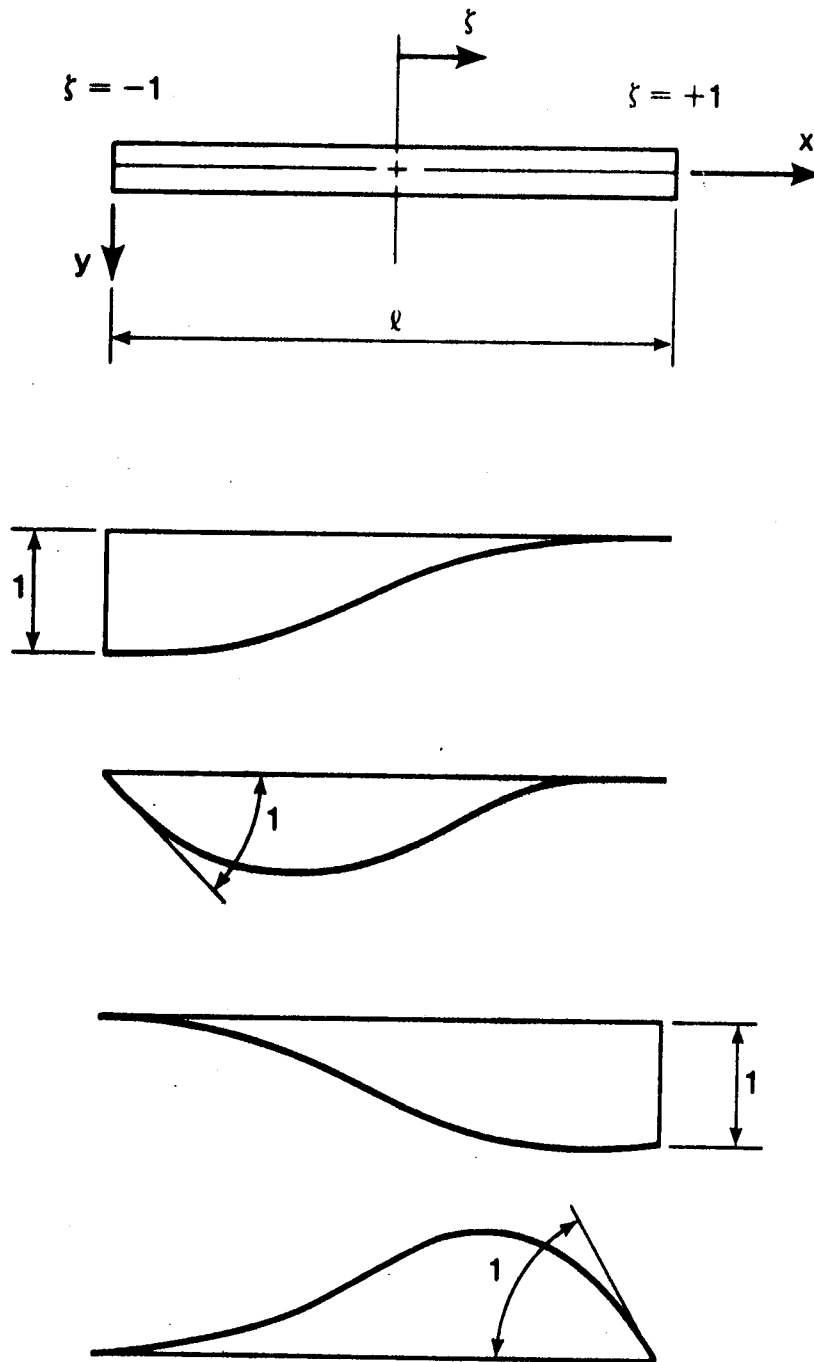


FIGURE A-2 Basic Functions for Cubic Polynomial

Substituting Eqs. A.2.4, and their derivatives, into Eq. A.1.11; using Eqs. A.2.5; carrying out the integration; and recognizing the arbitrary nature of δq ; Eqs. A.1.11 may be written as

$$[k_g] \{q\} = \{Q\} \quad (\text{A.2.6a})$$

in which the "secant stiffness matrix", $[k_g]$, can be subdivided into the "elastic stiffness matrix", $[k]$, and the "geometric stiffness matrix", $[k_g]$. That is

$$[k_s] = [k] + [k_g] \quad (\text{A.2.6b})$$

in which

$$[k] = \begin{bmatrix} EA/\ell & & & & & \\ 0 & \frac{12 EI}{\ell^3} & & & & \\ 0 & \frac{6 EI}{\ell^2} & \frac{4EI}{\ell} & & & \\ -EA/\ell & 0 & 0 & \frac{EA}{\ell} & & \\ 0 & \frac{-12 EI}{\ell^3} & \frac{-6 EI}{\ell^2} & 0 & \frac{12 EI}{\ell^3} & \\ 0 & \frac{6 EI}{\ell^2} & \frac{2 EI}{\ell} & 0 & \frac{-6 EI}{\ell^2} & \frac{4 EI}{\ell} \end{bmatrix} \quad \begin{matrix} \\ \\ \text{(SYM.)} \\ \\ \\ \end{matrix} \quad (\text{A.2.6c})$$

and

$$[k_g] = \frac{n}{\ell} \begin{bmatrix} 0 & & & & & \\ 0 & \frac{6}{5} & & & & \\ 0 & \frac{\ell}{10} & \frac{2\ell^2}{15} & & & \\ 0 & 0 & 0 & 0 & & \\ 0 & \frac{-6}{5} & \frac{-\ell}{10} & 0 & \frac{6}{5} & \\ 0 & \frac{\ell}{10} & \frac{-\ell^2}{30} & 0 & \frac{-\ell}{10} & \frac{2\ell^2}{15} \end{bmatrix} \quad \text{(A.2.6d)}$$

(SYM.)

The matrix $[k]$ is the standard elastic stiffness matrix commonly used for frame analysis (Ghali and Neville 1972). The matrix $[k_g]$ is called the geometric stiffness matrix (Chajes 1974; Porter and Powell 1971) and is a function of the element axial force.

APPENDIX B

DETAILS OF NONLINEAR ELASTIC FORMULATION

APPENDIX B

DETAILS OF NONLINEAR ELASTIC FORMULATION

This appendix presents the analytical development of the basic nonlinear equations used in this study. Also, a finite element model is developed and the finite element equilibrium equations are formulated.

B.1 Basic Equations

In Sect. 3.5.1 the incremental equilibrium equation for an element (Eq. 3.5.14) was written symbolically as

$$[k_T] \{\Delta q\} = \{\Delta Q\} \quad (B.1.1)$$

in which the influence coefficients $(k_T)_{ij}$ of the tangent stiffness matrix were evaluated by Eq. 3.5.16 which may be rewritten as

$$(k_T)_{ij} = \int_{\ell} \left(e_{1j} \frac{\partial u'_0}{\partial q_i} + e_{2j} \frac{\partial v'_0}{\partial q_i} + e_{3j} \frac{\partial v''_0}{\partial q_i} \right) \cdot dz \quad (B.1.2)$$

in which e_{1j} , e_{2j} , and e_{3j} are defined as

$$e_{1j} = \frac{\partial a_1}{\partial q_j} \quad (B.1.3a)$$

$$e_{2j} = \frac{\partial a_2}{\partial q_j} \quad (B.1.3b)$$

and

$$e_{3j} = \frac{\partial a_3}{\partial q_j} \quad (B.1.3c)$$

The quantities a_1 , a_2 , and a_3 are given by Eqs. 3.5.10. To evaluate the e_{ij} terms Eqs. 3.5.10 are differentiated with respect to q_j , which results in

$$e_{1j} = (1 + u'_0) \frac{\partial n}{\partial q_j} + n \frac{\partial u'_0}{\partial q_j} - v''_0 \frac{\partial m}{\partial q_j} - m \frac{\partial v''_0}{\partial q_j} \quad (\text{B.1.4a})$$

$$\begin{aligned} e_{2j} = & v'_0 \frac{\partial n}{\partial q_j} + n \frac{\partial v'_0}{\partial q_j} - \frac{v'_0 v''_0}{\sqrt{1-(v'_0)^2}} \left(2 + \frac{(v'_0)^2}{1-(v'_0)^2} \right) \frac{\partial m}{\partial q_j} \\ & - m \left[\frac{v'_0}{\sqrt{1-(v'_0)^2}} \left(2 + \frac{(v'_0)^2}{1-(v'_0)^2} \right) \frac{\partial v''_0}{\partial q_j} + \frac{v''_0}{\sqrt{1-(v'_0)^2}} \left(2 \right. \right. \\ & \left. \left. + \frac{3(v'_0)^4}{(1-(v'_0)^2)^2} + \frac{5(v'_0)^2}{1-(v'_0)^2} \right) \frac{\partial v'_0}{\partial q_j} \right] + \frac{v'_0 v''_0}{1-(v'_0)^2} \left(1 + \frac{(v'_0)^2}{1-(v'_0)^2} \right) \frac{\partial m^*}{\partial q_j} \\ & + m^* \left[\frac{2 v'_0 v''_0}{1-(v'_0)^2} \left(1 + \frac{(v'_0)^2}{1-(v'_0)^2} \right) \frac{\partial v''_0}{\partial q_j} + \frac{(v''_0)^2}{1-(v'_0)^2} \left(1 \right. \right. \\ & \left. \left. + \frac{4(v'_0)^4}{(1-(v'_0)^2)^2} + \frac{5(v'_0)^2}{1-(v'_0)^2} \right) \frac{\partial v'_0}{\partial q_j} \right] \quad (\text{B.1.4b}) \end{aligned}$$

and

$$\begin{aligned} e_{3j} = & - \left(1 + u'_0 + \frac{(v'_0)^2}{\sqrt{1-(v'_0)^2}} \right) \frac{\partial m}{\partial q_j} + v''_0 \left(1 + \frac{(v'_0)^2}{1-(v'_0)^2} \right) \frac{\partial m^*}{\partial q_j} \\ & - m \left[\frac{\partial u'_0}{\partial q_j} + \frac{v'_0}{\sqrt{1-(v'_0)^2}} \left(2 + \frac{(v'_0)^2}{1-(v'_0)^2} \right) \frac{\partial v'_0}{\partial q_j} \right] \end{aligned}$$

$$+ m^* \left[\left(1 + \frac{(v'_0)^2}{1 - (v'_0)^2} \right) \frac{\partial v''_0}{\partial q_j} + \frac{2v'_0 v''_0}{1 - (v'_0)^2} \left(1 + \frac{(v'_0)^2}{1 - (v'_0)^2} \right) \frac{\partial v'_0}{\partial q_j} \right]$$

(B.1.4c)

To evaluate the incremental force ΔQ_1 , of Eq. B.1.1, Eq. 3.5.17 is used. That is

$$\Delta Q_1 = Q_1 - \int_L \left(a_1 \frac{\partial u'_0}{\partial q_1} + a_2 \frac{\partial v'_0}{\partial q_1} + a_3 \frac{\partial v''_0}{\partial q_1} \right) \cdot dz \quad (\text{B.1.5})$$

All equations derived above apply to elastic and inelastic response.

B.2 Nonlinear Elastic Response

To specialize the problem to elastic response the material is assumed to be linearly elastic and the stress-strain relationship obeys Hooke's law (Eq. A.1.9).

To evaluate the stiffness coefficients $(k_T)_{ij}$ and the incremental forces ΔQ_1 , it is necessary to evaluate first the stress resultants n , m and m^* and also their derivatives $\frac{\partial n}{\partial q_j}$, $\frac{\partial m}{\partial q_j}$, and $\frac{\partial m^*}{\partial q_j}$ that appear in Eqs. 3.5.10 and B.1.4.

Substituting Eq. A.1.9 into the stress resultants defined in Eqs. 3.5.9 yields

$$n = \int_A E \cdot \epsilon_z \cdot dA \quad (\text{B.2.1a})$$

$$m = \int_A E \cdot \epsilon_z \cdot y \cdot dA \quad (\text{B.2.1b})$$

and

$$m^* = \int_A E \cdot \epsilon_z \cdot y^2 dA \quad (\text{B.2.1c})$$

Let the cross section properties for a symmetric section be defined as

$$\int_A dA = A \quad (\text{B.2.2a})$$

$$\int_A y \cdot dA = 0 \quad (\text{B.2.2b})$$

$$\int_A y^2 dA = I \quad (\text{B.2.2c})$$

$$\int_A y^3 dA = 0 \quad (\text{B.2.2d})$$

$$\int_A y^4 dA = I_4 \quad (\text{B.2.2e})$$

Substituting Eq. 3.5.5 into Eqs. B.2.1 and integrating, using the definitions given by Eqs. B.2.2 leads to

$$n = EA \left(u'_0 + \frac{(u'_0)^2}{2} + \frac{(v'_0)^2}{2} \right) + \frac{1}{2} EI \left((v''_0)^2 + \frac{(v'_0)^2 (v''_0)^2}{1 - (v'_0)^2} \right) \quad (\text{B.2.3a})$$

$$m = -EI \left(u'_0 v''_0 + v''_0 + \frac{(v'_0)^2 v''_0}{\sqrt{1 - (v'_0)^2}} \right) \quad (\text{B.2.3b})$$

and

$$m^* = EI \left(u'_0 + \frac{(u'_0)^2}{2} + \frac{(v'_0)^2}{2} \right) + \frac{1}{2} EI_4 \left((v''_0)^2 + \frac{(v'_0)^2 (v''_0)^2}{1 - (v'_0)^2} \right) \quad (\text{B.2.3c})$$

Differentiating Eqs. B.2.3 with respect to the generalized displacement q_j yields

$$\begin{aligned} \frac{\partial n}{\partial q_j} &= EA \left[(1 + u'_0) \frac{\partial u'_0}{\partial q_j} + v'_0 \frac{\partial v'_0}{\partial q_j} \right] \\ &+ EI \left[\frac{v'_0 (v''_0)^2}{1 - (v'_0)^2} \left(1 + \frac{(v'_0)^2}{1 - (v'_0)^2} \right) \frac{\partial v'_0}{\partial q_j} + v''_0 \left(1 + \frac{(v'_0)^2}{1 - (v'_0)^2} \right) \frac{\partial v''_0}{\partial q_j} \right] \end{aligned} \quad (\text{B.2.4a})$$

$$\begin{aligned} \frac{\partial m}{\partial q_j} &= -EI \left[v''_0 \frac{\partial u'_0}{\partial q_j} + (1 + u'_0) \frac{\partial v''_0}{\partial q_j} + \frac{v'_0 v''_0}{\sqrt{1 - (v'_0)^2}} \left(2 + \frac{(v'_0)^2}{1 - (v'_0)^2} \right) \frac{\partial v'_0}{\partial q_j} \right. \\ &\quad \left. + \frac{(v'_0)^2}{\sqrt{1 - (v'_0)^2}} \frac{\partial v''_0}{\partial q_j} \right] \end{aligned} \quad (\text{B.2.4b})$$

and

$$\frac{\partial m^*}{\partial q_j} = EI \left[(1 + u'_0) \frac{\partial u'_0}{\partial q_j} + v'_0 \frac{\partial v'_0}{\partial q_j} \right]$$

$$+ EI_4 \left[\frac{v'_0 (v''_0)^2}{1 - (v'_0)^2} \left(1 + \frac{(v'_0)^2}{1 - (v'_0)^2} \right) \frac{\partial v'_0}{\partial q_j} + v''_0 \left(1 + \frac{(v'_0)^2}{1 - (v'_0)^2} \right) \frac{\partial v''_0}{\partial q_j} \right] \quad (B.2.4c)$$

Equations B.2.3 and B.2.4 are expressions for the stress resultants and their derivatives, respectively, derived for an elastic element subjected to axial force and bending moments.

For an elastic element subjected only to axial force (truss element) the bending effect is eliminated and the displacements at any point along the element, Eqs. 3.2.3, become

$$u = u_0 \quad (B.2.5a)$$

and

$$v = v_0 \quad (B.2.5b)$$

Consequently

$$u' = u'_0 \quad (B.2.6a)$$

and

$$v' = v'_0 \quad (B.2.6b)$$

Substituting Eqs. B.2.6 into the strain expression given by Eq. 3.2.4 yields

$$\epsilon_z = u'_0 + \frac{1}{2} \left[(u'_0)^2 + (v'_0)^2 \right] \quad (B.2.7)$$

Substituting Eq. B.2.7 into Eqs. B.2.1 and integrating using Eqs. B.2.2 yields the stress resultants

$$n = EA \left[u'_o + \frac{(u'_o)^2}{2} + \frac{(v'_o)^2}{2} \right] \quad (\text{B.2.8a})$$

$$m = 0 \quad (\text{B.2.8b})$$

and

$$m^* = EI \left[u'_o + \frac{(u'_o)^2}{2} + \frac{(v'_o)^2}{2} \right] \quad (\text{B.2.8c})$$

Differentiating Eqs. B.2.8 with respect to q_j yields

$$\frac{\partial n}{\partial q_j} = EA \left[(1 + u'_o) \frac{\partial u'_o}{\partial q_j} + v'_o \frac{\partial v'_o}{\partial q_j} \right] \quad (\text{B.2.9a})$$

$$\frac{\partial m}{\partial q_j} = 0 \quad (\text{B.2.9b})$$

and

$$\frac{\partial m^*}{\partial q_j} = EI \left[(1 + u'_o) \frac{\partial u'_o}{\partial q_j} + v'_o \frac{\partial v'_o}{\partial q_j} \right] \quad (\text{B.2.9c})$$

B.3 Evaluation of Unbalanced Forces Vector $\{\Delta R\}$ For Finite Element Model

The incremental force ΔQ_i as given by Eq. B.1.5 can be evaluated knowing the quantities u'_o , v'_o and v''_o , their derivatives with respect to q_i , and the stress resultants n , m and m^* .

The quantities u'_o , v'_o and v''_o can be evaluated, from Eqs. 3.5.18 as

$$u'_o = \langle \phi' \rangle \{ \bar{U} \} \quad (\text{B.3.1a})$$

$$v'_0 = \langle \phi' \rangle \{\bar{V}\} \quad (\text{B.3.1b})$$

and

$$v''_0 = \langle \phi'' \rangle \{\bar{V}\} \quad (\text{B.3.1c})$$

Differentiating Eqs. B.3.1 with respect to q_1 yields

$$\frac{\partial u'_0}{\partial q_1} = \phi'_{q_1} \quad (\text{B.3.2a})$$

$$\frac{\partial v'_0}{\partial q_1} = \phi'_{q_1} \quad (\text{B.3.2b})$$

and

$$\frac{\partial v''_0}{\partial q_1} = \phi''_{q_1} \quad (\text{B.3.2c})$$

in which ϕ'_{q_1} or ϕ''_{q_1} is the term of the differentiated shape functions associated with the generalized displacement q_1 in $\{\bar{U}\}$ or $\{\bar{V}\}$ as defined in Fig. 3-7.

B.3.1 Vector of Incremental Forces $\{\Delta Q\}$ of Flexural Element

Substituting Eqs. B.3.2 into Eq. B.1.5 yields

$$\Delta Q_1 = Q_1 - \int_{\ell} a_1 \cdot \phi'_{q_1} \cdot dz \quad (\text{B.3.3a})$$

for $i = 1$ to 4; and

$$\Delta Q_1 = Q_1 - \int_{\ell} [a_2 \phi'_{q_1} + a_3 \phi''_{q_1}] \cdot dz \quad (\text{B.3.3b})$$

for $i = 5$ to 8 ; and the quantities a_1 , a_2 and a_3 are defined in Eqs. 3.5.10b, 3.5.10c, and 3.5.10d, respectively.

Arranging Eqs. B.3.3 in matrix form leads to

$$\{\Delta Q\} = \{Q\} - \int_{\ell} \left\{ \frac{a_1 \{\phi'\}}{a_2 \{\phi'\} + a_3 \{\phi''\}} \right\} dz \quad (B.3.4)$$

which can be written, symbolically, as

$$\{\Delta Q\} = \{Q\} - \{Q^R\} \quad (B.3.5)$$

in which $\{\Delta Q\}$ is the vector of incremental forces (8×1) associated with the vector of nodal displacements defined by Eq. 3.5.19b, $\{Q\}$ is the vector of applied loads and $\{Q^R\}$ is called the vector of resisting forces and is defined as

$$\{Q^R\} = \int_{\ell} \left\{ \frac{a_1 \{\phi'\}}{a_2 \{\phi'\} + a_3 \{\phi''\}} \right\} dz \quad (B.3.6)$$

To evaluate the vector $\{Q^R\}$ Gaussian integration method is used. The basic assumption in Gaussian numerical integration is that (Bathe and Wilson 1976)

$$\int_a^b \{F(r)\} dr = \alpha_1 \{F(r_1)\} + \alpha_2 \{F(r_2)\} + \dots + \alpha_n \{F(r_n)\} \quad (B.3.7)$$

in which $\{F(r)\}$ is the matrix to be integrated, $\alpha_1, \alpha_2, \dots$ and α_n are weighting factors, r_1, r_2, \dots and r_n are sampling points and $\{F(r_1)\}$ is the matrix $\{F(r)\}$ evaluated at the i th sampling point.

According to Eq. B.3.7, Eq. B.3.6 can be written as

$$\{Q^R\} = \sum_{i=1}^n \alpha_i \left\{ \frac{a_1 \{\phi'\}}{a_2 \{\phi'\} + a_3 \{\phi''\}} \right\}_i \quad (B.3.8)$$

in which n is the number of sampling points (Gauss points) assumed along the element and α_i is the weight associated with the i th Gauss point. Many references have tabulated a variety of sampling points and the corresponding weights (Loxan *et al.* 1942; Bathe and Wilson 1976).

In this study four sampling points are assumed along the element. For each Gauss point assumed the matrices $\{\phi'\}$ and $\{\phi''\}$ are evaluated. Also, the quantities u'_0 , v'_0 , and v''_0 are calculated using Eqs. B.3.1. At this point the stress resultants can be evaluated from Eqs. B.2.3. Consequently the quantities a_1 , a_2 , and a_3 can be calculated from Eqs. 3.5.10b, 3.5.10c, and 3.5.10d. Substituting the results into Eq. B.3.8 and using the appropriate weight yields the contribution of one Gauss point to the vector $\{Q^R\}$. Summing over all the Gauss points gives the vector of resisting force $\{Q^R\}$ which can be subtracted from the vector of applied loads $\{Q\}$ to obtain the vector of incremental forces $\{\Delta Q\}$ as defined in Eq. B.3.5.

B.3.2 Vector of Incremental Forces $\{\Delta Q\}$ of Truss Element

For an element subjected only to axial force the linear interpolation functions of Eqs. A.2.3a are used. Thus Eqs. B.3.2 become

$$\frac{\partial u'_0}{\partial q_1} = (\bar{\phi}_{q_1})' \quad (B.3.9a)$$

$$\frac{\partial v'_o}{\partial q_1} = (\bar{\phi}_{q_1})' \quad (\text{B.3.9b})$$

and

$$\frac{\partial v''_o}{\partial q_1} = 0 \quad (\text{B.3.9c})$$

Substituting Eqs. B.3.9 into Eq. B.1.5, and using Eqs. 3.5.10b, 3.5.10c, and 3.5.10d, yields

$$\Delta Q_1 = Q_1 - \int_{\ell} n(1 + u'_o) (\bar{\phi}_{q_1})' dz \quad (\text{B.3.10a})$$

for $i = 1, 2$; and

$$\Delta Q_1 = Q_1 - \int_{\ell} n v'_o (\bar{\phi}_{q_1})' dz \quad (\text{B.3.10b})$$

for $i = 3, 4$.

Writing Eqs. B.3.10 in matrix form leads to

$$\{\Delta Q\} = \{Q\} - \int_{\ell} \left\{ \frac{n(1 + u'_o) \{(\bar{\phi})'\}}{n v'_o \{(\bar{\phi})'\}} \right\} dz \quad (\text{B.3.11})$$

which can be written symbolically as

$$\{\Delta Q\} = \{Q\} - \{Q^R\} \quad (\text{B.3.12})$$

in which $\{\Delta Q\}$ is the vector of incremental forces associated with the vector of nodal displacements defined by Eq. 3.5.19c and it is a 4×1 vector.

Again the vector $\{Q^R\}$ can be evaluated by numerical integration using Gauss method explained above.

B.3.3 Assembly of Unbalanced Forces

To solve for the incremental displacements $\{\Delta r\}$ in Eq. 3.5.24 the vector of unbalanced forces $\{\Delta R\}$ must be evaluated. The incremental forces $\{\Delta Q\}$ are first obtained in local coordinate system by Eq. B.3.5. These forces can be assembled into the global coordinate system using Eq. 3.3.8 and the appropriate transformation. Assembling Eq. B.3.5 or Eq. B.3.12 into the global coordinate system yields

$$\{\Delta R\} = \{R\} - \{R^R\} \quad (B.3.13)$$

in which $\{\Delta R\}$ is the vector of unbalanced forces, $\{R\}$ is the assembled vector of applied loads and $\{R^R\}$ is the assembled vector of resisting forces.

B.4 Evaluation of Stiffness Matrix $[K_T]$

To solve for the incremental displacements $\{\Delta r\}$, in Eq. 3.5.24, the structure tangent stiffness matrix $[K_T]$ must be evaluated. In this section two different element stiffness matrices are developed, one for a flexural element and the other for a truss element. The element stiffness matrices are then assembled to form the structure stiffness matrix $[K_T]$.

B.4.1 Element Stiffness Matrix for a Flexural Element

The influence coefficient $(k_T)_{ij}$ must be evaluated to form the element stiffness matrix $[k_T]$. Substituting Eqs. B.3.2 into Eq. B.1.2 yields:

(a) for $1 \leq i \leq 4$

$$(k_T)_{ij} = \int_{\ell} e_{1j} \cdot \phi'_{q_i} \cdot dz \quad (B.4.1a)$$

and

(b) for $5 \leq i \leq 8$

$$(k_T)_{ij} = \int_{\ell} [e_{2j} \cdot \phi'_{q_i} + e_{3j} \cdot \phi''_{q_i}] dz \quad (B.4.1b)$$

in which e_{1j} , e_{2j} , and e_{3j} are defined in Eqs. B.1.4. Thus, the j th column in the element stiffness matrix $[k_T]$ can be written as

$$\{k_T\}_j = \int_{\ell} \left\{ \frac{\{\phi'\} \cdot e_{1j}}{\{\phi'\} e_{2j} + \{\phi''\} e_{3j}} \right\} dz \quad (B.4.2)$$

The full matrix $[k_T]$ can be written as

$$[k_T] = \int_{\ell} \left[\frac{\{\phi'\} \langle e_1 \rangle}{\{\phi'\} \langle e_2 \rangle + \{\phi''\} \langle e_3 \rangle} \right] dz \quad (B.4.3)$$

or it can be written, symbolically, as

$$[k_T] = \left[\frac{[k_1]}{[k_2] + [k_3]} \right] \quad (B.4.4)$$

in which $[k_T]$ is an 8×8 matrix, while $[k_1]$, $[k_2]$ and $[k_3]$ are 4×8 matrices defined as

$$\begin{aligned}
[k_1] = \int_{\ell} \{ \phi' \} & \left[(1 + u'_0) \left\langle \frac{\partial n}{\partial q} \right\rangle - v''_0 \left\langle \frac{\partial m}{\partial q} \right\rangle \right. \\
& \left. + n \left\langle \phi'_1 \right\rangle - m \left\langle \phi''_2 \right\rangle \right] \cdot dz
\end{aligned} \tag{B.4.5a}$$

$$\begin{aligned}
[k_2] = \int_{\ell} \{ \phi' \} & \left[v'_0 \left\langle \frac{\partial n}{\partial q} \right\rangle - \frac{v'_0 v''_0}{\sqrt{1 - (v'_0)^2}} \left(2 + \frac{v'_0}{1 - (v'_0)^2} \right) \left\langle \frac{\partial m}{\partial q} \right\rangle \right. \\
& + \frac{v'_0 (v''_0)^2}{1 - (v'_0)^2} \left(1 + \frac{(v'_0)^2}{1 - (v'_0)^2} \right) \left\langle \frac{\partial m^*}{\partial q} \right\rangle + n \left\langle \phi'_2 \right\rangle \\
& - m \left[\frac{v'_0}{\sqrt{1 - (v'_0)^2}} \left(2 + \frac{(v'_0)^2}{1 - (v'_0)^2} \right) \left\langle \phi''_2 \right\rangle \right. \\
& + \frac{v''_0}{\sqrt{1 - (v'_0)^2}} \left(1 + \frac{(v'_0)^2}{1 - (v'_0)^2} \right) \left(2 + \frac{3(v'_0)^2}{1 - (v'_0)^2} \right) \left\langle \phi'_2 \right\rangle \\
& + m^* \left(\frac{2 v'_0 v''_0}{1 - (v'_0)^2} \left(1 + \frac{(v'_0)^2}{1 - (v'_0)^2} \right) \left\langle \phi''_2 \right\rangle \right. \\
& \left. \left. + \frac{(v''_0)^2}{1 - (v'_0)^2} \left(1 + \frac{(v'_0)^2}{1 - (v'_0)^2} \right) \left(1 + \frac{4(v'_0)^2}{1 - (v'_0)^2} \right) \left\langle \phi'_2 \right\rangle \right) \right] dz
\end{aligned} \tag{B.4.5b}$$

and

$$\begin{aligned}
[k_3] = \int_{\ell} \{ \phi'' \} & \left[- \left(1 + u'_0 + \frac{(v'_0)^2}{\sqrt{1 - (v'_0)^2}} \right) \left\langle \frac{\partial m}{\partial q} \right\rangle \right. \\
& + v''_0 \left(1 + \frac{(v'_0)^2}{1 - (v'_0)^2} \right) \left\langle \frac{\partial m^*}{\partial q} \right\rangle - m \left(\left\langle \phi'_1 \right\rangle \right.
\end{aligned}$$

$$\begin{aligned}
& + \frac{v'_0}{\sqrt{1 - (v'_0)^2}} \left(2 + \frac{(v'_0)^2}{1 - (v'_0)^2} \right) \langle \phi'_2 \rangle \Bigg] \\
& + m^* \left[\frac{2 v'_0 v''_0}{1 - (v'_0)^2} \left(1 + \frac{(v'_0)^2}{1 - (v'_0)^2} \right) \langle \phi'_2 \rangle \right. \\
& \left. + \left(1 + \frac{(v'_0)^2}{1 - (v'_0)^2} \right) \langle \phi''_2 \rangle \right] \cdot dz
\end{aligned} \tag{B.4.5c}$$

In Eqs. B.4.5, $\langle \phi'_1 \rangle$, $\langle \phi'_2 \rangle$ and $\langle \phi''_2 \rangle$ are 1×8 row vectors defined as

$$\langle \phi'_1 \rangle = \langle \langle \phi' \rangle \vdots \langle 0 \rangle \rangle \tag{B.4.6a}$$

$$\langle \phi'_2 \rangle = \langle \langle 0 \rangle \vdots \langle \phi' \rangle \rangle \tag{B.4.6b}$$

and

$$\langle \phi''_2 \rangle = \langle \langle 0 \rangle \vdots \langle \phi'' \rangle \rangle \tag{B.4.6c}$$

; and the vectors $\langle \frac{\partial n}{\partial q} \rangle$, $\langle \frac{\partial m}{\partial q} \rangle$ and $\langle \frac{\partial m^*}{\partial q} \rangle$ are also 1×8 row vectors which are called the incremental stress resultant vectors.

In order to be able to use the Gaussian integration method to evaluate $[k_1]$, $[k_2]$, and $[k_3]$ the incremental stress resultant vectors must be evaluated at each Gauss point. This can be done as follows:

Substituting Eqs. B.3.2 into Eqs. B.2.4 yields

$$(a) \quad \text{for } 1 \leq j \leq 4$$

$$\frac{\partial n}{\partial q_j} = EA (1 + u'_0) \phi'_{q_j} \tag{B.4.7a}$$

$$\frac{\partial m}{\partial q_j} = -EI v_o'' \phi'_{q_j} \quad (B.4.7b)$$

$$\frac{\partial m^*}{\partial q_j} = EI (1 + u_o') \phi'_{q_j} \quad (B.4.7c)$$

and,

(b) for $5 \leq j \leq 8$

$$\begin{aligned} \frac{\partial n}{\partial q_j} = & EA v_o' \phi'_{q_j} + EI \left[\frac{v_o' (v_o'')^2}{1 - (v_o')^2} \left(1 + \frac{(v_o')^2}{1 - (v_o')^2} \right) \phi'_{q_j} \right. \\ & \left. + v_o'' \left(1 + \frac{(v_o')^2}{1 - (v_o')^2} \right) \phi''_{q_j} \right] \end{aligned} \quad (B.4.7d)$$

$$\begin{aligned} \frac{\partial m}{\partial q_j} = & -EI \left[\frac{v_o' (v_o'')^2}{\sqrt{1 - (v_o')^2}} \left(2 + \frac{(v_o')^2}{1 - (v_o')^2} \right) \phi'_{q_j} \right. \\ & \left. + \left(1 + u_o' + \frac{(v_o')^2}{\sqrt{1 - (v_o')^2}} \right) \phi''_{q_j} \right] \end{aligned} \quad (B.4.7e)$$

$$\begin{aligned} \frac{\partial m^*}{\partial q_j} = & EI v_o' \phi'_{q_j} + EI_4 \left[\frac{v_o' (v_o'')^2}{1 - (v_o')^2} \left(1 + \frac{(v_o')^2}{1 - (v_o')^2} \right) \phi'_{q_j} \right. \\ & \left. + v_o'' \left(1 + \frac{(v_o')^2}{1 - (v_o')^2} \right) \phi''_{q_j} \right] \end{aligned} \quad (B.4.7f)$$

Equations B.4.7 can be written in a column vector form as

listed in Table B-1.

$$\left\{ \frac{\partial n}{\partial q} \right\} = \left\{ \begin{array}{l} \frac{EA (1 + u'_0) \{\phi'\}}{\left(EA v'_0 + EI \frac{v'_0 (v''_0)^2}{1 - (v'_0)^2} \left(1 + \frac{(v'_0)^2}{1 - (v'_0)^2} \right) \right) \{\phi'\}} \\ + EI v''_0 \left(1 + \frac{(v'_0)^2}{1 - (v'_0)^2} \right) \{\phi''\} \end{array} \right\}$$

$$\left\{ \frac{\partial m}{\partial q} \right\} = \left\{ \begin{array}{l} \frac{- EI v''_0 \{\phi'\}}{- EI \frac{v'_0 v''_0}{\sqrt{1 - (v'_0)^2}} \left(2 + \frac{(v'_0)^2}{1 - (v'_0)^2} \right) \{\phi'\}} \\ - EI \left(1 + u'_0 + \frac{(v'_0)^2}{\sqrt{1 - (v'_0)^2}} \right) \{\phi''\} \end{array} \right\}$$

TABLE B-1 Incremental Stress Resultant Vectors
For Flexural Element

$$\left\{ \frac{\partial m^*}{\partial q} \right\} = \left\{ \begin{array}{l} \frac{EI (1 + u'_0) \{\phi'\}}{\left[EI v'_0 + EI_4 \frac{v'_0 (v''_0)^2}{1 - (v'_0)^2} \left(1 + \frac{(v'_0)^2}{1 - (v'_0)^2} \right) \right] \{\phi'\}} \\ + EI_4 v''_0 \left(1 + \frac{(v'_0)^2}{1 - (v'_0)^2} \right) \{\phi''\} \end{array} \right\}$$

Note:

$\left\{ \frac{\partial}{\partial q} \right\}$ is 8 x 1 column matrix

$\{\phi'\}$ and $\{\phi''\}$ are 4 x 1 column matrices

TABLE B-1 (Cont.) Incremental Stress Resultant
Vectors for Flexural Element

Now to evaluate $[k_T]$, the quantities u'_0 , v'_0 and v''_0 are calculated from Eqs. B.3.1 at each Gauss point. Thus the stress resultants can be evaluated from Eqs. B.2.3 and also the incremental stress resultant vectors can be evaluated as listed in Table B-1. At this stage the Gaussian integration method explained above is used to evaluate Eqs. B.4.5 leading to the element stiffness matrix given by Eq. B.4.4.

B.4.2 Element Stiffness Matrix for a Truss Element

For a truss element the influence coefficients $(k_T)_{ij}$ are obtained by substituting Eqs. B.3.9 into Eqs. B.1.2 to yield

$$(a) \text{ for } 1 \leq i \leq 2$$

$$(k_T)_{ij} = \int_{\ell} e_{1j} \cdot (\bar{\phi}_{q_1})' \cdot dz \quad (B.4.8a)$$

and

$$(b) \text{ for } 3 \leq i \leq 4$$

$$(k_T)_{ij} = \int_{\ell} e_{2j} (\bar{\phi}_{q_1})' dz \quad (B.4.8b)$$

The j th column in the element stiffness matrix can then be written as

$$\{k_T\}_j = \int_{\ell} \left\{ \begin{array}{c} \{(\bar{\phi})'\} e_{1j} \\ \{(\bar{\phi})'\} e_{2j} \end{array} \right\} dz \quad (B.4.9)$$

and the full matrix $[k_T]$ can be written as

$$[k_T] = \int_L \left[\frac{\{(\bar{\phi})'\} \langle e_1 \rangle}{\{(\bar{\phi})'\} \langle e_2 \rangle} \right] dz \quad (B.4.10)$$

or it can be written, symbolically, as

$$[k_T] = \begin{bmatrix} [k_1] \\ [k_2] \end{bmatrix} \quad (B.4.11)$$

in which $[k_T]$ is a 4 x 4 matrix and $[k_1]$ and $[k_2]$ are 2 x 4 matrices defined by Eqs. B.4.5a and B.4.5b. In such a case $\{(\bar{\phi})'\}$ replaces $\{\phi'\}$ and it is a 2 x 1 vector. Also $\langle(\bar{\phi}_1)'\rangle$, $\langle(\bar{\phi}_2)'\rangle$, and $\langle(\bar{\phi}_2)''\rangle$ replace $\langle\phi_1'\rangle$, $\langle\phi_2'\rangle$, and $\langle\phi_2''\rangle$, respectively. In this case $\langle(\bar{\phi}_1)'\rangle$, $\langle(\bar{\phi}_2)'\rangle$, and $\langle(\bar{\phi}_2)''\rangle$ are 1 x 4 matrices given as

$$\langle(\bar{\phi}_1)'\rangle = \left\langle \langle(\bar{\phi})'\rangle \vdots \langle 0 \rangle \right\rangle \quad (B.4.12a)$$

$$\langle(\bar{\phi}_2)'\rangle = \left\langle \langle 0 \rangle \vdots \langle(\bar{\phi})'\rangle \right\rangle \quad (B.4.12b)$$

and

$$\langle(\bar{\phi}_2)''\rangle = \left\langle \langle 0 \rangle \vdots \langle 0 \rangle \right\rangle \quad (B.4.12c)$$

in which $\langle\bar{\phi}\rangle$ is the shape functions for a truss element given by Eq. A.2.3a; and the incremental stress resultant vectors are 1 x 4 row vectors.

To evaluate the incremental stress resultant vectors Eqs. B.3.9 are substituted into Eqs. B.2.9 to obtain

(a) for $1 \leq j \leq 2$

$$\frac{\partial n}{\partial q_j} = EA (1 + u'_0) (\bar{\phi}_{q_j})' \quad (B.4.13a)$$

$$\frac{\partial m}{\partial q_j} = 0 \quad (\text{B.4.13b})$$

$$\frac{\partial m^*}{\partial q_j} = EI (1 + u'_0) (\bar{\phi}_{q_j})' \quad (\text{B.4.13c})$$

and

$$(b) \text{ for } 3 \leq j \leq 4$$

$$\frac{\partial n}{\partial q_j} = EA v'_0 (\bar{\phi}_{q_j})' \quad (\text{B.4.13d})$$

$$\frac{\partial \dot{m}}{\partial q_j} = 0 \quad (\text{B.4.13e})$$

$$\frac{\partial m^*}{\partial q_j} = EI v'_0 (\bar{\phi}_{q_j})' \quad (\text{B.4.13f})$$

Equations B.4.13 can be written in a column vector as given in Table B-2.

Substituting the incremental stress resultant vectors as given in Table B-2 and the stress resultants as given in Eqs. B.2.8 into Eqs. B.4.5a and B.4.5b, the matrices $[k_1]$ and $[k_2]$, in Eq. B.4.11, can be redefined as

$$[k_1] = \int_{\ell} \{(\bar{\phi})'\} \left[(1 + u'_0) \left\langle \frac{\partial n}{\partial q} \right\rangle + n \left\langle (\bar{\phi}_1)' \right\rangle \right] dz \quad (\text{B.4.14a})$$

and

$$[k_2] = \int_{\ell} \{(\bar{\phi})'\} \left[v'_0 \left\langle \frac{\partial n}{\partial q} \right\rangle + n \left\langle (\bar{\phi}_2)' \right\rangle \right] dz \quad (\text{B.4.14b})$$

$$\left\{ \frac{\partial n}{\partial q} \right\} = \left\{ \frac{EA (1 + u'_0) \{(\bar{\phi})'\}}{EA v'_0 \{(\bar{\phi})'\}} \right\}$$

$$\left\{ \frac{\partial m}{\partial q} \right\} = \{ 0 \}$$

$$\left\{ \frac{\partial m^*}{\partial q} \right\} = \left\{ \frac{EI (1 + u'_0) \{(\bar{\phi})'\}}{EI v'_0 \{(\bar{\phi})'\}} \right\}$$

Note

$\left\{ \frac{\partial}{\partial q} \right\}$ is 4 x 1 column matrix

$\{(\bar{\phi})'\}$ is 2 x 1 column matrix

TABLE B-2 Incremental Stress Resultant
Vectors for Truss Element

Integration leads to the element stiffness matrix $[k_T]$ in Eq. B.4.11.

B.4.3 Assembly of Structural Stiffness $[K_T]$

The assembly of element stiffness matrix into the structure stiffness matrix is explained in detail in Sect. 3.3.2.

APPENDIX C
LARGE DISPLACEMENT TRANSFORMATION

APPENDIX C

LARGE DISPLACEMENT TRANSFORMATION

Consider the element shown in Fig. C-1. The relation between the reference axis in local and global coordinate systems can be written as

$$Z = z \cos \alpha - y \sin \alpha \quad (C.1a)$$

and

$$Y = z \sin \alpha - y \cos \alpha \quad (C.1b)$$

Also the relation between the local displacement \tilde{u} and \tilde{v} and the global displacements \tilde{U} and \tilde{V} , at any point, can be expressed as

$$\tilde{u} = \tilde{U} \cos \alpha + \tilde{V} \sin \alpha \quad (C.2a)$$

and

$$\tilde{v} = \tilde{U} \sin \alpha - \tilde{V} \cos \alpha \quad (C.2b)$$

in which \tilde{u} and \tilde{v} are functions of z and y . Differentiating Eqs. C.2 with respect to z yields

$$\frac{\partial \tilde{u}}{\partial z} = \frac{\partial \tilde{U}}{\partial Z} \frac{\partial Z}{\partial z} \cos \alpha + \frac{\partial \tilde{V}}{\partial Z} \frac{\partial Z}{\partial z} \sin \alpha + \frac{\partial \tilde{U}}{\partial Y} \frac{\partial Y}{\partial z} \cos \alpha + \frac{\partial \tilde{V}}{\partial Y} \frac{\partial Y}{\partial z} \sin \alpha \quad (C.3a)$$

and

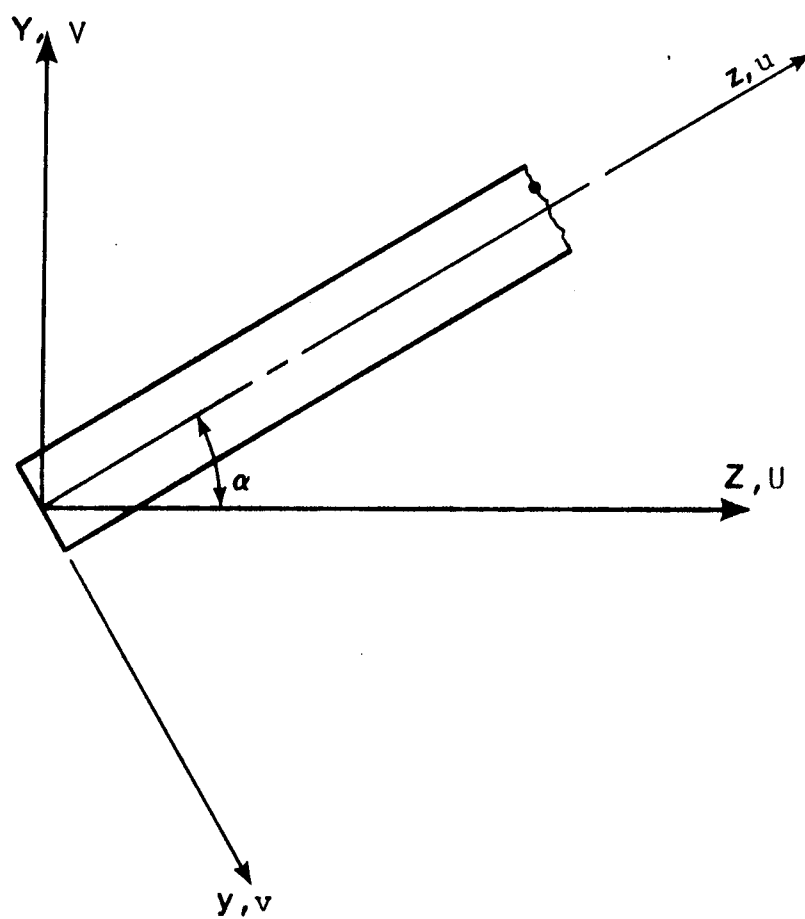


FIGURE C-1 Element Transformation

$$\frac{\partial \tilde{V}}{\partial z} = \frac{\partial \tilde{U}}{\partial Z} \frac{\partial Z}{\partial z} \sin \alpha - \frac{\partial \tilde{V}}{\partial Z} \frac{\partial Z}{\partial z} \cos \alpha + \frac{\partial \tilde{U}}{\partial Y} \frac{\partial Y}{\partial z} \sin \alpha - \frac{\partial \tilde{V}}{\partial Y} \frac{\partial Y}{\partial z} \cos \alpha \quad (C.3b)$$

Differentiating Eqs. C.1 results in

$$\frac{\partial Z}{\partial z} = \cos \alpha \quad (C.4)$$

$$\frac{\partial Y}{\partial z} = \sin \alpha \quad (C.5)$$

Also there is no change in angle between the axes after deformation.

This constraint has been approximated by imposing the condition that

$$\frac{\partial U}{\partial Y} = - \frac{\partial V}{\partial Z} \quad (C.6)$$

Substituting Eqs. C.4, C.5, and C.6 into Eqs. C.3 results in

$$\left. \frac{\partial \tilde{U}}{\partial z} \right|_{y=0} = \frac{\partial u}{\partial z} = \frac{\partial U}{\partial Z} \cos^2 \alpha + \frac{\partial V}{\partial Y} \sin^2 \alpha \quad (C.7a)$$

and

$$\left. \frac{\partial \tilde{V}}{\partial z} \right|_{y=0} = \frac{\partial v}{\partial z} = \frac{\partial U}{\partial Z} \cos \alpha \sin \alpha - \frac{\partial V}{\partial Y} \cos \alpha \sin \alpha - \frac{\partial V}{\partial Z} \quad (C.7b)$$

Introducing the notation

$$\theta = \frac{\partial V}{\partial Z} \quad (C.8)$$

then the transformation from local to global coordinate system may be written in a matrix form as

$$\begin{Bmatrix} u \\ u' \\ v \\ v' \end{Bmatrix} = \begin{bmatrix} c & s & & \\ & & c^2 & s^2 \\ s & -c & & \\ & & -1 & cs & -cs \end{bmatrix} \begin{Bmatrix} U \\ V \\ \theta \\ \frac{\partial U}{\partial Z} \\ \frac{\partial V}{\partial Y} \end{Bmatrix} \quad (\text{C.9})$$

in which c and s denote $\cos \alpha$ and $\sin \alpha$, respectively. The transformation matrix for the element is tabulated in Table 3-5.

APPENDIX D

CALCULATION OF SECTION PROPERTIES

AND STRESS RESULTANTS FOR

I-SECTION

APPENDIX D

CALCULATION OF SECTION PROPERTIES AND

STRESS RESULTANTS FOR I-SECTION

To evaluate the tangent stiffness matrix for an elastic element, it is necessary to know the cross section properties. In the case of inelastic analysis, it is important to evaluate the transformed section in order to evaluate the tangent stiffness matrix. Once the transformed section has been determined, the evaluation of the cross section properties is identical to that of any arbitrary elastic section.

In this Appendix the method of determining the transformed section is discussed. The equations for numerically evaluating section properties are presented and the equations used to evaluate the stress resultants for an inelastic section are given.

D.1 Determination of Transformed Section

For any set of nodal displacements the strain at any point on the element, due to axial and bending displacements, may be evaluated as (Eq. 3.5.5)

$$\epsilon_z = u'_o + \frac{u_o'^2}{2} + \frac{v_o'^2}{2} - y v_o'' \left(1 + u'_o + \frac{v_o'^2}{\sqrt{1 - v_o'^2}} \right) + \frac{y^2 v_o''^2}{2} \left(1 + \frac{v_o'^2}{1 - v_o'^2} \right) \quad (D.1.1)$$

Adding the residual strain at this particular point results in the total strain given as

$$\epsilon_{zt} = \epsilon_z + \epsilon_R \quad (D.1.2)$$

in which ϵ_{zt} is the total strain at any point in the z direction, ϵ_z is the strain given by Eq. D.1.1, and ϵ_R is the residual strain.

If the residual strain distribution varies in some arbitrary manner, as shown in Fig. D-1a, it can be approximated by linear segments, shown in Fig. D-1b.

For equilibrium

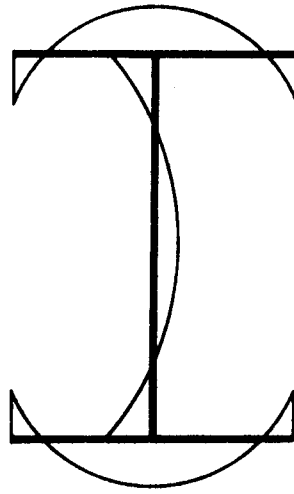
$$\int_A \sigma_R \cdot dA = 0 \quad (D.1.3a)$$

and

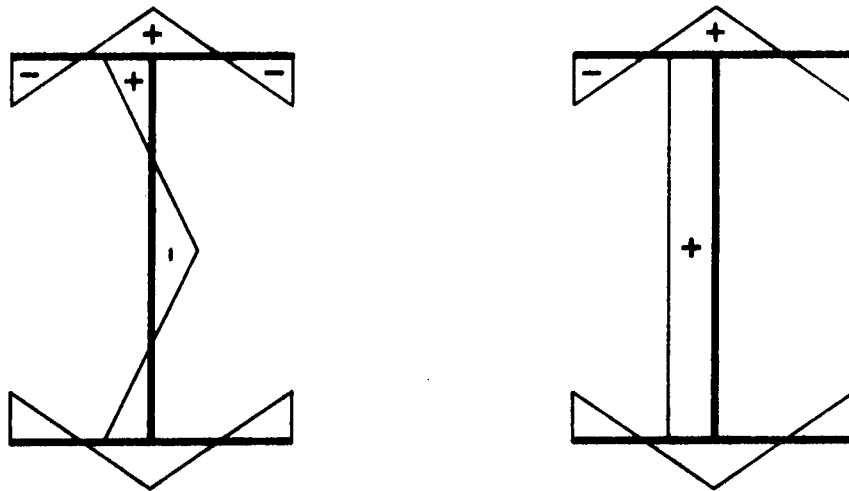
$$\int_A \sigma_R \cdot y \cdot dA = 0 \quad (D.1.3b)$$

Consider a plate segment of the cross section with a linear variation of residual strains. By superposition, the total strain distribution will also be linear in the segment.

The stress-strain curve used in the analysis is the tri-linear curve shown in Fig. D-2. To approximate the curve for mild steel curve 2, the dashed curve, is used. It is apparent from Fig. D-2 that the strain hardening of the material can approximately be accounted for in the analysis.



(a) Actual Residual Strain



(b) Assumed Residual Strain

FIGURE D-1 Residual Strain Distribution

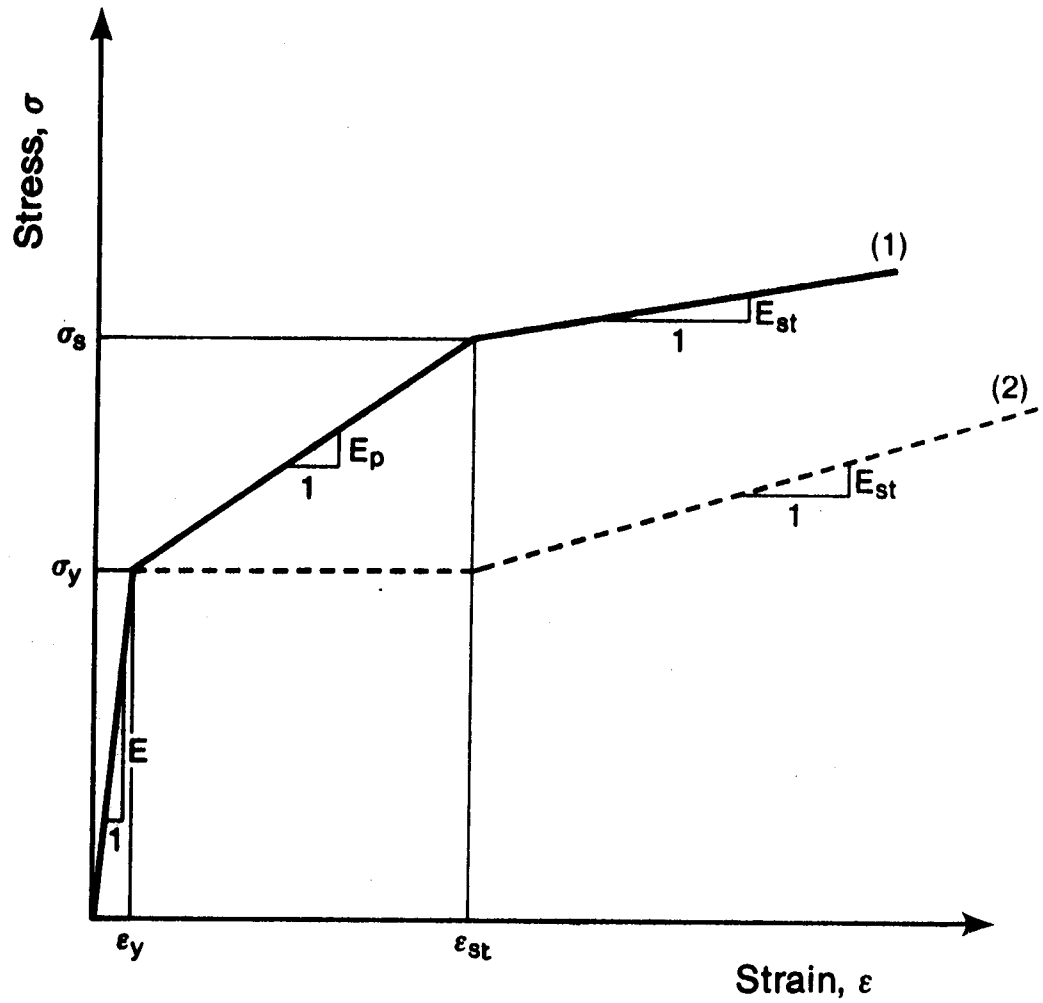


FIGURE D-2 Trilinear Stress-Strain Diagram

Consider a plate segment under a linear variation of strain as shown in Fig. D-3. When the strain at the two ends A and B are of the same sign, ϵ_A and ϵ_B may be in any of the three strain ranges given below:

$$\epsilon_B > \epsilon_{st} \qquad \epsilon_A > \epsilon_{st} \qquad (D.1.4a)$$

$$\epsilon_y \leq \epsilon_B \leq \epsilon_{st} \qquad \epsilon_y \leq \epsilon_A \leq \epsilon_{st} \qquad (D.1.4b)$$

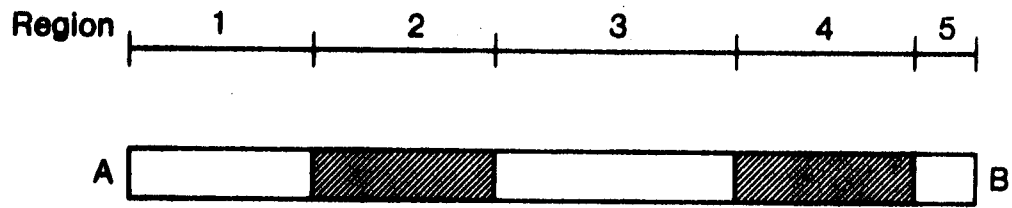
$$0 \leq \epsilon_B \leq \epsilon_y \qquad 0 \leq \epsilon_A < \epsilon_y \qquad (D.1.4c)$$

in which ϵ_y and ϵ_{st} are the yield strain and strain hardening strain respectively, defined in Fig. D-2.

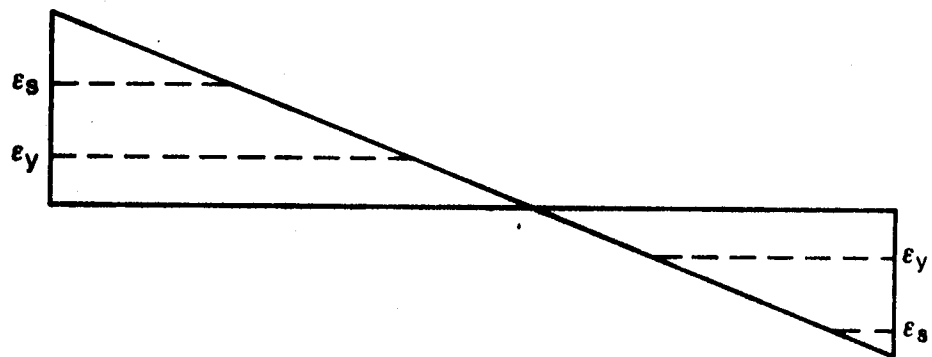
Thus, there are nine combinations of strain distribution when ϵ_A and ϵ_B are of the same sign. Also, there will be nine other combinations when they are of the opposite sign. In each segment of the cross section the tangent moduli E_t are determined from the strain distribution assuming no strain reversal. This divides the plate segment into at most five regions as shown in Fig. D-3, in which moduli are different (Rajasekaran 1971).

If each element of area is transformed such that the product of the current tangent modulus, E_t , times the original element of area, A , is equal to the original modulus, E , times the element of transformed area, A^t , then

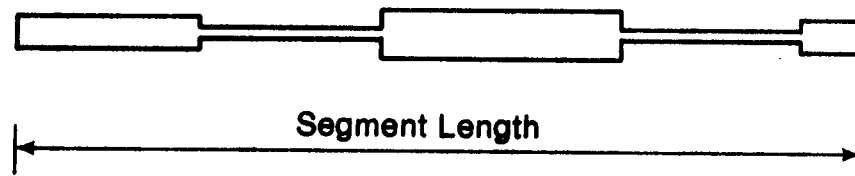
$$E_t \cdot A = E \cdot A^t \qquad (D.1.5)$$



(a) Plate Segment



(b) Strain Distribution



(c) Transformed Segment

FIGURE D-3 Transformed Section of a Plate Segment Region

In order to calculate the tangent properties it is sufficiently accurate to modify the thickness between the corresponding regions by the modular ratio according to the form

$$b_r^t = E_t b_r / E \quad (D.1.6)$$

in which b_r^t is the transformed thickness of a particular region r , and b_r is the original thickness of this region.

Now the section is transformed and the cross section properties of the transformed area can be evaluated as indicated in the following section.

D.2 Evaluation of Cross-Section Properties

Once the transformed thickness of each region is evaluated, the area and moment of inertia of each region are calculated about the centroidal axis of the transformed segment. Moments of inertia of each plate segment are then transformed to the global axis orientation of the cross section. Summing the properties for all segments gives the centroid and moment of inertia of the total cross section.

The section properties, A^t , I_1^t , I_2^t , I_3^t and I_4^t , needed for the inelastic analysis are defined, using Fig. D-4, as

$$A^t = \int_{A^t} dA^t \quad (D.2.2a)$$

$$I_1^t = \int_{A^t} y \cdot dA^t \quad (D.2.2b)$$

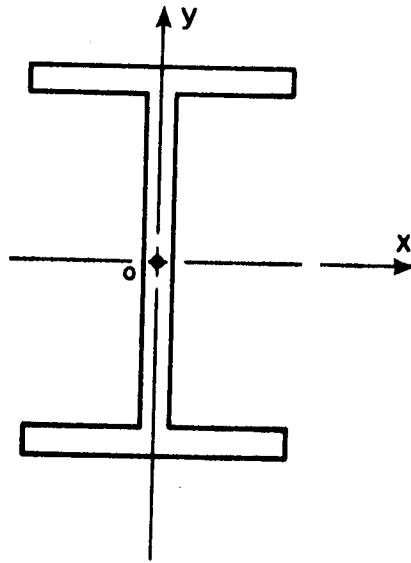


FIGURE D-4 Cross Section

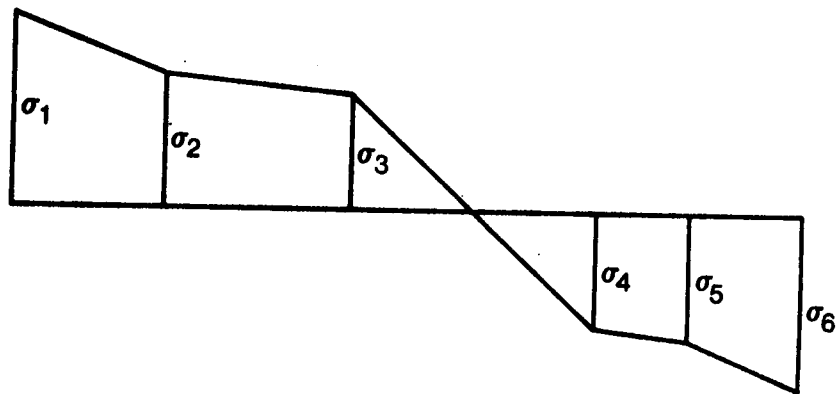


FIGURE D-5 Stresses in a Typical Plate Segment

$$I_2^t = \int_{A^t} y^2 \cdot dA^t \quad (D.2.2c)$$

$$I_3^t = \int_{A^t} y^3 \cdot dA^t \quad (D.2.2d)$$

and

$$I_4^t = \int_{A^t} y^4 \cdot dA^t \quad (D.2.2e)$$

These properties can be written in numerical form with respect to the x and y axes, of Fig. D-4, as

$$A^t = \sum_{k=1}^n A_k \quad (D.2.3a)$$

$$I_1^t = \sum_{k=1}^n A_k \cdot Y_k \quad (D.2.3b)$$

$$I_2^t = \sum_{k=1}^n (I_{xx})_k + \sum_{k=1}^n A_k Y_k^2 \quad (D.2.3c)$$

$$I_3^t = 3 \sum_{k=1}^n (I_{xx})_k Y_k + \sum_{k=1}^n A_k Y_k^3 \quad (D.2.3d)$$

and

$$I_4^t = \sum_{k=1}^n (I_{4xx})_k + 6 \sum_{k=1}^n (I_{xx})_k Y_k^2 + \sum_{k=1}^n A_k Y_k^4 \quad (D.2.3e)$$

in which $(I_{xx})_k$ is the moment of inertia of segment k about the centroidal axis x-x of this segment and $(I_{4xx})_k$ is defined by Eq. B.2.2e for the kth segment about x-x axis of the segment.

D.3 Evaluation of The Stress Resultants

From the stress-strain relationship shown in Fig. D-2, and assuming the strain distribution is known, the stresses in each region of the plate segment can be evaluated. The stress resultants may then be calculated numerically in the x-y reference system from their definitions. Referring to Fig. D-5, the numerical evaluation of the stress resultants can be written in the following forms (Rajasekaran 1971).

$$n = \int_A \sigma_z dA \quad (D.3.1a)$$

or

$$n = \sum_{k=1}^n \sum_{r=1}^5 \frac{1}{2} \ell_r t_k (\sigma_{ir} + \sigma_{jr}) \quad (D.3.1b)$$

also

$$m = \int_A \sigma_z y dA \quad (D.3.2a)$$

or

$$m = \sum_{k=1}^n \sum_{r=1}^5 \frac{\ell_r t_k}{6} \left[\sigma_{ir} (y_{jr} + 2y_{ir}) + \sigma_{jr} (y_{ir} + 2y_{jr}) \right] \quad (D.3.2b)$$

and

$$m^* = \int_A \sigma_z y^2 dA \quad (D.3.3a)$$

or

$$\begin{aligned}
 m^* = & \sum_{k=1}^n \sum_{r=1}^5 \frac{\ell_r t_k}{12} \left[\sigma_{ir} (4 y_{ir}^2 + 2 y_{jr}^2 - \ell_r^2) \right. \\
 & \left. + \sigma_{jr} (4 y_{jr}^2 + 2 y_{ir}^2 - \ell_r^2) \right] \quad (D.3.3b)
 \end{aligned}$$

in which r is the plate region, n is the number of plate segments, k is the plate segment index, t_k is the plate segment thickness, ℓ_r is the plate region length and i and j refer to the two ends of each region.

APPENDIX E

**INCREMENTAL STRESS RESULTANT VECTORS
FOR INELASTIC ELEMENT**

APPENDIX E
INCREMENTAL STRESS RESULTANT VECTORS
FOR INELASTIC ELEMENT

To evaluate the element tangent stiffness matrix, for an inelastic element, it is necessary to evaluate the incremental stress resultants $\frac{\partial n}{\partial q_j}$, $\frac{\partial m}{\partial q_j}$, and $\frac{\partial m^*}{\partial q_j}$, in Eqs. B.4.5. In this appendix the incremental stress resultant vectors are derived. The transformed section properties needed to evaluate such matrices are determined in Appendix D.

E.1 Incremental Stress Resultant Vectors

Consider variations in the stress resultants n , m , and m^* at any stage of loading. These variations can be written, from Eqs. 3.5.9, as

$$\delta n = \int_A E_t \delta \epsilon \, dA \quad (E.1.1a)$$

$$\delta m = \int_A E_t \delta \epsilon \, y \, dA \quad (E.1.1b)$$

and

$$\delta m^* = \int_A E_t \delta \epsilon \, y^2 \, dA \quad (E.1.1c)$$

in which E_t is the tangent modulus at this particular stage of loading.

From the transformed area concept, discussed in Sect. D.1, it can be written that

$$E_t \cdot dA = E dA^t \quad (E.1.2)$$

in which E is the original modulus and A and A^t are the original element of area and the element of transformed area, respectively. Thus Eqs. E.1.1 can be written as

$$\frac{\partial n}{\partial q_j} = \int_{A^t} E \frac{\partial \epsilon}{\partial q_j} dA^t \quad (E.1.3a)$$

$$\frac{\partial m}{\partial q_j} = \int_{A^t} E \frac{\partial \epsilon}{\partial q_j} y dA^t \quad (E.1.3b)$$

and

$$\frac{\partial m^*}{\partial q_j} = \int_{A^t} E \frac{\partial \epsilon}{\partial q_j} y^2 dA^t \quad (E.1.3c)$$

Let the transformed section properties be defined by Eqs. D.2.2. Differentiating Eq. 3.5.5 with respect to q_j and substituting into Eqs. E.1.3 and integrating using Eqs. D.2.2 yields

$$\frac{\partial n}{\partial q_j} = EA^t \cdot b_{1j} - EI_1^t \cdot b_{2j} + EI_2^t \cdot b_{3j} \quad (E.1.4a)$$

$$\frac{\partial m}{\partial q_j} = EI_1^t \cdot b_{1j} - EI_2^t \cdot b_{2j} + EI_3^t \cdot b_{3j} \quad (E.1.4b)$$

and

$$\frac{\partial m^*}{\partial q_j} = EI_2^t \cdot b_{1j} - EI_3^t \cdot b_{2j} + EI_4^t \cdot b_{3j} \quad (E.1.4c)$$

in which

$$b_{1j} = (1 + u'_0) \frac{\partial u'_0}{\partial q_j} + v'_0 \frac{\partial v'_0}{\partial q_j} \quad (E.1.5a)$$

$$b_{2j} = v''_0 \frac{\partial u'_0}{\partial q_j} + \frac{v'_0 v''_0}{\sqrt{1 - (v'_0)^2}} \left(2 + \frac{(v'_0)^2}{1 - (v'_0)^2} \right) \frac{\partial v'_0}{\partial q_j} + \left(1 + u'_0 + \frac{(v'_0)^2}{\sqrt{1 - (v'_0)^2}} \right) \frac{\partial v''_0}{\partial q_j} \quad (E.1.5b)$$

and

$$b_{3j} = \frac{v'_0 (v''_0)^2}{1 - (v'_0)^2} \left(1 + \frac{(v'_0)^2}{1 - (v'_0)^2} \right) \frac{\partial v'_0}{\partial q_j} + v''_0 \left(1 + \frac{(v'_0)^2}{1 - (v'_0)^2} \right) \frac{\partial v''_0}{\partial q_j} \quad (E.1.5c)$$

For each gauss point on the element the values u'_0 , v'_0 , and v''_0 are evaluated from Eqs. B.3.1. Then substituting Eqs. B.3.2 into Eqs. E.1.4 yields

(a) For $1 \leq j \leq 4$

$$\frac{\partial n}{\partial q_j} = [EA^t (1 + u'_0) - EI_1^t v''_0] \phi'_{qj} \quad (E.1.6a)$$

$$\frac{\partial m}{\partial q_j} = [EI_1^t (1 + u'_0) - EI_2^t v''_0] \phi'_{qj}$$

(E.1.6b)

and

$$\frac{\partial m^*}{\partial q_j} = [EI_2^t (1 + u'_0) - EI_3^t v''_0] \phi'_{qj}$$

(E.1.6c)

(b) For $5 \leq j \leq 8$

$$\frac{\partial n}{\partial q_j} = \left[EA^t v'_0 - EI_1^t \frac{v'_0 v''_0}{\sqrt{1 - (v'_0)^2}} \left(2 + \frac{(v'_0)^2}{1 - (v'_0)^2} \right) \right.$$

$$\left. + EI_2^t \frac{v'_0 (v''_0)^2}{1 - (v'_0)^2} \left(1 + \frac{(v'_0)^2}{1 - (v'_0)^2} \right) \right] \phi'_{qj}$$

$$+ \left[-EI_1^t \left(1 + u'_0 + \frac{(v'_0)^2}{\sqrt{1 - (v'_0)^2}} \right) + EI_2^t v''_0 \left(1 + \frac{(v'_0)^2}{1 - (v'_0)^2} \right) \right] \phi''_{qj}$$

(E.1.6d)

$$\frac{\partial m}{\partial q_j} = \left[EI_1^t v'_0 - EI_2^t \frac{v'_0 v''_0}{\sqrt{1 - (v'_0)^2}} \left(2 + \frac{(v'_0)^2}{1 - (v'_0)^2} \right) \right.$$

$$\left. + EI_3^t \frac{v'_0 (v''_0)^2}{1 - (v'_0)^2} \left(1 + \frac{(v'_0)^2}{1 - (v'_0)^2} \right) \right] \phi'_{qj}$$

$$+ \left[-EI_2^t \left(1 + u'_0 + \frac{(v'_0)^2}{\sqrt{1 - (v'_0)^2}} \right) + EI_3^t v''_0 \left(1 + \frac{(v'_0)^2}{1 - (v'_0)^2} \right) \right] \phi''_{qj}$$

(E.1.6e)

and

$$\begin{aligned} \frac{\partial m^*}{\partial q_j} = & \left[EI_2^t v_o' - EI_3^t \frac{v_o' v_o''}{\sqrt{1 - (v_o')^2}} \left(2 + \frac{(v_o')^2}{1 - (v_o')^2} \right) \right. \\ & + EI_4^t \frac{v_o' (v_o'')^2}{1 - (v_o')^2} \left(1 + \frac{(v_o')^2}{1 - (v_o')^2} \right) \left. \right] \phi_{qj}' \\ & + \left[-EI_3^t \left(1 + u_o' + \frac{(v_o')^2}{\sqrt{1 - (v_o')^2}} \right) + EI_4^t v_o'' \left(1 + \frac{(v_o')^2}{1 - (v_o')^2} \right) \right] \phi_{qj}'' \end{aligned} \quad (E.1.6f)$$

Equations E.1.6 are the incremental stress resultant equations for a flexural element, and can be written in a vector form as in Table E-1.

For a truss element the centroid of the transformed area of any cross section remains at the centroid of the elastic section because the section is subjected to axial force only resulting in uniform stress distribution. This leads to

$$I_1^t = 0 \quad (E.1.7a)$$

$$I_3^t = 0 \quad (E.1.7b)$$

Also for a truss element a linear interpolation function is used which leads to (Eq. B.3.1c)

$$v_o'' = \phi_{qj}'' = 0 \quad (E.1.7c)$$

$$\frac{\partial m}{\partial q_j} = [EI_1^t (1 + u'_0) - EI_2^t v''_0] \phi'_{qj} \quad (E.1.6b)$$

and

$$\frac{\partial m^*}{\partial q_j} = [EI_2^t (1 + u'_0) - EI_3^t v''_0] \phi'_{qj} \quad (E.1.6c)$$

(b) For $5 \leq j \leq 8$

$$\begin{aligned} \frac{\partial n}{\partial q_j} = & \left[EA^t v'_0 - EI_1^t \frac{v'_0 v''_0}{\sqrt{1 - (v'_0)^2}} \left(2 + \frac{(v'_0)^2}{1 - (v'_0)^2} \right) \right. \\ & + EI_2^t \frac{v'_0 (v''_0)^2}{1 - (v'_0)^2} \left(1 + \frac{(v'_0)^2}{1 - (v'_0)^2} \right) \left. \right] \phi'_{qj} \\ & + \left[-EI_1^t \left(1 + u'_0 + \frac{(v'_0)^2}{\sqrt{1 - (v'_0)^2}} \right) + EI_2^t v''_0 \left(1 + \frac{(v'_0)^2}{1 - (v'_0)^2} \right) \right] \phi''_{qj} \end{aligned} \quad (E.1.6d)$$

$$\begin{aligned} \frac{\partial m}{\partial q_j} = & \left[EI_1^t v'_0 - EI_2^t \frac{v'_0 v''_0}{\sqrt{1 - (v'_0)^2}} \left(2 + \frac{(v'_0)^2}{1 - (v'_0)^2} \right) \right. \\ & + EI_3^t \frac{v'_0 (v''_0)^2}{1 - (v'_0)^2} \left(1 + \frac{(v'_0)^2}{1 - (v'_0)^2} \right) \left. \right] \phi'_{qj} \\ & + \left[-EI_2^t \left(1 + u'_0 + \frac{(v'_0)^2}{\sqrt{1 - (v'_0)^2}} \right) + EI_3^t v''_0 \left(1 + \frac{(v'_0)^2}{1 - (v'_0)^2} \right) \right] \phi''_{qj} \end{aligned} \quad (E.1.6e)$$

and

$$\begin{aligned}
 \frac{\partial m^*}{\partial q_j} = & \left[EI_2^t v_o' - EI_3^t \frac{v_o' v_o''}{\sqrt{1 - (v_o')^2}} \left(2 + \frac{(v_o')^2}{1 - (v_o')^2} \right) \right. \\
 & \left. + EI_4^t \frac{v_o' (v_o'')^2}{1 - (v_o')^2} \left(1 + \frac{(v_o')^2}{1 - (v_o')^2} \right) \right] \phi_{q_j}' \\
 & + \left[-EI_3^t \left(1 + u_o' + \frac{(v_o')^2}{\sqrt{1 - (v_o')^2}} \right) + EI_4^t v_o'' \left(1 + \frac{(v_o')^2}{1 - (v_o')^2} \right) \right] \phi_{q_j}'' \\
 & \hspace{15em} (E.1.6f)
 \end{aligned}$$

Equations E.1.6 are the incremental stress resultant equations for a flexural element, and can be written in a vector form as in Table E-1.

For a truss element the centroid of the transformed area of any cross section remains at the centroid of the elastic section because the section is subjected to axial force only resulting in uniform stress distribution. This leads to

$$I_1^t = 0 \quad (E.1.7a)$$

$$I_3^t = 0 \quad (E.1.7b)$$

Also for a truss element a linear interpolation function is used which leads to (Eq. B.3.1c)

$$v_o'' = \phi_{q_j}'' = 0 \quad (E.1.7c)$$

$$\left\{ \frac{\partial n}{\partial q} \right\} = \left\{ \begin{aligned} & \frac{[EA^t (1 + u'_0) - EI_1^t v''_0] \{\phi'\}}{\left[EA^t v'_0 - EI_1^t \frac{v'_0 v''_0}{\sqrt{1 - (v'_0)^2}} \left(2 + \frac{(v'_0)^2}{1 - (v'_0)^2} \right) \right.} \\ & \quad \left. + EI_2^t \frac{v'_0 (v''_0)^2}{1 - (v'_0)^2} \left(1 + \frac{(v'_0)^2}{1 - (v'_0)^2} \right) \right] \{\phi'\}} \\ & + \left[EI_2^t v''_0 \left(1 + \frac{(v'_0)^2}{1 - (v'_0)^2} \right) - EI_1^t \left(1 + u'_0 + \frac{(v'_0)^2}{\sqrt{1 - (v'_0)^2}} \right) \right] \{\phi''\} \end{aligned} \right\}$$

$$\left\{ \frac{\partial m}{\partial q} \right\} = \left\{ \begin{aligned} & \frac{[EI_1^t (1 + u'_0) - EI_2^t v''_0] \{\phi'\}}{\left[EI_1^t v'_0 - EI_2^t \frac{v'_0 v''_0}{\sqrt{1 - (v'_0)^2}} \left(2 + \frac{(v'_0)^2}{1 - (v'_0)^2} \right) \right.} \\ & \quad \left. + EI_3^t \frac{v'_0 (v''_0)^2}{1 - (v'_0)^2} \left(1 + \frac{(v'_0)^2}{1 - (v'_0)^2} \right) \right] \{\phi'\}} \\ & + \left[EI_3^t v''_0 \left(1 + \frac{(v'_0)^2}{1 - (v'_0)^2} \right) \right. \\ & \quad \left. - EI_2^t \left(1 + u'_0 + \frac{(v'_0)^2}{\sqrt{1 - (v'_0)^2}} \right) \right] \{\phi''\} \end{aligned} \right\}$$

TABLE E-1 Incremental Stress Resultant Vectors
for Flexural Element

$$\left\{ \frac{\partial m^*}{\partial q} \right\} = \left\{ \begin{aligned} & \frac{[EI_2^t (1 + u'_0) - EI_3^t v''_0] \{\phi'\}}{\left[EI_2^t v'_0 - EI_3^t \frac{v'_0 v''_0}{\sqrt{1 - (v'_0)^2}} \left(2 + \frac{(v'_0)^2}{1 - (v'_0)^2} \right) \right.} \\ & \quad \left. + EI_4^t \frac{v'_0 (v''_0)^2}{1 - (v'_0)^2} \left(1 + \frac{(v'_0)^2}{1 - (v'_0)^2} \right) \right] \{\phi'\}} \\ & \quad + \left[EI_4^t v''_0 \left(1 + \frac{(v'_0)^2}{1 - (v'_0)^2} \right) \right. \\ & \quad \left. - EI_3^t \left(1 + u'_0 + \frac{(v'_0)^2}{\sqrt{1 - (v'_0)^2}} \right) \right] \{\phi''\} \end{aligned} \right\}$$

Note

$\left\{ \frac{\partial}{\partial q} \right\}$ is 8 x 1 column matrix

$\{\phi'\}$ and $\{\phi''\}$ are 4 x 1 column matrices

TABLE E-1 (Cont.) Incremental Stress Resultant
Vectors for Flexural Element

From Eqs. E.1.7, Eqs. E.1.6 can be modified for a truss element as

(a) For $1 \leq j \leq 2$

$$\frac{\partial n}{\partial q_j} = EA^t (1 + u'_0) (\bar{\phi}_{qj})' \quad (E.1.8a)$$

$$\frac{\partial m}{\partial q_j} = 0 \quad (E.1.8b)$$

$$\frac{\partial m^*}{\partial q_j} = EI_2^t (1 + u'_0) (\bar{\phi}_{qj})' \quad (E.1.8c)$$

(b) For $3 \leq j \leq 4$

$$\frac{\partial n}{\partial q_j} = EA^t v'_0 (\bar{\phi}_{qj})' \quad (E.1.8d)$$

$$\frac{\partial m}{\partial q_j} = 0 \quad (E.1.8e)$$

$$\frac{\partial m^*}{\partial q_j} = EI_2^t v'_0 (\bar{\phi}_{qj})' \quad (E.1.8f)$$

The column vectors arising from Eqs. E.1.8 are given in Table E-2. All section properties needed to form these matrices are given by Eqs. D.2.3. Once the incremental stress resultant vectors are formulated, for an inelastic element, they are used in Eq. B.4.4 or Eq. B.4.11 to evaluate the inelastic tangent stiffness matrix.

$$\left\{ \frac{\partial n}{\partial q} \right\} = \left\{ \frac{EA^t (1 + u'_0) \{ (\bar{\phi})' \}}{EA^t v'_0 \{ (\bar{\phi})' \}} \right\}$$

$$\left\{ \frac{\partial m}{\partial q} \right\} = \{ 0 \}$$

$$\left\{ \frac{\partial m^*}{\partial q} \right\} = \left\{ \frac{EI_2^t (1 + u'_0) \{ (\bar{\phi})' \}}{EI_2^t v'_0 \{ (\bar{\phi})' \}} \right\}$$

Note

$\left\{ \frac{\partial}{\partial q} \right\}$ is 4 x 1 column matrix

$\{ (\bar{\phi})' \}$ is 2 x 1 column matrix

TABLE E-2 Incremental Stress Resultant
Vectors for Truss Element